

Emergent random matrix universality in quantum operator dynamics

Oliver Lunt,^{1,2} Thomas Kriecherbauer,³ Kenneth T-R McLaughlin,⁴ and Curt von Keyserlingk²

¹*Clarendon Laboratory, Department of Physics, University of Oxford, United Kingdom*

²*Department of Physics, King's College London, United Kingdom*

³*Department of Mathematics, Universität Bayreuth, Germany*

⁴*Department of Mathematics, Tulane University, United States*

The memory function description of many-body quantum operator dynamics involves a carefully chosen split into ‘fast’ and ‘slow’ modes. An approximate model for the fast modes can then be used to solve for Green’s functions $G(z)$ of the slow modes. One common approach is to form a so-called Krylov operator basis $\{O_m\}_{m \geq 0}$, and then approximate the dynamics restricted to the ‘fast space’ $\{O_m\}_{m \geq n}$ for some large n . Denoting the fast space Green’s function by $G_n(z)$, in this work we prove that $G_n(z)$ exhibits universality in the $n \rightarrow \infty$ limit, approaching different universal scaling forms in different regions of the complex z -plane. This universality of $G_n(z)$ turns out to be precisely analogous to the universality of eigenvalue correlations in random matrix theory (RMT), even though there is *no explicit randomness* present in the Hamiltonian. At finite z , we show that $G_n(z)$ approaches the Wigner semicircle law, the same as the average resolvent in the bulk of the spectrum for the Gaussian Unitary Ensemble with a rescaled bandwidth. When $G(z)$ is the Green’s function of certain hydrodynamical variables, we show that at low frequencies $G_n(z)$ is instead governed by the Bessel universality class from RMT. As an application we give a new numerical method, the *spectral bootstrap*, for approximating spectral functions, including hydrodynamic transport data, from a finite number of Lanczos coefficients. Our proof is complex analytic in nature, involving a map to a Riemann-Hilbert problem which we solve using a steepest-descent-type method, rigorously controlled in the $n \rightarrow \infty$ limit. This proof technique assumes some analyticity and regularity conditions on the spectral function, and we comment on their possible connections to the eigenstate thermalization hypothesis. Also via the steepest-descent procedure, we are led to a related Coulomb gas optimization problem, and we discuss how a recent conjecture—the ‘Operator Growth Hypothesis’—implies that chaotic operator dynamics can generically be identified with the critical point of a confinement transition in this Coulomb gas. We then explain how this criticality has implications for the computational resources required to estimate transport coefficients to a given precision.

I. INTRODUCTION

Improvements in our understanding of many-body quantum systems can inform the development of new numerical algorithms to simulate them. For example, the realization that gapped 1D ground states have area law entanglement [1] justifies the great success of variational tensor network algorithms [2]. Moving beyond ground states, the study of many-body quantum dynamics presents a longstanding challenge. Due to the rapid growth of entanglement for generic interacting systems [3], the memory requirements for faithful tensor network descriptions typically grow exponentially in time [4]. Given this difficult state of affairs, it is worth asking: are there universal features of many-body quantum dynamics, and if so, how can we utilize this universality to design better algorithms?

Recently an array of algorithms have been proposed that apply new insights from quantum information and quantum chaos to the old problem of hydrodynamics [5–14]. These algorithms work by discarding information about a time-evolved quantum operator that can only be detected using very non-local probes, like high-order correlation functions. If one is primarily interested in physics described by low-order correlation functions, like linear response hydrodynamics, then such approximations can be worthwhile in order to reduce computational requirements. To develop intuition for why this could work, consider the autocorrelation function $C(t) = (O_0|O_0(t))$ of a normal-

ized local operator O_0 evolving in the Heisenberg picture as $O_0(t) = e^{iHt}O_0e^{-iHt}$, and for simplicity let us work at infinite temperature so that $(A|B) = \text{tr}[A^\dagger B] / \text{tr}[\mathbf{1}]$. The correlation function gives the probability amplitude at time t for the time-evolved operator to return to its starting point—that is, it measures the operator ‘back-flow’. Decomposing $O_0(t)$ as a superposition over operator paths, the dominant paths that contribute to $C(t)$ are those that involve only ‘simple’ local operators [12, 15]. The intuition is that, at least for ergodic dynamics, once an operator becomes sufficiently non-local, it is very unlikely to shrink down to a small operator again, and will therefore give a negligible contribution to $C(t)$. This suggests that one should be able to neglect such non-local operator histories while incurring only a small error in $C(t)$. Where these algorithms differ is in precisely how they choose to discard or approximate these non-local operators.

II. SYNOPSIS

In this paper we give a new approach to systematically approximate the contributions from complicated operator paths. As well as having a practical application in estimating Green’s functions, this also yields a new connection between quantum operator dynamics and random matrix theory. Our approach can be phrased in the language of

a standard tool from hydrodynamics, the Mori-Zwanzig memory function formalism [16–18], which separates operators into ‘fast’ and ‘slow’ modes. Given a Hamiltonian H and an initial operator O_0 , consider the Green’s function

$$G(z) = \left(O_0 \left| \frac{1}{z - \mathcal{L}} \right| O_0 \right), \quad (1)$$

where $\mathcal{L}(\cdot) = [H, \cdot]$ is the Liouvillian, and we are using a vectorized notation for operators, $O_0 \leftrightarrow |O_0\rangle$. Formally expanding the resolvent, we see that $G(z)$ will contain contributions from all operators of the form $\mathcal{L}^n |O_0\rangle$, $n = 0, 1, \dots$. Roughly speaking, the intuition is that the operators in the ‘slow space’ spanned by O_0 and low powers of the Liouvillian will give the dominant contributions to $G(z)$. To make this slightly more precise, let O_1 denote the operator obtained by orthogonalizing $\mathcal{L}|O_0\rangle$ against $|O_0\rangle$. Using some standard manipulations [18, 19], the Green’s function can be rewritten as

$$G(z) = \frac{1}{z - b_1^2 G_1(z)}, \quad (2)$$

where b_1 is a normalization factor, and $G_1(z)$ is given by

$$G_1(z) = \left(O_1 \left| \frac{1}{z - \mathcal{L}_1} \right| O_1 \right). \quad (3)$$

Here $\mathcal{L}_1 = \mathcal{Q}_1 \mathcal{L} \mathcal{Q}_1$, $\mathcal{Q}_1 \equiv \mathbb{1} - |O_0\rangle\langle O_0|$, is the Liouvillian projected on to the space orthogonal to the initial operator O_0 . $G_1(z)$ is the *memory function* associated with $G(z)$, but it can itself be thought of as the Green’s function for a new dynamical problem, with initial operator O_1 and dynamics generated by \mathcal{L}_1 . We can therefore repeat the same orthogonalization procedure recursively, eventually ending up with a continued fraction representation for the original Green’s function

$$G(z) = \frac{1}{z - \frac{b_1^2}{z - \dots - \frac{b_{n-1}^2}{z - b_n^2 G_n(z)}}} \quad (4)$$

This orthonormalization process produces a sequence of basis operators $\{O_n\}_{n=0}^{\infty}$ and normalization factors $\{b_n\}_{n=1}^{\infty}$, which are called the Lanczos operators and Lanczos coefficients respectively, because for a Hermitian H this process turns out to be equivalent to the Lanczos algorithm (see Section III). These coefficients can be calculated numerically for a given many-body model, up to some limit n_{\max} set by memory constraints. To calculate the true Green’s function $G(z)$, one then needs some means of terminating the continued fraction by choosing an appropriate expression for the level- n Green’s function

$$G_n(z) := \left(O_n \left| \frac{1}{z - \mathcal{L}_n} \right| O_n \right), \quad (5)$$

where $\mathcal{L}_n = \mathcal{Q}_n \mathcal{L} \mathcal{Q}_n$, $\mathcal{Q}_n = \mathbb{1} - \sum_{m=0}^{n-1} |O_m\rangle\langle O_m|$, is the Liouvillian restricted to the ‘fast space’ spanned by

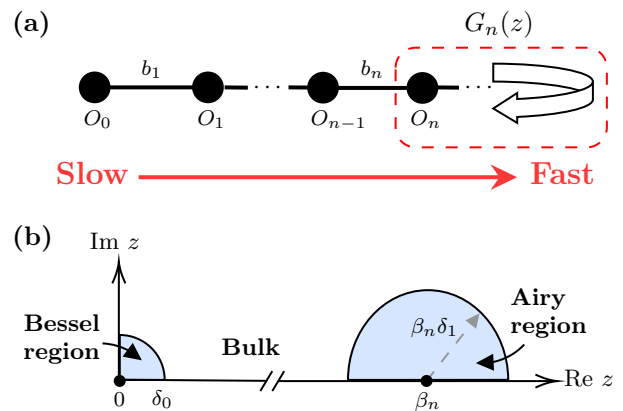


FIG. 1. (a) The semi-infinite 1D operator chain produced by the Lanczos algorithm. The level- n Green’s function $G_n(z) = \langle O_n | (z - \mathcal{L}_n)^{-1} | O_n \rangle$ is the effective Green’s function for operator dynamics restricted to sites n and above, which we call the ‘fast space’. A good model for the fast space dynamics encoded in $G_n(z)$ can be used to estimate the full Green’s function $G(z)$ via the continued fraction in Eq. (4). (b) $G_n(z)$ approaches *universal scaling forms* as $n \rightarrow \infty$, with different limits for different regions of the complex z -plane. The most prominent example is that $G_n(z)$ approaches the Wigner semicircle law in the ‘bulk’ of the spectrum, but there can be different behavior near the origin and the spectral edge. This emergent universality is precisely analogous to the universality of eigenvalue correlations of random matrices, even though there is *no explicit randomness* here. For illustration we show only the first quadrant, with the other quadrants obtained by reflection about the axes. Here δ_0 and δ_1 are small $\mathcal{O}(1)$ constants in units of the microscopic couplings, and $\beta_n \approx 2b_n$ determines the bandwidth of the bulk spectrum.

$\{O_m\}_{m \geq n}$. Much as the original Green’s function $G(z)$ captures the backflow of the original operator O_0 , the level- n Green’s function $G_n(z)$ encodes the backflow of operator dynamics in the fast space. The continued fraction representation shows that, if one can accurately describe the fast space dynamics, then one can leverage this to estimate the full many-body Green’s function $G(z)$. Choosing such an appropriate ‘terminator’ for $G_n(z)$ forms the basis of a numerical approach called the *recursion method* [19].

Since the eigenvalues of the Liouvillian $\mathcal{L}(\cdot) = [H, \cdot]$ are frequencies $\omega_{ij} = E_i - E_j$, our results are most easily stated in frequency space. As we will explain in detail in Section III, the spectral function

$$\Phi(\omega) := \int_{\mathbb{R}} e^{-i\omega t} \langle O_0 | O_0(t) \rangle dt \quad (6)$$

directly determines all the properties of the Lanczos basis. Assuming only a few physically motivated conditions on $\Phi(\omega)$, stated in Section S1 A, we show that, as $n \rightarrow \infty$, $G_n(z)$ approaches *universal scaling forms*. This universality can then be exploited to estimate the original Green’s function $G(z)$. As we will explain, the universality of $G_n(z)$ turns out to be precisely analogous to the universality of eigenvalue correlations of $n \times n$ random matrices.

Emergent universality in the $n \rightarrow \infty$ limit

When the memory function formalism was first developed it was hoped that, if n is sufficiently large, then all non-universal features of the original dynamical problem would be filtered out into the coefficients $\{b_n\}$, and then the level- n Green's function $G_n(z)$ could be approximated by assuming it is ultra short-range correlated in time, which amounts to setting $G_n(z)$ to be constant [18, 19]. In certain cases this turns out to be well-founded. As discussed in Section VI, one of our main results is that, as $n \rightarrow \infty$, for z in the ‘bulk’ of the spectrum, $G_n(z)$ approaches the Wigner semicircle law:

$$G_n(z) \approx \frac{2}{\beta_n^2} \left(z - \sqrt{z + \beta_n} \sqrt{z - \beta_n} \right). \quad (7)$$

Here β_n is an effective n -dependent frequency bandwidth approximated by $\beta_n \approx 2b_n$ as $n \rightarrow \infty$, and ‘bulk’ means $|z| > \delta_0$ and $|z/\beta_n \pm 1| > \delta_1$ for some small $\mathcal{O}(1)$ constants δ_0, δ_1 in units of the microscopic couplings (see Fig. 1(b)). That this should be called a semicircle is perhaps clearer from considering the corresponding bulk spectral function,

$$\Phi_n(\omega) = 2 \operatorname{Im} [G_n(\omega - i0^+)] \approx \frac{4}{\beta_n} \sqrt{1 - (\omega/\beta_n)^2}. \quad (8)$$

Note that this semicircle form of $G_n(z)$ is identical to the average global resolvent $\frac{1}{n} \operatorname{tr} [1/(z - M)]$ —which encodes dynamics in random matrix theory—for random $n \times n$ matrices M drawn from the Gaussian Unitary Ensemble [20], rescaled so that the bulk eigenvalue spectrum corresponds to the interval $[-\beta_n, \beta_n]$. Thus we see the emergence of random matrix-like universality—even though there is no explicit randomness present—in the bulk frequency profile of the ‘fast space’ operator dynamics, i.e., restricted to $\{O_m\}_{m \geq n}$. Since the bandwidth scales like $\beta_n \approx 2b_n$ to leading order in n , if the Lanczos coefficients grow indefinitely, $b_n \rightarrow \infty$, we conclude that $G_n(z) \approx \pm 2i/\beta_n + \mathcal{O}(z/\beta_n^2)$ is approximately constant to leading order in z/β_n , thereby justifying the assumption of short-range time correlations as $n \rightarrow \infty$. This also provides a precise sense in which the large- n dynamics are ‘fast’, since $G_n(z) = \mathcal{O}(1/\beta_n)$ tends to zero as $n \rightarrow \infty$.

For spectral functions $\Phi(\omega)$ which are complex analytic at $\omega = 0$, corresponding to autocorrelation functions $C(t)$ which decay exponentially in time, we further show that this semicircle behavior persists all the way down to zero frequency. We conjecture that this remains true even if $C(t)$ decays algebraically, provided it is faster than $1/t$ —but that there is a slower decay of the finite- n correction to the semicircle law in this case.

However, when the autocorrelation function $C(t)$ decays as a power-law slower than $1/t$, this results in power-law behavior of $G_n(z)$ near $z = 0$, so that the semicircle form is no longer appropriate. Such power-law decay in $C(t)$ is typical if the initial operator overlaps with a conserved quantity with sufficiently slow transport, say diffusive in

1D [18]. With hydrodynamics in mind, one of our principal goals will be to characterize how signatures of the long-time behavior of the autocorrelation function $C(t)$ imprint themselves on the Lanczos basis, and in turn how this affects the operator backflow encoded in the Green's functions $G_n(z)$. When the spectral function behaves like a power-law at low frequencies, we show that this modifies the behavior of $G_n(z)$ for $z \rightarrow 0$, such that the semicircle form breaks down, and $G_n(z)$ instead has an explicit expression in terms of Bessel functions (see Section VIB). This is a reflection of ‘Bessel universality’ that governs the low frequency behavior (see Fig. 1). With these fingerprints of low-frequency behavior in hand, we show how to approximate low-frequency data like hydrodynamic transport coefficients, using only a finite number of Lanczos coefficients as input (see Section V). We benchmark this approach on a range of physical models, including the mixed field Ising model and the XXZ spin chain, finding results that are competitive with tensor network methods.

Orthogonal polynomials and large- n expansions

Our technical approach is to make use of some powerful machinery from complex analysis, developed in the study of orthogonal polynomials [21–27]. This is relevant because the Lanczos algorithm can be naturally phrased in the language of orthogonal polynomials (see Section III). Indeed, the n th Lanczos basis operator $|O_n\rangle$ is given by

$$|O_n\rangle = p_n(\mathcal{L})|O_0\rangle, \quad (9)$$

where the polynomials $p_n(\omega)$ are orthonormal with respect to the spectral function, i.e.,

$$\int_{\mathbb{R}} p_m(\omega) p_n(\omega) \frac{\Phi(\omega)}{2\pi} d\omega = \delta_{mn}. \quad (10)$$

One can similarly write an expression for the level- n Green's function $G_n(z)$ in terms of these orthogonal polynomials (see Eq. (11)). The complex analytic machinery works by devising a Riemann-Hilbert problem whose solution encodes essential data about these orthogonal polynomials with respect to $\Phi(\omega)$, which in turn gives us information about the Lanczos basis (see Section S2 for details). The advantage of this formulation is that it permits approximate solutions, controlled in the limit $n \rightarrow \infty$, even without knowing the explicit form of the spectral function $\Phi(\omega)$. Instead one only needs to know some ‘high level’ features of $\Phi(\omega)$, like its rate of decay at high frequencies, and whether it has a power-law at low frequencies. Then one can use a technique similar to steepest descent to obtain a $1/n$ expansion of the polynomials $p_n(\omega)$ (Sections V and VII), the recurrence coefficients b_n (Theorem 1), the level- n Green's function $G_n(z)$ (Section VI), and other related quantities. We remark that the $n \rightarrow \infty$ limit is quite natural, in the sense that we expect the operator Krylov space $\mathcal{K} = \operatorname{span}\{\mathcal{L}^n O_0\}_{n \geq 0}$ to be infinite dimensional in the thermodynamic limit,

for generic local operators O_0 and generic Hamiltonians. This provides one with the means to perform a large- n expansion of the operator dynamics, even when there is no explicit large parameter in the Hamiltonian.

Since this steepest descent approach involves deformation of contours into the complex plane, our proof technique requires us to make some assumptions about the complex analytic structure of the spectral function $\Phi(\omega)$ near the real frequency axis; this is the main technical caveat to our work, and we discuss it in more detail in Sections S1 A and S1 B. However, numerical evidence suggests that some of our results may remain valid, at least to leading order in n , assuming only weaker conditions than analyticity, such as differentiability of $\Phi(\omega)$. Indeed, a recent breakthrough result in random matrix theory proved universality assuming only a very mild local continuity condition [28], and it would be interesting to see if these techniques could be adapted for our purposes.

Lanczos dynamics and random matrix universality

As previously discussed, one of our main results is that, as $n \rightarrow \infty$, the level- n Green's function $G_n(z)$ approaches universal scaling forms, the most prominent example being the Wigner semicircle law for z in the bulk of the spectrum. In what follows, we will discuss how the universality of $G_n(z)$ and related quantities is analogous, in a precise sense, to the universality of eigenvalue correlations of random matrices. Mathematically, this shared universality can be understood from the fact that both Lanczos operator dynamics and random matrix theory can be formulated in the language of orthogonal polynomials. These polynomials themselves exhibit universal scaling forms in the $n \rightarrow \infty$ limit, which then implies universality in both Lanczos operator dynamics and random matrix theory. While these formulations in terms of orthogonal polynomials are well-known to practitioners of both fields, it is worth spelling out how they work in some detail.

In the Lanczos context, we already saw the connection with orthogonal polynomials in Eqs. (9) and (10): the n th Lanczos operator O_n can be written in terms of the n th orthogonal polynomial $p_n(\omega)$ with respect to the spectral function $\Phi(\omega) = \int_{\mathbb{R}} e^{-i\omega t} C(t) dt$. To get from there to the level- n Green's function, one can employ the useful identity [29]

$$G_n(z) = \frac{1}{b_n} \frac{C_n(z)}{C_{n-1}(z)}, \quad (11)$$

$$\text{where } C_n(z) \equiv \int_{\mathbb{R}} \frac{p_n(\omega)}{z - \omega} \frac{\Phi(\omega)}{2\pi} d\omega.$$

Unfortunately, $G_n(z)$ does not, in general, have an interpretation as a simple low-order correlation function of a random matrix ensemble. In that sense, the result for the bulk of the spectrum is a special case—albeit one that applies almost everywhere in the complex z plane—where $G_n(z)$ approaches the Wigner semicircle law, and

can then indeed be identified with a simple RMT correlation function. But nonetheless, even away from the bulk, $G_n(z)$ does still approach universal scaling forms, which can be understood in terms of universality of the orthogonal polynomials $p_n(\omega)$ in the $n \rightarrow \infty$ limit.

In the random matrix theory context, orthogonal polynomials provide a useful tool for computing eigenvalue correlation functions [30]. Consider an ensemble of $n \times n$ random Hermitian matrices M with probability density $P(M) \propto \exp(-\text{tr}[Q(M)])$, for some function Q called the *potential*. The Gaussian unitary ensemble (GUE) corresponds to $Q(x) = x^2$, but it can be useful to consider more general functions Q to introduce correlations between matrix elements. One can instead consider the distribution on the eigensystem of M rather than its matrix elements; for general Q , integrating out the eigenvectors produces a distribution on the eigenvalues given by

$$P_Q(\lambda_1, \dots, \lambda_n) \propto \left(\prod_{i < j} |\lambda_i - \lambda_j|^2 \right) \prod_i e^{-Q(\lambda_i)}, \quad (12)$$

resulting in the familiar Vandermonde determinant $\prod_{i < j} |\lambda_i - \lambda_j|^2$ responsible for eigenvalue repulsion. It is then natural to consider the k -point eigenvalue correlation function $R_k(\lambda_1, \dots, \lambda_k)$ defined by

$$R_k(\lambda_1, \dots, \lambda_k) = \frac{n!}{(n-k)!} \int_{\mathbb{R}} \dots \int_{\mathbb{R}} P_Q(\lambda_1, \dots, \lambda_k, \lambda_{k+1}, \dots, \lambda_n) d\lambda_{k+1} \dots d\lambda_n. \quad (13)$$

The key fact linking RMT and orthogonal polynomials is that R_k can be expressed as a $k \times k$ matrix determinant,

$$R_k(\lambda_1, \dots, \lambda_k) = \det \left[\left(\hat{K}_n(\lambda_i, \lambda_j) \right)_{1 \leq i, j \leq k} \right], \quad (14)$$

where each matrix element is given by evaluating a 2-point correlation kernel $\hat{K}_n(\lambda_i, \lambda_j)$. The kernel is defined by

$$\hat{K}_n(\lambda_i, \lambda_j) = \sqrt{e^{-Q(\lambda_i)} e^{-Q(\lambda_j)}} \sum_{m=0}^{n-1} p_m(\lambda_i) p_m(\lambda_j), \quad (15)$$

where the p_m are orthogonal polynomials satisfying

$$\int_{\mathbb{R}} p_k(\lambda) p_l(\lambda) e^{-Q(\lambda)} d\lambda = \delta_{kl}. \quad (16)$$

Thus we see that eigenvalue statistics of random matrices can be described in terms of orthogonal polynomials with respect to $e^{-Q(\lambda)}$, the potential defining the random matrix ensemble. One of the deepest facts about random matrices is that their eigenvalue statistics can be *universal*, when probed on a local scale [31]. Here ‘local scale’ means that we consider correlations over $\mathcal{O}(1)$ separations in units of the inverse local eigenvalue density, and ‘universal’ means they are independent of the exact eigenvalue probability distribution. Given the formulation in terms of orthogonal polynomials in Eq. (16),

one can derive RMT universality from universality of the orthogonal polynomials themselves.

To relate Lanczos operator dynamics to random matrix theory, let us summarize the discussion so far: the Lanczos basis operators O_n are related to orthogonal polynomials with respect to $\Phi(\omega)/2\pi$ (see Eq. (10)), while RMT eigenvalue statistics are related to orthogonal polynomials with respect to $e^{-Q(\lambda)}$ (see Eq. (16)). Therefore, under the identification of weight functions:

$$\boxed{\frac{\Phi(\omega)}{2\pi} \equiv e^{-Q(\omega)}}, \quad (17)$$

we see that there is a connection between:

n th Lanczos operator $O_n \rightsquigarrow n \times n$ random matrices

Much as one can derive RMT universality from universality of the orthogonal polynomials defining the matrix ensemble, one can derive universality of the level- n Green's function $G_n(z)$ and related quantities from universality of the orthogonal polynomials with respect to the spectral function $\Phi(\omega)$. Universal asymptotics of orthogonal polynomials is a much older phenomenon than RMT universality, going back to work in the 1920s of Plancherel and Rotach on $n \rightarrow \infty$ asymptotics for the Hermite polynomials ($Q(x) = x^2$) [32]. One of our technical contributions is proving so-called 'Plancherel-Rotach asymptotics' of the orthogonal polynomials for a large class of spectral functions obeying physically-motivated conditions (described in Section S1 A). From there, one is led to universality for the level- n Green's function.

Coulomb gas confinement transition, quantum chaos, and the operator growth hypothesis

Stemming from the foundational work of Dyson [33], a key concept in random matrix theory (RMT) is the Coulomb gas [34]. To give context for our result about a Coulomb gas confinement transition, let us briefly illustrate where this comes from, both in random matrix theory and in Lanczos operator dynamics.

To compute eigenvalue correlation functions in RMT, one needs to consider integrals with respect to the eigenvalue probability distribution $P_Q(\lambda_1, \dots, \lambda_n)$. For reasons that will soon become apparent, it turns out to be important to rescale by an n -dependent factor, $\lambda_i \rightarrow \beta_n x_i$, where the scale factor β_n is determined by Q and the x_i are $\mathcal{O}(1)$; for $Q(\lambda) = \lambda^2$ we have $\beta_n = \sqrt{2n}$. Then, defining the rescaled potential $V_n(x) \equiv Q(\beta_n x)/n$, one can rewrite Eq. (12) as

$$P_Q(\lambda_1, \dots, \lambda_n) \propto e^{-[\sum_{i \neq j} \log |x_i - x_j|^{-1} + n \sum_i V_n(x_i)]}, \quad (18)$$

and so one expects the leading contributions to come from tuples $\mathbf{x} = (x_1, \dots, x_n)$ for which the exponent is minimal. For any such tuple \mathbf{x} , if we introduce the normalized

counting measure $d\psi_{\mathbf{x}}(y) = \frac{1}{n} \sum_{i=1}^n \delta(y - x_i) dy$, then we are led to consider the Coulomb gas energy functional

$$E_{V_n}[\psi] = \int_{\mathbb{R}} \int_{\mathbb{R}} \log |x - y|^{-1} d\psi(x) d\psi(y) + \int_{\mathbb{R}} V_n(x) d\psi(x). \quad (19)$$

In the $n \rightarrow \infty$ limit, eigenvalue correlation functions will be dominated by configurations ψ which minimize this Coulomb gas energy. The rescaling $\lambda_i \rightarrow \beta_n x_i$ served the purpose of ensuring that the two energy terms are of comparable magnitude as $n \rightarrow \infty$. In general, this minimal configuration gives the *mean eigenvalue density profile* for the random matrix ensemble defined by the potential Q . For $Q(\lambda) = \lambda^2$, the minimizing configuration is the Wigner semicircle law.

Remarkably, the same Coulomb gas ensemble also plays a central role in the $n \rightarrow \infty$ asymptotics of orthogonal polynomials [25]. The easiest way to see this is through the following explicit formula for the orthogonal polynomials $p_n(\omega)$ with respect to the weight function $e^{-Q(\omega)}$:

$$p_n(\omega) \propto \int \cdots \int \left(\prod_{i=1}^n (\omega - \omega_i) \right) P_Q(\omega_1, \dots, \omega_n) d\omega_1 \cdots d\omega_n, \quad (20)$$

where the probability density $P_Q(\omega_1, \dots, \omega_n)$ was defined in Eq. (16). In other words, $p_n(\omega)$ can be expressed as an average over all degree- n polynomials, weighted by the *same* probability measure as that which governed the eigenvalue distribution of the random matrix ensemble defined by the potential Q . In this context, the minimal energy configuration of the charge- n Coulomb gas—which we call $\sigma_n(\omega)$ —gives the *limiting density distribution of zeros* of the orthogonal polynomials with respect to $e^{-Q(\omega)}$. In our Riemann-Hilbert steepest descent analysis (Section S2), the support of this minimal energy configuration is analogous to the 'oscillatory region' of a WKB approximation, and yields the dominant contribution to the steepest descent problem as $n \rightarrow \infty$.

With the relevance of the Coulomb gas established, we can now discuss its confinement transition and the connection to quantum chaos. For systems with local interactions, one can show that the spectral function must decay at least exponentially as $|\omega| \rightarrow \infty$ [35–37], which translates, via Eq. (17), into the requirement that the potential $Q(\omega)$ grow at least linearly at large ω . This is enough to conclude that the Coulomb gas is always confined, in the sense that, for any finite n , the equilibrium Coulomb gas density $\sigma_n(\omega)$ has finite support. However, within the confined phase, there can be a further phase transition between 'weak confinement' and 'strong confinement' (see Fig. 2) [38–41]. These phases are distinguished by whether the Coulomb gas density is approximately uniform or not within the bulk of its support.

Importantly, the order parameter for this transition is the equilibrium density at *low frequencies*, $\sigma_n(\omega \approx 0)$. In the weakly confined phase, $\sigma_n(\omega)$ has an algebraic divergence as $\omega \rightarrow 0$, while in the strongly confined phase it is approximately constant there; at the critical point, there

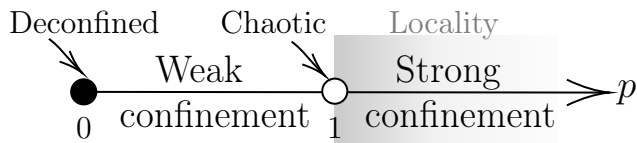


FIG. 2. Phase diagram of Coulomb gas confinement with a single-particle potential $Q(\omega)$, controlled by the large frequency decay of the spectral function $\Phi(\omega) \sim \exp[-Q(\omega)]$. Locality of the Hamiltonian forces the potential to grow polynomially at large ω , $Q(|\omega| \rightarrow \infty) \sim |\omega|^p$, with $p \geq 1$. The operator growth hypothesis [10] posits that chaotic systems generically have $p = 1$. A Coulomb gas with finite charge (i.e. finite n) is confined for all $p > 0$ since the two-particle repulsion is only logarithmic, while the potential is polynomial. However, there is a transition between ‘weak’ and ‘strong’ confinement at $p = 1$, precisely at the boundary imposed by locality. This has implications for numerical applications.

is instead a logarithmic divergence as $\omega \rightarrow 0$ (see Fig. 4 for an example). What is interesting is that, despite being diagnosed by the density near $\omega = 0$, the transition itself is primarily driven by the rate of *high frequency* decay of the spectral function. In particular, the weakly confined phase, the critical point, and the strongly confined phase, correspond to $\Phi(\omega \rightarrow \infty)$ decaying subexponentially, exponentially, and superexponentially respectively (Fig. 2). This critical exponential decay—the slowest possible decay consistent with locality [35–37]—coincides with the behavior that is expected to occur *generically* for chaotic systems with local interactions; this is the content of a recent conjecture in quantum chaos, the ‘Operator Growth Hypothesis’ (OGH) [10]. Thus, assuming the OGH, there is a sense in which chaotic systems are generically marginal. Since this confinement transition is related to the density of zeros of the orthogonal polynomials $p_n(\omega)$, which in turn govern the Lanczos operators O_n via Eq. (9), this marginality has implications for the computational efficiency of numerical applications, as we will discuss. One of our contributions (Lemma 2) is showing that this confinement phase structure is robust, in the sense that we prove it occurs for a wide class of spectral functions assuming only a fairly weak specification of how they decay at high frequencies (see Section S1 A).

Comparison with eigenstate thermalization

The main technical caveat to our work is that we also impose some regularity and analyticity conditions on $\Phi(\omega)$ in order to prove rigorous statements; we discuss this in detail in Section S1 A. But with these conditions in mind, let us discuss the relationship between the appearance of random matrix theory (RMT) in our work, and more familiar appearances of RMT in quantum many-body physics, namely through the eigenstate thermalization hypothesis (ETH) [42, 43]. The ETH postulates that the matrix elements of a local operator O in the energy

eigenbasis of a chaotic local Hamiltonian take the form

$$\langle E_m | O | E_n \rangle = O(\bar{E}) \delta_{mn} + e^{-S(\bar{E})/2} f_O(\bar{E}, \omega) R_{mn}, \quad (21)$$

where $\bar{E} \equiv (E_m + E_n)/2$, $\omega \equiv E_n - E_m$, and $S(\bar{E})$ is the thermodynamic entropy at energy \bar{E} . RMT appears through the entropic factor $e^{-S(\bar{E})/2}$ and the random matrix R , which is postulated to be distributed according to a Gaussian random matrix ensemble [43].

An important part of the ETH is that the functions $O(\bar{E})$ and $f_O(\bar{E}, \omega)$ are postulated to be *smooth* functions of their arguments. For our purposes, working in the thermodynamic limit, we do assume some smoothness properties of the spectral function $\Phi(\omega)$, which coincides with the function $|f_O(E_{av}, \omega)|^2$ at the average energy $E_{av} = \text{tr}[H]/\text{tr}[\mathbf{1}]$ of the infinite temperature state [43]. Therefore, arguably the most natural class of physical systems that one might expect to obey our assumptions about the spectral function are those that obey the ETH. However, the RMT universality we discuss in our work appears to be distinct in nature from the appearance of random matrix theory in the ETH, since it really owes itself to the *regularity* of spectral functions (and the consequence of that on the Lanczos orthogonal polynomials), which can be achieved even in non-ergodic single-particle and integrable systems. Indeed, we also find some evidence of this RMT universality in the integrable XXZ chain, where the presence of integrability should violate the ETH (although a weak version may persist [44]). Validity of the ETH may therefore be a sufficient but not necessary condition for the RMT universality we discuss here, but a fuller investigation of these connections is an important topic for future work.

Numerical application: the spectral bootstrap

The recursion method is a numerical technique based around the continued fraction representation for the full Green’s function $G(z)$; traditionally it requires one to make an educated guess for the functional form of the level- n Green’s function $G_n(z)$ [19]. Our approach allows us to rigorously derive the functional behavior of $G_n(z)$, showing how this changes for z in different regions of the complex plane (see Fig. 1). This provides a principled means of terminating the continued fraction and thereby approximating the full Green’s function $G(z)$.

We show how to use this control afforded by the large- n limit to produce an approximation of the spectral function $\Phi(\omega)$ using a finite number of Lanczos coefficients. Our focus is particularly on the low frequency behavior, and we show how to extract diffusion constants, as well as transport coefficients in models with nondiffusive transport, such as the isotropic Heisenberg model which has superdiffusive spin transport [45]. We also show how to generalize these ideas to finite frequencies. The simplest case is when the semicircle form for the level- n Green’s function $G_n(z)$ is valid at the target frequency, because

then only a single parameter, the frequency bandwidth β_n , needs to be specified in order to fully fix the semicircle Green's function—and β_n can be simply approximated from the Lanczos coefficients via $\beta_n = 2b_n[1 + \mathcal{O}(1/n)]$ (see Theorem 1). However, there are also more complicated cases, such as when $\Phi(\omega)$ has a low-frequency power-law, where an additional phase, arising from an integral over the Coulomb gas density, needs to be specified in order to approximate $G_n(z)$. This is the content of our ‘spectral bootstrap’ algorithm. It works by using the appropriate $n \rightarrow \infty$ asymptotics of the orthogonal polynomials $p_n(\omega)$ to formulate a first-order ordinary differential equation in frequency space involving the spectral function and the desired phase factor. Iteratively solving this ODE gives a finite- n approximation to the spectral function, using only the first n Lanczos coefficients as input.

One interesting aspect of this is that the convergence rate of this approximation at $\omega = 0$ is determined by a combination of the high- and low-frequency behavior of the spectral function $\Phi(\omega)$, owing to the manifestation of the Coulomb gas confinement transition in the Coulomb gas density at low frequencies. We show that the rate of convergence is $1/\text{poly}(n)$ when the spectral function $\Phi(\omega \rightarrow \infty)$ decays superexponentially, regardless of the low-frequency scaling of $\Phi(\omega)$. However, when $\Phi(\omega \rightarrow \infty)$ decays only (quasi-)exponentially—which is the case conjectured to be generic for chaotic quantum systems by the Operator Growth Hypothesis [10]—then the convergence rate is only $1/\text{poly}(\log n)$ if $\Phi(\omega \rightarrow 0) \sim |\omega|^\rho$ with $\rho \neq 0$. We recover $1/\text{poly}(n)$ scaling when $\rho = 0$, but this is likely a consequence of the fact that, for $\rho = 0$, our assumptions on $\Phi(\omega)$ amount to assuming analyticity at $\omega = 0$, i.e. that the correlation function $C(t)$ decays exponentially in time. We conjecture that when $0 < \Phi(0) < \infty$ but $\Phi(\omega)$ is not analytic at $\omega = 0$ due to hydrodynamic tails, then the convergence rate again reduces to $1/\text{poly}(\log n)$. However, despite this worst-case theoretical convergence, in practice we find that the spectral bootstrap can still often give surprisingly accurate estimates using only a modest number of Lanczos coefficients (see e.g. Fig. 8).

Marginality and quantum chaos

One curious aspect of this work concerns the connection between ‘marginality’ and chaotic operator dynamics. In our work the spectral function $\Phi(\omega)$ takes center stage, since it completely characterizes the Lanczos basis. In that role it functions mainly as the density of a measure $d\mu(\omega) = (\Phi(\omega)/2\pi)d\omega$ on \mathbb{R} , where it defines the particular set of orthogonal polynomials constructed by the Lanczos algorithm. Its origin in quantum operator dynamics is left somewhat implicit, entering only through constraints at high- and low-frequencies coming from considerations of locality and hydrodynamics.

Our numerical algorithm, the spectral bootstrap, gives one solution to the ‘spectral inverse problem’ of recovering the measure $\Phi(\omega)/2\pi$ from its moments (which

is equivalent to recovery from the Lanczos coefficients [46]). Relatedly, the ‘Hamburger moment problem’ asks whether there exists a measure μ generating a given set of moments, and if so whether this measure is unique [47]. If it is unique then we say the moment problem for μ is *determinate*, and if not then it is *indeterminate*. By definition it is then impossible to uniquely recover a measure from its moments if the corresponding moment problem is indeterminate. Crucially, it is well known that the moment problem is determinate for all measures which decay at least *exponentially* at infinity, meaning $\int_{\mathbb{R}} e^{c|x|} d\mu(x) < \infty$ for some $c > 0$ [48]. For example, the ‘Freud weights’ $d\mu(x) = \exp(-|x|^p)dx$ are determinate for $p \geq 1$ and indeterminate for $p < 1$ [48].

What seems curious is that this determinate-indeterminate boundary happens to be precisely where the Operator Growth Hypothesis (OGH) conjectures generic spectral functions of locally interacting quantum chaotic systems should fall, in the sense that they should generically have exponentially decaying spectral functions, $\Phi(\omega \rightarrow \infty) \sim \exp[-\mathcal{O}(\omega)]$ [10]. It is fitting, then, that in our spectral bootstrap algorithm we find that the error bounds at $\omega = 0$ decay increasingly slowly the slower the high-frequency decay of the spectral function, as discussed in the previous section. These error bounds control how large n must be to approximate $\Phi(\omega = 0)$ to a given precision ϵ , so we see that the inverse problem becomes increasingly difficult as the determinate-indeterminate boundary is approached, before becoming impossible (by definition) in the indeterminate regime.

Thus, according to the OGH, recovery of spectral functions of chaotic systems is *exponentially hard* in n as a function of the inverse precision $1/\epsilon$. From the vantage of the original operator growth problem, it is not so surprising that chaotic systems are hard to simulate; for example, it is known that the operator entanglement entropy generically grows linearly in time for chaotic systems [49], rendering tensor network descriptions challenging. But it is perhaps surprising that, in the context of the Lanczos algorithm, where entanglement entropy plays no obvious role, nonetheless the spectral theory should conspire so as to make this problem hard.

To be clear, in the context of this section, quantum chaos is a *sufficient but not necessary* condition for marginality. More generally the requirement for marginality is (quasi-)linear growth of Lanczos coefficients, and there are examples of non-chaotic systems exhibiting this growth, such as certain operators in many-body localized systems [50].

Relation to previous work

We note that the appearance of the Wigner semicircle law in the level- n Green's function $G_n(z)$ was recognized by Ref. [51], but only in the context of a *finite*-dimensional system where n is so large that the Lanczos coefficients have plateaued (typically this happens once n is of order

the system size), so they can utilize rigorous results from Ref. [29]. Our analysis is instead focused on interacting systems in the thermodynamic limit, where the Lanczos coefficients will generically grow indefinitely. We show that it is the $n \rightarrow \infty$ limit (i.e., not the plateau itself), which results in emergent random matrix universality. Besides the interpretational difference, this is relevant for numerical applications to interacting systems, where one will generically not see a plateau without incurring finite-size effects. We also show how the universal scaling form for $G_n(z)$ can be modified away from the Wigner semicircle law, the most prominent example being Bessel universality near $z = 0$ when the spectral function $\Phi(\omega)$ has a low-frequency power-law. Connections between the Lanczos algorithm and random matrix theory were also discussed in Ref. [52], but not with a focus on universality akin to that of eigenvalue correlations, as we discuss here. More generally, Ref. [53] gives a comprehensive review of quantum dynamics in Krylov space.

Future directions

Previously we saw that, in the Lanczos context, it is actually the high-frequency scaling of the spectral function $\Phi(\omega)$ that determines the computational difficulty of recovering $\Phi(\omega)$ at low frequencies. But it is often the case that one is principally interested in characterizing the low-frequency behavior of a system, say for computing hydrodynamic transport coefficients, and the accuracy of estimates of high-frequency properties are of lesser concern. That motivates studying potential modifications of the system's dynamics which cause $\Phi(\omega)$ to decay superexponentially as $\omega \rightarrow \infty$, thereby improving the error bound scaling, while ideally having minimal impact on $\Phi(\omega)$ near $\omega = 0$. One possibility is to use operator truncation approaches, such as in dissipaton-assisted operator evolution [5] and similar techniques. Provided the modification is such that the effective Liouvillian is still self-adjoint, then the Lanczos approach is valid; anything of the form $\mathcal{L}_{\text{eff}} = \mathcal{D}\mathcal{L}\mathcal{D}$ for some self-adjoint dissipator \mathcal{D} would suffice. Depending on the dissipator, this may also have the dual benefit of reducing the computational requirements to compute the Lanczos coefficients up to a given n , due to a suppression of operator trajectories.

All of the results in this paper concern operator dynamics generated by a time-independent and Hermitian Hamiltonian H . An obvious question is whether the notion of universality discussed in this paper can be generalized to other types of operator dynamics. For Floquet dynamics generated by a unitary U , this question is likely quite tractable, and will involve asymptotics of orthogonal polynomials on the unit circle [54], corresponding to the spectra of unitary operators (for related work see [55]). Where the situation is both less clear and possibly richer is that of open quantum system dynamics [56–60]. With dynamics generated by a Lindbladian \mathcal{L} with nontrivial jump operators, the spectrum of \mathcal{L} now generically lies in

the complex plane, so the analysis will now involve polynomials orthogonal on the plane rather than on a contour. This is a much less well-developed field [61, 62], and it is an exciting task to examine whether there can be new types of universality in open system operator dynamics.

One of our main results is the appearance of the Wigner semicircle law in the level- n Green's function $G_n(z)$ describing the dynamics restricted to the ‘fast space’ $\{O_m\}_{m \geq n}$. One can heuristically argue for this result using the recursion relation Eq. (79) between $G_n(z)$ and $G_{n+1}(z)$, where the Wigner semicircle appears as a fixed point (see Section VI). This recursion bears some resemblance to the R -transform from free probability [63], but ‘deformed’ by the ratio b_{n+1}/b_n . Recently, the language of free probability was used to generalize the eigenstate thermalization hypothesis (ETH) to higher-order correlation functions [64, 65]. It is an interesting topic for future work to explore potential connections between universality in Lanczos dynamics and the generalized ETH.

Acknowledgements

We thank Alexander Avdoshkin, Xiangyu Cao, Pieter Claeys, Fabian Essler, Michael Flynn, Jorge Kurchan, Jean-Bernard Lasserre, Doron Lubinsky, Sheehan Olver, Daniel Parker, and Gabriele Pinna for helpful discussions. Some of the numerical computations were performed using King's College London's CREATE cluster [66]. O.L. was supported by EPSRC through grant number EP/Y005058/2. K.M. gratefully acknowledges the support of a Royal Society Wolfson Fellowship (grant number: RSWVF/R2/212003). C.vK. was supported by a UKRI FLF through MR/T040947/1, MR/T040947/2 and MR/Z000297/1.

CONTENTS

I. Introduction	1	C. Riemann-Hilbert problem for U	43
II. Synopsis	1	D. Equilibrium measures for complex log-Freud weights	44
Emergent universality in the $n \rightarrow \infty$ limit	3	E. Logarithmic transform of the equilibrium measure, and the Riemann-Hilbert problem for T	46
Orthogonal polynomials and large- n expansions	3	F. Analytic continuation of the equilibrium measure and its logarithmic transform	47
Lanczos dynamics and random matrix universality	4	G. Riemann-Hilbert problem for S : contour deformation and ‘opening the lens’	48
Coulomb gas confinement transition, quantum chaos, and the operator growth hypothesis	5	H. Parametrix N for the outside region	49
Comparison with eigenstate thermalization	6	I. Local parametrix P near the endpoints $z = \pm 1$	50
Numerical application: the spectral bootstrap	6	J. Local parametrix P near the origin	54
Marginality and quantum chaos	7	K. Riemann-Hilbert problem for R	59
Relation to previous work	7	S3. Extracting the recurrence coefficients: proof of Theorem 1	62
Future directions	8	A. Reversing the transformations	62
Acknowledgements	8	B. Recurrence coefficients from residue calculus	62
III. Background	10	C. Scaling of the leading coefficient y_n	65
IV. Hydrodynamic contributions to the Lanczos coefficients	11	S4. Asymptotics of the orthogonal polynomials	66
A. Coulomb gas, universality, and confinement	12	A. Behavior near the origin	66
V. Hydrodynamics from the zero mode	16	B. Expressions for the spectral bootstrap	68
A. Extracting the low frequency power-law	16	C. Level- n Green’s function	71
B. Extracting hydrodynamic transport coefficients	17	S5. Airy bootstrap	74
VI. Universality of the level- n Green’s function	19	S6. Detailed analysis of the equilibrium measure	76
A. Frequencies in the bulk	20	A. Behavior of the equilibrium measure near the origin	76
B. Frequencies near $\omega = 0$	21	B. Uniform lower bounds for the equilibrium measure on the real line	79
C. Frequencies near the edges $\omega = \pm\beta_n$	21	C. Behavior of the equilibrium measure near the endpoints	81
VII. The spectral bootstrap: approximating the spectral function at finite frequencies	22	D. Decay of contributions from the lens boundaries	83
A. The bulk bootstrap: $\rho = 0$	22	Glossary of Symbols	85
B. Generalization to arbitrary ρ : the Bessel bootstrap	25		
VIII. Random matrix universality	27		
A. Background	27		
B. Universality in quantum operator dynamics	28		
C. Scaling of the equilibrium measure	31		
References	32		
S1. Class of spectral functions (weights)	36		
A. Definition of potentials	36		
B. Comments on analyticity requirements	37		
C. Properties of log-Freud weights	38		
S2. Riemann-Hilbert steepest descent analysis	42		
A. Fundamental Riemann-Hilbert problem for Y	42		
B. Proof overview	43		

III. BACKGROUND

A time-evolved operator $A(t) := e^{iHt} A e^{-iHt}$ can be expanded as a sum of nested commutators,

$$e^{iHt} A e^{-iHt} = A + it[H, A] + \frac{(it)^2}{2!} [H, [H, A]] + \dots \quad (22)$$

This suggests that if we want to understand the growth of $A(t)$, a natural object to study is the *Krylov space* $\mathcal{K} := \text{span}\{\mathcal{L}^k(A)\}_{k=0}^\infty$, where $\mathcal{L}(\cdot) := [H, \cdot]$ is the Liouvillian superoperator. To probe this space, it is convenient to construct an orthonormal basis for \mathcal{K} using the Gram-Schmidt process. When \mathcal{L} is self-adjoint, this reduces to the *Lanczos algorithm*, where successive basis vectors for \mathcal{K} can be defined by a recurrence relation containing only three terms, rather than all previous basis vectors. We will use a vector notation $|A\rangle$ for operators, and for now we take the inner product to be the Hilbert-Schmidt product $\langle A|B\rangle := \text{tr}[A^\dagger B] / \text{tr}[\mathbf{1}]$, so we are effectively working at infinite temperature. Starting with a self-adjoint operator $|A\rangle$, we initialize the recurrence with $|O_{-1}\rangle := 0$ and $|O_0\rangle := b_0^{-1}|A\rangle$, where $b_0 := \sqrt{\langle A|A\rangle} \equiv \|A\|$. Then we recursively define

$$|A_n\rangle := \mathcal{L}|O_{n-1}\rangle - b_{n-1}|O_{n-2}\rangle, \quad (23a)$$

$$b_n := \sqrt{\langle A_n|A_n\rangle}, \quad (23b)$$

$$|O_n\rangle := b_n^{-1}|A_n\rangle. \quad (23c)$$

We will refer to the basis $\{|O_n\rangle\}_{n=0}^\infty$ as the *Lanczos basis*, and throughout will consider the generic case where \mathcal{K} is infinite-dimensional in the thermodynamic limit.

As well as the basis vectors themselves, the Lanczos algorithm produces a sequence of numbers $\{b_n\}_{n=1}^\infty$ which we will interchangeably refer to as the *recurrence* or *Lanczos coefficients*. It turns out that these numbers are enough to fully characterize the action of \mathcal{L} within \mathcal{K} ; indeed, the restriction $\mathcal{L}_\mathcal{K}$ of \mathcal{L} to \mathcal{K} can be represented in the Lanczos basis by a tridiagonal matrix

$$\mathcal{L}_\mathcal{K} = \begin{pmatrix} 0 & b_1 & 0 & 0 & \dots \\ b_1 & 0 & b_2 & 0 & \dots \\ 0 & b_2 & 0 & b_3 & \dots \\ 0 & 0 & b_3 & 0 & \ddots \\ \vdots & \vdots & \vdots & \ddots & \ddots \end{pmatrix}. \quad (24)$$

That the diagonal elements are all zero is a generic consequence of *Hermiticity*, since $\langle O|\mathcal{L}|O\rangle = 0$ follows for any self-adjoint O simply by using the definition $\mathcal{L}(\cdot) = [H, \cdot]$ with self-adjoint H , and inductively one can show that $i^n O_n$ is self-adjoint.

The tridiagonal form lends itself to interpreting $\mathcal{L}_\mathcal{K}$ as a tight-binding model on a semi-infinite chain, where the sites are the operators $\{O_n\}_{n=0}^\infty$, and the hopping strengths are the recurrence coefficients $\{b_n\}_{n=1}^\infty$. We can visualize the operator evolution $A(t)$ as a single-particle problem, with a wavefunction initially localized on site

$n = 0$ of the chain, which then spreads out along the chain over time. The autocorrelation function $C(t) := \langle A|A(t)\rangle$ corresponds to the probability amplitude for the operator wavefunction to be found back at its starting point at time t .

The *spectral function* $\Phi(\omega)$ defined as

$$\Phi(\omega) := \int_{\mathbb{R}} e^{-i\omega t} C(t) dt, \quad (25)$$

plays a significant role in the Lanczos algorithm. In particular, the Lanczos algorithm has a natural formulation in terms of the *orthogonal polynomials* with respect to the weight function $w(\omega) = \Phi(\omega)/2\pi$. To see this, we start from

$$C(t) = \langle A|e^{i\mathcal{L}t}|A\rangle = \int_{\mathbb{R}} e^{i\omega t} \frac{\Phi(\omega)}{2\pi} d\omega, \quad (26)$$

and evaluate the k th derivative with respect to t at $t = 0$. Assuming $\Phi(\omega)$ decays sufficiently quickly as $|\omega| \rightarrow \infty$ (more on this later), this gives

$$\langle A|\mathcal{L}^k|A\rangle = \int_{\mathbb{R}} \omega^k \frac{\Phi(\omega)}{2\pi} d\omega. \quad (27)$$

Since \mathcal{L} has real spectrum, $\omega_{ij} = E_i - E_j$, if we then define the inner product between real polynomials $p, q: \mathbb{R} \rightarrow \mathbb{R}$

$$\langle p, q \rangle := \langle p(\mathcal{L})A|q(\mathcal{L})A \rangle, \quad (28)$$

one can use linearity of the inner product and Eq. (27) to write this as

$$\langle p, q \rangle = \int_{\mathbb{R}} p(\omega)q(\omega) \frac{\Phi(\omega)}{2\pi} d\omega, \quad (29)$$

so, as claimed, $\Phi(\omega)/2\pi$ appears as the relevant weight function. A defining property of orthonormal polynomials with respect to an even weight function on \mathbb{R} is that they obey a three-term recursion relation of the form [46, 67]

$$b_n p_n(\omega) = \omega p_{n-1}(\omega) - b_{n-1} p_{n-2}(\omega). \quad (30)$$

Comparing this to the Lanczos recursion relation, we deduce that the n th Lanczos vector $|O_n\rangle$ is given by

$$|O_n\rangle = p_n(\mathcal{L})|A\rangle, \quad (31)$$

where $p_n(\omega) = y_n \omega^n + \dots$, $y_n > 0$, is the n th order orthonormal polynomial with respect to the inner product Eq. (28) [68, 69]. Thus, by studying the orthogonal polynomials with respect to the spectral function $\Phi(\omega)/2\pi$, we can understand properties of the Lanczos operators.

Note that this argument is very general, so that we can also easily apply it to operator inner products other than the Hilbert-Schmidt product. In particular, at finite temperature, we can consider the following family of inner products [19]

$$\langle A|B\rangle_\beta^g := \frac{1}{\beta} \int_0^\beta g(\lambda) \langle A^\dagger e^{-\lambda H} B e^{\lambda H} \rangle_\beta d\lambda - \langle A^\dagger \rangle_\beta \langle B \rangle_\beta, \quad (32)$$

where $\langle B \rangle_\beta = \text{tr}[e^{-\beta H} B] / \mathcal{Z}$ is a thermal expectation value, $\mathcal{Z} = \text{tr}[e^{-\beta H}]$ is the partition function, and $g(\lambda)$ is any function defined on the thermal circle $[0, \beta]$ satisfying

$$g(\lambda) \geq 0, \quad g(\beta - \lambda) = g(\lambda), \quad \frac{1}{\beta} \int_0^\beta g(\lambda) d\lambda = 1.$$

One can then perform a version of the Lanczos algorithm where operators are orthogonal with respect to this inner product. Examples include $g(\lambda) = [\delta(\lambda) + \delta(\lambda - \beta)]/2$ for linear response, and the Wightman product $g(\lambda) = \delta(\lambda - \beta/2)$. The autocorrelation function and spectral function are then $C_\beta^g(t) := (A|A(t))_\beta^g$ and $\Phi_\beta^g(\omega) := \int_{-\infty}^\infty e^{-i\omega t} C_\beta^g(t) dt$, and the polynomial inner product defined by $\langle p, q \rangle_\beta^g := (p(L^\dagger)A|q(L)A)_\beta^g$ can be written as

$$\langle p, q \rangle_\beta^g = \int_{-\infty}^\infty p(\omega)q(\omega) \frac{\Phi_\beta^g(\omega)}{2\pi} d\omega, \quad (33)$$

with the generalized spectral function $\Phi_\beta^g(\omega)/2\pi$ again appearing as the weight function. Since all our work is premised on assumptions made about the spectral function, we expect our conclusions to hold not only at infinite temperature, but also at high enough finite temperatures, given a suitable choice of inner product.

IV. HYDRODYNAMIC CONTRIBUTIONS TO THE LANCZOS COEFFICIENTS

We saw in Section III that the spectral function $\Phi(\omega) := \int_{\mathbb{R}} e^{-i\omega t} C(t) dt$ determines all the properties of the Lanczos basis. However, for a given interacting many-body Hamiltonian H , we do not generally have a hope of exactly calculating $\Phi(\omega)$. Instead, the approach we will take is to impose a few physically motivated conditions on $\Phi(\omega)$, and study their implications.

1. We take $\Phi(\omega) = \Phi(-\omega)$ to be an *even* function. This is true because at infinite temperature we have $C(-t) = C(t)$ for Hermitian H and Hermitian A , so its Fourier transform satisfies $\Phi(-\omega) = \Phi(\omega)^*$. Then $\Phi(\omega) = \Phi(-\omega)$ follows because $\Phi(\omega)$ is real, which is clear from its spectral decomposition.
2. We fix the $|\omega| \rightarrow \infty$ behavior of $\Phi(\omega)$, taking it to decay at least exponentially in $|\omega|$. This is provably true at high temperatures for *local* lattice Hamiltonians with a bounded local Hilbert space [35–37], and forms part of the motivation for the operator growth hypothesis [10].
3. Since we are interested in signatures of the $|t| \rightarrow \infty$ behavior of $C(t)$, we impose a condition on the $\omega \rightarrow 0$ behavior of its Fourier transform $\Phi(\omega)$. To model $C(t) \sim 1/|t|^{1+\rho}$ as $|t| \rightarrow \infty$, we require $\Phi(\omega) \sim |\omega|^\rho$ as $\omega \rightarrow 0$. Such power-law decay in $C(t)$ is typical if the initial operator overlaps with a conserved quantity with sufficiently slow transport, say diffusive [18].

Since $\Phi(\omega) \geq 0$ and is even, we can always write it in the form $\Phi(\omega) \equiv \exp[-Q(\omega)]$ for some even real-valued function $Q(\omega)$. However, since we are interested in hydrodynamic spectral functions, which typically have an algebraic divergence $\Phi(\omega) \sim |\omega|^\rho$ as $\omega \rightarrow 0$, it will prove helpful to factorize out this divergence, and decompose $\Phi(\omega)$ as

$$\Phi(\omega)/2\pi \equiv |\omega|^\rho e^{-Q(\omega)}. \quad (34)$$

In principle $\Phi(\omega)$ may also have algebraic behavior near other frequencies, in which case we would also factorize those out [27]. But for simplicity we will focus on the case where there is only an algebraic divergence at $\omega = 0$. The function $Q(x)$ so defined is called the *potential* (we will later make precise the sense in which this is a potential). We can impose the $|\omega| \rightarrow \infty$ condition on $\Phi(\omega)$ by asking that, for large enough ω , $Q(\omega)$ is positive and grows at least linearly with ω . We also ask that $Q(\omega)$ is smooth near $\omega = 0$ so as not to interfere with the power-law $|\omega|^\rho$, and more generally is finite at finite ω ; this requires assuming $\Phi(\omega) > 0$, which should be generically true for interacting systems.

Our first main result, Theorem 1, is a statement about the recurrence coefficients $\{b_n\}$ associated with spectral functions of the form in Eq. (34). It is an asymptotic statement, controlled in the limit $n \rightarrow \infty$ of large Lanczos number. This limit is analogous to the large matrix dimension limit in random matrix theory [25], and similarly will lead to universal behavior.

Our results are valid for a wide class of potentials Q which obey a few conditions. In particular, we consider potentials which, for some exponents $p \geq 1, q \in \mathbb{R}$, grow as $|\omega| \rightarrow \infty$ like

$$|\omega|^p (\log |\omega|)^{q-\epsilon} \leq Q(\omega) \leq |\omega|^p (\log |\omega|)^{q+\epsilon}, \quad (35)$$

where ϵ can be taken to zero as $|\omega| \rightarrow \infty$. We will informally write this as $Q(\omega) \sim |\omega|^p \log^q |\omega|$, and give a formal definition in Section S1 A. The constraint that $p \geq 1$ is a translation of the bound that $\Phi(\omega)$ must decay at least exponentially, given local Hamiltonian dynamics [35]. We include the possibility of a log-correction ($q \neq 0$) to Q to account for the fact that the exponential bound on $\Phi(\omega)$ receives a log-correction ($q = 1$) in one spatial dimension, owing to geometric constraints on operator growth not present in higher dimensions [10, 35].

It is well established that the scaling of $\Phi(\omega)$ as $|\omega| \rightarrow \infty$ determines the *leading* behavior of the b_n as $n \rightarrow \infty$ [70]. What we show in Theorem 1 is that the hydrodynamic power-law imprints itself on the *subleading* behavior of b_n in a universal manner. Some of the quantities appearing in the theorem, namely β_n and $h_n(x)$, are defined in terms of a classical Coulomb gas problem we will introduce in the next section. The reason for studying this Coulomb gas is that it controls the location of the dominant contributions to the recurrence coefficients.

Theorem 1 (Informal). Consider $\Phi(\omega)/2\pi \equiv |\omega|^\rho \exp[-Q(\omega)]$, where $\rho > -1$, and Q is an even function scaling like $Q(\omega) \sim |\omega|^p \log^q |\omega|$ as $|\omega| \rightarrow \infty$, for some $p \geq 1$ and $q \in \mathbb{R}$. Further assume that $Q(\omega)$ is ‘smooth enough’ (see discussion below). Then the recurrence coefficients b_n associated with $\Phi(\omega)$ have a large- n expansion given by

$$b_n = \frac{\beta_n}{2} \left[1 + \rho \left(\frac{1}{h_n(1)} - (-1)^n \frac{1}{h_n(0)} \right) \frac{1}{n} + \dots \right], \quad (36)$$

where the scaling of β_n is given in Eq. (44), the scaling of $h_n(1)$ and $h_n(0)$ are given in Lemmas 1 and 2, and the dots indicate terms subleading in n .

The case $p = 1$ of (quasi-)exponential decay—most relevant for generic chaotic systems according to the operator growth hypothesis [10]—turns out to be marginal, with the above expression simplifying to

$$b_n = \frac{\beta_n}{2} \left[1 + \frac{\rho}{2} \left(1 - (-1)^n \frac{1}{(\log n)^{1+o(1)}} \right) \frac{1}{n} + \dots \right], \quad (37)$$

provided $q > -1$. (Local interactions enforce $q \geq 0$.)

If $p > 1$, then this expression instead simplifies to

$$b_n = \frac{\beta_n}{2} \left[1 + \frac{\rho}{2p} \left(1 - (-1)^n (p-1) \right) \frac{1}{n} + \dots \right], \quad (38)$$

for all $q \in \mathbb{R}$.

The requirement that Q is ‘smooth enough’ is the main technical caveat to our results; we explain what we mean by this in Section S1 A. This theorem is proved in Section S3, with the scaling of the \dots error term discussed in Section S3 B 5.

This theorem shows that the hydrodynamic power-law, $\Phi(\omega) \sim |\omega|^\rho$ as $\omega \rightarrow 0$, shows up as a *multiplicative correction* to the leading scaling governed by β_n , whose scaling depends only on the $|\omega| \rightarrow \infty$ asymptotics via Eq. (44). The subleading hydrodynamic term displays *staggering* due to the factor $(-1)^n$, but the magnitude of the staggering decays to zero as $n \rightarrow \infty$. Many authors have noted examples where such staggering is sufficient to give singular $\omega \rightarrow 0$ behavior [19, 71–77]. Our result proves in a wide class of models that this staggering *necessarily* arises from the low-frequency behavior. Hermiticity is an important ingredient in producing the specific $(-1)^n$ form: it enters in the proof via the identity

$$(-1)^n = \exp \left(2\pi i \int_0^{\beta_n} \sigma_n(\omega) d\omega \right), \quad (39)$$

where $\sigma_n(\omega)$ is the charge density of a Coulomb gas distribution that we will define more fully in Section IV A. This identity follows very generically by symmetry, since the distribution has total charge n by construction, $\int_{-\beta_n}^{\beta_n} \sigma_n(\omega) d\omega = n$, and $\sigma_n(\omega)$ is *even*, the latter com-

ing from the evenness of the spectral function, which is a property of Hermitian systems. Thus we have $\int_0^{\beta_n} \sigma_n(\omega) d\omega = n/2$, giving the staggering factor $(-1)^n$. It is also worth emphasizing that this is a contribution from the $\omega = 0$ behavior of the spectral function; that is why the lower limit of the integral in Eq. (39) is zero. This $(-1)^n$ staggering factor also has the same origins as the sign of the polynomials at zero, $\text{sgn}[p_{2n}(0)] = (-1)^n$ (c.f. Eq. (57)), which again is a generic property of even weight functions [67].

Notice that the case $p = 1$ is marginal, in the sense that the staggered multiplicative correction associated with the hydrodynamics scales like $1/n \log n$, rather than $1/n$ for $p > 1$. This is a signature of the Coulomb gas confinement transition discussed in Section IV A. This transition is primarily a consequence of the *high frequency* scaling of the spectral function, but it affects the hydrodynamic signature because of its manifestation in a logarithmically divergent equilibrium charge density at *low frequencies*.

We emphasize that the operator growth hypothesis [10] conjectures that chaotic many-body quantum systems generically have $p = 1$, and so are marginal in this sense. The possibility of a log-correction for $p = 1$ was noted in [75]. Note that $p = 1$ scaling is not restricted to chaotic models—certain many-body localized models have been shown to also exhibit this scaling (with a $q = 1$ log-correction) [50]. There is numerical evidence that the case $p = 2$, corresponding to $b_n \sim \sqrt{n}$, holds for interacting integrable systems at infinite temperature [10, 19, 78, 79]. We can also consider non-interacting systems as the limit $p \rightarrow \infty$, such that $b_n \sim n^0$ and the spectral function has compact support (see [80, Theorem 7.4]).

It is tempting to extract the value of ρ by fitting the Lanczos coefficients to the relevant asymptotic form given in Theorem 1. In practice, we have found that, while this method gives qualitatively correct answers for ρ , it tends to give rather large error bars, since one is attempting to fit the coefficient of a small subleading correction. Instead, we recommend following the procedure outlined in Section V A for extracting ρ from the leading scaling of the zero mode in the Krylov space, which amplifies the effects of the staggered subleading term coming from the low-frequency power-law.

Example 1. As a check of Theorem 1, we can consider the generalized Hermite polynomials, which have weight function $\Phi(\omega)/2\pi = |\omega|^\rho \exp[-\omega^2]$. With $Q(\omega) = \omega^2$, we can determine $\beta_n = \sqrt{2n}$ from Eq. (43), and $h_n(0) = h_n(1) = 4$ from Eq. (51) (in agreement with Lemmas 1 and 2 with $p = 2$). Substituting into Theorem 1, we get agreement to $\mathcal{O}(1/n)$ with the exact recurrence coefficients, which are known to be $b_n = \frac{1}{\sqrt{2}} \sqrt{n + \frac{1}{2} [1 - (-1)^n] \rho}$ [81].

A. Coulomb gas, universality, and confinement

Now let us explain the Coulomb gas problem which played a role in Theorem 1. As outlined in Section II,

this Coulomb gas arises naturally both in the context of random matrix theory and orthogonal polynomials, and finding the minimum energy Coulomb gas configuration will give us a handle on the regions which dominantly contribute to the Lanczos coefficients.

Given a potential $Q(\omega)$ determined from the spectral function by Eq. (34), we define a Coulomb gas energy functional E_Q as follows. We take as input a charge density function $\sigma : \mathbb{R} \rightarrow \mathbb{R}_{\geq 0}$ (defined on frequency space), and give it an energy consisting of two terms,

$$E_Q[\sigma] := - \int_{\mathbb{R}} \int_{\mathbb{R}} \log |\omega_1 - \omega_2| \sigma(\omega_1) \sigma(\omega_2) d\omega_1 d\omega_2 \quad (40)$$

$$+ \int_{\mathbb{R}} Q(\omega) \sigma(\omega) d\omega,$$

namely a logarithmic repulsion between charges, and a single-particle energy determined by the potential Q . For a given Lanczos index n , we imagine distributions with total charge n , so that $\int_{\mathbb{R}} \sigma(\omega) d\omega = n$. We then want to consider the distribution σ_n with charge n that minimizes the energy $E_Q[\sigma]$, so that

$$\sigma_n := \operatorname{argmin}_{\sigma} \left\{ E_Q[\sigma] : \int_{\mathbb{R}} \sigma(\omega) d\omega = n \right\}. \quad (41)$$

We will refer to σ_n as the *equilibrium density*. For large enough n , one can show that σ_n is indeed uniquely defined and continuous under reasonable assumptions on Q [82]. Let us make a few observations about this equilibrium density. Since the potential $Q(x)$ must grow at least linearly for $|x| \rightarrow \infty$ due to constraints from locality, while the two-particle repulsion is only logarithmic, we conclude that for any finite n , the charge will remain at a finite distance from the origin. This means that $\sigma_n(\omega)$ has support within some finite interval we denote by

$$\operatorname{supp} \sigma_n \equiv (-\beta_n, \beta_n), \quad (42)$$

which we refer to as the ‘bulk’. This distribution is even, $\sigma_n(-\omega) = \sigma_n(\omega)$, because Q is even. As $n \rightarrow \infty$ the density $\sigma_n(\omega)$ gives the density of zeros of the orthogonal polynomials with respect to the weight $e^{-Q(\omega)}$ [82], and the dominant contribution to the recurrence coefficients will come from this bulk frequency range $(-\beta_n, \beta_n)$. This interval is analogous to the oscillatory region in a WKB approximation [22, 83]. Note that, for technical convenience, we do not include the power law $|\omega|^\rho$ in the Coulomb gas potential, instead handling it by other means (Szegő functions).

The distance β_n is referred to as the *n*th *Mhaskhar-Rakhmanov-Saff* (MRS) number [82, 84, 85], and is defined for even Q as the positive solution to the integral equation

$$\frac{1}{2\pi} \int_{-1}^1 \frac{\beta_n s Q'(\beta_n s)}{\sqrt{1-s^2}} ds = n. \quad (43)$$

This solution is unique for large enough n . How does β_n scale with n ? Clearly, the slower the growth of the single-particle potential Q , the more the charge will spread out.

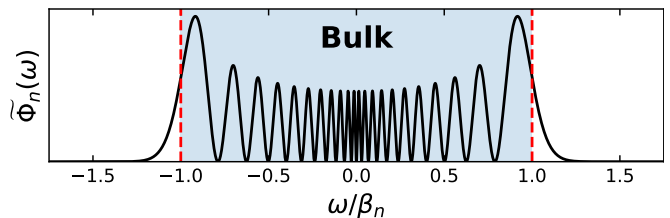


FIG. 3. The n th spectral function $\tilde{\Phi}_n(\omega) = p_n(\omega)^2 \Phi(\omega)$ for the toy spectral function $\Phi(\omega)/2\pi = \operatorname{sech}(\pi\omega)$ and $n = 20$. This governs the dynamics of O_n with respect to the *full* Liouvillian \mathcal{L} , not the restricted Liouvillian \mathcal{L}_n (see Fig. 7 for the latter). In this case $\beta_n \approx \sqrt{n(n-1)}$ [86], with the linear scaling $\beta_n \sim \mathcal{O}(n)$ reflecting the exponential decay of $\Phi(\omega \rightarrow \infty)$. One can see that $\tilde{\Phi}_n(\omega)$ is peaked near $|\omega| = \beta_n$, and as $n \rightarrow \infty$ this becomes increasingly sharp. The region $|\omega| \leq \beta_n$ is referred to as the ‘bulk’, and is analogous to the oscillatory region in a WKB approximation. For $|\omega| \gg \beta_n$, $\tilde{\Phi}_n(\omega)$ is exponentially small. When $\Phi(\omega \rightarrow 0) \sim |\omega|^\rho$ has a power-law at $\omega = 0$, the orthogonal polynomials $p_n(\omega)$ behave differently near the origin (see e.g. Theorem 2).

It turns out that the growth of Q and β_n are related by

$$Q(\omega) \sim |\omega|^p \log^q |\omega| \text{ as } |\omega| \rightarrow \infty \quad (44)$$

$$\Downarrow$$

$$\beta_n \sim \left(\frac{n}{\log^q n} \right)^{1/p} \text{ as } n \rightarrow \infty.$$

It is straightforward to verify this scaling when Q is literally a polynomial, e.g. $Q(\omega) = \omega^{2m}$, but it continues to hold when $Q(\omega)$ is sufficiently ‘polynomial-like’ as $|\omega| \rightarrow \infty$ (see Lemma S1). The locality constraint on Q translates into $p \geq 1$, so that β_n grows at most linearly in local systems. It is well known, as we will see in Theorem 1, that the scaling of β_n fixes the leading behavior of the recurrence coefficients b_n , which are given by $b_n \approx \beta_n/2$ to leading order in n [70]. Note that by construction β_n depends only on Q and so is independent of the hydrodynamic exponent ρ , so the hydrodynamics will only show up at *subleading* orders in the recurrence coefficients.

One way to understand the MRS number β_n is as an n -dependent frequency bandwidth. From Eq. (43) it is easy to see that if we introduce a frequency scale ω_0 by mapping $Q(\omega) \mapsto Q(\omega/\omega_0)$, then β_n transforms as $\beta_n \mapsto \omega_0 \beta_n$, so β_n indeed has units of frequency. Furthermore, if we consider the spectral function $\tilde{\Phi}_n(\omega) := \int_{\mathbb{R}} e^{-i\omega t} \langle O_n | e^{i\mathcal{L}t} | O_n \rangle dt$ for the dynamics of the n th Lanczos operator O_n under the full Liouvillian \mathcal{L} , then from Eq. (31) we can see that this is related to the original spectral function by

$$\tilde{\Phi}_n(\omega) = p_n(\omega)^2 \Phi(\omega). \quad (45)$$

(Note $\tilde{\Phi}_n(\omega)$ is not to be confused with the spectral function $\Phi_n(\omega)$ related to $G_n(z)$; they correspond to dynamics generated by \mathcal{L} and \mathcal{L}_n respectively). A remarkable result

due to Mhaskar and Saff [87] shows that, under certain conditions on Q , the MRS number β_n provides an asymptotically sharp characterization of where this weighted polynomial is peaked, so $\operatorname{argmax}_{\omega \geq 0} \tilde{\Phi}_n(\omega) \xrightarrow{n \rightarrow \infty} \beta_n$. One can understand the scaling in Eq. (44) as coming from the tradeoff between the growth of the degree $2n$ polynomial $p_n(\omega)^2$ and the decay of the spectral function $\Phi(\omega \rightarrow \infty) \sim \exp[-\mathcal{O}(\omega^p \log^q \omega)]$. Physically, β_n therefore represents the frequency bandwidth over which the n th spectral function $\tilde{\Phi}_n(\omega)$ is non-negligible. For frequencies $|\omega| \gg \beta_n$, $\tilde{\Phi}_n(\omega)$ will be exponentially small (see Fig. 3 for an example); this region is analogous to the ‘classically forbidden’ region in a WKB analysis, and will give only exponentially small contributions to the Lanczos coefficients.

Given a minimizing density distribution σ_n , it is helpful to define a related distribution

$$\psi_n(x) := \frac{\beta_n}{n} \sigma_n(\beta_n x), \quad (46)$$

which is normalized to 1 and has support $[-1, 1]$. We refer to ψ_n as the rescaled equilibrium density. It is the energy minimizing distribution with charge 1 for the ‘rescaled potential’

$$V_n(x) := \frac{1}{n} Q(\beta_n x). \quad (47)$$

The rescaling by β_n in the definition of V_n washes out the non-universal details of Q when n is large. For example, for the class of potentials we consider, if $Q(x) \sim x^p$ as $x \rightarrow \infty$, then for any finite x we have

$$\lim_{n \rightarrow \infty} V_n(x) = \kappa_p |x|^p, \quad (48)$$

where $\kappa_p = \Gamma[\frac{1}{2}] \Gamma[\frac{p}{2}] / \Gamma[\frac{p+1}{2}]$ [88, Lemma 3.2]. This emergent dominance of the high frequency scaling means that the equilibrium density $\psi_n(x)$ has several displays of *universality* in the $n \rightarrow \infty$ limit, with the same properties as if the potential were the corresponding ‘Freud potential’ $Q^{(p)}(x) \equiv \kappa_p |x|^p$. These potentials have $\beta_n = n^{1/p}$, and an equilibrium measure given by the ‘Ullman distribution’ [82]

$$\psi^{(p)}(x) := \frac{1}{\pi} \int_{|x|}^1 \frac{pu^{p-1}}{\sqrt{u^2 - x^2}} du. \quad (49)$$

One simple manifestation of this is that, quite generally, the density $\psi_n(x)$ vanishes like $\sqrt{1-x^2}$ at the endpoints $x = \pm 1$; this has a manifestation in the famous Wigner semicircle law of random matrix theory [30], but holds near the edge more generally beyond Gaussian ensembles. Other universal properties of the equilibrium Coulomb gas distribution are more easily stated in terms of a function $h_n(x)$ defined by

$$\psi_n(x) =: \frac{1}{2\pi} h_n(x) \sqrt{1-x^2}, \quad (50)$$

for $x \in [-1, 1]$. The values of $h_n(x)$ at $x = 0$ and $x = 1$ appeared in Theorem 1 describing hydrodynamic corrections to the Lanczos coefficients.

For large enough n (but $\mathcal{O}(1)$ in terms of the microscopic couplings), we show that the minimum energy configuration of E_Q is obtained when $h_n(x)$ is given by

$$h_n(x) = \frac{1}{\pi} \int_{-1}^1 \frac{V'_n(s) - V'_n(x)}{s-x} \frac{ds}{\sqrt{1-s^2}}. \quad (51)$$

We then show that $h_n(x)$ displays universal behavior at the origin $x = 0$ and the endpoints $x = \pm 1$, similar to that of the Ullman distribution Eq. (49). This behavior depends only on the $|\omega| \rightarrow \infty$ behavior of Q , provided it is sufficiently smooth near the origin, essentially because of the large- n scaling of $V_n(x)$ given by Eq. (48).

As an example, for our class of spectral functions, at the edge of the bulk we have:

Lemma 1 (Informal). *If $Q(\omega) \sim |\omega|^p \log^q |\omega|$ as $|\omega| \rightarrow \infty$ for some $p > 0$ and $q \in \mathbb{R}$, then*

$$\lim_{n \rightarrow \infty} h_n(1) = 2p. \quad (52)$$

We test this result numerically for the mixed field Ising model in Section S5. Note that $h_n(x)$ is even if $Q(x)$ is even, so the same conclusion holds for $h_n(-1)$.

The behavior of $h_n(0)$ is more interesting, since it is sensitive to a *confinement transition* in the Coulomb gas, between ‘strong confinement’ for $p > 1$ to ‘weak confinement’ for $p < 1$ (see Fig. 2) [38–41]. Despite this confinement transition being driven primarily by the *high frequency* behavior of the spectral function, it turns out to manifest in a divergent density at *low frequencies*, as codified in Lemma 2. This means it will have an imprint on the signatures of hydrodynamics on the recurrence coefficients b_n , as we saw in Theorem 1. The following result is stated in terms of $h_n(0)$, but can be translated back to a confinement transition in the original equilibrium density $\sigma_n(0)$ using Eqs. (46) and (50).

Lemma 2 (Informal). *Suppose $Q(\omega) \sim |\omega|^p \log^q |\omega|$ as $|\omega| \rightarrow \infty$ for some $p \geq 1$ and $q \in \mathbb{R}$.*

If $p > 1$, then for all $q \in \mathbb{R}$ we have

$$\lim_{n \rightarrow \infty} h_n(0) = \frac{2p}{p-1}, \quad (53)$$

while in the marginal case $p = 1$, as $n \rightarrow \infty$ we have

$$h_n(0) = (\log n)^{1+o(1)} \quad (54)$$

provided $q > -1$. (Local interactions enforce $q \geq 0$.)

We prove Lemmas 1 and 2 in Section S6. It is interesting to now recall the *operator growth hypothesis* (OGH) [10], which posits that operators undergoing chaotic many-body dynamics generically grow as fast as possible under locality constraints. These constraints stipulate that the

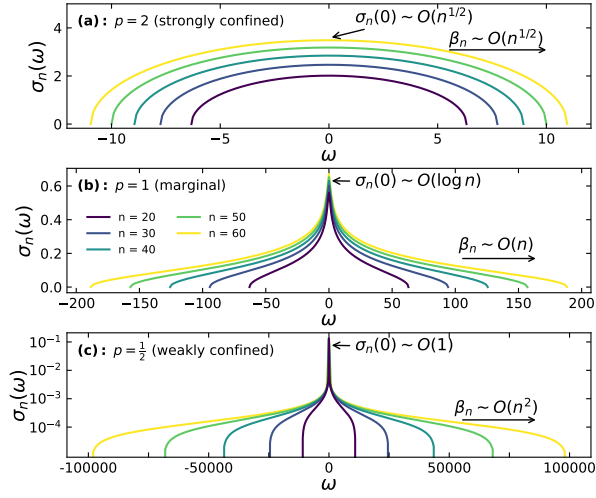


FIG. 4. Illustration of the confinement transition using the potential $Q(\omega) = (1 + \omega^2)^{p/2}$ for different growth exponents p . The values $p = \frac{1}{2}$ and $p = 2$ lie in the weakly and strongly confined phases respectively, while $p = 1$ is marginal. All systems with local interactions should have $p \geq 1$. The confinement transition can be diagnosed via the equilibrium density $\sigma_n(0)$ at zero frequency. In the strongly confined phase $\sigma_n(0) \sim \mathcal{O}(n/\beta_n)$ grows algebraically with n , reducing to logarithmic growth $\sigma_n(0) \sim \mathcal{O}(\log n)$ at the critical point (or $\sigma_n(0) \sim \mathcal{O}(\log^2 n)$ in one spatial dimension). In the weakly confined phase, $\sigma_n(0) \sim \mathcal{O}(1)$ does not grow with n .

spectral function must decay at least exponentially with ω , so that $Q(\omega) \sim |\omega|^p$ with $p \geq 1$, and hence b_n grows no faster than $\mathcal{O}(n)$. The OGH therefore amounts to the statement that chaotic many-body systems generically have $p = 1$; here we see that this implies they can be identified with the critical point of a Coulomb gas confinement transition (see Fig. 2). Systems with spectral functions decaying superexponentially ($p > 1$) will instead lie in the strongly confined phase of the Coulomb gas.

The confinement transition can be heuristically understood as follows. We have already seen that the large frequency scaling of the potential $Q(\omega) \sim |\omega|^p \log^q |\omega|$ determines the width β_n of the equilibrium charge density distribution $\sigma_n(\omega)$ via Eq. (44). The confinement transition is related to the relative scaling of the bandwidth β_n and the total charge n . For $p > 1$, β_n grows slower than n , so the average charge density $n/(2\beta_n)$ increases with n ; heuristically, the charge is increasingly ‘packed in’. A useful diagnostic is the charge density at zero frequency, $\sigma_n(\omega = 0)$, which is related to $h_n(0)$ via

$$\sigma_n(0) = \frac{1}{2\pi} \frac{n}{\beta_n} h_n(0). \quad (55)$$

Lemma 2 tells us that $h_n(0)$ is $\mathcal{O}(1)$ for $p > 1$, where the $\mathcal{O}(1)$ refers to scaling with n . Combining this with the scaling of β_n given in Eq. (44), we conclude that $\sigma_n(0) \sim \mathcal{O}(n/\beta_n)$ increases algebraically with n , with the same n -scaling as the average charge density. In this sense the charge density is approximately uniform (in ω)

in the bulk. An example is shown in Fig. 4(a), where we show the equilibrium density $\sigma_n(\omega)$ for the toy potential $Q(\omega) = (1 + \omega^2)^{p/2}$ with $p = 2$.

By contrast, in the (locality forbidden) weakly confined phase ($p < 1$), the bandwidth β_n grows faster than n , so the average charge density $n/(2\beta_n)$ decreases with n . However, the charge is now distributed differently at low frequencies compared with the rest of the bulk; the density profile is peaked at $\omega = 0$, where it becomes $\sigma_n(0) \sim \mathcal{O}(1)$. An example is shown in Fig. 4(c). One can understand this divergence from the behavior of the derivative $Q'(\omega) \sim \omega^{p-1}$, which for $p < 1$ grows algebraically as ω becomes smaller. For our class of spectral functions we only assume that this behavior holds at large frequencies, but when n is large this scaling still governs the behavior of the rescaled potential $V'_n(s) = (\beta_n/n)Q'(\beta_n s)$ for $s \sim \mathcal{O}(1)$ (c.f. Eq. (48)). As such, for $x = 0$ the integrand of Eq. (51) diverges algebraically as s approaches zero, until the divergence is eventually cut off by our differentiability assumption on Q . This gives rise to a contribution scaling like $h_n(0) \sim \mathcal{O}(n^{(1-p)/p})$, so that $\sigma_n(0) \sim \mathcal{O}(1)$.

Finally, in the marginal case $p = 1$ relevant for chaotic systems, the bandwidth β_n grows at the same rate as the total charge n (up to logarithmic factors depending on q). By a similar argument to the $p < 1$ case, the derivative $V'_n(s)$ is now approximately constant for $s \sim \mathcal{O}(1)$, so the integrand of Eq. (51) has a logarithmic divergence as $s \rightarrow 0$. This is again cut off at very small $s \sim \mathcal{O}(1/\beta_n)$ by our differentiability assumption on Q , with the end result that $h_n(0)$ diverges like $\mathcal{O}(\log n)$. Any logarithmic corrections to $Q(\omega) \sim |\omega| \log^q |\omega|$ do not affect the logarithmic scaling of $h_n(0)$ provided $q > -1$. The case $q = -1$ corresponds to the transition to weak confinement; this is also where the Hamburger moment problem for $\Phi(\omega)$ becomes indeterminate [89], which follows from Carleman’s condition [47]. Note that local interactions enforce $q \geq 0$ if $p = 1$ [35]. The scaling of $\sigma_n(0)$ is then $\sigma_n(0) \sim \mathcal{O}(nh_n(0)/\beta_n)$, giving $\sigma_n(0) \sim \mathcal{O}(\log n)$ for $\beta_n \sim n$ and $\sigma_n(0) \sim \mathcal{O}(\log^2 n)$ for $\beta_n \sim n/\log n$, the latter case relevant in one spatial dimension [10].

Before proceeding, we note that the convergence of the equilibrium Coulomb gas density to the asymptotic forms indicated in Lemmas 1 and 2 can be extremely slow, depending on the functional form for Q . When Q is an even-order polynomial, $Q(x) \sim \mathcal{O}(x^{2m})$, then it is known that the finite n corrections to $h_n(0)$ and $h_n(1)$ scale like $\mathcal{O}(n^{-1/2m})$ [22]. When Q is not necessarily an actual polynomial, but merely of polynomial-growth as we treat here, then in general the rate of convergence depends on how quickly Q approaches its asymptotic scaling $Q(x) \sim x^p \log^q x$. In toy examples we have also found that convergence of $h_n(0)$ tends to be slower than that of $h_n(1)$, particularly in the quasi-linear case $p = 1$ where $h_n(0)$ has a logarithmic divergence. Having said that, this slow convergence will not necessarily be a problem for estimating e.g. diffusion constants: in Section VB we show how to eliminate the dependence on these slowly converging Coulomb gas densities. After developing some

technical tools, we perform some quantitative checks of the convergence of the equilibrium measure to the Ullman distribution Eq. (49) in Section VIII C. We find, at the values of n typically available for numerical simulations, that the Ullman distribution successfully describes the large-scale qualitative shape of the true equilibrium measure, but at finite n there remain significant fluctuations which must be accounted for in order to get quantitative accuracy in estimates of the spectral function.

V. HYDRODYNAMICS FROM THE ZERO MODE

So far we have given a large- n expansion of the Lanczos coefficients b_n , showing how a low-frequency power-law in the spectral function, $\Phi(\omega \rightarrow 0) \sim |\omega|^\rho$, shows up as a subleading correction to the leading scaling of the Lanczos coefficients. In this section we explain how by studying the zero mode $|\omega = 0\rangle_{\mathcal{K}}$ of the Liouvillian $\mathcal{L}_{\mathcal{K}}$ within the Krylov space, satisfying $\mathcal{L}_{\mathcal{K}}|\omega = 0\rangle_{\mathcal{K}} = 0$, one can extract the value of the low frequency power-law exponent ρ , as well as hydrodynamic transport coefficients encoded in $\lim_{\omega \rightarrow 0} \Phi(\omega)/|\omega|^\rho$. The advantage of studying the zero mode over directly analyzing the Lanczos coefficients is that the zero mode amplifies the effects of the small subleading terms in the Lanczos coefficients, such that the hydrodynamics is manifest in the *leading* behavior of the zero mode as $n \rightarrow \infty$.

A. Extracting the low frequency power-law

If we expand $|\omega = 0\rangle_{\mathcal{K}} = \sum_{n=0}^{\infty} c_n |O_n\rangle$ in the Lanczos basis, then Eq. (31) tells us that

$$\frac{c_n}{c_0} = \frac{p_n(0)}{p_0(0)}, \quad (56)$$

where $p_0(0) = \|A\|^{-1}$ for an initial operator $|A\rangle$. It is a general property of orthogonal polynomials with respect to even weight functions that they have definite parity [67], $p_n(-x) = (-1)^n p_n(x)$, and hence $c_n = 0$ for odd n . Furthermore, by using the recurrence relation in Eq. (30), we find the recursive formula $p_{2n}(0) = -(b_{2n-1}/b_{2n})p_{2n-2}(0)$, and hence

$$\frac{p_{2n}(0)}{p_0(0)} = (-1)^n \frac{b_{2n-1}}{b_{2n}} \frac{b_{2n-3}}{b_{2n-2}} \dots \frac{b_1}{b_2}. \quad (57)$$

Because this quantity involves the ratio of even and odd Lanczos coefficients, it amplifies the effects of the even/odd staggering in the subleading corrections to the Lanczos coefficients indicated in Theorem 1. Previous authors have noted that this is analogous to the origin of the localized zero mode in the Su-Schrieffer-Heeger chain [71, 72, 90]. Our next result gives us a precise handle on how the low-frequency power-law imprints itself on the scaling of this zero mode:

Theorem 2 (Informal). *Given the spectral function $\Phi(\omega) \equiv |\omega|^\rho \exp[-Q(\omega)]$, so that $\Phi(\omega) \sim |\omega|^\rho$ as $\omega \rightarrow 0$ for some $\rho > -1$, then as $n \rightarrow \infty$ we have*

$$p_{2n}(0)^2 = \frac{C_\rho}{e^{-Q(0)}} \frac{[\pi\sigma_{2n}(0)]^\rho}{\beta_{2n}} [1 + o(1)], \quad (58)$$

where σ_{2n} and β_{2n} are respectively the density and support of the equilibrium Coulomb gas distribution defined in Section IV A, and the constant C_ρ is given by

$$C_\rho = \frac{2^{1-\rho}}{\Gamma\left[\frac{1}{2}(1+\rho)\right]^2}. \quad (59)$$

See Section S4 A 1 for a proof; the $o(1)$ error term is given by the RHS of Eq. (S2.126). For the purposes of numerically extracting the value of ρ , it is worth isolating the n -dependence of $p_{2n}(0)^2$. The scaling of β_{2n} is given in Eq. (44), and the scaling of $\sigma_{2n}(0) = (2n/\beta_{2n})h_{2n}(0)/2\pi$ can be deduced from Lemma 2, leading to the following.

Corollary 1. *With $\Phi(\omega) \equiv |\omega|^\rho \exp[-Q(\omega)]$, for $n \rightarrow \infty$ we have*

$$p_{2n}(0)^2 \sim \mathcal{O}\left(\frac{[nh_{2n}(0)]^\rho}{\beta_{2n}^{1+\rho}}\right). \quad (60)$$

With $Q(x) \sim |x|^p \log^q |x|$ as $|x| \rightarrow \infty$, this leads to

$$p_{2n}(0)^2 \sim \begin{cases} n^{-\frac{1}{p} + \rho(1 - \frac{1}{p})} (\log n)^{\frac{q}{p}(1+\rho)}, & \text{for } p > 1, q \in \mathbb{R}, \\ n^{-1} (\log n)^{\rho + q(1+\rho)}, & \text{for } p = 1, q > -1, \end{cases} \quad (61)$$

where the \sim indicates only the overall n -dependence, and for $p = 1$ we have dropped the $o(1)$ subleading exponent in $h_n(0) = (\log n)^{1+o(1)}$ from Lemma 2.

In Table I we summarize some of the most physically relevant cases for the scaling of $p_{2n}(0)^2$. The statements about chaotic dynamics are made according to the operator growth hypothesis [10], while the statement about integrable systems is based on numerical evidence only.

Since we must have $1 + \rho > 0$ in order for the spectral function to be Lebesgue integrable across $\omega = 0$, we see that $\sum_n p_{2n}(0)^2$ diverges algebraically for $p > 1$, but polylogarithmically for $p = 1$, so the zero mode is *marginally*

Dynamical class	p	q	$\mathcal{O}(p_{2n}(0)^2)$	$\mathcal{O}(\sum_{m=0}^n p_{2m}(0)^2)$
Chaotic ($d > 1$)	1	0	$(\log n)^\rho/n$	$(\log n)^{1+\rho}$
Chaotic ($d = 1$)	1	1	$(\log n)^{1+2\rho}/n$	$(\log n)^{2(1+\rho)}$
Interacting integrable	2	0	$n^{\frac{1}{2}(-1+\rho)}$	$n^{\frac{1}{2}(1+\rho)}$
Non-interacting	∞	0	n^ρ	$n^{1+\rho}$

TABLE I. Zero mode amplitude $p_{2n}(0)^2$ scaling as a function of the low-frequency power-law exponent $\Phi(\omega \rightarrow 0) \sim |\omega|^\rho$ and the high-frequency behavior $\Phi(\omega \rightarrow \infty) \sim \omega^p \log^q \omega$.

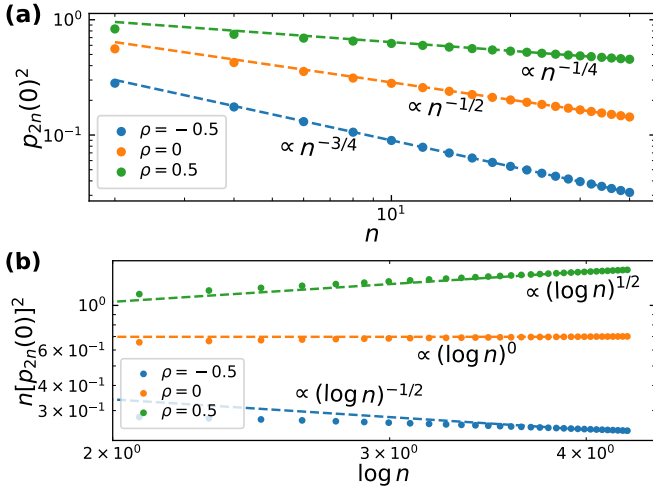


FIG. 5. Scaling of the zero mode amplitudes $p_{2n}(0)^2$ as a function of the power-law exponent ρ governing the low-frequency spectral function $\Phi(\omega \rightarrow 0) \sim |\omega|^\rho$. **(a)** Toy model $\Phi(\omega)/2\pi = |\omega|^\rho \exp[-Q(\omega)]$ with $Q(\omega) = (1 + \omega^2 + \omega^4)^{1/2}$. This model has $p = 2$, so $p_{2n}(0)^2$ scales algebraically as $p_{2n}(0)^2 \sim n^{\frac{1}{2}(\rho-1)}$. **(b)** Toy model $\Phi(\omega)/2\pi = |\omega|^\rho \exp[-Q(\omega)]$ with $Q(\omega) = (1 + \omega^2 + \omega^4)^{1/4}$. This model has $p = 1$, so $np_{2n}(0)^2$ scales polylogarithmically as $np_{2n}(0)^2 \sim (\log n)^\rho$. (Note the axes are log-scale, so for case **(b)** the x-axis is linear in $\log \log n$.)

delocalized for $p = 1$. Unlike the original Su-Schrieffer-Heeger chain, here the zero mode is not a true localized eigenstate; although its support does decay further into the bulk of the Lanczos chain, it does so too slowly to be localized. The only case in which the zero mode is normalizable is when the spectral function has a delta-function peak at zero frequency. In Fig. 5 we test this scaling numerically for some toy spectral functions, finding good agreement with the predictions of Theorem 2.

Having fixed the values of p and q from the leading behavior of the Lanczos coefficients $b_n \sim (n/\log^q n)^{1/p}$, one can extract the value of the power-law exponent ρ by computing $p_{2n}(0)^2$ and fitting to the relevant asymptotic form indicated in Corollary 1. In practice, we have found this to be more robust than attempting to extract ρ by fitting the subleading terms in Theorem 1, since here one is fitting to the leading behavior of $p_{2n}(0)^2$. Generally this procedure works well for $p > 1$, i.e. sublinear Lanczos coefficients. However, for $p = 1$, where the Lanczos coefficients are (quasi-)linear, we have found that n has to be extremely large before this procedure gives the correct value of ρ , and so in this case it might be best to assume the value of ρ on phenomenological grounds. We attribute this to the potentially very slow convergence of the Coulomb gas density $h_n(0)$ to its asymptotic form given in Lemma 2. While this slow convergence seems troubling, our algorithms for extracting hydrodynamic coefficients like diffusion constants, discussed in the next section, do *not* rely on the asymptotics for the Coulomb gas. In fact, one of our contributions is showing how to eliminate $h_n(0)$ from the equations that will determine

the hydrodynamic coefficients.

B. Extracting hydrodynamic transport coefficients

Now let us apply this to develop a numerical algorithm for computing diffusion constants and other transport coefficients. To warm up, let us consider diffusion. The infinite temperature dc conductivity σ_{dc} , rescaled by the temperature [91], is given by the Kubo formula [92]

$$\sigma_{\text{dc}} = \lim_{\tau \rightarrow \infty} \lim_{L \rightarrow \infty} \int_0^\tau \frac{(\mathcal{J}|\mathcal{J}(t))}{L} dt, \quad (62)$$

where \mathcal{J} is the total current for the conserved charge, and L is the system size. Now we set our initial Lanczos operator to be $A := \mathcal{J}/\sqrt{L}$, the zero wavevector component of the Fourier transform of the current density, and take the thermodynamic limit $L \rightarrow \infty$. For a translationally invariant system, the Lanczos algorithm can be run in Fourier space with minimal modification compared with real space [10, Appendix C]. Since $(\mathcal{J}|\mathcal{J}(t)) = (\mathcal{J}|\mathcal{J}(-t))$ at infinite temperature, we have

$$\sigma_{\text{dc}} = \frac{1}{2} \int_{-\infty}^{\infty} (A|A(t)) dt = \frac{1}{2} \Phi(0). \quad (63)$$

Given our ansatz $\Phi(\omega)/2\pi = |\omega|^\rho \exp[-Q(\omega)]$, we have

$$\lim_{\omega \rightarrow 0} \frac{\Phi(\omega)}{|\omega|^\rho} = 2\pi e^{-Q(0)}. \quad (64)$$

For regular diffusion we expect the dc conductivity σ_{dc} to be finite, which corresponds to $\rho = 0$. To obtain the diffusion constant, one can use the Einstein relation $D = \sigma_{\text{dc}}/\chi$, where χ is the static susceptibility.

The first thing to notice is that Eq. (58) contains this factor $\exp[-Q(0)]$ which gives us the value of $\lim_{\omega \rightarrow 0} \Phi(\omega)/|\omega|^\rho$. However, despite being able to exactly compute $p_{2n}(0)$ via Eq. (57), the problem with using Eq. (58) on its own to extract $\exp[-Q(0)]$ is that it also contains the factor $\sigma_n(0)$ related to the density of the equilibrium measure at the origin, and in general computing $\sigma_n(0)$ exactly requires already knowing the spectral function (since one needs to know Q). While Lemma 2 indicates that $\sigma_n(0) = (1/2\pi)(nh_n(0)/\beta_n)$ exhibits some universal scaling as $n \rightarrow \infty$, this asymptotic scaling can take a long time to set in, so given only a modest number of Lanczos coefficients, it would be preferable to rely only on quantities we can compute exactly or approximately using a finite number of Lanczos coefficients. Fortunately, it turns out to be possible to eliminate the leading-order dependence on $\sigma_n(0)$ using the precise asymptotics of the partial sums of the amplitudes $p_{2n}(0)^2$. We define

$$K_n(x, y) := \sum_{m=0}^{n-1} p_m(x)p_m(y), \quad (65)$$

which is known as the ‘Christoffel-Darboux kernel’ in the language of orthogonal polynomials [93]. Using our Riemann-Hilbert analysis, we have

Lemma 3. *Given the spectral function $\Phi(\omega) \equiv |\omega|^\rho \exp[-Q(\omega)]$, so that $\Phi(\omega) \sim |\omega|^\rho$ as $\omega \rightarrow 0$ for some $\rho > -1$, then as $n \rightarrow \infty$ we have*

$$K_n(0,0) = \frac{\hat{c}_\rho}{e^{-Q(0)}} [\pi\sigma_n(0)]^{1+\rho} [1 + o(1)], \quad (66)$$

where the $o(1)$ error term is given in the RHS of Eq. (S2.126), and the constant \hat{c}_ρ is given by

$$\hat{c}_\rho := \frac{1}{2^{1+\rho} \Gamma[\frac{1}{2}(1+\rho)] \Gamma[\frac{1}{2}(3+\rho)]}. \quad (67)$$

Combining Lemma 3 and Theorem 2 gives

$$\pi\sigma_{2n}(0) = 2(1+\rho) \frac{K_{2n}(0,0)}{\beta_{2n} p_{2n}(0)^2} [1 + o(1)], \quad (68)$$

leading to the following result:

Theorem 3. *With $\Phi(\omega) \sim |\omega|^\rho$ as $\omega \rightarrow 0$, we have*

$$\lim_{\omega \rightarrow 0} \frac{\Phi(\omega)}{|\omega|^\rho} = \lim_{n \rightarrow \infty} \frac{c_\rho [K_{2n}(0,0)]^\rho}{[\beta_{2n} p_{2n}(0)^2]^{1+\rho}}, \quad (69)$$

where the constant c_ρ is given by

$$c_\rho = \frac{4\pi(1+\rho)^\rho}{\Gamma[\frac{1}{2}(1+\rho)]^2}. \quad (70)$$

For the reader's convenience, we can use Eqs. (57) and (65) to give the following more explicit expression in terms of Lanczos coefficients:

$$\lim_{\omega \rightarrow 0} \frac{\Phi(\omega)}{|\omega|^\rho} = \lim_{n \rightarrow \infty} c_\rho \|A\|^2 \frac{\left[1 + \sum_{k=1}^{n-1} \left(\frac{b_{2k-1}}{b_{2k}} \dots \frac{b_1}{b_2}\right)^2\right]^\rho}{\left[\beta_{2n} \left(\frac{b_{2n-1}}{b_{2n}} \dots \frac{b_1}{b_2}\right)^2\right]^{1+\rho}}, \quad (71)$$

where A is the initial Lanczos operator, $O_0 = A/\|A\|$. By Theorem 1 we know that $\beta_{2n} = 2b_{2n}[1 + \mathcal{O}(1/n)]$, so from Eq. (71) we can see that simply approximating $\beta_{2n} \approx 2b_{2n}$ also results in a small $\mathcal{O}(1/n)$ relative error in $\lim_{\omega \rightarrow 0} \Phi(\omega)/|\omega|^\rho$. All of the subtle effects from sub-leading staggered terms in the Lanczos coefficients are captured in $p_{2n}(0)^2$ and $K_{2n}(0,0)$, which we can compute exactly using the first $2n$ Lanczos coefficients.

To start our benchmarks, we begin with regular diffusion. In this case $\Phi(0)$ for the current operator is nonzero, corresponding to $\rho = 0$. In this special case, Theorem 3 becomes

$$\Phi(0) = \lim_{n \rightarrow \infty} \frac{4}{\beta_{2n} p_{2n}(0)^2}, \quad (72)$$

$$= \lim_{n \rightarrow \infty} \frac{4\|A\|^2}{\beta_{2n}} \left(\frac{b_{2n}}{b_{2n-1}} \frac{b_{2n-2}}{b_{2n-3}} \dots \frac{b_2}{b_1}\right)^2, \quad (73)$$

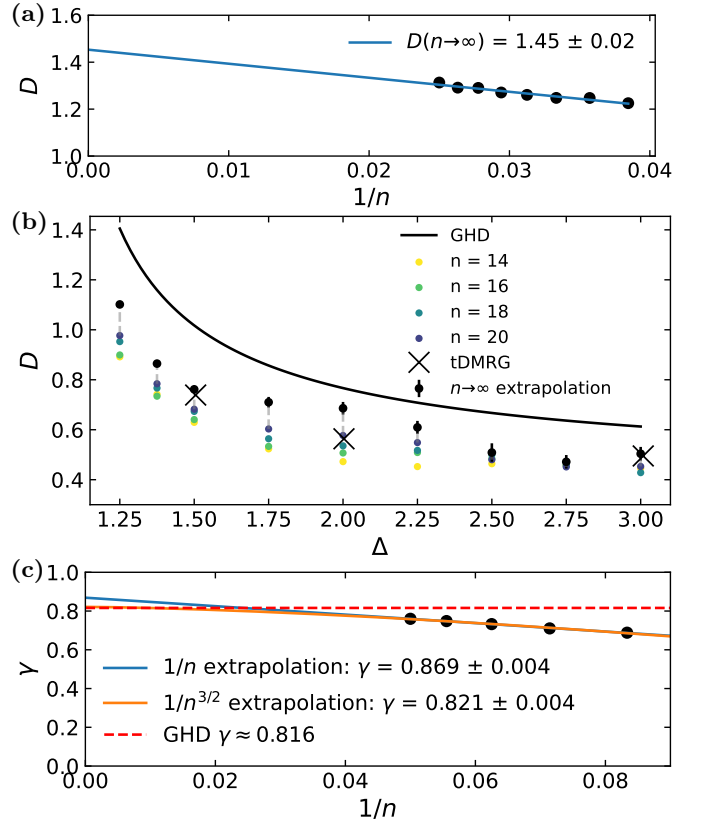


FIG. 6. (a) Energy diffusion constant of the mixed field Ising chain using Theorem 3 with $\rho = 0$ and up to $n = 40$ Lanczos coefficients. (b) Spin diffusion constant of the XXZ spin chain as a function of the anisotropy Δ using Theorem 3 with $\rho = 0$ and up to $n = 20$ Lanczos coefficients, compared with the prediction Eq. (76) from generalized hydrodynamics (GHD) [96, 97]. The black dots show the result of a linear extrapolation in $1/n$ to $n \rightarrow \infty$, and the crosses show tDMRG data from Ref. [98]. (c) Coefficient γ of the time-dependent spin diffusion constant $D(t) \sim \gamma t^{1/3}$ for the isotropic Heisenberg chain using Theorem 3 with $\rho = -1/3$ and up to $n = 20$ Lanczos coefficients. Extrapolations in $1/n$ and $1/n^{3/2}$ give slightly different predictions, with the $1/n^{3/2}$ result agreeing better with the GHD prediction $\gamma \approx 0.816$ [99, 100].

where in the second line we used Eq. (57) to replace $p_{2n}(0)^2$. A similar formula appears in Ref. [94], based on considerations motivated by the operator growth hypothesis (OGH) [10] (see also Ref. [95]). Our derivation shows that this behavior does not necessarily require the system to obey the OGH in order for it to valid.

We start with the mixed field Ising model,

$$H_{\text{MFIM}} = \sum_{i=1}^L (Z_i Z_{i+1} + g_x X_i + g_z Z_i), \quad (74)$$

which has energy diffusion for generic values of g_x and g_z [3]. The energy current operator is defined by a continuity equation to be $\mathcal{J} = \sum_i g_x (Y_i Z_{i+1} - Z_i Y_{i+1})$, so given the initial Lanczos operator $A := \mathcal{J}/\sqrt{L}$, in the thermodynamic limit we have $\|A\|^2 = \lim_{L \rightarrow \infty} (\mathcal{J}|\mathcal{J})/L = 2g_x^2$,

which is needed to compute $p_{2n}(0)$ via Eq. (57). The infinite temperature static energy susceptibility is $\chi = \lim_{L \rightarrow \infty} [\langle H_{\text{MFIM}}^2 \rangle - \langle H_{\text{MFIM}} \rangle^2] / L = 1 + g_x^2 + g_z^2$. Fixing $g_x = 1.4$ and $g_z = 0.9045$, Fig. 6(a) shows the result of using Theorem 3 with $\rho = 0$ to extract the energy diffusion constant D . A linear extrapolation in $1/n$ on the predictions from up to $n = 40$ Lanczos coefficients gives an estimate of $D(n \rightarrow \infty) = 1.45 \pm 0.02$, close to the prediction $D = 1.4\text{--}1.45$ from tensor network methods [5, 9].

For a more challenging example, we study spin diffusion in the XXZ chain,

$$H_{\text{XXZ}} = \frac{1}{4} \sum_i (X_i X_{i+1} + Y_i Y_{i+1} + \Delta Z_i Z_{i+1}), \quad (75)$$

which has diffusive spin transport for $\Delta > 1$ [91]. The spin current operator is defined by a continuity equation to be $\mathcal{J} = \frac{1}{4} \sum_i (X_i Y_{i+1} - Y_i X_{i+1})$, so $\|A\|^2 = 1/8$. The infinite temperature static spin susceptibility is $\chi = \lim_{L \rightarrow \infty} [\langle (S_{\text{tot}}^z)^2 \rangle - \langle S_{\text{tot}}^z \rangle^2] / L = 1/4$. Performing a linear extrapolation in $1/n$ on the predictions from up to $n = 20$ Lanczos coefficients, Fig. 6(b) shows that the resulting diffusion constants come reasonably close to the prediction from generalized hydrodynamics [96, 97],

$$D_{\text{XXZ}} = \frac{2 \sinh \eta}{9\pi} \sum_{s=1}^{\infty} (1+s) \left[\frac{s+2}{\sinh \eta s} - \frac{s}{\sinh \eta (s+2)} \right], \quad (76)$$

where $\eta := \text{arcosh } \Delta$. We note that $n = 20$ is still relatively small, but even at these small values the predictions are close to those obtained using tensor network methods like tDMRG [98].

Finally, to test the method for $\rho \neq 0$, we study spin transport in the isotropic Heisenberg chain (i.e. $\Delta = 1$ for the XXZ spin chain). This has recently been discovered to have superdiffusive spin transport at infinite temperature [45], with a current-current correlator decaying like $\langle \mathcal{J} \mathcal{J}(t) \rangle \sim (\gamma \chi / 3) t^{-2/3}$ as $t \rightarrow \infty$, leading to a time-dependent diffusion constant growing like $D(t) \sim \gamma t^{1/3}$. The value of γ can be extracted from the Lanczos coefficients of the spin current operator using Theorem 3 with $\rho = -1/3$ via the relation

$$\gamma = \frac{\chi \sqrt{3}}{\Gamma[\frac{1}{3}]} \lim_{\omega \rightarrow 0} \frac{\Phi(\omega)}{|\omega|^{-1/3}}, \quad (77)$$

where we used the fact that $\int_{\mathbb{R}} e^{-i\omega t} |t|^{-2/3} dt = \sqrt{3} \Gamma[1/3] |\omega|^{-1/3}$. Generalized hydrodynamics gives the prediction $\gamma = (2/3)(10\pi/27)^{4/3} \approx 0.816$ [99, 100]. Using only $n = 20$ Lanczos coefficients, we obtain predictions close to this result (Fig. 6(c)). Interestingly, we find extrapolating in $n^{-3/2}$ gives better agreement with the GHD prediction than extrapolating in n^{-1} .

VI. UNIVERSALITY OF THE LEVEL- n GREEN'S FUNCTION

In this section we will explore emergent universality in Green's functions, and explain how the results of the previous section can be interpreted in terms of this universality. Let $\mathcal{L}_n = (\mathcal{L}_{ij})_{i,j \geq n}$ denote the tridiagonal Liouvillian matrix restricted to sites n and above, and let

$$G_n(z) := \left(O_n \left| \frac{1}{z - \mathcal{L}_n} \right| O_n \right), \quad (78)$$

which we refer to as the 'level- n Green's function'. Due to the tridiagonal structure of the Liouvillian, $G_n(z)$ obeys the recursion relation [19]

$$G_n(z) = \frac{1}{z - b_{n+1}^2 G_{n+1}(z)}. \quad (79)$$

Recurring this gives a continued fraction expansion for the original Green's function $G(z) \equiv G_0(z)$ (taking $\|A\| = 1$ for notational simplicity)

$$G(z) = \frac{1}{z - \frac{b_1^2}{z - \dots \frac{b_{n-1}^2}{z - b_n^2 G_n(z)}}} \quad (80)$$

In practice one can only compute some finite number of coefficients $\{b_k\}_{k=1}^n$, so one must somehow terminate the continued fraction expansion at level- n . Simply setting $G_n(z) = 0$ is a bad idea because it amounts to terminating the Lanczos chain after site n , which gives unphysical reflections of the operator wavefunction off the hard boundary, leading to very slow convergence with n . A better approach is to choose a model for $G_n(z)$ which is designed to accurately capture the operator backflow. The 'recursion method' [19] is a popular numerical technique where one chooses such a 'terminator' level- n Green's function based on some high level features of the spectral function, like its high-frequency decay and any algebraic singularities. The existence of appropriate terminators is something of a lottery because one needs exact expressions for all three of the Lanczos coefficients, the spectral function, and the Green's function. These solutions are usually expressed in terms of special functions, and there is no guarantee an exactly solvable model will exist with all the appropriate characteristics. With our Riemann-Hilbert approach, we can analyze the $n \rightarrow \infty$ asymptotic behavior of $G_n(z)$ directly, bypassing the need for these exactly solvable models.

We prove that, as $n \rightarrow \infty$, $G_n(z)$ approaches different universal scaling forms in different regions of the complex plane. The simplest case is when z is sufficiently far from the special points $z = 0$ and $z = \pm \beta_n$. In this case we show that $G_n(z)$ approaches the Wigner semicircle law, the same as the average global resolvent $\frac{1}{n} \text{tr} [1/(z - M)]$ for random $n \times n$ matrices M drawn from the Gaussian

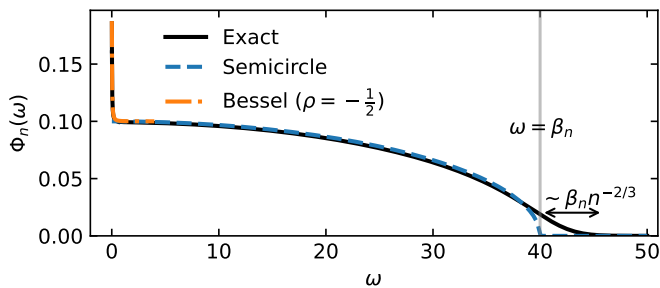


FIG. 7. The spectral function $\Phi_n(\omega) = 2 \text{Im}[G_n(\omega - i0^+)]$ corresponding to the level- n Green's function $G_n(z)$, shown for the toy spectral function $\Phi(\omega) = |\omega|^{-1/2} \text{sech}(\pi\omega)$ and $n = 40$. The Wigner semicircle law Eq. (82) describes the behavior very well in the bulk, but breaks down near $\omega = 0$ due to the low frequency power-law in the spectral function. Instead the behavior near $\omega = 0$ is described by the universal Bessel form corresponding to Eq. (84). Near the endpoint $\omega = \beta_n$ the behavior is described by Airy universality.

Unitary Ensemble [20] with a suitably rescaled bandwidth. If the spectral function $\Phi(\omega)$ is complex analytic at $\omega = 0$, this semicircle behavior persists all the way down to $z = 0$. On the other hand, if $\Phi(\omega \rightarrow 0) \sim |\omega|^\rho$ has a low-frequency power law, then the semicircle law breaks down near $\omega = 0$, and $G_n(z)$ instead is described by a form dictated by the Bessel universality class. Finally, near the edge of the spectrum, $z \approx \pm\beta_n$, the behavior of $G_n(z)$ is described by the Airy universality class. We show an example of this in Fig. 7 for the toy spectral function $\Phi(\omega) = |\omega|^{-1/2} \text{sech}(\pi\omega)$, where we focus on the behavior along the real line, as encoded in the corresponding spectral function $\Phi_n(\omega) = 2 \text{Im}[G_n(\omega - i0^+)]$. Since in this case we know the spectral function $\Phi(\omega)$, we can numerically compute $G_n(z)$ using a formula expressing it as a ratio of two Cauchy-Stieltjes transforms (see Eq. (S4.42)).

A. Frequencies in the bulk

First let us consider frequencies sufficiently far from the special points $z = 0$ and $z = \pm\beta_n$, where the level- n Green's function $G_n(z)$ takes on a particularly simple form as $n \rightarrow \infty$. In Section S4C we show that, as $n \rightarrow \infty$, $\beta_n G_n(\beta_n z)$ approaches a universal scaling form

$$\beta_n G_n(\beta_n z) \approx 2 \left(z - \sqrt{z + 1} \sqrt{z - 1} \right), \quad (81)$$

for all z satisfying $|z| > \delta_0$ and $|z/\beta_n \pm 1| > \delta_1$, where δ_0 and δ_1 are small but $\mathcal{O}(1)$ constants (see Fig. 1), and we use the principal branch of the square root, so the RHS has a branch cut along $[-1, 1]$. Thus, away from the special points $z = 0$ and $z = \pm\beta_n$, the only free parameter determining $G_n(z)$ is the frequency bandwidth β_n , which can be approximated up to $\mathcal{O}(1/n)$ relative error by $\beta_n \approx 2b_n$ (c.f. Theorem 1). When the spectral function $\Phi(\omega)$ is complex analytic at $\omega = 0$, we prove this semicircle

behavior extends all the way to $z = 0$. One can then understand the special case Eq. (73) of our formula for recovering $\Phi(\omega = 0)$ from the Lanczos coefficients as being equivalent to substituting $G_n(\pm i0^+) \approx \mp 2i/\beta_n \approx \mp i/b_n$ into the continued fraction expansion for $G(z)$. Although our proof technique in this case requires analyticity at $\omega = 0$, our numerical tests in Section VB suggest that this scaling $G_n(\pm i0^+) \approx \mp 2i/\beta_n$ may still be accurate to leading order in n , even without such strong analyticity requirements.

Within the ‘bulk’ frequency range $\delta_0 < |\omega| < (1 - \delta_1)\beta_n$, the spectral function corresponding to Eq. (81) is

$$\begin{aligned} \Phi_n(\omega) &:= \int_{-\infty}^{\infty} e^{-i\omega t} \langle O_n | e^{i\mathcal{L}_n t} | O_n \rangle dt \\ &= i [G_n(\omega + i0^+) - G_n(\omega - i0^+)] \\ &\approx \frac{4}{\beta_n} \sqrt{1 - (\omega/\beta_n)^2}, \end{aligned} \quad (82)$$

namely the *semicircle law* famous from random matrix theory (RMT) [20]. Thus we see the emergence of RMT universality in the bulk frequency response of the operators O_n restricted to the ‘fast space’. To leading order in $\omega/\beta_n \ll 1$, this spectral function is constant, providing some justification for approximating the large- n dynamics by white noise, as was the original intuition for the Mori-Zwanzig memory function formalism [18, 19]. In the next section we will show how this can fail near $\omega = 0$.

Although this is not how we prove it (see Section S4C for the actual proof), a quick way to arrive at Eq. (81) is to *assume* the existence of the limit $\beta_n G_n(\beta_n z) \xrightarrow{n \rightarrow \infty} f(z)$ (in particular that this limit is the same for both even and odd n —this assumption can fail near $z = 0$). Then, using the properties $\lim_{n \rightarrow \infty} b_n/\beta_n = 1/2$ (c.f. Theorem 1) and $\lim_{n \rightarrow \infty} b_{n+1}/b_n = 1$, one concludes from Eq. (79) that $f(z)$ must solve the fixed point equation

$$f(z) = \frac{1}{z - \frac{1}{4}f(z)}. \quad (83)$$

The RHS of Eq. (81) is then the unique solution of this fixed point, subject to the requirement that $f(z)$ is separately analytic in \mathbb{C}_\pm and approaches zero like $\mathcal{O}(1/z)$ as $z \rightarrow \infty$ (these properties follow from the resolvent representation of $G_n(z)$).

Without going into the details of the actual proof, let us note that the origin of the semicircle law behavior for $G_n(z)$ seems somewhat different to its origin for Gaussian random matrix ensembles. For the latter, the semicircle law arises because the equilibrium measure of the Gaussian potential $Q(\omega) = -\log[\exp(-\omega^2)] = \omega^2$ is the semicircle law (c.f. Eq. (49) for $p = 2$). In that context, the equilibrium measure governs the average eigenvalue density as $n \rightarrow \infty$. However, here the semicircle law for $G_n(z)$ arises for a much wider class of potentials, even when the corresponding equilibrium measure does *not* approach the semicircle law. The main ingredient to get the semicircle law for $G_n(z)$ seems to be that the equilibrium density $\sigma_n(\omega)$ is nonzero throughout the whole

interval $(-\beta_n, \beta_n)$, and that it vanishes like a square root as ω approaches the endpoints $\pm\beta_n$ (this is called ‘regular’ behavior). We prove this is the case for large enough n for our class of spectral functions (see Lemma S6), subject to the regularity condition that $Q'(\omega) > 0$ for large enough ω . In this sense the universal form Eq. (81) seems quite generic, but it would be possible to violate it locally if e.g. the spectral function contained spectral gaps.

In the language of the recursion method [19, 101], the Green’s function in Eq. (81) is known as the ‘square root terminator’, and is one of the simplest ways to terminate the infinite continued fraction for the true Green’s function. Indeed, within the approximation $\beta_n \approx 2b_n$, it amounts to setting all $b_{n+k} \mapsto b_n$, $k = 0, 1, 2, \dots$, to be equal, so that \mathcal{L}_n is just a constant tridiagonal matrix with b_n on the off-diagonals. Our results show that, remarkably, this simple square root terminator is sufficient to accurately compute diffusion constants ($\rho = 0$). In fact, we have even more freedom: any terminator satisfying $G_n(\omega \pm i0^+) \approx \mp 2i/\beta_n$ as $\omega \rightarrow 0$ would work just as well. For example, this means that it is *not* necessary to match the high frequency tail of the true spectral function (this is not generally true if $\rho \neq 0$ —see Section VIII B). In related work, we explore this ‘stitching freedom’ in more detail [102].

We discuss the error term of Eq. (81) in Section S4 C. In brief, for $z = \mathcal{O}(1)$ there is a multiplicative error of $\mathcal{O}(1/n)$. For $\rho = 0$ this is true for all z , but if $\rho \neq 0$ the error can become larger as $z \rightarrow 0$, reaching $\mathcal{O}(1/\sigma_n(0))$ at $z \sim 1/\beta_n$ (corresponding to a physical frequency $\omega = \beta_n z$ of $\mathcal{O}(n^0)$). This is $\tilde{\mathcal{O}}(1/n^{(p-1)/p})$ for $p > 1$, but only $\mathcal{O}(1/(\log n)^{1+q+o(1)})$ in the marginal case $p = 1$. (We remind the reader that, for $p = 1$, $q \geq 0$ is guaranteed by locality, with $q \geq 1$ in $d = 1$ spatial dimensions [10, 35].)

B. Frequencies near $\omega = 0$

In the limit $\omega \rightarrow 0$, the distinction between even and odd n is important for $\rho \neq 0$; we will discuss the even case. In the order of limits where $\omega \rightarrow 0$ before $n \rightarrow \infty$, we can show

$$G_{2n}(\omega \pm i0^+) \approx \frac{-2}{\beta_{2n}} \left(\frac{J_{\frac{1}{2}(\rho-1)} \pm iY_{\frac{1}{2}(\rho-1)}}{J_{\frac{1}{2}(\rho+1)} \pm iY_{\frac{1}{2}(\rho+1)}} \right) [\pi\sigma_{2n}(0)\omega], \quad (84)$$

where J_ν and Y_ν are Bessel functions of the first and second kind respectively, and our shorthand indicates all Bessel functions should be evaluated with the argument $\pi\sigma_{2n}(0)\omega$ (this is a linear approximation of $\pi I_{2n}(\omega) = \pi \int_0^\omega \sigma_{2n}(s) ds \approx \pi\sigma_{2n}(0)\omega$). See Section S4 C for a derivation. The appearance of Bessel functions here is an indication of the Bessel universality governing the behavior near the origin due to the spectral function scaling $\Phi(\omega \rightarrow 0) \sim |\omega|^\rho$. Let us now illustrate the relation to our discussion of the zero mode in the previous section.

Taking $\omega \rightarrow 0$ of Eq. (84) gives

$$\lim_{\omega \rightarrow 0^+} \frac{\text{Im}[G_{2n}(\omega \pm i0^+)]}{|\omega|^\rho} \approx \mp \pi C_\rho \frac{[\pi\sigma_{2n}(0)]^\rho}{\beta_{2n}}, \quad (85)$$

where the constant C_ρ was defined in Eq. (59). By using Eq. (80), one can show that if $-1 < \rho < 1$ then we can recover the behavior of the original Green’s function at the origin using

$$\lim_{\omega \rightarrow 0^+} \frac{\text{Im}[G(\omega \pm i0^+)]}{|\omega|^\rho} = \frac{1}{p_{2n}(0)^2} \lim_{\omega \rightarrow 0^+} \frac{\text{Im}[G_{2n}(\omega \pm i0^+)]}{|\omega|^\rho}, \quad (86)$$

where we have used the recursive formula Eq. (57) for $p_{2n}(0)$. Finally, to get the spectral function we use

$$\Phi(\omega) = \mp 2 \text{Im}[G(\omega \pm i0^+)]. \quad (87)$$

Combining Eqs. (85) to (87), we get

$$\lim_{\omega \rightarrow 0^+} \frac{\Phi(\omega)}{|\omega|^\rho} \approx 2\pi C_\rho \frac{[\pi\sigma_{2n}(0)]^\rho}{\beta_{2n} p_{2n}(0)^2}. \quad (88)$$

The connection to the previous section comes from noticing that this is precisely what we would get by combining the asymptotics of $p_{2n}(0)^2$ from Theorem 2 with the identity $\lim_{\omega \rightarrow 0} \Phi(\omega)/|\omega|^\rho = 2\pi e^{-Q(0)}$. The final step to get Theorem 3 is to eliminate $\pi\sigma_{2n}(0)$ using Eq. (68), which is done for practical reasons so that we can express everything in terms of Lanczos coefficients. As discussed in Section S4 C, these expressions have a multiplicative error of $\mathcal{O}(1/\sigma_n(0))$.

C. Frequencies near the edges $\omega = \pm\beta_n$

Near the edge of the spectrum, meaning $|z/\beta_n \pm 1| < \delta_1$ for a small $\mathcal{O}(1)$ constant δ_1 , the Wigner semicircle law for $G_n(z)$ again breaks down, and instead the behavior is governed by the Airy universality class. This is analogous to the behavior near the turning points of a WKB approximation [83], or the maximal eigenvalue distribution of a random matrix ensemble [103]. We refer the reader to Section S4 C for the full expression for $G_n(z)$ in terms of Airy functions, and simply state here the leading behavior precisely at the endpoint β_n , where we have

$$G_{n,\pm}(\beta_n) \approx \frac{2}{\beta_n} \left(\frac{2 \text{Ai}(0) \sqrt{f'_n(1)} + e^{\pm \frac{i\pi}{3}} \sqrt{2} \text{Ai}'(0)(\rho+1)}{2 \text{Ai}(0) \sqrt{f'_n(1)} + e^{\pm \frac{i\pi}{3}} \sqrt{2} \text{Ai}'(0)(\rho-1)} \right), \quad (89)$$

with $f'_n(1) = (nh_n(1)/\sqrt{2})^{2/3} \sim \mathcal{O}(n^{2/3})$, and where $\text{Ai}(0) = (3^{2/3}\Gamma[\frac{2}{3}])^{-1}$ and $\text{Ai}'(0) = -(3^{1/3}\Gamma[\frac{1}{3}])^{-1}$. The appearance of the Airy function Ai is a reflection of the Airy universality near the spectral edge. From this expression we see that the corresponding spectral function $\Phi_n(\omega) = \mp 2 \text{Im}[G_{n,\pm}(\omega)]$ does not vanish precisely at $\omega = \beta_n$, as the semicircle law would predict, but instead scales to zero like $\mathcal{O}(\beta_n^{-1}n^{-1/3})$. As discussed in Section S4 C, this expression for $G_{n,\pm}(\beta_n)$ has a multiplicative error of $\mathcal{O}(1/n)$.

VII. THE SPECTRAL BOOTSTRAP: APPROXIMATING THE SPECTRAL FUNCTION AT FINITE FREQUENCIES

In this section we explain how to extend ideas from the previous section to extract the spectral function at finite frequencies. The high-level summary is that, using the appropriate $n \rightarrow \infty$ asymptotics of the orthogonal polynomials, we formulate a first-order differential equation involving the spectral function and the equilibrium density of the Coulomb gas defined in Section IV A. Together with an initial condition at $\omega = 0$ provided to us by Hermiticity (i.e. $\Phi(-\omega) = \Phi(\omega)$), this differential equation can be iteratively solved to give a finite n approximation to the spectral function at finite frequencies. The convergence of this approximation is determined by the convergence of the polynomial asymptotics.

We refer to this general procedure of using orthogonal polynomial asymptotics to give a differential equation for the spectral function as the *spectral bootstrap*. In order for this to work well, it is important to derive asymptotics taking into account all the relevant ‘high-level’ features of the spectral function, such as algebraic singularities, spectral gaps, etc. We will focus on a particular instance of this idea, where the spectral function $\Phi(\omega)/2\pi \equiv |\omega|^\rho \exp[-Q(\omega)]$ has a power-law at $\omega = 0$ but is otherwise smooth. To warm up we will start by taking $\rho = 0$, so that the spectral function is also smooth at $\omega = 0$. The procedure for $\rho \neq 0$ is conceptually similar, but the equations involved are a little more complicated. For $\rho = 0$, the whole frequency range $\omega \in (-\beta_n, \beta_n)$ is referred to as the ‘bulk’ (see Fig. 3), and the following procedure is controlled for all frequencies inside the bulk and away from the edges $\omega \approx \pm\beta_n$. Since β_n increases with n , for computationally accessible values of n the size of the bulk is large enough to capture the frequency range where the spectral function is non-negligible.

We remark that if one is only interested in recovering the spectral function $\Phi(\omega)$ in the bulk, there is a much simpler procedure than what we are about to describe:

1. Approximate the level- n Green’s function by the universal ‘semicircle form’

$$G_n(z) \approx \frac{2}{\beta_n^2} (z - \sqrt{z + \beta_n} \sqrt{z - \beta_n}),$$

from Eq. (81), where we approximate $\beta_n \approx 2b_n$.

2. Substitute $G_n(z)$ into the continued fraction in Eq. (80) to obtain the full Green’s function $G(z)$.
3. Compute $\Phi(\omega) = 2 \operatorname{Im} G(\omega - i0^+)$.

For $\rho = 0$, this simple procedure gives numerically identical results to the spectral bootstrap algorithm we will describe in the next section. However, for $\rho \neq 0$, the behavior of $\Phi(\omega)$ near $\omega = 0$ is strongly influenced by the behavior of the Coulomb gas density $\sigma_n(\omega)$, which can have strong fluctuations as a function of ω . Unfortunately, even for finite n , computing $\sigma_n(\omega)$ exactly requires already knowing the full spectral function $\Phi(\omega)$, which

would defeat the point. What we show is how to iteratively compute an approximation to $\sigma_n(\omega)$, controlled in the $n \rightarrow \infty$ limit, and in turn how this can be used to obtain a finite n approximation of the spectral function $\Phi(\omega)$. As a byproduct, having access to $\sigma_n(\omega)$ is also useful in checking the emergence of random matrix universality in this quantum operator growth problem—we will discuss this in more detail in Section VIII.

As well as the ‘bulk’ and ‘Bessel’ versions of the spectral bootstrap we will describe imminently, one can also formulate a version suited for frequencies near the spectral edge $|\omega| \approx \beta_n$. In this region there is Airy universality, as in Section VIC, and one must formulate polynomial asymptotics which are relevant for this universality class. We defer the exposition of this ‘Airy bootstrap’ to Section S5.

A. The bulk bootstrap: $\rho = 0$

In terms of the Coulomb gas density $\sigma_n(x)$ discussed in Section IV A, we define

$$\theta_n(\omega) := -\pi \int_{\omega}^{\beta_n} \sigma_n(\omega') d\omega' - \frac{\pi}{4}. \quad (90)$$

We will see shortly that $\theta_n(\omega)$ acts as a phase factor in a WKB-like asymptotic for the orthogonal polynomials. However, let us first briefly discuss some consequences of Hermiticity. For an arbitrary spectral function, all one knows about σ_n is that it integrates to n over some interval whose right endpoint is β_n . But for an *even* spectral function, which for us is guaranteed by Hermiticity, we know that $\sigma_n(\omega)$ is even and supported on $[-\beta_n, \beta_n]$, so that $\int_0^{\beta_n} \sigma_n(x) dx = n/2$ (the same integral gave the staggering factor $(-1)^n$ in the recurrence coefficients, c.f. Theorem 1). Thus we can rewrite $\theta_n(\omega)$ as

$$\theta_n(\omega) = \pi I_n(\omega) - \frac{n\pi}{2} - \frac{\pi}{4}, \quad (91)$$

where $I_n(\omega)$ is defined as

$$I_n(\omega) := \int_0^{\omega} \sigma_n(\omega') d\omega'. \quad (92)$$

Note that $I_n(0) = 0$, independent of the density distribution σ_n . This is important because it sets the initial condition for the first-order differential equation we will derive below. Although this is manifest from its definition, this discussion shows that it is really Hermiticity that gives us an initial condition at $\omega = 0$. For a non-even weight function, one would only have an initial condition for $\theta_n(\omega)$ at $\omega = \beta_n$.

The Riemann-Hilbert analysis gives us access to detailed asymptotic formulae for the orthogonal polynomials, controlled as $n \rightarrow \infty$. In the orthogonal polynomials literature, these are known as Plancherel-Rotach asymptotics [32].

We have the following generalization of Theorem 2 for $\rho = 0$ to finite frequencies (see Section S4 for a proof)

$$p_{n-1}(\omega) \approx \frac{-1}{\sqrt{\Phi(\omega)}} \sqrt{\frac{2}{\beta_n}} \left[\left(\frac{\beta_n - \omega}{\beta_n + \omega} \right)^{1/4} \cos \theta_n(\omega) + \left(\frac{\beta_n + \omega}{\beta_n - \omega} \right)^{1/4} \sin \theta_n(\omega) \right], \quad (93)$$

$$p_n(\omega) \approx \frac{1}{\sqrt{\Phi(\omega)}} \sqrt{\frac{2}{\beta_n}} \left[\left(\frac{\beta_n - \omega}{\beta_n + \omega} \right)^{1/4} \cos \theta_n(\omega) - \left(\frac{\beta_n + \omega}{\beta_n - \omega} \right)^{1/4} \sin \theta_n(\omega) \right], \quad (94)$$

where at this level of approximation we are setting $\beta_n \approx 2b_n$ (see Theorem 1 for $\rho = 0$). The first thing to notice is that $p_{n-1}(\omega)$ and $p_n(\omega)$ are both pointwise proportional to $1/\sqrt{\Phi(\omega)}$; this important feature is quite generic for orthogonal polynomials, and we will see that it continues to hold in other frequency regimes. We can combine these equations and use Eq. (91) to get the first of our bootstrap equations:

$$\Phi(\omega) \approx \frac{4}{\beta_n} \frac{1}{p_{n-1}(\omega)^2 + p_n(\omega)^2} \frac{\beta_n - (-1)^n \omega \sin[2\pi I_n(\omega)]}{\sqrt{\beta_n^2 - \omega^2}}. \quad (95)$$

Note that we used *two* polynomials, p_{n-1} and p_n , in order to avoid dividing by zero: it is a general property of orthogonal polynomials that the zeros of p_{n-1} and p_n interlace [104], which guarantees $p_{n-1}(\omega)^2 + p_n(\omega)^2 > 0$.

Given n Lanczos coefficients $\{b_k\}_{k=1}^n$, the orthogonal polynomials $p_k(\omega)$ can be computed exactly up to order n using the recursion relation Eq. (30), so if we knew the phase function $I_n(\omega)$, then we would be able to recover the spectral function $\Phi(\omega)$ from Eq. (95). However, $I_n(\omega) = \int_0^\omega \sigma_n(\omega') d\omega'$ is defined in terms of the equilibrium measure σ_n , and computing that *exactly* via Eqs. (46), (50) and (51) requires prior knowledge of Φ , precisely the function we are trying to estimate in the first place.

Our solution is to derive a large- n approximation for $\sigma_n(\omega)$ using the polynomial asymptotics Eqs. (93) and (94). If we differentiate either of these equations with respect to ω , we will get terms involving the derivative $I'_n(\omega) = \sigma_n(\omega)$, which is what we want. However, we will also get terms involving the derivative $\Phi'(\omega)$, which is a new unknown. The trick is to consider a certain ‘determinantal’ combination of derivatives. In particular, the Christoffel-Darboux formula [67] shows that the diagonal Christoffel-Darboux kernel $K_n(\omega, \omega) = \sum_{k=0}^{n-1} p_k(\omega)^2$ can be expressed as

$$K_n(\omega, \omega) = b_n \det \begin{pmatrix} p_{n-1}(\omega) & p'_{n-1}(\omega) \\ p_n(\omega) & p'_n(\omega) \end{pmatrix}. \quad (96)$$

This determinantal structure ensures exact cancellation of the terms involving the unwanted derivative $\Phi'(\omega)$. More explicitly, if we write the asymptotics in Eqs. (93) and (94) as $p_{n-1}(\omega) \equiv \Phi(\omega)^{-1/2} \alpha_{n-1}(\omega)$ and $p_n(\omega) \equiv \Phi(\omega)^{-1/2} \alpha_n(\omega)$, then we have (suppressing ω arguments for ease of notation)

$$\begin{aligned} K_n &= b_n \det \begin{pmatrix} \Phi^{-1/2} \alpha_{n-1} & (\Phi^{-1/2} \alpha_{n-1})' \\ \Phi^{-1/2} \alpha_n & (\Phi^{-1/2} \alpha_n)' \end{pmatrix}, \\ &= b_n \Phi^{-1} \det \begin{pmatrix} \alpha_{n-1} & \alpha'_{n-1} \\ \alpha_n & \alpha'_n \end{pmatrix} - \frac{b_n}{2} \Phi' \Phi^{-2} \det \begin{pmatrix} \alpha_{n-1} & \alpha_{n-1} \\ \alpha_n & \alpha_n \end{pmatrix}, \\ &= b_n \Phi^{-1} [\alpha_{n-1} \alpha'_n - \alpha'_{n-1} \alpha_n]. \end{aligned}$$

Thus the term proportional to $\Phi'(\omega)$ vanishes as claimed due to rank deficiency. This argument does not rely on the detailed form of the polynomial asymptotics, other than the fact that $p_{n-1}(\omega)$ and $p_n(\omega)$ are both pointwise proportional to $\Phi(\omega)^{-1/2}$, and so will generalize to other frequency regimes discussed in subsequent sections.

Now, carrying out the relevant derivatives of Eqs. (93) and (94) and rearranging, we get the second of our bootstrap equations:

$$\sigma_n(\omega) \approx \frac{\Phi(\omega)}{2\pi} K_n(\omega, \omega) + (-1)^n \frac{\beta_n \cos[2\pi I_n(\omega)]}{2\pi(\beta_n^2 - \omega^2)}. \quad (97)$$

The kernel $K_n(\omega, \omega)$ can be calculated in terms of the orthogonal polynomials using Eq. (96), which we remind the reader can be computed exactly in terms of the Lanczos coefficients $\{b_k\}_{k=1}^n$ using the three-term recurrence Eq. (30). Eq. (97) was proven by different means for a similar class of spectral functions in [105, Theorem 9.5], but only with the first term on the RHS, which dominates the second term by a factor of $\mathcal{O}(\beta_n)$ when ω is $\mathcal{O}(1)$.

Since $\partial_\omega I_n(\omega) = \sigma_n(\omega)$, Eqs. (95) and (97) constitute a first-order ordinary differential equation for $I_n(\omega)$ which is closed at leading order in n , and whose solution yields $\Phi(\omega)$ as a byproduct. Crucially, we also have the initial condition $I_n(0) = 0$, allowing us to iteratively solve this differential equation and thereby obtain a finite- n approximation to the spectral function. Given a choice of frequency spacing $\delta\omega \ll 1$ and a maximum frequency ω_{\max} satisfying $0 < \omega_{\max} \ll \beta_n$, the algorithm works as follows:

0. Set $\omega = 0$ and $I_n(0) = 0$.
1. Compute $\Phi(\omega)$ using Eq. (95).
2. Compute $\sigma_n(\omega)$ using Eq. (97).
3. Set $I_n(\omega + \delta\omega) = I_n(\omega) + \sigma_n(\omega) \times \delta\omega$.

4. Increment $\omega \mapsto \omega + \delta\omega$.

5. Repeat steps 1-4 until $\omega = \omega_{\max}$, then terminate.

As an example we will again consider the mixed field Ising model (MFIM). We will compare the results to those obtained through the ‘simple procedure’ described at the start of the section where we replace the level- n Green’s function $G_n(z)$ by the universal ‘semicircle’ form in Eq. (81), as well as to the spectral function resulting from Fourier transforming the real-time autocorrelation function $(\mathcal{J}|\mathcal{J}(t))/\sqrt{L}$ obtained using time-evolving block decimation (TEBD). For the spectral bootstrap we compute $n = 40$ Lanczos coefficients, going up to $\omega_{\max} = 0.99\beta_n$, with $\beta_n \approx 2b_n \approx 46.1$ for $n = 40$ in the MFIM. For the real-time evolution, we go up to $t_{\max} = 10$ using a timestep of $dt = 0.01$, with a maximum bond dimension of $\chi_{\max} = 512$ and a system size $L = 201$ large enough that finite-size effects are negligible over these timescales. We can see from the main panel of Fig. 8(a) that the spectral bootstrap and semicircle approximation give numerically identical results throughout this bulk frequency range, providing an important self-consistency check. The spectral bootstrap also generally agrees well with the Fourier transform data at low to moderate frequencies. There is some deviation around $\omega = 0$, but it is hard to do a fair comparison because it is not clear how to systematically convert between n and t_{\max} . As a rough indication of computational effort, our Julia implementation of the Lanczos algorithm took ~ 30 min and ~ 60 GiB RAM on a single CPU core to compute $n = 40$ Lanczos coefficients for the MFIM, while our TEBD simulation performed using TeNPy [106] took ~ 30 h on 8 cores using ~ 2 GiB RAM. However, the TEBD runtime is highly parameter dependent, and could be reduced by using a larger dt or a smaller χ_{\max} . At any rate, the initial $\omega = 0$ step of the spectral bootstrap corresponds to the $\rho = 0$ case of the procedure for extracting diffusion constants described in Section VB, and in Fig. 6(a) we already demonstrated quantitative accuracy in the $n \rightarrow \infty$ limit.

More noticeable differences between the spectral bootstrap and the Fourier transformed correlator can be found at high frequencies, as shown in the left inset of Fig. 8(a). What is striking about the spectral bootstrap data is that we are able to resolve the log-correction due to geometric constraints on operator growth in 1D [10]: Lanczos coefficients growing like $b_n \sim n/\log n$ correspond to a spectral function decaying like $\Phi(\omega \rightarrow \infty) \sim \exp[-\mathcal{O}(\omega \log \omega)]$ (c.f. Eq. (44)), rather than the generic exponential bound $\Phi(\omega \rightarrow \infty) \sim \exp[-\mathcal{O}(\omega)]$ expected in higher dimensions. Further evidence for this is shown in Fig. 8(b), where we find that $\log[\Phi(\omega)]/\omega \log \omega$ plateaus at large frequencies, while without the log correction $\log[\Phi(\omega)]/\omega$ continues to decay. The estimates appear to be well converged with n provided we restrict to $|\omega| < \beta_n$ (which is why the smaller n curves stop at smaller ω). Convincingly resolving this log-correction had previously required going to much larger n using a Monte-Carlo algorithm that exploits the lack of a sign-problem for operator growth in

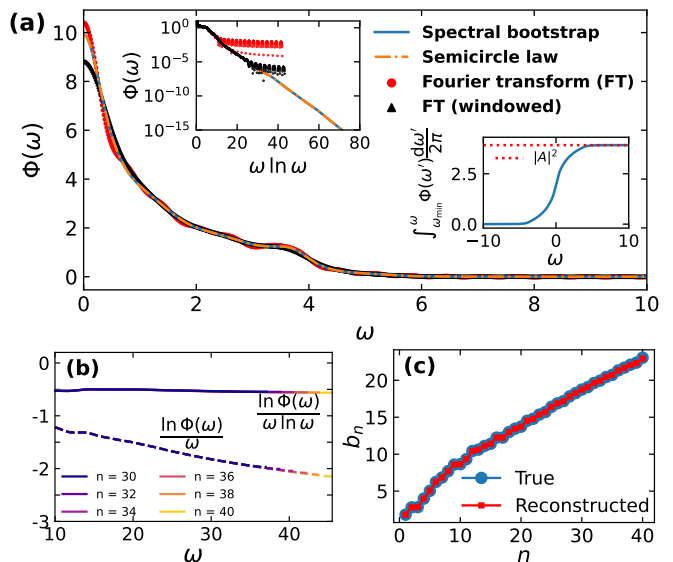


FIG. 8. (a) The $n = 40$ approximation to the spectral function of the energy current operator of the mixed field Ising model, with a comparison between the spectral bootstrap and approximating the level- n Green’s function by the ‘semicircle form’ in Eq. (81), and the Fourier transform (FT) of the real-time correlator $C(t) = (\mathcal{J}|\mathcal{J}(t))/L$ up to $t_{\max} = 10$. We also show the Fourier transform of $C(t)$ multiplied by the cosine window $\frac{1}{2}[1 + \cos(\pi t/t_{\max})]$ in order to reduce spectral leakage due to the finite t_{\max} . The left inset demonstrates the high-frequency scaling $\Phi(\omega) \sim \exp[-\mathcal{O}(\omega \log \omega)]$ expected in one spatial dimension [10]. The right inset verifies the sum rule for the approximate spectral function obtained using the spectral bootstrap. (b) The spectral function $\Phi(\omega)$ obtained using the spectral bootstrap, rescaled in two ways, as evidence that $\Phi(\omega)$ decays like $\Phi(\omega \rightarrow \infty) \sim \exp[-\mathcal{O}(\omega \log \omega)]$ rather than $\Phi(\omega \rightarrow \infty) \sim \exp[-\mathcal{O}(\omega)]$. (c) Reconstructed Lanczos coefficients b_n , calculated using the estimate of the spectral function obtained using the spectral bootstrap, and compared with the exact Lanczos coefficients. The close agreement is strong evidence that the spectral bootstrap is producing a good approximation to the true spectral function.

the MFIM [50, 107].

Getting the correct high-frequency tail from the Fourier transformed real-time correlation function can be challenging due to spectral leakage arising from cutting off the Fourier transform integral at a finite t_{\max} . Indeed, we can see in the left inset to Fig. 8(a) that the spectral function from the Fourier transform does not have the expected quasi-exponential high-frequency decay. The standard fix to this problem of spectral leakage is to multiply the real-time correlator by a windowing function before taking the Fourier transform [108]. We also show in Fig. 8(a) the results from multiplying by a simple finite cosine window $\frac{1}{2}[1 + \cos(\pi t/t_{\max})]$. This extends the maximum frequency at which the Fourier transform data agrees with the high frequency tail of the spectral bootstrap, but still eventually leads to an unphysical plateau at very high frequencies. This high frequency tail could likely be improved further by both reducing dt and increasing

t_{\max} , at the cost of increased computational resources. Fig. 8(b) shows that the high-frequency tail of the spectral bootstrap is converged with n at least up to $\omega \approx 40$, so this Lanczos approach appears to be particularly well suited to reliably extracting high-frequency information.

To further verify the accuracy of the spectral function approximation $\Phi_{\text{est}}(\omega)$ obtained using the spectral bootstrap, we attempt to reconstruct the exact sequence of Lanczos coefficients by carrying out the three-term recurrence relation Eq. (30) for the orthogonal polynomials, but computing the norm

$$b_n^2 = \int_{\mathbb{R}} [\omega p_{n-1}(\omega) - b_{n-1} p_{n-2}(\omega)]^2 \frac{\Phi(\omega)}{2\pi} d\omega \quad (98)$$

by numerically evaluating the integral with $\Phi(\omega)$ approximated by $\Phi_{\text{est}}(\omega)$. We can only compute this integral up to the maximum frequency $\omega_{\max} = 0.99\beta_n$ for which we performed the spectral bootstrap, but this is sufficient to capture almost all of the norm contributing to b_n , for reasons discussed in Section IV A. The result is shown in Fig. 8(c), where we find very close agreement between the exact and the reconstructed Lanczos sequence, thus providing strong evidence that the spectral bootstrap yields a good approximation to the true spectral function (see Fig. 10(c) for more examples). As a final nontrivial check, the right inset to Fig. 8(a) shows that the sum rule $\int_{\mathbb{R}} \Phi(\omega) d\omega / 2\pi = \langle A | A \rangle$ is verified very accurately. Using the spectral function extracted in the range $\omega \in [-0.99\beta_n, 0.99\beta_n]$, we find that the sum rule is satisfied up to a relative error of $\sim 10^{-6}$.

Before proceeding, we remark that it is also possible to start this bulk bootstrap at some nonzero frequency ω_0 as follows. Use the semicircle approximation (Eq. (81)) to the level- n Green's function $G_n(\omega_0 \pm i0^+)$ to approximate the spectral function $\Phi(\omega_0)$, as described at the start of Section VII. Then numerically solve Eq. (95) to determine $I_n(\omega_0) \pmod{1}$ and use Eq. (97) to compute $\sigma_n(\omega_0)$. Then one can proceed with the main routine of the bulk spectral bootstrap. This ability to start away from the special points $\omega = 0, \pm\beta_n$ is a particular feature of the bulk bootstrap, owing to the fact that the bulk Green's function in Eq. (81) contains only a single free parameter, β_n , which can be directly estimated from the Lanczos coefficients.

B. Generalization to arbitrary ρ : the Bessel bootstrap

The algorithm outlined in the previous section made use of the $n \rightarrow \infty$ asymptotics of the orthogonal polynomials. When $\rho \neq 0$ these asymptotics are modified, particularly near $\omega = 0$, the location of the power-law. Once we have the correct asymptotics, however, then the differential equation can be solved iteratively as before. We will aim to capture the ‘envelope function’ $\Phi(\omega)/|\omega|^\rho \equiv 2\pi \exp[-Q(\omega)]$, since this is what is needed to determine the values of hydrodynamic transport coefficients.

For the initial step at $\omega = 0$, we use the result of Theorem 3, which we restate here, together with a result relating this to the equilibrium density at the origin:

$$e^{-Q(0)} \approx \frac{2(1+\rho)^\rho}{\Gamma\left[\frac{1}{2}(1+\rho)\right]^2} \frac{[K_n(0,0)]^\rho}{[\beta_n(p_{n-1}(0)^2 + p_n(0)^2)]^{1+\rho}}, \quad (99)$$

$$\sigma_n(0) \approx \frac{2}{\pi} \left(\Gamma\left[\frac{1}{2}(1+\rho)\right] \Gamma\left[\frac{1}{2}(3+\rho)\right] e^{-Q(0)} K_n(0,0) \right)^{\frac{1}{1+\rho}}. \quad (100)$$

These are the $\omega \rightarrow 0^+$ limits of the following equations which we will use for $\omega > 0$. For the envelope function we have

$$e^{-Q(\omega)} \approx \frac{1}{p_{n-1}(\omega)^2 + p_n(\omega)^2} \frac{1}{\sqrt{\beta_n^2 - \omega^2}} \frac{\pi I_n(\omega)}{\omega^\rho} \left[\left(J_{\frac{1}{2}(\rho-1)}^2 + J_{\frac{1}{2}(\rho+1)}^2 \right) (\pi I_n(\omega)) \right. \\ \left. - (-1)^n \frac{\omega}{\beta_n} \left(2J_{\frac{1}{2}(\rho-1)} J_{\frac{1}{2}(\rho+1)} \right) (\pi I_n(\omega)) \cos \left\{ \rho \arcsin \left(\frac{\omega}{\beta_n} \right) \right\} \right], \quad (101)$$

where $I_n(\omega)$ is defined as before in Eq. (92), J_α is a Bessel function of the first kind, and we are using the shorthand $(J_\alpha^2 + J_\beta^2)(x) \equiv J_\alpha^2(x) + J_\beta^2(x)$, $(J_\alpha J_\beta)(x) \equiv J_\alpha(x) J_\beta(x)$, etc. For the equilibrium density we have

$$\sigma_n(\omega) \approx \frac{4}{\pi} \frac{K_n(\omega, \omega) \omega^\rho e^{-Q(\omega)}}{\pi I_n(\omega)} \frac{1}{\left[J_{\frac{1}{2}(\rho-1)}^2 + J_{\frac{1}{2}(\rho+1)}^2 - J_{\frac{1}{2}(\rho-3)} J_{\frac{1}{2}(\rho+1)} - J_{\frac{1}{2}(\rho-1)} J_{\frac{1}{2}(\rho+3)} \right] (\pi I_n(\omega))}. \quad (102)$$

We derive these expressions in Section S4B. One can check that they reduce to Eqs. (95) and (97) upon sending

$\rho \rightarrow 0$. Unlike for $\rho = 0$, where the asymptotics were valid out to $\omega = \mathcal{O}(\beta_n)$, these asymptotics are in principle valid only for ω within some $\mathcal{O}(1)$ window around $\omega = 0$, essentially the ‘hydrodynamic’ frequency regime where we expect the power-law to dominate the behavior of the spectral function. Note that, taking $\omega = \mathcal{O}(1)$, Eqs. (101) and (102) have been slightly simplified by dropping some terms which are subleading as $n \rightarrow \infty$; see Eqs. (S4.22) and (S4.23) for the full expressions. In practice we have found that these simplified expressions give numerical results very close to those of the full expressions, provided n is large enough that $\omega/\beta_n \ll 1$.

The appearance of the Bessel functions in these equations is a signature of ‘Bessel universality’, akin to that found in random matrix ensembles whose probability measures behave as a power-law near the origin [27, 109]. For larger ω , one could then switch to the asymptotics in the ‘bulk’, which should then be valid up until $|\omega| \lesssim \beta_n$ like those stated for $\rho = 0$, but in practice we have found that just using the Bessel asymptotics gives good results for the frequency regime where the spectral function is non-negligible.

With these asymptotics in hand, we now have another first-order differential equation which we can iteratively solve as follows to obtain a finite n approximation to the spectral function. We initialize by setting $\omega = 0$ and $I_n(0) = 0$, computing $e^{-Q(0)}$ via Eq. (99) and $\sigma_n(0)$ via Eq. (100), then setting $I_n(\delta\omega) = I_n(0) + \sigma_n(0) \times \delta\omega$ and incrementing $\omega \mapsto \omega + \delta\omega$. Then the main routine is conceptually identical to the procedure outlined for $\rho = 0$:

1. Compute $e^{-Q(\omega)}$ using Eq. (101).
2. Compute $\sigma_n(\omega)$ using Eq. (102).
3. Set $I_n(\omega + \delta\omega) = I_n(\omega) + \sigma_n(\omega) \times \delta\omega$.
4. Increment $\omega \mapsto \omega + \delta\omega$.
5. Repeat steps 1-4 until $\omega = \omega_{\max}$, then terminate.

To illustrate this generalized spectral bootstrap (SB), we try to reconstruct the envelope functions of some toy spectral functions of the form $\Phi(\omega)/2\pi = |\omega|^\rho \exp[-Q(\omega)]$ for $\rho = -\frac{1}{2}$, again comparing with the recursion method (RM) [19]. Fig. 9(a) shows the comparison for $Q(x) = \frac{1}{2}(x^6 - 5x^4 + 20x^2 + 1)^{1/3}$. This function has no special significance other than the fact that $Q(x) \sim \mathcal{O}(x^2)$, so we have $b_n \sim \mathcal{O}(\sqrt{n})$. Here there is an exactly solvable model available for the recursion method which has the relevant features of Gaussian decay and a zero frequency power-law [19]. The model spectral function is $\tilde{\Phi}(\omega) = \frac{2\pi/\omega_0}{\Gamma[\frac{1}{2}(1+\rho)]} |\omega/\omega_0|^\rho \exp[-(\omega/\omega_0)^2]$, where ω_0 and ρ are tunable parameters. Crucially, its Lanczos coefficients are known to be $b_{2k-1} = \omega_0 \sqrt{(2k-1+\rho)/2}$ and $b_{2k} = \omega_0 \sqrt{2k/2}$, and its Green’s function is $\tilde{G}(z) = (iz/\omega_0^2) \exp[-(z/\omega_0)^2] E_{\frac{1}{2}(1+\rho)}[-(z/\omega_0)^2]$, where $E_\alpha(x)$ is the generalized exponential integral. We recover the envelope function from the RM using $e^{-Q(\omega)} = |\omega|^{-\rho} \Phi(\omega)/2\pi$

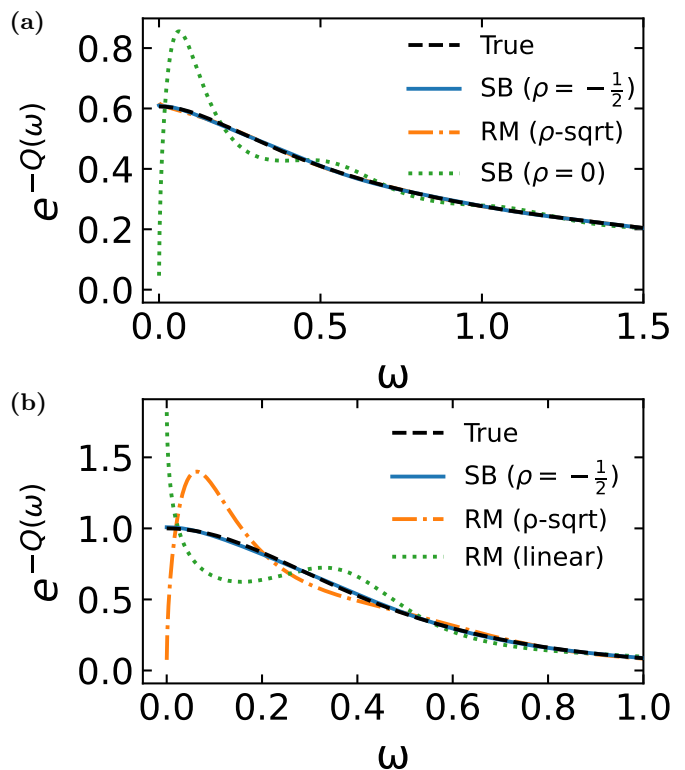


FIG. 9. Reconstructing the spectral envelope function $\exp[-Q(\omega)]$ for a toy spectral function $\Phi(\omega)/2\pi = |\omega|^{-1/2} \exp[-Q(\omega)]$, using the spectral bootstrap (SB) and the recursion method (RM). (a) $Q(\omega) = \frac{1}{2}(\omega^6 - 5\omega^4 + 20\omega^2 + 1)^{1/3}$, which has $b_n \sim \mathcal{O}(\sqrt{n})$. Here there is an appropriate exact ‘stitching function’ for the RM (see main text), so the RM and the $\rho = -1/2$ SB work equally well. The $\rho = 0$ SB curve illustrates the errors one can make by not accounting for the power-law. (b) Same as (a), except now $Q(\omega) = -\log \operatorname{sech} \pi\omega$, which has $b_n \sim \mathcal{O}(n)$. Only the $\rho = -\frac{1}{2}$ SB accurately recovers the spectral function. Now there is no available stitching function with the appropriate power-law behavior, so the RM performs poorly. For the RM one has exact solutions with the right low frequency power-law but the wrong high frequency tail (ρ -sqrt), or no low frequency power-law but the right high frequency tail (linear), neither of which gives the correct result at low frequencies.

with $\Phi(\omega) = 2 \operatorname{Im} G(\omega - i\epsilon)$, $\epsilon = 10^{-14}$. In this case, the SB and the RM with $\rho = -1/2$ give essentially identical results. We also show the result of $e^{-Q(\omega)} = |\omega|^{1/2} \Phi(\omega)/2\pi$ where $\Phi(\omega)$ is computed using the SB with $\rho = 0$, showing that one can get large errors near $\omega = 0$ if one does not take into account the power-law, although at larger ω the agreement does become better.

This first example showed that, when we have available an exactly solvable spectral function that captures the relevant features of the high-frequency decay and the low-frequency power-law, then the recursion method can work very well. One problem with the recursion method, though, is that the existence of these special solutions is not guaranteed for all problems of interest (see Ref. [19] for a review). In order for the recursion method to work

well, one needs to have an exact model solution for all three of the spectral function, the Green's function, and the Lanczos coefficients. Unfortunately, while there is a power-law solution available with Gaussian high-frequency decay, to our knowledge there is no such solution available which has both a low-frequency power-law and *exponential* decay. This is potentially a problem because the operator growth hypothesis posits that such exponential decay is generic for chaotic quantum systems [10]. Fig. 9(b) shows that when $\rho \neq 0$ it is important to get both of these ingredients correct to accurately capture the $\omega \rightarrow 0$ behavior of the spectral function. We consider the toy spectral function $\Phi(\omega)/2\pi = |\omega|^{-1/2} \text{sech}(\pi\omega)$, which decays exponentially as $\omega \rightarrow \infty$. The $\rho = -\frac{1}{2}$ spectral bootstrap (SB) captures the true spectral function very well. However, since there is now no available exact solution, the RM performs poorly. One could try using the Meixner-Pollaczek solution from Ref. [10] to capture the high-frequency tail while ignoring the low frequency power-law, which is labeled 'RM (linear)'. Or one could try using the exact solution from the previous example to get the low frequency power-law correct, at the cost of getting the high-frequency tail wrong, which is labeled 'RM (ρ -sqrt)'. However, both of these approaches result in large errors at low frequencies, and so only the $\rho = -\frac{1}{2}$ spectral bootstrap correctly captures the true low frequency behavior of the spectral function. This highlights one of the advantages of the spectral bootstrap over the recursion method: it does not require any exact solutions, and so can be equally employed for a wide range of growth behaviors of the Lanczos coefficients.

From the discussion in Section VI, we know that for $\rho = 0$ there is a great deal of freedom in choosing the stitching function for the recursion method, and in particular it is *not* necessary for the stitching function to have a high frequency decay matching that of the true spectral function; one only needs that the level- n Green's function satisfies $G_n(\omega \pm i0^+) \approx \mp i/b_n$ as $\omega \rightarrow 0$ and $n \rightarrow \infty$, which is much more generic. One then might wonder why for $\rho \neq 0$ we no longer have such freedom, since it appears to be necessary to also match the high frequency behavior (the relevance of matching the low frequency behavior is perhaps more intuitive). This is because the nontrivial low-frequency behavior of $\Phi(\omega \rightarrow 0) \sim |\omega|^\rho$ couples to the equilibrium density $\sigma_n(0)$ when $\rho \neq 0$ (c.f. Theorem 1 and Eq. (58)), and $\sigma_n(0)$ depends nontrivially on the high frequency decay of the spectral function (c.f. Lemma 2), being sensitive to a Coulomb gas confinement transition. This coupling is seen most explicitly in Eq. (84), where we show that the level $2n$ Green's function $G_{2n}(\omega \pm i0^+)$ is primarily a function of $\pi\sigma_{2n}(0)\omega$ as $\omega \rightarrow 0$ and $n \rightarrow \infty$.

VIII. RANDOM MATRIX UNIVERSALITY

While we developed the spectral bootstrap with the practical aim of recovering the spectral function $\Phi(\omega)$ from its Lanczos coefficients, as a byproduct we also get

an estimate of the equilibrium measure $\sigma_n(\omega)$. We can use this to perform various self-consistency checks. In particular, while we cannot usually verify that a given many-body spectral function obeys all the assumptions under which we derive our results, we can at least check that our estimates of $\Phi(\omega)$ and $\sigma_n(\omega)$ are consistent with the behavior expected given those assumptions. One notable example is the emergence of 'universality' akin to that governing eigenvalue correlations in random matrix theory (RMT) [31]. Just as universality appears in the $n \rightarrow \infty$ of $n \times n$ random matrices, here it should appear in the limit $n \rightarrow \infty$ of large Lanczos index. From a physical point of view, this RMT-like universality is interesting because it seems to be 'superuniversal', in the sense that it can appear not only for chaotic models, which might be expected from studies of eigenstate thermalization [43], but also in integrable and non-interacting models, provided they have sufficiently smooth spectral functions in the thermodynamic limit. What changes between these classes of operator dynamics is the n -dependence of the frequency scale on which this RMT universality appears, due to the different scaling of b_n .

A. Background

Given a spectral function $\Phi(\omega)$, we can define a unitarily-invariant ensemble of $n \times n$ Hermitian random matrices whose eigenvalues are distributed according to

$$P(\boldsymbol{\lambda})d^n\boldsymbol{\lambda} = \frac{1}{Z_n} \left(\prod_{i<j} |\lambda_i - \lambda_j|^2 \right) \prod_i \frac{\Phi(\lambda_i)}{2\pi} d\lambda_i, \quad (103)$$

where $\boldsymbol{\lambda} = (\lambda_1, \dots, \lambda_n)$ with the ordering $\lambda_1 \leq \lambda_2 \leq \dots \leq \lambda_n$, and Z_n is a normalization constant. The bracketed prefactor is the Vandermonde determinant which gives rise to level repulsion. We consider this random matrix ensemble because its eigenvalue distribution will be governed by the same Coulomb gas as that controlling the Lanczos operators via the orthogonal polynomials $p_n(\omega)$.

For any $1 \leq m \leq n-1$, let

$$R_m(\lambda_1, \dots, \lambda_m) = \frac{n!}{(n-m)!} \int_{\mathbb{R}} \dots \int_{\mathbb{R}} P(\lambda_1, \dots, \lambda_m, \lambda_{m+1}, \dots, \lambda_n) d\lambda_{m+1} \dots d\lambda_n \quad (104)$$

denote the m -point eigenvalue correlation function. A remarkable property of these random matrix ensembles is that all of the correlation functions can be written in terms of a determinant of a 2-point correlation kernel [30],

$$R_m(\lambda_1, \dots, \lambda_m) = \det \left[\left(\hat{K}_n(\lambda_i, \lambda_j) \right)_{1 \leq i, j \leq m} \right]. \quad (105)$$

The correlation kernel \hat{K}_n is a weighted version of the Christoffel-Darboux kernel K_n defined in Eq. (65),

$$\hat{K}_n(\omega_a, \omega_b) = \sqrt{w(\omega_a)w(\omega_b)} K_n(\omega_a, \omega_b), \quad (106)$$

where $w(\omega) = \Phi(\omega)/2\pi$ is the weight function defining the random matrix ensemble. In the Lanczos language, from Eq. (31) we can see that $\hat{K}_n(\omega_a, \omega_b)$ is the integral kernel (in frequency space) of the projection superoperator \mathcal{P}_n on to the first n Lanczos operators [25]

$$\mathcal{P}_n = \sum_{m=0}^{n-1} |O_m\rangle\langle O_m|, \quad (107)$$

which is the complement of the projector $\mathcal{Q}_n = \mathbb{1} - \mathcal{P}_n$ used to construct the level- n Green's function $G_n(z)$ (Section VI). By studying $\hat{K}_n(\omega_a, \omega_b)$, we can characterize this slow/fast operator projection in frequency space.

A further remarkable property of random matrix ensembles is that for large- n their eigenvalue correlations often display *universality* [31]. This manifests in $\hat{K}_n(\omega_a, \omega_b)$ approaching a universal form in different sections of the spectrum when probed on the appropriate scale, independent of the precise form of the weight w . For example, for ω in the 'bulk' of the spectrum, $|\omega| \ll \beta_n$, we get

$$\frac{1}{\sigma_n(\omega)} \hat{K}_n \left(\omega + \frac{u}{\sigma_n(\omega)}, \omega + \frac{v}{\sigma_n(\omega)} \right) \xrightarrow{n \rightarrow \infty} \mathbb{S}(u, v), \quad (108)$$

for $u, v \in \mathbb{R}$, so for large- n the local eigenvalue correlations are described by the *sine kernel*

$$\mathbb{S}(u, v) = \frac{\sin[\pi(u - v)]}{\pi(u - v)}. \quad (109)$$

Note that the RHS of Eq. (108) is translation invariant, provided ω is within the bulk of the spectrum.

If the weight function has a power-law at the origin, $w(x) = |x|^\rho e^{-Q(x)}$, then this affects the local eigenvalue correlations near the origin. Rather than the sine kernel, at $\omega = 0$ we instead have *Bessel universality*:

$$\frac{1}{\sigma_n(0)} \hat{K}_n \left(\frac{u}{\sigma_n(0)}, \frac{v}{\sigma_n(0)} \right) \xrightarrow{n \rightarrow \infty} e^{-\frac{i\rho}{2}(\arg u + \arg v)} \mathbb{J}_{\rho/2}(u, v), \quad (110)$$

where $\mathbb{J}_{\rho/2}$ is the Bessel kernel given by

$$\mathbb{J}_{\rho/2}(u, v) = \pi \sqrt{u} \sqrt{v} \frac{J_{\rho+1}(\pi u) J_{\rho-1}(\pi v) - J_{\rho-1}(\pi u) J_{\rho+1}(\pi v)}{2(u - v)} \quad (111)$$

with J_α a Bessel function of the first kind.

Finally, for eigenvalues near the edge of the spectrum, $\omega \approx \beta_n$, the bulk sine universality gives way to *Airy universality*, such that

$$\frac{\beta_n}{c_n n^{2/3}} \hat{K}_n \left(\beta_n + \frac{\beta_n}{c_n n^{2/3}} u, \beta_n + \frac{\beta_n}{c_n n^{2/3}} v \right) \xrightarrow{n \rightarrow \infty} \mathbb{A}(u, v), \quad (112)$$

where $c_n := (h_n(1)/\sqrt{2})^{2/3}$ is $\mathcal{O}(1)$ (note $c_n n^{2/3} = f'_n(1)$ by Eq. (S5.2)), and the Airy kernel \mathbb{A} is given by

$$\mathbb{A}(u, v) = \frac{\text{Ai}(u) \text{Ai}'(v) - \text{Ai}(v) \text{Ai}'(u)}{u - v}, \quad (113)$$

where Ai is the Airy function of the first kind.

Theorem 4. For our class of spectral functions (see Section S1 A for a definition), the corresponding correlation kernels \hat{K}_n satisfy the universal scalings Eqs. (108), (110) and (112) in the relevant sections of the spectrum.

This theorem follows as a direct consequence of the $n \rightarrow \infty$ asymptotics we established for the orthogonal polynomials, such as Eqs. (93) and (94) in the bulk of the spectrum. See Section S4 for the full asymptotic expressions.

B. Universality in quantum operator dynamics

While we can prove the emergence of universality for spectral functions obeying our assumptions, it would be gratifying to see this also emerge in more familiar many-body quantum models, even though we cannot explicitly verify that our assumptions hold. Indeed, universality is a very generic phenomenon [28, 110, 111], particularly in the bulk, and it may well hold even if some of our assumptions are violated (such as our analyticity requirements). Using the spectral bootstrap algorithm described in Section VII, we can estimate both the weight function $w(\omega) = \Phi(\omega)/2\pi$ and the equilibrium measure $\sigma_n(\omega)$ for a given many-body model, using only a finite number of its Lanczos coefficients. We can then perform a self-consistent check that these approximations reproduce the universal scalings Eqs. (108), (110) and (112).

The evidence we will present for universality in many-body models comes with a qualification. To test for universality requires explicitly knowing the spectral function $\Phi(\omega)$ and the equilibrium measure $\sigma_n(\omega)$, but for most interacting many-body models this is not analytically tractable. For models where we do not know $\Phi(\omega)$, we use our spectral bootstrap algorithm to first obtain a finite- n approximation to $\Phi(\omega)$ and $\sigma_n(\omega)$. The qualification is that this algorithm *assumes* the validity of Plancherel-Rotach asymptotics for the orthogonal polynomials (e.g. Eqs. (93) and (94)), from which universality can be derived as a consequence [22]. (But we do prove these asymptotics hold under reasonable assumptions on the spectral function.) To avoid circularity, we perform independent cross-checks of these estimates of $\Phi(\omega)$ and $\sigma_n(\omega)$, such as the ability to reconstruct the numerically exact Lanczos coefficients (Fig. 10(c)). If these checks are passed convincingly, which turns out to be the case for the physical models we consider, then this gives strong evidence that we have obtained accurate estimates of the true spectral function and equilibrium measure. With those in hand, it is then reasonable to test for universality.

Before proceeding, we make a practical consideration. The statements of universality in Eqs. (108), (110) and (112) are made under the approximation that the equilibrium density $\sigma_n(\omega)$ is locally constant. This approximation becomes increasingly well justified as $n \rightarrow \infty$, but for the finite n we have available to us numerically,

this approximation is not necessarily so good, particularly near the origin for exponentially decaying spectral functions which are at the Coulomb gas confinement transition (see Fig. 10(b) for some physical examples). We will adopt a practice that is standard in the random matrix theory literature, namely ‘unfolding’ the spectrum [112], which involves transforming to new coordinates that account for variation of the local density. Fixing a frequency ω at which we want to test for universality, we define

$$F_{n,\omega}(x) := \int_{\omega}^x \sigma_n(s) ds, \quad (114)$$

$$= I_n(x) - I_n(\omega),$$

where $I_n(\omega) = \int_0^{\omega} \sigma_n(s) ds$ was defined in Eq. (92). Now note that, if we approximate $\sigma_n(s) \approx \sigma_n(\omega)$ as constant in Eq. (114), then each of the arguments of the kernel \hat{K}_n in Eq. (108) can be expressed in terms of the inverse function $F_{n,\omega}^{-1}(u) \approx \omega + u/\sigma_n(\omega)$. Then the statement Eq. (108) of bulk universality at frequency ω can be rewritten as

$$\left(\frac{F_{n,\omega}^{-1}(u) - F_{n,\omega}^{-1}(v)}{u - v} \right) \hat{K}_n \left(F_{n,\omega}^{-1}(u), F_{n,\omega}^{-1}(v) \right) \xrightarrow{n \rightarrow \infty} \mathbb{S}(u, v). \quad (115)$$

The point is that, even in the situation where the equilibrium density $\sigma_n(\omega)$ is not constant and $F_{n,\omega}$ must be inverted numerically, this formulation of bulk universality will account for that variation, and so one can still expect to observe the sine kernel. (The inverse $F_{n,\omega}^{-1}$ is well-defined because $F_{n,\omega}$ is the integral of a positive function $\sigma_n(\omega) > 0$, so is increasing.) The statement Eq. (110) of Bessel universality can be expressed in the same way by setting $\omega = 0$, with only the RHS changing to the Bessel kernel instead of the sine kernel. The statement Eq. (112) of Airy universality around $\omega = \beta_n$ can also be made with the same LHS, but with $F_{n,\beta_n}(x)$ redefined as

$$\text{(Airy)} \quad F_{n,\beta_n}(x) := f_n(x/\beta_n), \quad (116)$$

where f_n is defined in Eq. (S5.1).

1. Sine universality in the bulk

First we check for sine universality in the bulk of the spectrum, taking as examples the chaotic mixed field Ising model (MFIM), the interacting integrable XXZ chain, and the non-interacting transverse field Ising model (TFIM). We take the initial Lanczos operator to be the total energy current for the MFIM, the total spin current for the $\Delta = 2$ XXZ model, and $\frac{1}{\sqrt{L}} \sum_x Y_x Y_{x+1}$ for the TFIM (with XX interactions), and compute $n = 40, 20, 40$ Lanczos coefficients respectively. Since in each case we expect the autocorrelation function $C(t)$ to decay faster than $1/t$, such that $0 < |\Phi(\omega = 0)| < \infty$, we set $\rho = 0$ and start testing for bulk universality at $\omega = 0$. Note that, for $\rho = 0$, our assumptions on the spectral function (Section S1 A)

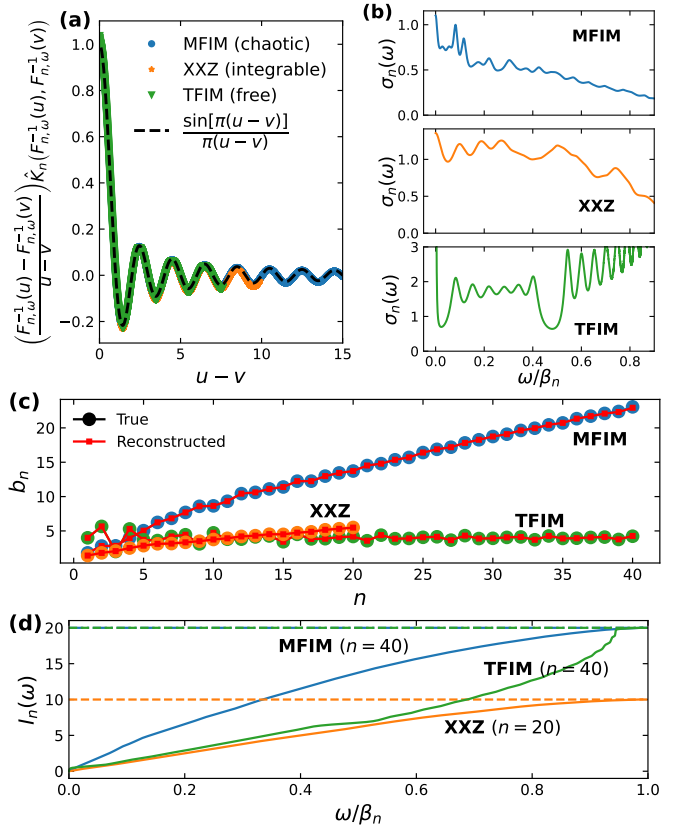


FIG. 10. (a) Sine kernel universality [c.f. Eqs. (109) and (115)] in the bulk spectra of the chaotic mixed field Ising model (MFIM), the interacting integrable XXZ chain, and the non-interacting transverse field Ising model (TFIM). There are no free fitting parameters; everything is extracted from the Lanczos coefficients using the spectral bootstrap (Section VII A). (b) Equilibrium densities $\sigma_n(\omega)$ estimated using the spectral bootstrap algorithm. Note the significant variation of $\sigma_n(\omega)$ with ω , which necessitates the unfolding procedure. (c) Reconstructed Lanczos coefficients b_n , calculated using the estimate of the spectral function obtained using the spectral bootstrap, and compared with the exact Lanczos coefficients. (d) Cumulative integrals $I_n(\omega) = \int_0^{\omega} \sigma_n(\omega') d\omega'$ of the equilibrium measures from panel (b), showing that they integrate to $I_n(\omega = \beta_n) = n/2$, as expected from Eqs. (41) and (42).

required for our Riemann-Hilbert analysis amount to assuming analyticity of $\Phi(\omega)$ at $\omega = 0$, which does not explicitly account for possible effects of power-law decay of $C(t)$ faster than $1/t$ on the analytic structure of $\Phi(\omega)$. The test of bulk universality we are about to perform thereby gives us a probe to see whether this non-analyticity affects the universality class near $\omega = 0$.

We estimate the weight function $w(\omega) = \Phi(\omega)/2\pi$ and the equilibrium density $\sigma_n(\omega)$ throughout the bulk frequency spectrum by carrying out the ‘bulk bootstrap’ algorithm, described in Section VII, in the frequency range $\omega \in [0, 0.99\beta_n]$, with $\beta_{n=40} \approx 46.1$ for MFIM, $\beta_{n=20} \approx 11.2$ for XXZ, and $\beta_{n=40} \approx 8.5$ for TFIM. As a check of the accuracy of our estimate of $\Phi(\omega)$, like in

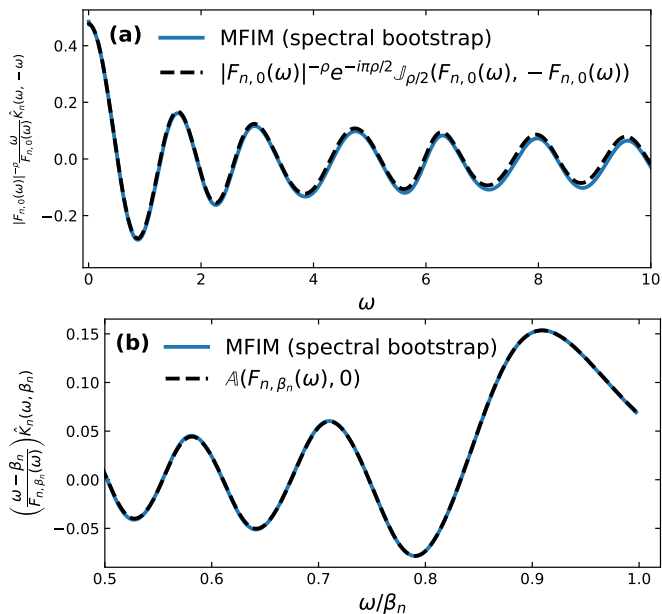


FIG. 11. (a) Bessel universality near $\omega = 0$ in the mixed field Ising model (MFIM). The initial Lanczos operator is the local energy density; since energy transport is diffusive in this model, the spectral function should scale like $\Phi(\omega \rightarrow 0) \sim |\omega|^\rho$ with $\rho = -\frac{1}{2}$. There is good agreement with the corresponding Bessel kernel $\mathbb{J}_{\rho/2}$ (Eq. (111)) in an $\mathcal{O}(1)$ region around the origin. (b) Airy universality near the spectral edge $\omega = \beta_n$ in the MFIM. We compare the results from the spectral bootstrap to the Airy kernel \mathbb{A} (Eq. (113)), finding very close agreement.

Fig. 8(c) we again use it to reconstruct the Lanczos coefficients for these models by evaluating the three-term recurrence Eq. (30), with the results shown in Fig. 10(c), where we find very good agreement. For the MFIM energy current, in Fig. 8(a) we also found good agreement with the spectral function obtained by Fourier transforming the real-time autocorrelation function obtained by TEBD, providing another independent accuracy test. To check the accuracy of the equilibrium measure $\sigma_n(\omega)$, as shown in Fig. 10(b), we compute the cumulative integral $I_n(\omega) = \int_0^\omega \sigma_n(\omega') d\omega'$. By the definitions Eqs. (41) and (42) and the even symmetry $\sigma_n(-\omega) = \sigma_n(\omega)$, we should have the sum rule $I_n(\omega = \beta_n) = n/2$. As shown in Fig. 10(d), we find this is well satisfied in all three models. This sum rule is not enforced by the spectral bootstrap, so this is a nontrivial check of the accuracy of our estimates of $\sigma_n(\omega)$.

With this assurance, we then use these estimates of $\Phi(\omega)$ and $\sigma_n(\omega)$ to numerically compute the inverse function $F_{n,\omega}^{-1}$, and then evaluate the LHS of Eq. (115), with the kernel $K_n(x, y) = \sum_{m=0}^{n-1} p_m(x)p_m(y)$ computed from the exact recurrence coefficients $\{b_n\}$ using the three-term recurrence Eq. (30). The results are shown in Fig. 10(a), where we see that all three models collapse on to the sine kernel $\mathbb{S}(u, v) = \sin[\pi(u - v)]/\pi(u - v)$, indicating the emergence of sine universality in the bulk. We emphasize that there are no free fitting parameters—everything is

computed from the Lanczos coefficients—so getting such close agreement is nontrivial. Note that the curve continues for larger separations $u - v$ for the MFIM than the XXZ model and then the TFIM simply because the frequency bandwidth β_n is larger, allowing us to probe larger separations before hitting the edge of the spectrum. This verification of bulk universality can be seen as an *a posteriori* explanation of the effectiveness of our spectral bootstrap algorithm to estimate the spectral functions of these physical models.

2. Bessel universality at the origin

Next we check for Bessel universality near $\omega = 0$, which is expected when the spectral function has a power-law at the origin, $\Phi(\omega \rightarrow 0) \sim |\omega|^\rho$. We will consider the energy density $h_0 = \frac{1}{2}(Z_{-1}Z_0 + Z_0Z_1) + g_x X_0 + g_z Z_0$ at site zero of the mixed field Ising model (MFIM), which should have $\Phi(\omega \rightarrow 0) \sim |\omega|^{-1/2}$ (i.e. $\rho = -\frac{1}{2}$) due to energy diffusion [3]. We compute $n = 40$ Lanczos coefficients for this model, and then use the ‘Bessel bootstrap’ described in Section VII B to extract the spectral function and the equilibrium measure. After checking again that these estimates successfully reproduce the true Lanczos coefficients (not shown), we then evaluate the LHS of Eq. (115) for $v = -u$ and using $F_{n,\omega=0}$ (note the RHS of Eq. (115) should now be replaced by $e^{-i\pi\rho/2}\mathbb{J}_{\rho/2}(u, -u)$). For clarity, we opt to plot as a function of the physical frequency ω , with $u = F_{n,0}(\omega)$. Note that, due to the even symmetry of the spectral function, we have $v = -u = F_{n,0}(-\omega)$. To account for the $\omega \rightarrow 0$ divergent power-law of both the spectral function and the $\rho = -\frac{1}{2}$ Bessel kernel, we rescale both sides by $|u|^{-\rho} = |F_{n,0}(\omega)|^{-\rho}$ when plotting. The results are shown in Fig. 11(a). We find good agreement with the Bessel kernel for $\mathcal{O}(1)$ frequencies, providing evidence for Bessel universality at $\omega = 0$ for this model. There is gradually increasing disagreement for larger frequencies, but this is not surprising since Bessel universality is only expected to hold in an $\mathcal{O}(1)$ -sized region around the origin (c.f. Fig. 1(b) and Section VII B).

3. Airy universality at the edge

Finally we check for Airy universality at the edge of the spectrum, $\omega \approx \beta_n$. We consider again the mixed field Ising model, and take the energy current as our initial Lanczos operator, computing $n = 40$ Lanczos coefficients. We use the ‘Airy bootstrap’ of Section S5 to approximate the spectral function $\Phi(\omega)$ and the equilibrium measure $\sigma_n(\omega)$ for frequencies in a range $\omega \in [\omega_{\min}, \beta_n]$ close to the edge $\omega = \beta_n$. With these estimates, we evaluate the LHS of Eq. (115), with the RHS now replaced by the Airy kernel $\mathbb{A}(u, v)$ (Eq. (113)). Note that, for Airy universality, the unfolding map F_n must now be defined according to Eq. (116). Since our spectral bootstrap algorithm estimates the weight only up to the spectral edge $\omega = \beta_n$,

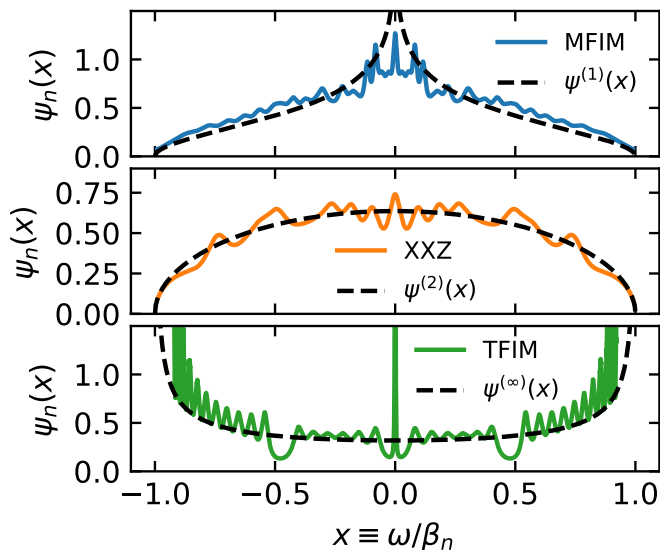


FIG. 12. Rescaled equilibrium measures $\psi_n(x) = (\beta_n/n)\sigma_n(\beta_n x)$ for the mixed field Ising model (MFIM), the XXZ chain, and the transverse field Ising model (TFIM), as extracted using the spectral bootstrap. Given that they respectively have $b_n \sim \mathcal{O}(n/\log n)$, $b_n \sim \mathcal{O}(\sqrt{n})$, and $b_n \sim \mathcal{O}(1)$, we compare with the equilibrium measures $\psi^{(p)}(x)$ for the Freud weights with equivalent growth rates, as indicated in Eqs. (117) to (119). In each case, $\psi^{(p)}$ captures the qualitative shape of the equilibrium measure for the physical model, but there are significant fluctuations, which have implications for quantitative extraction of the spectral function.

we will fix $v = 0$, where $F_{n,\omega=\beta_n}^{-1}(v = 0) = \beta_n$, and take the other argument u to be negative. Again for clarity we plot in terms of the physical frequency ω , so negative $u = F_{n,\beta_n}(\omega)$ corresponds to frequencies below $\omega = \beta_n$. The results are shown in Fig. 11(b). We find very good agreement with the Airy kernel, indicating the emergence of Airy universality near the edge of the spectrum in the mixed field Ising model.

C. Scaling of the equilibrium measure

Since our class of spectral functions behaves like the Freud weights $w^{(p)}(x) = \exp(-\kappa_p|x|^p)$ at large frequency scales (c.f. Eq. (48)), it is also interesting to compare our estimates of the rescaled equilibrium measure $\psi_n(x) = (\beta_n/n)\sigma_n(\beta_n x)$ with the corresponding function $\psi^{(p)}(x)$ for the Freud weights, which is given by the Ullman distribution defined in Eq. (49) [82]. For our physical test systems, we will use the same models as in Section VIII B 1—the mixed field Ising model (MFIM), the XXZ chain, and the transverse field Ising model (TFIM)—take the same initial Lanczos operators, and extract the equilibrium measure in the same way. Since these models have Lanczos coefficients growing like $b_n \sim \mathcal{O}(n/\log n)$, $b_n \sim \mathcal{O}(n^{1/2})$, and $b_n \sim \mathcal{O}(1)$ respectively, we will com-

pare to the following cases of the Ullman distribution:

$$\psi^{(p=1)}(x) = \frac{1}{\pi} \operatorname{artanh}\left(\sqrt{1-x^2}\right), \quad (117)$$

$$\psi^{(p=2)}(x) = \frac{2}{\pi} \sqrt{1-x^2}, \quad (118)$$

$$\psi^{(p \rightarrow \infty)}(x) = \frac{1}{\pi} \frac{1}{\sqrt{1-x^2}}. \quad (119)$$

Notice that $\psi^{(p=2)}(0)$ and $\psi^{(p \rightarrow \infty)}(0)$ are finite, while $\psi^{(p=1)}(x)$ has a logarithmic divergence as $x \rightarrow 0$. This is an instance of the Coulomb gas confinement transition discussed in Section IV A, which occurs at $p = 1$. The divergence of $\psi^{(p \rightarrow \infty)}(x)$ as $|x| \rightarrow 1$ is consistent with the scaling $h_n(1) \xrightarrow{n \rightarrow \infty} 2p$ in Lemma 1. For $p \rightarrow \infty$, the rescaled potential $V_n(x) = Q(\beta_n x)/n$ approaches a box potential which is zero for $|x| \leq 1$ and infinite outside, and the logarithmic repulsion between charges causes a build up of charge at the boundaries $x = \pm 1$ of the box.

The comparisons between the rescaled equilibrium measures $\psi_n(x)$ for the physical models and the corresponding Ullman distributions are shown in Fig. 12. Again we note there are no free fitting parameters. In each case the Ullman distribution $\psi^{(p)}(x)$ gives a good qualitative description of the large-scale profile of the equilibrium measure, but the physical equilibrium measures have significant fluctuations on smaller scales. These are a reflection of the fact that the nonuniversal structure of these spectral functions has not yet been washed out by the rescaling by β_n . Given these noticeable fluctuations, if one is aiming for quantitative accuracy in recovering a spectral function from Lanczos coefficients, it is not usually enough to simply approximate the equilibrium measure $\sigma_n(\omega)$ by a rescaled Ullman distribution $(n/\beta_n)\psi^{(p)}(\omega/\beta_n)$. Rather, one has to account for these fluctuations by using something like the spectral bootstrap to more accurately extract the equilibrium measure.

We emphasize that we considered this class of ‘Freud-like’ weights for our proofs because they are sufficiently regular to be amenable to rigorous proofs, but we expect the expressions for the polynomial asymptotics to be more universal, at least to leading order in $n \rightarrow \infty$. Thus we do not think there is a sense in which we have inadvertently assumed Freud-like behavior, so any agreement should be interpreted as a statement about the physical behavior of these models.

- sponse Theory*, SpringerBriefs in Mathematical Physics, Vol. 13 (Springer International Publishing, Cham, 2017).
- [38] C. M. Canali, M. Wallin, and V. E. Kravtsov, Nonuniversality in random-matrix ensembles with soft level confinement, *Physical Review B* **51**, 2831 (1995).
- [39] V. Freilikher, E. Kanzieper, and I. Yurkevich, Unitary random-matrix ensemble with governable level confinement, *Physical Review E* **53**, 2200 (1996).
- [40] V. Freilikher, E. Kanzieper, and I. Yurkevich, Theory of random matrices with strong level confinement: Orthogonal polynomial approach, *Physical Review E* **54**, 210 (1996).
- [41] T. Claeys, I. Krasovsky, and O. Minakov, Weak and Strong Confinement in the Freud Random Matrix Ensemble and Gap Probabilities, *Communications in Mathematical Physics* **402**, 833 (2023).
- [42] M. Srednicki, Chaos and quantum thermalization, *Physical Review E* **50**, 888 (1994).
- [43] L. D'Alessio, Y. Kafri, A. Polkovnikov, and M. Rigol, From quantum chaos and eigenstate thermalization to statistical mechanics and thermodynamics, *Advances in Physics* **65**, 239 (2016).
- [44] V. Alba, Eigenstate thermalization hypothesis and integrability in quantum spin chains, *Physical Review B* **91**, 155123 (2015).
- [45] S. Gopalakrishnan and R. Vasseur, Superdiffusion from Nonabelian Symmetries in Nearly Integrable Systems, *Annual Review of Condensed Matter Physics* **15**, 159 (2024).
- [46] W. Gautschi, *Orthogonal Polynomials: Computation and Approximation*, Numerical Mathematics and Scientific Computation (Oxford University Press, Oxford, New York, 2004).
- [47] N. I. Akhiezer, *The Classical Moment Problem and Some Related Questions in Analysis* (SIAM, 1965).
- [48] E. Levin and D. S. Lubinsky, Orthogonal polynomials for weights close to indeterminacy, *Journal of Approximation Theory* **147**, 129 (2007).
- [49] C. Jonay, D. A. Huse, and A. Nahum, Coarse-grained dynamics of operator and state entanglement (2018), [arXiv:1803.00089](https://arxiv.org/abs/1803.00089).
- [50] X. Cao, A statistical mechanism for operator growth, *Journal of Physics A: Mathematical and Theoretical* **54**, 144001 (2021).
- [51] A. Kar, L. Lamprou, M. Rozali, and J. Sully, Random matrix theory for complexity growth and black hole interiors, *Journal of High Energy Physics* **2022**, 16 (2022).
- [52] V. Balasubramanian, J. M. Magan, and Q. Wu, Tridiagonalizing random matrices, *Physical Review D* **107**, 126001 (2023).
- [53] P. Nandy, A. S. Matsoukas-Roubeas, P. Martínez-Azcona, A. Dymarsky, and A. del Campo, Quantum Dynamics in Krylov Space: Methods and Applications (2024), [arXiv:2405.09628](https://arxiv.org/abs/2405.09628).
- [54] B. Simon, *Orthogonal Polynomials on the Unit Circle: Part 1: Classical Theory* (American Mathematical Soc., 2009).
- [55] P. Suchsland, R. Moessner, and P. W. Claeys, Krylov complexity and Trotter transitions in unitary circuit dynamics, *Physical Review B* **111**, 014309 (2025).
- [56] A. Bhattacharya, P. Nandy, P. P. Nath, and H. Sahu, Operator growth and Krylov construction in dissipative open quantum systems, *Journal of High Energy Physics* **2022**, 81 (2022).
- [57] B. Bhattacharjee, X. Cao, P. Nandy, and T. Pathak, Operator growth in open quantum systems: Lessons from the dissipative SYK, *Journal of High Energy Physics* **2023**, 54 (2023).
- [58] B. Bhattacharjee, P. Nandy, and T. Pathak, Operator dynamics in Lindbladian SYK: A Krylov complexity perspective, *Journal of High Energy Physics* **2024**, 94 (2024).
- [59] A. Bhattacharya, P. Nandy, P. P. Nath, and H. Sahu, On Krylov complexity in open systems: An approach via bi-Lanczos algorithm, *Journal of High Energy Physics* **2023**, 66 (2023).
- [60] N. S. Srivatsa and C. von Keyserlingk, Operator growth hypothesis in open quantum systems, *Physical Review B* **109**, 125149 (2024).
- [61] F. Balogh, M. Bertola, S.-Y. Lee, and K. D. T.-R. McLaughlin, Strong Asymptotics of the Orthogonal Polynomials with Respect to a Measure Supported on the Plane, *Communications on Pure and Applied Mathematics* **68**, 112 (2015).
- [62] M. Kieburg, A. B. J. Kuijlaars, and S. Lahiry, Orthogonal polynomials in the normal matrix model with two insertions (2024), [arXiv:2408.12952](https://arxiv.org/abs/2408.12952).
- [63] J. A. Mingo and R. Speicher, *Free Probability and Random Matrices*, Fields Institute Monographs, Vol. 35 (Springer, New York, NY, 2017).
- [64] S. Pappalardi, L. Foini, and J. Kurchan, Eigenstate Thermalization Hypothesis and Free Probability, *Physical Review Letters* **129**, 170603 (2022).
- [65] S. Pappalardi, F. Fritzsche, and T. Prosen, Full Eigenstate Thermalization via Free Cumulants in Quantum Lattice Systems, *Physical Review Letters* **134**, 140404 (2025).
- [66] King's Computational Research, Engineering and Technology Environment (CREATE) (2024).
- [67] G. Szegő, *Orthogonal Polynomials*, Colloquium Publications, Vol. 23 (American Mathematical Society, 1939).
- [68] Y. Saad, *Numerical Methods for Large Eigenvalue Problems* (New York, N.Y. : Manchester University Press, J. Wiley and Sons. Halsted Press., 1992).
- [69] W. Mück and Y. Yang, Krylov complexity and orthogonal polynomials, *Nuclear Physics B* **984**, 115948 (2022).
- [70] D. S. Lubinsky, H. N. Mhaskar, and E. B. Saff, A proof of Freud's conjecture for exponential weights, *Constructive Approximation* **4**, 65 (1988).
- [71] D. J. Yates, A. G. Abanov, and A. Mitra, Dynamics of almost strong edge modes in spin chains away from integrability, *Physical Review B* **102**, 195419 (2020).
- [72] D. J. Yates, A. G. Abanov, and A. Mitra, Lifetime of Almost Strong Edge-Mode Operators in One-Dimensional, Interacting, Symmetry Protected Topological Phases, *Physical Review Letters* **124**, 206803 (2020).
- [73] A. Dymarsky and M. Smolkin, Krylov complexity in conformal field theory, *Physical Review D* **104**, L081702 (2021).
- [74] F. Ballar Trigueros and C.-J. Lin, Krylov complexity of many-body localization: Operator localization in Krylov basis, *SciPost Physics* **13**, 037 (2022).
- [75] B. Bhattacharjee, X. Cao, P. Nandy, and T. Pathak, Krylov complexity in saddle-dominated scrambling, *Journal of High Energy Physics* **2022**, 174 (2022).
- [76] E. Rabinovici, A. Sánchez-Garrido, R. Shir, and J. Sonner, Krylov localization and suppression of complexity, *Journal of High Energy Physics* **2022**, 211 (2022).
- [77] E. Rabinovici, A. Sánchez-Garrido, R. Shir, and J. Son-

- ner, Krylov complexity from integrability to chaos, *Journal of High Energy Physics* **2022**, 151 (2022).
- [78] M. H. Lee, Ergodic Theory, Infinite Products, and Long Time Behavior in Hermitian Models, *Physical Review Letters* **87**, 250601 (2001).
- [79] R. Heveling, J. Wang, and J. Gemmer, Numerically probing the universal operator growth hypothesis, *Physical Review E* **106**, 014152 (2022).
- [80] P. G. Nevai, *Orthogonal Polynomials* (American Mathematical Soc., 1979).
- [81] G. Mastroianni and G. V. Milovanović, *Interpolation Processes - Basic Theory and Applications*, Springer Monographs in Mathematics (Springer, Berlin, Heidelberg, 2008).
- [82] E. Saff and V. Totik, *Logarithmic Potentials with External Fields* (Springer Berlin, Heidelberg, 1997).
- [83] B. C. Hall, *Quantum Theory for Mathematicians*, Graduate Texts in Mathematics, Vol. 267 (Springer, New York, NY, 2013).
- [84] H. N. Mhaskar and E. B. Saff, Extremal problems for polynomials with exponential weights, *Transactions of the American Mathematical Society* **285**, 203 (1984).
- [85] E. A. Rakhmanov, On Asymptotic Properties of Polynomials Orthogonal on the Real Axis, *Mathematics of the USSR-Sbornik* **47**, 155 (1984).
- [86] Y. Chen and M. E. H. Ismail, Asymptotics of extreme zeros of the Meixner-Pollaczek polynomials, *Journal of Computational and Applied Mathematics 7th ICCAM 96 Congress*, **82**, 59 (1997).
- [87] H. N. Mhaskar and E. B. Saff, Where does the sup norm of a weighted polynomial live?, *Constructive Approximation* **1**, 71 (1985).
- [88] D. S. Lubinsky and E. B. Saff, Uniform and mean approximation by certain weighted polynomials, with applications, *Constructive Approximation* **4**, 21 (1988).
- [89] J. A. Shohat and J. D. Tamarkin, *The Problem of Moments*, Mathematical Surveys No. 1 (American Mathematical Soc., 1943).
- [90] W. P. Su, J. R. Schrieffer, and A. J. Heeger, Solitons in Polyacetylene, *Physical Review Letters* **42**, 1698 (1979).
- [91] B. Bertini, F. Heidrich-Meisner, C. Karrasch, T. Prosen, R. Steinigeweg, and M. Žnidarič, Finite-temperature transport in one-dimensional quantum lattice models, *Reviews of Modern Physics* **93**, 025003 (2021).
- [92] R. Kubo, Statistical-Mechanical Theory of Irreversible Processes. I. General Theory and Simple Applications to Magnetic and Conduction Problems, *Journal of the Physical Society of Japan* **12**, 570 (1957).
- [93] B. Simon, *The Christoffel-Darboux Kernel* (2008), arxiv:0806.1528.
- [94] J. Wang, M. H. Lamann, R. Steinigeweg, and J. Gemmer, Diffusion constants from the recursion method, *Physical Review B* **110**, 104413 (2024).
- [95] M. Füllgraf, J. Wang, and J. Gemmer, Lanczos-Pascal approach to correlation functions in chaotic quantum systems (2025), arXiv:2503.17555.
- [96] S. Gopalakrishnan and R. Vasseur, Kinetic Theory of Spin Diffusion and Superdiffusion in XXZ Spin Chains, *Physical Review Letters* **122**, 127202 (2019).
- [97] J. De Nardis, D. Bernard, and B. Doyon, Diffusion in generalized hydrodynamics and quasiparticle scattering, *SciPost Physics* **6**, 049 (2019).
- [98] C. Karrasch, J. E. Moore, and F. Heidrich-Meisner, Real-time and real-space spin and energy dynamics in one-dimensional spin- $\frac{1}{2}$ systems induced by local quantum quenches at finite temperatures, *Physical Review B* **89**, 075139 (2014).
- [99] J. De Nardis, S. Gopalakrishnan, E. Ilievski, and R. Vasseur, Superdiffusion from Emergent Classical Solitons in Quantum Spin Chains, *Physical Review Letters* **125**, 070601 (2020).
- [100] J. De Nardis, S. Gopalakrishnan, R. Vasseur, and B. Ware, Stability of Superdiffusion in Nearly Integrable Spin Chains, *Physical Review Letters* **127**, 057201 (2021).
- [101] R. Haydock, The Recursive Solution of the Schrodinger Equation, in *Solid State Physics*, Vol. 35, edited by H. Ehrenreich, F. Seitz, and D. Turnbull (Academic Press, 1980) pp. 215–294.
- [102] G. Pinna, O. Lunt, and C. von Keyserlingk, Approximation theory for Green's functions via the Lanczos algorithm (2025), arXiv:2505.00089.
- [103] C. A. Tracy and H. Widom, Level-spacing distributions and the Airy kernel, *Communications in Mathematical Physics* **159**, 151 (1994).
- [104] G. Freud, *Orthogonal Polynomials* (Pergamon Press, 1971).
- [105] E. Levin and D. S. Lubinsky, *Orthogonal Polynomials for Exponential Weights* (Springer Science & Business Media, 2012).
- [106] J. Hauschild and F. Pollmann, Efficient numerical simulations with Tensor Networks: Tensor Network Python (TeNPy), *SciPost Physics Lecture Notes* **5**, 10.21468/SciPostPhysLectNotes.5 (2018).
- [107] A. De, U. Borla, X. Cao, and S. Gazit, Stochastic sampling of operator growth dynamics, *Physical Review B* **110**, 155135 (2024).
- [108] S. R. White and I. Affleck, Spectral function for the $S = 1$ Heisenberg antiferromagnetic chain, *Physical Review B* **77**, 134437 (2008).
- [109] G. Akemann, P. H. Damgaard, U. Magnea, and S. Nishigaki, Universality of random matrices in the microscopic limit and the Dirac operator spectrum, *Nuclear Physics B* **487**, 721 (1997).
- [110] L. Erdős, Universality of Wigner random matrices: A survey of recent results, *Russian Mathematical Surveys* **66**, 507 (2011).
- [111] D. S. Lubinsky, Bulk universality holds in measure for compactly supported measures, *Journal d'Analyse Mathématique* **116**, 219 (2012).
- [112] T. A. Brody, J. Flores, J. B. French, P. A. Mello, A. Pandey, and S. S. M. Wong, Random-matrix physics: Spectrum and strength fluctuations, *Reviews of Modern Physics* **53**, 385 (1981).
- [113] J. Maldacena and D. Stanford, Remarks on the Sachdev-Ye-Kitaev model, *Physical Review D* **94**, 106002 (2016).
- [114] M. Dodelson, C. Iossa, R. Karlsson, and A. Zhiboedov, A thermal product formula, *Journal of High Energy Physics* **2024**, 36 (2024).
- [115] T. Kasuga and R. Sakai, Orthonormal polynomials with generalized Freud-type weights, *Journal of Approximation Theory* **121**, 13 (2003).
- [116] K. T.-R. McLaughlin and P. D. Miller, The dbar steepest descent method for orthogonal polynomials on the real line with varying weights (2008), arXiv:0805.1980.
- [117] L. V. Delacrétaz, Heavy operators and hydrodynamic tails, *SciPost Physics* **9**, 034 (2020).
- [118] A. Raj, P. Glorioso, S. Gopalakrishnan, and

- V. Oganessian, [Diffusion cascade in a model of interacting random walkers](#) (2024), [arXiv:2412.05222](#).
- [119] T. Kriecherbauer and K. T.-R. McLaughlin, Strong asymptotics of polynomials orthogonal with respect to Freud weights, [International Mathematics Research Notices](#) **1999**, 299 (1999).
- [120] A. S. Fokas, A. R. Its, and A. V. Kitaev, The isomonodromy approach to matrix models in 2D quantum gravity, [Communications in Mathematical Physics](#) **147**, 395 (1992).
- [121] A. B. J. Kuijlaars, K. T. R. McLaughlin, W. Van Assche, and M. Vanlessen, The Riemann–Hilbert approach to strong asymptotics for orthogonal polynomials on $[-1,1]$, [Advances in Mathematics](#) **188**, 337 (2004).
- [122] M. Vanlessen, Strong asymptotics of the recurrence coefficients of orthogonal polynomials associated to the generalized Jacobi weight, [Journal of Approximation Theory](#) **125**, 198 (2003).
- [123] M. Vanlessen, Strong Asymptotics of Laguerre-Type Orthogonal Polynomials and Applications in Random Matrix Theory, [Constructive Approximation](#) **25**, 125 (2007).
- [124] M. Abramowitz and I. A. Stegun, *Handbook of Mathematical Functions: With Formulas, Graphs, and Mathematical Tables* (Courier Corporation, 1965).

Supplemental Material

S1. CLASS OF SPECTRAL FUNCTIONS (WEIGHTS)

A. Definition of potentials

We want to consider weights $w(\omega) \equiv \Phi(\omega)/2\pi$ which decay at least exponentially at large ω . We will decompose them as $w(\omega) \equiv |\omega|^p \exp[-Q(\omega)]$, where Q is called the *potential*. Given the exponential decay of w , $Q(\omega)$ should grow at least linearly as $|\omega| \rightarrow \infty$. To model this behavior, we will consider a class of weights inspired by the ‘very smooth Freud weights’ of Refs. [70, 88], which they denote by $\text{VSF}(p)$, with p an exponent governing the degree of the polynomial growth of $Q(\omega) \sim |\omega|^p$ as $|\omega| \rightarrow \infty$. Our weights will be a subset of $\text{VSF}(p)$, where we add the requirement of analyticity, and also require a specification of the logarithmic corrections to the leading polynomial growth of $Q(\omega)$.

Our Riemann-Hilbert analysis draws heavily from Ref. [22], where they take Q to be a polynomial of even order. However, we are particularly interested in the marginal case where $Q(\omega \rightarrow \infty)$ grows linearly with $|\omega|$, since the Operator Growth Hypothesis [10] conjectures this to be generic for spectral functions in chaotic many-body quantum systems. But it is clearly not possible to simultaneously have i) $Q(\omega) \sim |\omega|$ as $|\omega| \rightarrow \infty$, and ii) Q be a polynomial. This was a primary motivation for considering this generalized class $\text{VSLF}(p, q)$ of ‘polynomial-like’ weights.

Definition S1 ($\text{VSLF}(p, q)$): log-Freud potentials of order (p, q) . Let $Q : \mathbb{R} \rightarrow \mathbb{R}$ be real-analytic, even, and satisfy

$$Q'(\omega) > 0, \quad \text{for } \omega \text{ large enough}, \quad (\text{S1.1})$$

$$\lim_{\omega \rightarrow \infty} \left(\frac{\omega Q''(\omega)}{Q'(\omega)} \right) = p - 1, \quad (\text{S1.2})$$

$$\lim_{\omega \rightarrow \infty} \left(\log(\omega) \left[-p + \frac{\omega Q'(\omega)}{Q(\omega)} \right] \right) = q. \quad (\text{S1.3})$$

for some $p > 0$ and $q \in \mathbb{R}$. Then we shall call Q a *log-Freud* potential of order (p, q) and write $Q \in \text{VSLF}(p, q)$.

We will see in Eq. (S1.11) that these potentials grow as $Q(\omega) \sim |\omega|^p (\log |\omega|)^{q+o(1)}$ as $|\omega| \rightarrow \infty$, where the $o(1)$ in the exponent refers to scaling with ω . In this sense assumptions Eqs. (S1.2) and (S1.3) are similar to but slightly weaker than assuming $Q \in \Theta(|\omega|^p (\log |\omega|)^q)$. We make the assumption Eq. (S1.1) for technical convenience; it allows us to prove that for large enough n we need consider only the simplest case, where the support of the equilibrium measure consists of a single interval (see Section S2D). Similar analyses have been performed in the more complicated case where the support consists of multiple disjoint intervals, but mostly for so-called ‘varying weights’ of the form $w(x) = \exp[-nQ(x)]$ where the weight depends on n [24, 27].

In order to apply Riemann-Hilbert techniques, we also need to assume that some of these properties continue to hold in a region of the complex plane near the real axis.

Definition S2 ($\text{CVSLF}(p, q, \theta, \gamma)$): complex log-Freud potentials of order (p, q) . For an angle $0 < \theta \leq \pi/2$, define the ‘complex cone’ C_θ by

$$C_\theta := \{z : |\arg z| < \theta\} \cup \{z : |\arg z| > \pi - \theta\}, \quad (\text{S1.4})$$

using the convention $-\pi < \arg z \leq \pi$. We consider the open cone, so $z = 0$ is not included in C_θ . Now suppose there is some $0 < \theta \leq \pi/2$ and $\gamma > 0$ such that $Q \in \text{VSLF}(p, q)$ can be analytically continued to $C_\theta \cup \{z : |z| < \gamma\}$, the union of C_θ and the disk of radius γ centered at the origin (see Fig. S1). Also assume that Eqs. (S1.2) and (S1.3) generalize to this region, in the sense that for z restricted to C_θ we have

$$\lim_{|z| \rightarrow \infty} \frac{z Q''(z)}{Q'(z)} = p - 1, \quad (\text{S1.5})$$

$$\lim_{|z| \rightarrow \infty} \left(\log(z) \left[-p + \frac{z Q'(z)}{Q(z)} \right] \right) = q. \quad (\text{S1.6})$$

Given these properties, we say that Q is a complex log-Freud potential of order (p, q) , and write $Q \in \text{CVSLF}(p, q, \theta, \gamma)$.

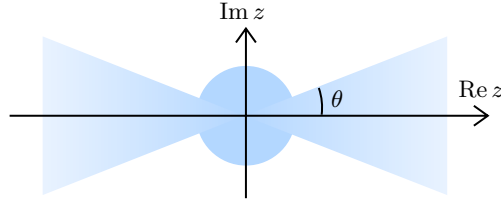


FIG. S1. We require the potential $Q(z)$ defined in Eq. (34) to have an analytic continuation to the shaded region of the complex plane, where $0 < \theta \leq \pi/2$ is any positive angle. This region is the union of the ‘complex cone’ C_θ (see Eq. (S1.4)) and a disk of constant radius around $z = 0$.

Our proofs will apply for $Q \in \text{CVSLF}(p, q, \theta, \gamma)$ in all cases where the corresponding Hamburger moment problem is determined. This encompasses $p > 1, q \in \mathbb{R}$, and $p = 1, q > -1$.

Example S1. All even polynomials with positive leading coefficient, $Q(x) = q_{2m}x^{2m} + \dots$, $q_{2m} > 0$, lie in $\text{CVSLF}(p, q, \theta, \gamma)$ with $p = 2m$, $q = 0$, $\theta = \pi/2$, $\gamma = \infty$.

Example S2. Certain fractional powers of polynomials satisfy our assumptions, e.g. $Q(x) = \sqrt{1+x^2}$ has $p = 1$, $q = 0$, $0 < \theta < \pi/2$, and $0 < \gamma < 1$. A similar example is $Q(x) = \sqrt{1+x^2} \log(1+x^2)$, which has $p = 1, q = 1$.

Example S3. The symmetric Meixner-Pollaczek weights have $w(x) = \exp[-Q(x)] = \Gamma(\lambda + ix)\Gamma(\lambda - ix)$. (Q can then be defined as in Eq. (S1.9) below.) With $\lambda > 0$, we have $p = 1$, $q = 0$, $0 < \theta < \pi/2$, and $0 < \gamma < \lambda$. These weights appear in a rescaled form as the 2-point Wightman spectral function in the SYK model [113, 114], and were utilized in Ref. [10] to give an exactly solvable spectral function with exponential decay for use with the recursion method [19].

Example S4. Taking $Q'(z) = \text{erf}(z) = (2/\sqrt{\pi}) \int_0^z e^{-t^2} dt$ gives an example of a $p = 1$ potential which is also entire, unlike the previous $p = 1$ examples. The conditions Eqs. (S1.5) and (S1.6) hold for $0 < \theta < \pi/4$.

B. Comments on analyticity requirements

Regarding the definition of the class CVSLF, the reason we need analyticity in a cone of constant argument rather than, say, a strip of constant width, is that we need this region of analyticity to be invariant under rescaling $z \mapsto z/\beta$ for $\beta > 0$. Note that θ could be very small; we just require that it is a positive constant. We also require $Q(z)$ to be analytic in a disk of constant radius around $z = 0$. Handling the fact that this disk is *not* invariant under rescaling is one of the technical achievements of our work. Note that this analyticity requirement on Q is not in general the same as requiring $\Phi(z)$ to be analytic at $z = 0$, since we are explicitly factorizing out a low-frequency power law, c.f. Eq. (34), which is supposed to capture the main non-analyticity of $\Phi(z)$.

Typically, we are more used to talking about analytic continuations of Green’s functions than of spectral functions. Suppose we have a retarded Green’s function $G_R(z)$, defined in the lower-half plane by

$$G_R(z) := \left(O_0 \left| \frac{1}{z - \mathcal{L}} \right| O_0 \right) = \int_{\mathbb{R}} \frac{\Phi(\omega) d\omega}{z - \omega} \frac{1}{2\pi}, \quad z \in \mathbb{C}_-. \quad (\text{S1.7})$$

By construction $G_R(z)$ is analytic in the lower-half plane, and $\Phi(\omega) = 2 \text{Im} \lim_{\epsilon \rightarrow 0^+} G_R(\omega - i\epsilon)$. Now suppose that $G_R(z)$ has an analytic continuation across a section of the real line to some subset $\Omega \subseteq \mathbb{C}_+ \cup \mathbb{R}$ of the upper-half plane. We can use this to define an analytic continuation of the spectral function by

$$\Phi(z) := \frac{1}{i} (G_R(z) + G_R(-z)). \quad (\text{S1.8})$$

$\Phi(z)$ is then analytic in $\Omega \cup (-\Omega)$, and satisfies $\Phi(-z) = \Phi(z)$. So, for example, if $G_R(z)$ has a diffusive pole at $z = iDk^2$, then $\Phi(z)$ would have poles at $z = \pm iDk^2$. Having analytically continued $\Phi(z)$ in this way, $Q(z)$ would then be defined such that Eq. (34) is satisfied. In the case $\rho = 0$, this can be achieved by taking

$$Q(z) = -\log \left(\frac{\Phi(0)}{2\pi} \right) - \int_0^z \frac{\Phi'(s)}{\Phi(s)} ds, \quad (\text{S1.9})$$

where the integral is along any path where $\Phi(s) > 0$ and avoiding any poles. Then $\exp[-Q(z)] = \Phi(z)/2\pi$ by construction. A similar construction is possible for $\rho \neq 0$ given an analytic continuation of $|\omega|^\rho$ to the relevant quadrant of the complex plane.

Note that we do *not* show that the violation of these analyticity conditions on Q necessarily leads to a modification of our results. Versions of some of our results have been proven, though not always with explicit constants, only using assumptions about the behavior of the spectral function on the real line, see e.g. [105, 115]. Rather than using Riemann-Hilbert techniques, which rely quite crucially on analyticity, it may also be possible to prove similar statements using a $\bar{\partial}$ steepest descent method [116], which does not require such strong analyticity assumptions on Q , at the expense of getting weaker error bounds.

One potential violation of our analyticity conditions could come from systems with a ‘diffuson cascade’ [117, 118], which can lead to an infinite series of poles in k -space retarded Green’s functions $G_R(z, k)$ accumulating all the way down to the real z axis, as opposed to the conventional expectation of just a simple pole at $z = iDk^2$ [18]. Handling such singular points would require a modification of our analysis which goes beyond the scope of this work (though see [119] for some work in this direction). However, despite their analyticity conditions, our calculations give certain predictions that can be tested numerically. We find that they are obeyed well even in some interacting non-integrable systems that might be expected to have a diffuson cascade. This suggests that, even if we weaken our analyticity conditions, some of our conclusions may continue to hold.

C. Properties of log-Freud weights

First we adapt some results from Refs. [70, 88] to characterize the asymptotic behavior of these weights on the real line. Note that those references include a requirement on the 3rd derivative of Q in the definition of their VSF(p) class, which we do not include in our VSLF(p, q) definition, since it is not necessary to prove any of the properties relevant for our purposes. When quoting results from Refs. [70, 88], we will sometimes use the shorthand $Q \in \text{VSF}(p)$, with the implicit understanding that the relevant proof uses only properties of the VSF(p) class that we do include in our definition of the VSLF(p, q) class.

Definition S3 (n th Mhaskar-Rakhmanov-Saff (MRS) number β_n). Given an even potential $Q(x)$ and a positive integer n , define β_n as the positive solution to the integral equation

$$\frac{1}{2\pi} \int_{-1}^1 \frac{\beta_n s Q'(\beta_n s)}{\sqrt{1-s^2}} ds = n. \quad (\text{S1.10})$$

As discussed in Section IV A of the main text, the MRS number β_n is important because it sets the bandwidth of the region in which the weighted orthogonal polynomials $p_n(x)w(x)^{1/2}$ are non-negligible. This also turns out to set the location of the dominant contribution to the Riemann-Hilbert problem for the orthogonal polynomials, and the leading behavior of the recurrence coefficients is given by $b_n \approx \beta_n/2$.

Lemma S1. *Suppose $Q \in \text{VSLF}(p, q)$ for some $p > 0$, $q \in \mathbb{R}$. Then the following hold.*

(i) $xQ'(x)$ is increasing for large enough x .

(ii) For any $\epsilon > 0$, there exists x_0 such that for $|x| \geq x_0$ we have

$$|x|^p (\log |x|)^{q-\epsilon/2} \leq |Q(x)| \leq |x|^p (\log |x|)^{q+\epsilon/2}. \quad (\text{S1.11})$$

(iii) For any $\epsilon > 0$, there exists x_0 such that for $|x| \geq x_0$ we have

$$|x|^{p-1} (\log |x|)^{q-\epsilon/2} \leq |Q'(x)| \leq |x|^{p-1} (\log |x|)^{q+\epsilon/2}. \quad (\text{S1.12})$$

(iv) For large enough n , the n th MRS number β_n for Q is uniquely defined, monotonically increasing, and furthermore

$$\lim_{n \rightarrow \infty} \frac{\beta_n Q'(\beta_n)}{n} = \frac{p}{\lambda_p}, \quad (\text{S1.13})$$

where λ_p is defined by

$$\lambda_p = \frac{\Gamma(\frac{p+1}{2})}{\Gamma(\frac{1}{2}) \Gamma(\frac{p}{2})}. \quad (\text{S1.14})$$

(v) Uniformly for s in any compact subinterval of $(0, \infty)$, we have

$$\lim_{n \rightarrow \infty} \frac{1}{n} \beta_n s Q'(\beta_n s) = \frac{p}{\lambda_p} s^p. \quad (\text{S1.15})$$

(vi) For any $\epsilon > 0$, if n is large enough then we have

$$\left(\frac{n}{(\log n)^{q+\epsilon/2}} \right)^{1/p} \leq \beta_n \leq \left(\frac{n}{(\log n)^{q-\epsilon/2}} \right)^{1/p}. \quad (\text{S1.16})$$

Proof. (i) This is [88, Lemma 3.1(i)], whose proof we repeat here. Eqs. (S1.1) and (S1.2) imply that for large enough x we have

$$\frac{d}{dx} [xQ'(x)] = Q'(x) \left[1 + \frac{xQ''(x)}{Q'(x)} \right], \quad (\text{S1.17})$$

$$\geq Q'(x)(p/2) > 0. \quad (\text{S1.18})$$

(ii) Fixing $\epsilon > 0$, for large enough x Eq. (S1.3) yields

$$\frac{p}{x} + \frac{q - \epsilon/2}{x \log x} \leq \frac{Q'(x)}{Q(x)} \leq \frac{p}{x} + \frac{q + \epsilon/2}{x \log x}. \quad (\text{S1.19})$$

Integrating w.r.t. x and exponentiating then gives the result (the integration constant can be absorbed by slightly increasing ϵ).

(iii) The condition in Eq. (S1.3) implies

$$\lim_{x \rightarrow \infty} \left[\frac{xQ'(x)}{Q(x)} \right] = p. \quad (\text{S1.20})$$

Fixing $0 < \epsilon' < p$, for x large enough this limit implies

$$(p - \epsilon'/2) \frac{Q(x)}{x} \leq Q'(x) \leq (p + \epsilon'/2) \frac{Q(x)}{x}. \quad (\text{S1.21})$$

Then we apply Eq. (S1.11) to get

$$(p - \epsilon'/2)x^{p-1} (\log x)^{q-\epsilon/2} \leq Q'(x) \leq (p + \epsilon'/2)x^{p-1} (\log x)^{q+\epsilon/2}. \quad (\text{S1.22})$$

We can get rid of the constants $(p \pm \epsilon'/2)$ by slightly increasing ϵ , and so we obtain Eq. (S1.12).

(iv) This is [88, Lemma 3.2(i) and (ii)], the proofs of which directly carry over because $Q \in \text{VSF}(p)$.

(v) This follows after using [88, Lemma 3.1(ii)], which states that for $Q \in \text{VSF}(p)$, uniformly for s in any compact subinterval of $(0, \infty)$ we have

$$\lim_{n \rightarrow \infty} \frac{Q'(\beta_n s)}{Q'(\beta_n)} = s^{p-1}. \quad (\text{S1.23})$$

The statement then follows by combining this with Eq. (S1.13), since

$$\lim_{n \rightarrow \infty} \frac{1}{n} \beta_n s Q'(\beta_n s) = \lim_{n \rightarrow \infty} \frac{\beta_n Q'(\beta_n)}{n} \frac{Q'(\beta_n s)}{Q'(\beta_n)} s = \frac{p}{\lambda_p} s^{p-1} s = \frac{p}{\lambda_p} s^p.$$

(vi) We will prove the upper bound on β_n , with the lower bound proceeding analogously. From Eq. (S1.13) we have $\lim_{n \rightarrow \infty} \beta_n Q'(\beta_n)/n = p/\lambda_p$, and hence, given $0 < \epsilon' < p/\lambda_p$, for sufficiently large n we have

$$\frac{\beta_n Q'(\beta_n)}{n} \leq \frac{p}{\lambda_p} + \frac{\epsilon'}{2}.$$

Then lower bounding $Q'(\beta_n)$ using Eq. (S1.12) gives

$$\beta_n \leq \left(\frac{p}{\lambda_p} + \frac{\epsilon'}{2} \right)^{1/p} \left(\frac{n}{(\log \beta_n)^{q-\epsilon/2}} \right)^{1/p}.$$

Since $Q \in \text{VSF}(p)$, we can apply [70, Lemma 3.3(iii)], which gives the bound $\beta_n \geq n^{1/(p+\epsilon')}$ for $0 < \epsilon' < p$, and hence $\log \beta_n \geq (p + \epsilon')^{-1} \log n$. Using this to bound the $\log \beta_n$ factor on the RHS, and redefining ϵ to absorb the constant prefactor, we get the upper bound in Eq. (S1.16). \square

Next we generalize some of these properties to the region of the complex plane where Q is assumed to be complex analytic. First we generalize the upper bound of Eq. (S1.12) to this complex region.

Lemma S2. *Assume $Q \in \text{CVSLF}(p, q, \theta, \gamma)$. For any $\epsilon > 0$, there exists A such that for $z \in C_\theta$ with $|z| \geq A$ we have*

$$|Q'(z)| \leq |z|^{p-1} (\log |z|)^{q+\epsilon/2}. \quad (\text{S1.24})$$

Proof. One may proceed as in the proofs of properties (ii) and (iii) of Lemma S1 where the starting point Eq. (S1.19) is replaced by the estimate

$$\left| \frac{Q'(z)}{Q(z)} - \frac{p}{z} - \frac{q}{z \log z} \right| \leq \frac{\epsilon/2}{|z \log z|}. \quad (\text{S1.25})$$

\square

Second we generalize [88, Lemma 3.1(ii)] to the complex region.

Lemma S3. *Assume $Q \in \text{CVSLF}(p, q, \theta, \gamma)$. Then uniformly for z in any compact subset of C_θ with $\text{Re } z > 0$, we have*

$$\lim_{\beta \rightarrow \infty} \frac{Q'(\beta z)}{Q'(\beta)} = z^{p-1}, \quad (\text{S1.26})$$

with the behavior for $\text{Re } z < 0$ given by symmetry, since $Q'(z)$ is assumed odd.

Proof. Throughout we consider $z \in C_\theta$ with $\text{Re } z > 0$. First note that C_θ is invariant under rescaling, so $z \in C_\theta \Rightarrow \beta z \in C_\theta$ for $\beta > 0$. Then we use the observation that

$$\log Q'(\beta z) - \log Q'(\beta) - (p-1) \log z = \int_\beta^{\beta z} \left[\frac{u Q''(u)}{Q'(u)} - (p-1) \right] \frac{du}{u}, \quad (\text{S1.27})$$

where the integral is along the straight line contour $u(t) = \beta[1 + t(z-1)]$, $t \in [0, 1]$, connecting β and βz . This contour remains within C_θ because the subset of C_θ with $\text{Re } z > 0$ is convex. By the assumption Eq. (S1.5), given $\epsilon > 0$, for sufficiently large β we have

$$\left| \frac{u Q''(u)}{Q'(u)} - (p-1) \right| \leq \epsilon \quad (\text{S1.28})$$

for all u along the contour. Then changing variables from u to t and applying the bound gives

$$|\log Q'(\beta z) - \log Q'(\beta) - (p-1) \log z| \leq \epsilon \int_0^1 \left| \frac{z-1}{1+t(z-1)} \right| dt, \quad (\text{S1.29})$$

where we note that the β dependence has disappeared from the RHS. Since $\text{Re } z > 0$, the integrand denominator is always nonzero, so the integral converges, and hence there exists finite $c_z > 0$, independent of β , such that

$$|\log Q'(\beta z) - \log Q'(\beta) - (p-1) \log z| \leq \epsilon c_z. \quad (\text{S1.30})$$

Since ϵ can be taken arbitrarily small by increasing β , so that $\epsilon c_z \rightarrow 0$ uniformly for z in any compact subset of C_θ , we have

$$\lim_{\beta \rightarrow \infty} [\log Q'(\beta z) - \log Q'(\beta)] = (p-1) \log z. \quad (\text{S1.31})$$

Exponentiating both sides then gives Eq. (S1.26). \square

Combining this lemma with Lemma S1(iv), we get the complex analogue of Lemma S1(v) (the proof is identical):

Lemma S4. *Uniformly for z in any compact subset of C_θ ,*

$$\lim_{n \rightarrow \infty} \frac{1}{n} \beta_n z Q'(\beta_n z) = \frac{p}{\lambda_p} z^p. \quad (\text{S1.32})$$

Next we mention a useful corollary of the proof of Eq. (S1.26). The first part follows from the integral inequality

$$\int_{\beta s}^{\beta} \frac{Q''(u)}{Q'(u)} du \geq \int_{\beta s}^{\beta} \frac{p-1-\epsilon}{u} du, \quad (\text{S1.33})$$

for $0 < s \leq 1$ with βs large enough so that the estimate (S1.28) can be obtained from condition (S1.2). The second part follows after using Eq. (S1.13).

Corollary S1. *Assume $\epsilon > 0$ and $\beta > 0$. Then there exists $A > 0$ such that*

$$Q'(\beta s) \leq Q'(\beta) s^{p-1-\epsilon} \quad (\text{S1.34})$$

for all $A/\beta \leq s \leq 1$. Thus, for sufficiently large n and all $A/\beta_n \leq s \leq 1$, we have

$$0 < V'_n(s) = \frac{\beta_n}{n} Q'(\beta_n s) \leq \frac{2p}{\lambda_p} s^{p-1-\epsilon}. \quad (\text{S1.35})$$

Finally, since it will be relevant later, we consider the Lagrange multiplier $l_n \in \mathbb{R}$, which appears in the Euler-Lagrange equation

$$g_{n,+}(x) + g_{n,-}(x) - V_n(x) - l_n = 0, \quad \text{for } x \in [-1, 1], \quad (\text{S1.36})$$

for the Coulomb gas energy minimization problem discussed in Section IV A, which will be relevant in Section S2 D 3. Here $V_n(x) = Q(\beta_n x)/n$ is the rescaled potential, and g_n is the logarithmic transform of the equilibrium measure, which we will define later in Eq. (S2.31). The Lagrange multiplier l_n can be determined using the expression

$$l_n = -2 \log 2 - \frac{2}{\pi} \int_0^1 \frac{V_n(s)}{\sqrt{1-s^2}} ds. \quad (\text{S1.37})$$

(This follows from [82, Theorem IV.3.1], where in their language we have $l_n = -2C_{\frac{1}{2}V_n}$.) For our class of weights, the limiting value is the same as that for the simple Freud weight $\kappa_p |x|^p$, where $\kappa_p = 1/\lambda_p$ with λ_p defined in Eq. (S1.14).

Lemma S5. *For $Q \in \text{VSLF}(p, q)$ with $p > 0$, we have*

$$\lim_{n \rightarrow \infty} l_n = -2 \log 2 - \frac{2}{p}. \quad (\text{S1.38})$$

Thus the Lagrange multiplier should be $\mathcal{O}(1)$ and negative for sufficiently large n .

Proof. By [88, Lemma 3.2(iii)] (our weights satisfy all the relevant conditions), we have $\lim_{n \rightarrow \infty} V_n(s) = \kappa_p |s|^p$ uniformly for s in compact subsets of \mathbb{R} . This implies pointwise convergence of the integrand for $s \in (0, 1)$. In order to apply the dominated convergence theorem we appeal to Corollary S1, choosing ϵ so that $p-1-\epsilon > -1$. However, this upper bound is only available for $s \in [A/\beta_n, 1]$. Observe that the remaining part of the integral can be bounded by

$$\int_0^{A/\beta_n} \frac{|V_n(s)|}{\sqrt{1-s^2}} ds \leq \frac{1}{\sqrt{1-(A/\beta_n)^2}} \frac{1}{n\beta_n} \int_0^A |Q(u)| du \leq \mathcal{O}\left(\frac{1}{n\beta_n}\right), \quad (\text{S1.39})$$

which goes to zero as $n \rightarrow \infty$. Then using the dominated convergence theorem gives

$$\lim_{n \rightarrow \infty} l_n = -2 \log 2 - \frac{2}{\pi} \int_0^1 \frac{\kappa_p s^p}{\sqrt{1-s^2}} ds, \quad (\text{S1.40})$$

$$= -2 \log 2 - \frac{2}{p}, \quad (\text{S1.41})$$

where the final step comes from explicitly evaluating the integral and simplifying using Eq. (S1.14) with $\kappa_p = 1/\lambda_p$. \square

S2. RIEMANN-HILBERT STEEPEST DESCENT ANALYSIS

To obtain $n \rightarrow \infty$ asymptotics of the orthogonal polynomials with respect to $w(x) \equiv \Phi(x)/2\pi$, we make use of a ‘steepest descent’-inspired analysis of a Riemann-Hilbert problem (RHP) associated with w [21–27]. This fundamental RHP looks for a 2×2 matrix-valued function Y which is analytic in $\mathbb{C} \setminus \mathbb{R}$, with a specified jump across \mathbb{R} that is related to $w(x)$. This RHP is formulated in such a way to have a unique solution which encodes much valuable information about the orthogonal polynomials with respect to w .

A. Fundamental Riemann-Hilbert problem for Y

Let us decompose $w(x) \equiv |x|^\rho e^{-Q(x)}$, and note that we must have $\rho > -1$ in order for w to be integrable. Throughout we will assume $w(-x) = w(x)$ is even, and to account for the power-law at $x = 0$, we will need to add an extra condition to ensure uniqueness of the solution to the RHP. Then we look for a 2×2 matrix-valued function $Y(z)$ satisfying the following conditions.

(Y_a) $Y(z)$ is analytic in $\mathbb{C} \setminus \mathbb{R}$.

(Y_b) $Y(z)$ takes continuous boundary values $Y_\pm(x) := \lim_{y \rightarrow 0^\pm} Y(x + iy)$ such that

$$Y_+(x) = Y_-(x) \begin{pmatrix} 1 & w(x) \\ 0 & 1 \end{pmatrix}, \quad \text{for } x \in \mathbb{R} \setminus \{0\}. \quad (\text{S2.1})$$

(Y_c) $Y(z)$ has the following asymptotic behavior at infinity:

$$Y(z) = [\mathbb{1} + \mathcal{O}(1/z)] \begin{pmatrix} z^n & 0 \\ 0 & z^{-n} \end{pmatrix}, \quad \text{as } |z| \rightarrow \infty \text{ for } z \in \mathbb{C} \setminus \mathbb{R}. \quad (\text{S2.2})$$

(Y_d) $Y(z)$ has the following behavior near $z = 0$:

$$Y(z) = \begin{cases} \mathcal{O} \begin{pmatrix} 1 & |z|^\rho \\ 1 & |z|^\rho \end{pmatrix}, & \rho < 0; \\ \mathcal{O} \begin{pmatrix} 1 & 1 \\ 1 & 1 \end{pmatrix}, & \rho \geq 0, \end{cases} \quad (\text{S2.3})$$

as $z \rightarrow 0$ for $z \in \mathbb{C} \setminus \mathbb{R}$, where the \mathcal{O} notation is taken elementwise. (For noneven weights with $\rho = 0$, the second column of $Y(z)$ would diverge as $\mathcal{O}(\log |z|)$ as $z \rightarrow 0$, but this logarithmic divergence is exactly canceled for an even weight.)

Then by the result of Fokas, Its and Kitaev [120] (see also [25, 27, 121, 122]), we have

Theorem S1. *The unique solution to the above RHP is given by*

$$Y(z) = \begin{pmatrix} P_n(z) & C[P_n w](z) \\ c_n P_{n-1}(z) & c_n C[P_{n-1} w](z) \end{pmatrix}, \quad (\text{S2.4})$$

where the $P_n(x)$ are the monic orthogonal polynomials associated with w . Here $c_n = -2\pi i y_{n-1}^2$, with $y_{n-1} > 0$ the coefficient of the leading term in the corresponding normalized orthogonal polynomial $p_{n-1}(x) = y_{n-1} x^{n-1} + \dots$, and

$$C[f](z) := \frac{1}{2\pi i} \int_{-\infty}^{\infty} \frac{f(s)}{s-z} ds, \quad z \in \mathbb{C} \setminus \mathbb{R}$$

is the Cauchy-Stieltjes transform of $f \in L^2(\mathbb{R})$. Furthermore, there exists $Y_1 \in \mathbb{C}^{2 \times 2}$ such that

$$Y(z) \begin{pmatrix} z^{-n} & 0 \\ 0 & z^n \end{pmatrix} = \mathbb{1} + \frac{Y_1}{z} + \mathcal{O} \left(\frac{1}{|z|^2} \right) \quad \text{as } |z| \rightarrow \infty.$$

The recurrence coefficient b_n and the leading coefficient y_n are then given by

$$b_n = \sqrt{(Y_1)_{12}(Y_1)_{21}}, \quad (\text{S2.5})$$

$$y_n = \frac{1}{\sqrt{-2\pi i (Y_1)_{12}}}. \quad (\text{S2.6})$$

Note that many authors in the orthogonal polynomials literature label what we call b_n as b_{n-1} , but we will stick with this convention to be consistent with the physics literature, which typically starts at b_1 rather than b_0 .

For a proof that Eq. (S2.4) solves this Riemann-Hilbert problem, see Sec 3.2 of Ref. [25]; the crucial point is that the Cauchy-Stieltjes transform satisfies the operator identity $C_+ - C_- = \text{Id}$, where $C_{\pm}[f](x) = \lim_{y \rightarrow 0^+} C[f](x \pm iy)$ denote its limits on the \pm sides of the contour (c.f. the Sokhotski–Plemelj theorem). For a proof that this is the unique solution for $Y(z)$, see Lemma 2.3 of Ref. [121].

B. Proof overview

The initial Riemann-Hilbert problem (RHP) is too complicated to solve immediately, so we perform a sequence of transformations which gradually simplify the problem until it is solvable by standard techniques. We can then reverse the transformations to obtain the desired asymptotics of $Y(z)$. We denote the sequence of transformations by

$$Y \mapsto U \mapsto T \mapsto S \mapsto R$$

- $Y \mapsto U$ is a simple rescaling by the Mhaskar-Rakhmanov-Saff number β_n , so that the dominant contributions will come from near the interval $[-1, 1]$ in the rescaled coordinates. This finite interval is the analogue of a point of stationary phase when performing a saddle point approximation of a contour integral.
- $U \mapsto T$ involves the function $g_n(z) = \int_{-1}^1 \log(z-t)\psi_n(t)dt$, the logarithmic transform of the equilibrium measure. This step normalizes the RHP at infinity, since $\exp[ng_n(z)] \approx z^n$ as $z \rightarrow \infty$. Furthermore, as $n \rightarrow \infty$, $\psi_n(t)$ approximates the density of zeros $\{x_{j,n}\}$ of the orthogonal polynomials with respect to $\exp[-Q(x)]$ when appropriately rescaled from $[-\beta_n, \beta_n]$ to $[-1, 1]$ [22, 82]. Morally we have

$$\exp[ng_n(z)] \approx \exp \left[n \int_{-1}^1 \log(z-t) \left(\frac{1}{n} \sum_{j=1}^n \delta(t - x_{j,n}/\beta_n) \right) dt \right] = \prod_{j=1}^n (z - x_{j,n}/\beta_n) = \beta_n^{-n} P_n(\beta_n z),$$

where P_n are the monic orthogonal polynomials. For technical convenience we will always define the equilibrium measure with respect to Q ; this means that for $\rho \neq 0$ the density of zeros of the orthogonal polynomials with respect to the full weight $|x|^\rho \exp[-Q(x)]$ is slightly different to that with respect to $\exp[-Q(x)]$ alone, with an enhancement or suppression near $x = 0$ depending on whether ρ is negative or positive. In the end this still provides a good enough approximation away from $x = 0$ to be useful, and we will handle the effects of the power-law more explicitly using a Szegő function (see Section S2H).

- $T \mapsto S$ involves a factorization of the jump matrix, and a subsequent deformation of the jump contours into the complex plane. Under this deformation, oscillatory terms transform into terms which decay with n and are usually subleading. In most cases these terms decay exponentially with n , but in the marginal case where $w(\omega)$ decays only exponentially in ω , these terms decay more slowly with n .
- $S \mapsto R$ is the most technically involved step. We explicitly construct a parametrix S_{par} which approximately solves the RHP for S . This construction is most delicate near the endpoints of the jump contour, and at the location of the power-law; here we construct approximate local solutions out of appropriate special functions: Airy functions near the endpoints ± 1 , and Bessel functions near the origin. We then set $R = SS_{\text{par}}^{-1}$, so that R has a jump matrix which is uniformly close enough to the identity that the RHP for R can be solved using standard techniques. One can think of R as a ‘residual’, and $R(z) \approx \mathbf{1}$ to leading order in n .

C. Riemann-Hilbert problem for U

In terms of the Mhaskar-Rakhmanov-Saff number β_n defined in Eq. (S1.10), we define

$$U(z) = \beta_n^{-(n+\rho/2)\sigma_3} Y(\beta_n z) \beta_n^{(\rho/2)\sigma_3}, \quad \text{for } z \in \mathbb{C} \setminus \mathbb{R}, \quad (\text{S2.7})$$

where $\sigma_3 = \begin{pmatrix} 1 & 0 \\ 0 & -1 \end{pmatrix}$ is the third Pauli matrix. Given that Y is the unique solution to the RHP stated above, one can verify that U is the unique solution to an equivalent RHP, stated as follows.

$(U_a) U(z)$ is analytic in $\mathbb{C} \setminus \mathbb{R}$;

(U_b) $U(z)$ takes continuous boundary values $U_{\pm}(x) := \lim_{y \rightarrow 0^{\pm}} U(x + iy)$ such that

$$U_+(x) = U_-(x) \begin{pmatrix} 1 & |x|^{\rho} e^{-nV_n(x)} \\ 0 & 1 \end{pmatrix} \quad (\text{S2.8})$$

for $x \in \mathbb{R} \setminus \{0\}$, where $V_n(x) := Q(\beta_n x)/n$ is the rescaled potential.

(U_c) U satisfies the same behaviour as $z \rightarrow \infty$ as Y does, given by Eq. (S2.2).

(U_d) U satisfies the same behaviour near $z = 0$ as Y does, given by Eq. (S2.3).

D. Equilibrium measures for complex log-Freud weights

In this section we wish to construct the equilibrium measure for the rescaled potential $V_n(x) := Q(\beta_n x)/n$. To that end, for z in the domain of analyticity of $V_n(z)$, define the function

$$h_n(z) := \frac{1}{2\pi i} \oint_{\Gamma_z} \frac{V'_n(s) ds}{s - z r(s)}, \quad (\text{S2.9})$$

where $r(s) = (s + 1)^{1/2}(s - 1)^{1/2}$, taking principal branches of powers such that $r(s) \sim +s$ as $s \rightarrow \infty$, and Γ_z is any simple closed anticlockwise oriented contour within the domain of analyticity of V_n and with $[-1, 1] \cup \{z\}$ in its interior. Now note that

$$\oint_{\Gamma_z} \frac{1}{r(s)} \frac{ds}{s - z} = 0, \quad (\text{S2.10})$$

because the integrand is analytic outside Γ_z , so we can deform the contour to infinity. Then, in order to deal with any potential singularities, we are free to rewrite

$$h_n(z) = \frac{1}{2\pi i} \oint_{\Gamma_z} \frac{V'_n(s) - V'_n(z)}{s - z} \frac{ds}{r(s)} \quad (\text{S2.11})$$

This is helpful because the integrand now has zero residue at the pole $s = z$. In order to obtain an expression for $h_n(x)$ on the real line, we pull the contour through z (at zero cost because the residue is zero), and then deform it around $[-1, 1]$, obtaining

$$h_n(x) = \frac{1}{\pi} \int_{-1}^1 \frac{V'_n(s) - V'_n(x)}{s - x} \frac{ds}{\sqrt{1 - s^2}}, \quad x \in \mathbb{R}, \quad (\text{S2.12})$$

where we used $r_+(s) = i\sqrt{1 - s^2}$. Since V_n is even, we can also write this as

$$h_n(x) = \frac{2}{\pi} \int_0^1 \frac{xV'_n(x) - sV'_n(s)}{x^2 - s^2} \frac{ds}{\sqrt{1 - s^2}}. \quad (\text{S2.13})$$

1. Definition of the equilibrium measure

Having defined $h_n(z)$ in Eq. (S2.9) (reducing to Eq. (S2.13) on the real line), we now define the ‘candidate’ equilibrium measure $\psi_n(x)$ for $x \in [-1, 1]$ by

$$\psi_n(x) := \frac{1}{2\pi} \sqrt{1 - x^2} h_n(x), \quad x \in [-1, 1]. \quad (\text{S2.14})$$

We will show that this candidate function $\psi_n(x)$ is indeed the true equilibrium measure for $V_n(x)$ by verifying that the Euler-Lagrange variational conditions for the energy minimization problem are satisfied (for large enough n). We will furthermore show that $\psi_n(x)$ is ‘regular’ in the sense that it is positive in $(-1, 1)$ and vanishes like a square root as $|x| \rightarrow 1$. This means we will get Airy universality near the endpoints $x = \pm 1$.

2. Support of the equilibrium measure

Lemma S6. *Suppose $Q \in \text{VSLF}(p, q)$ with $p \geq 1$, and q arbitrary for $p > 1$ but constrained to $q > -1$ for $p = 1$. Then there exists $n_0 \in \mathbb{N}$ such that, for every $M > 0$, there exists a constant $C > 0$ such that for all $n \geq n_0$ we have $h_n(x) > C$ for all $|x| < M$.*

We defer the proof of this statement to Section S6 B. The fact that for sufficiently large n we have $h_n(x) > 0$ for $|x| \leq 1$ implies via Eq. (S2.14) that the equilibrium measure $\psi_n(x) > 0$ for $|x| < 1$ and vanishes like a square root as $|x| \rightarrow 1$, as claimed.

3. Check of the Euler-Lagrange variational conditions

Lemma S7. *Define $g_n(z) := \int_{-1}^1 \log(z-t)\psi_n(t)dt$ for $z \in \mathbb{C} \setminus [-1, 1]$. Then for large enough n the following Euler-Lagrange variational conditions are satisfied (c.f. [22]).*

$$(i) \quad g_{n,+}(x) + g_{n,-}(x) - V_n(x) - l_n = 0, \text{ for } |x| \leq 1.$$

$$(ii) \quad g_{n,+}(x) + g_{n,-}(x) - V_n(x) - l_n < 0, \text{ for } |x| > 1.$$

The strict inequality in (ii) means that ψ_n is ‘regular’ (for large enough n).

Proof. Part (i) follows from the discussion in [82, Theorem IV.3.1], and does not require a large n limit. Part (ii) follows by combining Lemma S6 with the relation

$$g_{n,+}(x) + g_{n,-}(x) - V_n(x) - l_n = - \int_1^x h_n(t) \sqrt{t^2 - 1} dt, \quad \text{for } |x| > 1, \quad (\text{S2.15})$$

which we will now prove. We essentially rehash the relevant part of the proof of [24, Lemma 3.2]. We start from the Hilbert transform

$$H\psi_n(t) := \frac{1}{\pi} \int_{-1}^1 \frac{\psi_n(s)}{t-s} ds, \quad (\text{S2.16})$$

where f denotes a principal value integral, and integrate t from 1 to x to give

$$\int_1^x H\psi_n(t) dt = \frac{1}{\pi} \int_{-1}^1 \psi_n(s) (\log|x-s| - \log|1-s|) ds. \quad (\text{S2.17})$$

(This integration is justified for sufficiently smooth ψ_n ; see proof of [82, Theorem IV.3.1].) Since $g_{n,+}(x) + g_{n,-}(x) = 2 \int_{-1}^1 \log|x-s|\psi_n(s)ds$ for $x \in \mathbb{R}$, this means

$$g_{n,+}(x) + g_{n,-}(x) - [g_{n,+}(1) + g_{n,-}(1)] = 2\pi \int_1^x H\psi_n(t) dt. \quad (\text{S2.18})$$

The variational condition gives $g_{n,+}(1) + g_{n,-}(1) = V_n(1) + l_n$, and so

$$g_{n,+}(x) + g_{n,-}(x) - V_n(x) - l_n = 2\pi \int_1^x \left(H\psi_n(t) - \frac{V'_n(t)}{2\pi} \right) dt. \quad (\text{S2.19})$$

It remains to show that

$$H\psi_n(t) - \frac{V'_n(t)}{2\pi} = -\frac{1}{2\pi} h_n(t) \sqrt{t^2 - 1}, \quad \text{for } t > 1. \quad (\text{S2.20})$$

This will follow the proof of [24, Theorem 3.1]. Define the function

$$F_n(z) := \frac{1}{\pi i} \int_{-1}^1 \frac{\psi_n(s)}{s-z} ds, \quad z \in \mathbb{C} \setminus [-1, 1], \quad (\text{S2.21})$$

which on $[-1, 1]$ has the jump

$$F_{n,\pm}(x) = \pm\psi_n(x) + iH\psi_n(x), \quad x \in [-1, 1]. \quad (\text{S2.22})$$

However, differentiating the variational condition on $[-1, 1]$ gives

$$H\psi_n(x) = \frac{V'_n(x)}{2\pi}, \quad x \in [-1, 1]. \quad (\text{S2.23})$$

It follows that F_n satisfies the following scalar Riemann-Hilbert problem,

$$F_{n,+}(x) + F_{n,-}(x) = \frac{iV'_n(x)}{\pi}, \quad x \in [-1, 1], \quad (\text{S2.24})$$

$$F_{n,+}(x) - F_{n,-}(x) = 0, \quad x \in \mathbb{R} \setminus [-1, 1], \quad (\text{S2.25})$$

$$F_n(z) = \frac{-1}{i\pi z} + \mathcal{O}(z^{-2}), \quad z \rightarrow \infty, \quad (\text{S2.26})$$

which has the standard solution

$$F_n(z) = r(z) \frac{1}{\pi i} \int_{-1}^1 \frac{iV'_n(s)/(2\pi)}{r_+(s)} \frac{ds}{s-z}, \quad z \in \mathbb{C} \setminus \mathbb{R}, \quad (\text{S2.27})$$

where $r(z) = (z-1)^{1/2}(z+1)^{1/2}$. For nonreal z in the domain of analyticity of V_n , we can rewrite

$$F_n(z) = \frac{iV'_n(z)}{2\pi} + \frac{1}{2\pi i} h_n(z) r(z), \quad (\text{S2.28})$$

where $h_n(z)$ is given by the contour integral

$$h_n(z) = \frac{1}{2\pi i} \oint_{\Gamma_z} \frac{V'_n(s)}{r(s)} \frac{ds}{s-z}, \quad (\text{S2.29})$$

which for $z \rightarrow x \in [-1, 1]$ gives the familiar expression for $h_n(x)$ from the definition of the equilibrium measure. For $t > 1$ we have

$$F_n(t) = \frac{iV'_n(t)}{2\pi} + \frac{1}{2\pi i} h_n(t) \sqrt{t^2 - 1}, \quad (\text{S2.30})$$

and the expression Eq. (S2.20) comes from noticing that $H\psi_n(t) = -iF_n(t)$ for $t \in \mathbb{R} \setminus [-1, 1]$. \square

E. Logarithmic transform of the equilibrium measure, and the Riemann-Hilbert problem for T

Given the rescaled equilibrium measure $\psi_n(x)$ for $V_n(x) = Q(\beta_n x)/n$ (see Section S2D), we define its logarithmic transform $g_n(z)$ by

$$g_n(z) := \int_{-1}^1 \log(z-t) \psi_n(t) dt, \quad \text{for } z \in \mathbb{C} \setminus (-\infty, 1], \quad (\text{S2.31})$$

where we take the principal branch of the logarithm. For z approaching the real axis, we have the limiting values $g_{n,\pm}(x) := \lim_{y \rightarrow 0^+} g_n(x \pm iy)$ given by

$$g_{n,\pm}(x) = \int_{-1}^1 \log|x-t| \psi_n(t) dt \pm \begin{cases} i\pi, & x \leq -1, \\ i\pi \int_x^1 \psi_n(t) dt, & -1 < x < 1, \\ 0, & x \geq 1. \end{cases} \quad (\text{S2.32})$$

The following proposition is immediate from Eqs. (S2.31) and (S2.32).

Proposition S1. *For all $n \in \mathbb{N}$, the following holds.*

(a) g_n is analytic and $g_n|_{\mathbb{C}_\pm}$ have continuous extensions to \mathbb{C}_\pm .

(b) The map $z \mapsto e^{ng_n(z)}$ possesses an analytic continuation to $\mathbb{C} \setminus [-1, 1]$, and

$$e^{ng_n(z)} z^{-n} = 1 + \mathcal{O}\left(\frac{1}{|z|}\right), \quad \text{as } z \rightarrow \infty. \quad (\text{S2.33})$$

In terms of the logarithmic transform $g_n(z)$, we define the matrix-valued function T by

$$T(z) = e^{-\frac{nl_n}{2}\sigma_3} U(z) e^{\frac{nl_n}{2}\sigma_3} e^{-ng_n(z)\sigma_3}. \quad (\text{S2.34})$$

Given that $U(z)$ satisfies the Riemann-Hilbert problem (U_a) - (U_d) , one can combine Eqs. (S2.32) and (S2.33) to verify that $T(z)$ satisfies the following equivalent Riemann-Hilbert problem.

(T_a) $T(z)$ is analytic in $\mathbb{C} \setminus \mathbb{R}$.

(T_b) T satisfies the following jump relations on \mathbb{R} :

$$T_+(x) = T_-(x) \begin{pmatrix} e^{-n(g_{n,+}(x)-g_{n,-}(x))} & |x|^\rho \\ 0 & e^{n(g_{n,+}(x)-g_{n,-}(x))} \end{pmatrix}, \quad \text{for } x \in [-1, 1] \setminus \{0\}, \quad (\text{S2.35})$$

$$T_+(x) = T_-(x) \begin{pmatrix} 1 & |x|^\rho e^{n(g_{n,+}(x)+g_{n,-}(x)-V_n(x)-l_n)} \\ 0 & 1 \end{pmatrix}, \quad \text{for } |x| > 1. \quad (\text{S2.36})$$

(T_c) $T(z) = \mathbb{1} + \mathcal{O}(1/z)$ as $z \rightarrow \infty$.

(T_d) $T(z)$ has the same behavior as $Y(z)$ as $z \rightarrow 0$, given by Eq. (S2.3).

Notice that, by (T_c) , the Riemann-Hilbert problem is now normalized at infinity. Furthermore, by Lemmas S6 and S7, the jump matrix is exponentially close to the identity for $|x| > 1$. For $|x| < 1$, we see from Eq. (S2.32) that the diagonal elements of the jump matrix are complex phases which rapidly oscillate for large n ; these can be viewed as the analogue of the ‘fast phase’ arising in the analysis of linear differential equations in the WKB limit [22].

F. Analytic continuation of the equilibrium measure and its logarithmic transform

In terms of $h_n(z)$, which is defined by Eq. (S2.9) within the domain of analyticity of $V_n(z)$, we can define an analytic continuation $\hat{\psi}_n(z)$ of the equilibrium measure by

$$\hat{\psi}_n(z) = \frac{1}{2\pi i} r(z) h_n(z), \quad (\text{S2.37})$$

with $r(z) = (z+1)^{1/2}(z-1)^{1/2}$. Since $h_n(z)$ is analytic, while $r(z)$ flips sign across $[-1, 1]$, we have

$$\hat{\psi}_{n,+}(x) = -\hat{\psi}_{n,-}(x) = \psi_n(x), \quad \text{for } x \in (-1, 1), \quad (\text{S2.38})$$

$$\hat{\psi}_{n,+}(x) = \hat{\psi}_{n,-}(x), \quad \text{for } x \in \mathbb{R} \setminus (-1, 1), \quad (\text{S2.39})$$

so $\hat{\psi}_n(z)$ is an analytic continuation of $\psi_n(x)$ to \mathbb{C}_+ , and similarly $-\hat{\psi}_n(z)$ provides an analytic continuation to \mathbb{C}_- . Finally, having defined these continuations, we define

$$\phi_n(z) := -\pi i \int_1^z \hat{\psi}_n(y) dy, \quad \text{for } z \in \mathbb{C} \setminus \mathbb{R}, \quad (\text{S2.40})$$

where the path of integration does not cross the real axis. By using the analyticity of $\hat{\psi}_n(z)$ and the fact that $\int_0^1 \psi_n(x) dx = 1/2$ by symmetry, one can show that $\phi_n(z)$ can equivalently be written as

$$\phi_n(z) = \pm \frac{i\pi}{2} - \pi i \int_0^z \hat{\psi}_n(y) dy, \quad \text{for } z \in \mathbb{C}_\pm, \quad (\text{S2.41})$$

where again the path of integration does not cross the real axis. Note that Eq. (S2.39) implies that $\phi_n(z)$ is analytic across $\mathbb{R} \setminus (-1, 1)$. Also, Eq. (S2.41) shows that $2\phi_{n,+}(0) = 2\pi i \int_0^1 \psi_n(t) dt = \pi i$. This is a special property of *even* weight functions, but should be true generically given that symmetry. This factor (exponentiated) is what ends up giving rise to the $(-1)^n$ staggering factor in the recurrence coefficients, so here we see that this is a direct consequence of the $x \rightarrow -x$ symmetry, which itself is a consequence of unitarity.

For the logarithmic transform, note that by Eq. (S2.32) we have

$$g_{n,+}(x) - g_{n,-}(x) = \begin{cases} 2\pi i, & x \leq -1, \\ 2\pi i \int_x^1 \psi_n(t) dt, & |x| < 1, \\ 0, & x \geq 1. \end{cases} \quad (\text{S2.42})$$

From Eqs. (S2.38) and (S2.40) we deduce that the functions $2\phi_n(z)$ and $-2\phi_n(z)$ provide analytic continuations of $(g_{n,+} - g_{n,-})(z)$ into the upper and lower half planes respectively.

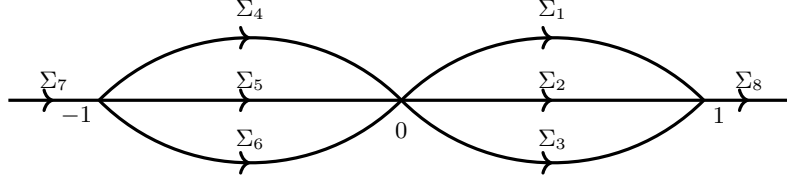


FIG. S2. The lens shaped contour $\Sigma = \bigcup_{j=1}^6 \Sigma_j$.

G. Riemann-Hilbert problem for S : contour deformation and ‘opening the lens’

Next we notice that the jump matrix for $T(x)$ on $x \in [-1, 1]$ can be factorized as

$$\begin{pmatrix} e^{-n(g_{n,+}(x)-g_{n,-}(x))} & |x|^\rho \\ 0 & e^{n(g_{n,+}(x)-g_{n,-}(x))} \end{pmatrix} = \begin{pmatrix} 1 & 0 \\ |x|^{-\rho} e^{n(g_{n,+}(x)-g_{n,-}(x))} & 1 \end{pmatrix} \begin{pmatrix} 0 & |x|^\rho \\ -|x|^{-\rho} & 0 \end{pmatrix} \begin{pmatrix} 1 & 0 \\ |x|^{-\rho} e^{-n(g_{n,+}(x)-g_{n,-}(x))} & 1 \end{pmatrix}. \quad (\text{S2.43})$$

Remembering that $\pm 2\phi_n(z)$ provides an analytic continuation of $g_{n,+} - g_{n,-}$ to \mathbb{C}_\pm , and defining the analytic continuation of $|x|^\rho$ to be

$$\omega(z) = \begin{cases} (-z)^\rho, & \text{if } \text{Re } z < 0, \\ z^\rho, & \text{if } \text{Re } z > 0, \end{cases} \quad (\text{S2.44})$$

with principal branches of powers, we define the matrix-valued function S as follows.

$$S(z) = \begin{cases} T(z), & \text{for } z \text{ outside the lens,} \\ T(z) \begin{pmatrix} 1 & 0 \\ -\omega(z)^{-1} e^{-2n\phi_n(z)} & 1 \end{pmatrix}, & \text{for } z \text{ in the upper parts of the lens,} \\ T(z) \begin{pmatrix} 1 & 0 \\ \omega(z)^{-1} e^{-2n\phi_n(z)} & 1 \end{pmatrix}, & \text{for } z \text{ in the lower parts of the lens.} \end{cases} \quad (\text{S2.45})$$

By the upper parts of the lens, we mean the regions enclosed by $\Sigma_1 \cup \Sigma_2$ and $\Sigma_4 \cup \Sigma_5$, and by the lower parts of the lens, we mean the regions enclosed by $\Sigma_3 \cup \Sigma_2$ and $\Sigma_6 \cup \Sigma_5$, with the contours Σ_j shown schematically in Fig. S2. Because of the shape of these contours, this step is often referred to as ‘opening the lens’.

Given the conditions for the Riemann-Hilbert problem for T , one can verify that S is the unique solution of the following Riemann-Hilbert problem.

(S_a) $S(z)$ is analytic in $\mathbb{C} \setminus \Sigma$.

(S_b) S satisfies the following jump relations on Σ :

$$S_+(z) = S_-(z) \begin{pmatrix} 1 & 0 \\ \omega(z)^{-1} e^{-2n\phi_n(z)} & 1 \end{pmatrix}, \quad \text{for } z \in \Sigma \cap \mathbb{C}_\pm, \quad (\text{S2.46})$$

$$S_+(x) = S_-(x) \begin{pmatrix} 0 & |x|^\rho \\ -|x|^{-\rho} & 0 \end{pmatrix}, \quad \text{for } x \in (-1, 1) \setminus \{0\}, \quad (\text{S2.47})$$

$$S_+(x) = S_-(x) \begin{pmatrix} 1 & |x|^\rho e^{n(g_{n,+}(x)+g_{n,-}(x)-V_n(x)-I_n)} \\ 0 & 1 \end{pmatrix}, \quad \text{for } |x| > 1. \quad (\text{S2.48})$$

(S_c) $S(z) = \mathbb{1} + \mathcal{O}(1/z)$ as $z \rightarrow \infty$.

(S_d) For $\rho < 0$, the matrix function $S(z)$ has the following behavior as $z \rightarrow 0$:

$$S(z) = \mathcal{O} \begin{pmatrix} 1 & |z|^\rho \\ 1 & |z|^\rho \end{pmatrix}, \quad \text{as } z \rightarrow 0, z \in \mathbb{C} \setminus \Sigma. \quad (\text{S2.49})$$

For $\rho > 0$, the matrix function $S(z)$ has the following behavior as $z \rightarrow 0$:

$$S(z) = \begin{cases} \mathcal{O} \begin{pmatrix} 1 & 1 \\ 1 & 1 \end{pmatrix}, & \text{as } z \rightarrow 0 \text{ from outside the lens,} \\ \mathcal{O} \begin{pmatrix} |z|^{-\rho} & 1 \\ |z|^{-\rho} & 1 \end{pmatrix}, & \text{as } z \rightarrow 0 \text{ from inside the lens.} \end{cases} \quad (\text{S2.50})$$

We already know from Lemma S7 that the jump matrix for $|x| > 1$ is exponentially close in n to the identity matrix. For the new jump on $\Sigma \cap \mathbb{C}_\pm$, we will show in Lemma S12 that $\sup_{z \in \Sigma} |e^{-2n\phi_n(z)}| \xrightarrow{n \rightarrow \infty} 0$, so this jump matrix will also tend to the identity as $n \rightarrow \infty$. Precisely how fast this happens depends on the scaling of $\text{Re}[\phi_n(z)]$ with n . We will see later that in most cases we can get $\exp[-n\phi_n(z)]$ to decay superpolynomially in n . However, in the marginal case where the weight $w(x)$ decays only exponentially as $|x| \rightarrow \infty$, the decay of $\exp[-n\phi_n(z)]$ with n will be slower, only super-polylogarithmic in the worst case (see Lemma S12 for details).

H. Parametrix N for the outside region

Since the jumps for $S(z)$ for z away from $(-1, 1)$ decay with n , it is useful to solve the Riemann-Hilbert problem for only the jump on $(-1, 1)$, whose solution we will denote by $N(z)$.

Riemann-Hilbert problem for N

(N_a) $N : \mathbb{C} \setminus [-1, 1] \rightarrow \mathbb{C}^{2 \times 2}$ is analytic.

(N_b) $N_+(x) = N_-(x) \begin{pmatrix} 0 & |x|^\rho \\ -|x|^{-\rho} & 0 \end{pmatrix}$ for $x \in (-1, 1) \setminus \{0\}$.

(N_c) $N(z) = \mathbf{1} + \mathcal{O}\left(\frac{1}{|z|}\right)$ as $|z| \rightarrow \infty$.

We will construct a solution to this RH problem in terms of the Szegő function D associated with $|x|^\rho$ on $(-1, 1)$. This is a scalar function which is the solution to a multiplicative scalar RH problem with the following conditions.

Riemann-Hilbert problem for D

(D_a) $D : \mathbb{C} \setminus [-1, 1] \rightarrow \mathbb{C}$ is analytic and nonzero.

(D_b) $D_+(x)D_-(x) = |x|^\rho$ for $x \in (-1, 1) \setminus \{0\}$.

(D_c) $\lim_{z \rightarrow \infty} D(z) = D_\infty$ exists and is a positive real number.

In this case, one can check that the Szegő function is given by

$$D(z) = \frac{z^{\rho/2}}{\varphi(z)^{\rho/2}}, \quad (\text{S2.51})$$

where

$$\varphi(z) := z + (z+1)^{1/2}(z-1)^{1/2} \quad (\text{S2.52})$$

is the conformal map from $\mathbb{C} \setminus [-1, 1]$ to the exterior of the unit circle; $\varphi(z)$ has a branch cut along $[-1, 1]$ and behaves like $\varphi(z) \approx 2z$ as $z \rightarrow \infty$.

Having obtained D , it turns out that the solution to the RH problem for N is [26]

$$N(z) = \begin{pmatrix} D_\infty & 0 \\ 0 & \frac{1}{D_\infty} \end{pmatrix} \begin{pmatrix} \frac{a(z)+a^{-1}(z)}{2} & \frac{a(z)-a^{-1}(z)}{2i} \\ \frac{a(z)-a^{-1}(z)}{-2i} & \frac{a(z)+a^{-1}(z)}{2} \end{pmatrix} \begin{pmatrix} \frac{1}{D(z)} & 0 \\ 0 & D(z) \end{pmatrix}, \quad (\text{S2.53})$$

where

$$a(z) := \frac{(z-1)^{1/4}}{(z+1)^{1/4}} \quad \text{and} \quad D_\infty := \lim_{z \rightarrow \infty} D(z) = 2^{-\rho/2}. \quad (\text{S2.54})$$

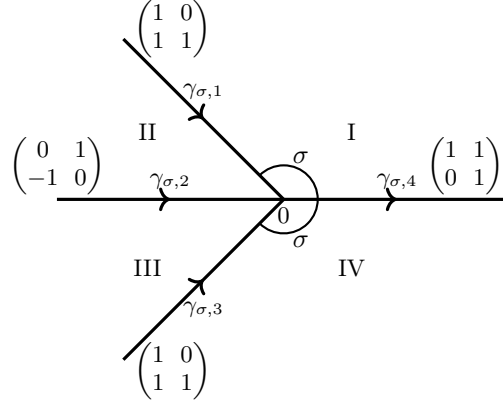


FIG. S3. The oriented contour γ_σ and the jump matrix v_1 for Ψ on γ_σ . The four straight rays $\gamma_{\sigma,1}, \dots, \gamma_{\sigma,4}$ divide the complex plane into four regions I, II, III, and IV.

Since $N(z)$ is a product of three matrices each with $\det = 1$, we have $\det N(z) = 1$, so $N(z)$ is invertible. Furthermore, as $z \rightarrow \infty$, this matrix scales as

$$N(z) = \mathbb{1} + \frac{i}{2z} \begin{pmatrix} 0 & 2^{-\rho} \\ -2^\rho & 0 \end{pmatrix} + \mathcal{O}\left(\frac{1}{z^2}\right), \quad (\text{S2.55})$$

and as $z \rightarrow 0$ it scales as

$$N(z) \sim \mathcal{O} \begin{pmatrix} z^{-\rho/2} & z^{\rho/2} \\ z^{-\rho/2} & z^{\rho/2} \end{pmatrix}, \quad (\text{S2.56})$$

where the big- \mathcal{O} notation is taken elementwise.

I. Local parametrix P near the endpoints $z = \pm 1$

While it is true that the jumps of $S(z)$ decay with n for z away from the real axis, these jumps become nonnegligible at the points $z = 0$ and $z = \pm 1$ where the contour Σ meet the real axis. We need to construct ‘local parametrices’ which approximately solve the Riemann-Hilbert problem for S near these points, and handle any potential singularities.

In this subsection we will construct the parametrices for the endpoints $z = \pm 1$, which we will build out of Airy functions (because the equilibrium measure is regular for large enough n). Our analysis here is standard and will closely follow that of Refs. [22, 123]. First we focus on the parametrix near $z = 1$, since the construction near $z = -1$ will be closely related by symmetry. We will make use of the function $h_n(z)$ defined in Eq. (S2.9), which is analytic in the region of analyticity of V_n , which by assumption contains a neighbourhood of $z = 1$. We will construct the parametrix $P(z)$ in a disk $U_{\delta_2} = \{z \in \mathbb{C} : |z - 1| < \delta_2\}$ around $z = 1$, where the radius $\delta_2 > 0$ is a small constant. $P(z)$ is the solution to the following Riemann-Hilbert problem.

Riemann-Hilbert problem for P

(P_a) P is analytic in $U_{\delta_2} \setminus \Sigma$.

(P_b) $P_+(z) = P_-(z)v_S(z)$ for $z \in \Sigma \cap U_{\delta_2}$, with v_S the jump matrix for S .

(P_c) $P(z)N(z)^{-1} \sim \mathbb{1} + \mathcal{O}(1/n)$ as $n \rightarrow \infty$, uniformly for z on the boundary ∂U_δ of the disk U_δ for δ in compact subsets of $(0, \delta_2)$.

The construction of P involves three steps. First we will construct a matrix-valued function that satisfies conditions (P_a) and (P_b). In order to do this we will transform this RHP into a RHP for $P^{(1)}$ with constant jump matrices and then construct a solution of the latter RHP. Finally, we will take the matching condition (P_c) into account.

1. Transformation to constant jump matrices

Following Ref. [123], in order to transform to constant jump matrices, we seek the parametrix P near 1 in the following form

$$P(z) = E(z)P^{(1)}(z)e^{-n\phi_n(z)\sigma_3}z^{-(1/2)\rho\sigma_3}, \quad \text{for } z \in U_{\delta_2} \setminus \Sigma, \quad (\text{S2.57})$$

with E an invertible analytic matrix-valued function in U_{δ_2} , to be determined to ensure that the matching condition (P_c) is satisfied. Since E is invertible and analytic, one can use Eqs. (S2.38) to (S2.40) to show that the jump matrix for $P^{(1)}$ is piecewise constant:

$$P_+^{(1)}(z) = \begin{cases} P_-^{(1)}(z) \begin{pmatrix} 1 & 0 \\ 1 & 1 \end{pmatrix}, & z \in (\Sigma_1 \cup \Sigma_3) \cap U_{\delta_2}, \\ P_-^{(1)}(z) \begin{pmatrix} 0 & 1 \\ -1 & 0 \end{pmatrix}, & z \in \Sigma_2 \cap U_{\delta_2} = (1 - \delta_2, 1), \\ P_-^{(1)}(z) \begin{pmatrix} 1 & 1 \\ 0 & 1 \end{pmatrix}, & z \in \Sigma_8 \cap U_{\delta_2} = (1, 1 + \delta_2). \end{cases} \quad (\text{S2.58})$$

We will determine $P^{(1)}$ subject to these constant jump matrices by an explicit construction based on an auxiliary problem for $\Psi(\zeta)$ in the ζ -plane with jumps on the oriented contour $\gamma_\sigma = \cup_{j=1}^4 \gamma_{\sigma,j}$, shown in Fig. S3, consisting of four straight rays

$$\gamma_{\sigma,1} : \arg \zeta = \sigma, \quad \gamma_{\sigma,2} : \arg \zeta = \pi, \quad \gamma_{\sigma,3} : \arg \zeta = -\sigma, \quad \gamma_{\sigma,4} : \arg \zeta = 0,$$

with $\sigma \in (\pi/3, \pi)$. These four rays divide the complex plane into four regions I, II, III, and IV, also shown in Fig. S3.

Riemann-Hilbert problem for Ψ

(Ψ_a) Ψ is analytic in $\mathbb{C} \setminus \gamma_\sigma$.

(Ψ_b) $\Psi_+(\zeta) = \Psi_-(\zeta)v_1(\zeta)$ for $\zeta \in \gamma_\sigma$, where v_1 is the piecewise constant matrix-valued function on γ_σ defined as shown in Fig. S3, i.e., $v_1(\zeta) = \begin{pmatrix} 1 & 0 \\ 1 & 1 \end{pmatrix}$ for $\zeta \in \gamma_{\sigma,1}$, etc. This means that Ψ has the same jumps on γ_σ as $P^{(1)}$ does on $\Sigma_S \cap U_{\delta_2}$.

(Ψ_c) Ψ has the following behaviour at infinity,

$$\begin{aligned} \Psi(\zeta) &\sim \zeta^{-\sigma_3/4} \frac{1}{\sqrt{2}} \begin{pmatrix} 1 & 1 \\ -1 & 1 \end{pmatrix} \\ &\times \left[\mathbf{1} + \sum_{k=1}^{\infty} \frac{1}{2} \left(\frac{2}{3} \zeta^{3/2} \right)^{-k} \begin{pmatrix} (-1)^k (s_k + t_k) & s_k - t_k \\ (-1)^k (s_k - t_k) & s_k + t_k \end{pmatrix} \right] e^{-(\pi i/4)\sigma_3} e^{-(2/3)\zeta^{3/2}\sigma_3}, \end{aligned} \quad (\text{S2.59})$$

as $\zeta \rightarrow \infty$, uniformly for $\zeta \in \mathbb{C} \setminus \gamma_\sigma$ and σ in compact subsets of $(\pi/3, \pi)$. Here,

$$s_k = \frac{\Gamma(3k + \frac{1}{2})}{54^k k! \Gamma(k + \frac{1}{2})}, \quad t_k = -\frac{6k + 1}{6k - 1} s_k, \quad \text{for } k \geq 1. \quad (\text{S2.60})$$

It is well known [22, 25] that, with $\varpi := e^{2\pi i/3}$ and Ai the Airy function, the solution to this RHP is

$$\Psi(\zeta) = \sqrt{2\pi} e^{-\pi i/12} \times \begin{cases} \begin{pmatrix} \text{Ai}(\zeta) & \text{Ai}(\varpi^2 \zeta) \\ \text{Ai}'(\zeta) & \varpi^2 \text{Ai}'(\varpi^2 \zeta) \end{pmatrix} e^{-(\pi i/6)\sigma_3}, & \zeta \in \text{I}, \\ \begin{pmatrix} \text{Ai}(\zeta) & \text{Ai}(\varpi^2 \zeta) \\ \text{Ai}'(\zeta) & \varpi^2 \text{Ai}'(\varpi^2 \zeta) \end{pmatrix} e^{-(\pi i/6)\sigma_3} \begin{pmatrix} 1 & 0 \\ -1 & 1 \end{pmatrix}, & \zeta \in \text{II}, \\ \begin{pmatrix} \text{Ai}(\zeta) & -\varpi^2 \text{Ai}(\varpi \zeta) \\ \text{Ai}'(\zeta) & -\text{Ai}'(\varpi \zeta) \end{pmatrix} e^{-(\pi i/6)\sigma_3} \begin{pmatrix} 1 & 0 \\ 1 & 1 \end{pmatrix}, & \zeta \in \text{III}, \\ \begin{pmatrix} \text{Ai}(\zeta) & -\varpi^2 \text{Ai}(\varpi \zeta) \\ \text{Ai}'(\zeta) & -\text{Ai}'(\varpi \zeta) \end{pmatrix} e^{-(\pi i/6)\sigma_3}, & \zeta \in \text{IV}, \end{cases} \quad (\text{S2.61})$$

With this definition, we can now specify the precise form of the contour Σ near $z = 1$: Σ is defined in U_{δ_2} as the inverse f_n -image of $\gamma_\sigma \cap f_n(U_{\delta_2})$, where $f_n(z)$ is a biholomorphic map between the z - and ζ -planes to be constructed in the next section. We then define

$$P^{(1)}(z) := \Psi(f_n(z)), \quad \text{for } z \in U_{\delta_2} \setminus f_n^{-1}(\gamma_\sigma). \quad (\text{S2.62})$$

2. Construction of biholomorphic map

Proposition S2. *There exists a $\delta_2 > 0$ such that for sufficiently large n there exists a function $f_n : U_{\delta_2} \rightarrow f_n(U_{\delta_2}) \subset \mathbb{C}$ with the following properties.*

- (a) $f_n : U_{\delta_2} \rightarrow f_n(U_{\delta_2})$ is biholomorphic.
- (b) $f_n(U_{\delta_2} \cap \mathbb{R}) = f_n(U_{\delta_2}) \cap \mathbb{R}$, $f_n(U_{\delta_2} \cap \mathbb{C}_{\pm}) = f_n(U_{\delta_2}) \cap \mathbb{C}_{\pm}$.
- (c) $\frac{2}{3}(f_n(z))^{3/2} = -n\phi_n(z)$ for all $z \in U_{\delta_2} \setminus (-\infty, 1]$.

Proof (adapted from [123], Prop 3.19). Given the analyticity of $h_n(z)$ near $z = 1$, we will explicitly construct $f_n(z)$ as follows. We define the auxiliary function $\hat{\varphi}_n : \mathbb{C} \setminus (-\infty, 1] \rightarrow \mathbb{C}$ by

$$\hat{\varphi}_n(z) = \frac{3}{4}(z-1)^{-3/2} \int_1^z h_n(s)(s+1)^{1/2}(s-1)^{1/2} ds, \quad (\text{S2.63})$$

$$= \frac{h_n(1)}{\sqrt{2}} + \frac{3}{4}(z-1)^{-3/2} \int_1^z \left[h_n(s)(s+1)^{1/2} - h_n(1)\sqrt{2} \right] (s-1)^{1/2} ds. \quad (\text{S2.64})$$

Note that $\hat{\varphi}_n(z)$ actually has no jumps across $(-1, 1)$ because both $(z-1)^{-3/2}$ and $(s-1)^{1/2}$ flip sign, so we already know that $\hat{\varphi}_n(z)$ has an analytic continuation to $U_{\delta} \setminus \{1\}$ for some $\delta > 0$. To deal with the potential difficulty at $z = 1$, note that, for $|s-1| < \delta$, Cauchy's theorem tells us that

$$\begin{aligned} \left| h_n(s)(s+1)^{1/2} - h_n(1)\sqrt{2} \right| &= \left| (s-1) \frac{1}{2\pi i} \oint_{|w-1|=2\delta} \frac{h_n(w)(w+1)^{1/2} - h_n(1)\sqrt{2}}{(w-1)(w-s)} dw \right|, \\ &\leq \frac{|s-1|}{\delta} \sup_{|w-1|=2\delta} \left| h_n(w)(w+1)^{1/2} - h_n(1)\sqrt{2} \right|. \end{aligned}$$

In Lemma S11 we prove that, for sufficiently large n and sufficiently small δ , there exists a constant $\epsilon > 0$ (independent of n) such that $|h_n(w) - h_n(1)| < \epsilon$ for $|w-1| < 2\delta$. Together with Lemma 1, which tells us that $h_n(1) = 2p + o(1)$, it is easy to see that there is a constant $c > 0$ such that for $|s-1| < \delta$ and sufficiently large n we have

$$\left| h_n(s)(s+1)^{1/2} - h_n(1)\sqrt{2} \right| \leq c|s-1|. \quad (\text{S2.65})$$

Inserting this into Eq. (S2.64), we conclude there is a constant $C_1 > 0$ such that for sufficiently large n we have

$$|\hat{\varphi}_n(z) - \hat{\varphi}_n(1)| \leq C_1|z-1|, \quad \text{for } |z-1| < \delta, \quad (\text{S2.66})$$

where $\hat{\varphi}_n(1) = h_n(1)/\sqrt{2}$. Therefore the isolated singularity of $\hat{\varphi}_n(z)$ at $z = 1$ is removable, so that $\hat{\varphi}_n$ is indeed analytic for $z \in U_{\delta}$. Having established these properties of $\hat{\varphi}_n(z)$, we then define the function

$$\varphi_n(z) := (z-1)(\hat{\varphi}_n(z))^{2/3}, \quad \text{for } z \in U_{\delta}. \quad (\text{S2.67})$$

Since $\hat{\varphi}_n(1) = h_n(1)/\sqrt{2}$ and $h_n(1) = 2p + o(1)$ by Lemma 1, we conclude that $\text{Re}[\hat{\varphi}_n(z)] > 0$ for $z \in U_{\delta}$ and sufficiently large n . This implies that $\varphi_n(z)$ is analytic for $z \in U_{\delta}$.

To establish that $\varphi_n(z)$ is injective, observe that, by Eqs. (S2.66) and (S2.67) and Lemmas 1 and S11, $\varphi_n(z)$ is uniformly (in n and z) bounded in U_{δ} . By Cauchy's theorem for derivatives, this implies that $\varphi_n''(z)$ is also uniformly (in n and z) bounded in U_{δ} for a smaller δ . Since $\hat{\varphi}_n(1) = h_n(1)/\sqrt{2} \neq 0$, we have $\varphi_n'(1) = (h_n(1)/\sqrt{2})^{2/3}$, so that

$$\left| \varphi_n'(z) - (h_n(1)/\sqrt{2})^{2/3} \right| = \left| \int_1^z \varphi_n''(s) ds \right| \leq C_2|z-1|, \quad \text{for } z \in U_{\delta},$$

for some constant $C_2 > 0$ and sufficiently large n . By Lemma 1 we know there exists $h_0 > 0$ such that $h_n(1) > h_0$ for sufficiently large n , and so by the inverse function theorem we conclude there exists $0 < \delta_2 < \delta$ such that φ_n is injective and hence biholomorphic in U_{δ_2} .

Finally, we define the biholomorphic map $f_n(z)$ by

$$f_n(z) := n^{2/3}\varphi_n(z). \quad (\text{S2.68})$$

Property (b) follows from the fact that φ_n and its inverse φ_n^{-1} are real on the real axis, while property (c) follows from

$$\phi_n(z) = -\frac{2}{3}(z-1)^{3/2}\hat{\varphi}_n(z), \quad (\text{S2.69})$$

which follows from Eqs. (S2.40) and (S2.63). \square

To calculate residues we will need the values of $\hat{\varphi}_n(1)$ and $\hat{\varphi}'_n(1)$, which can be calculated from the values of $h_n(1)$ and $h'_n(1)$ via

$$\hat{\varphi}_n(1) = \frac{1}{\sqrt{2}}h_n(1), \quad (\text{S2.70})$$

$$\hat{\varphi}'_n(1) = \frac{3\sqrt{2}}{40}[h_n(1) + 4h'_n(1)]. \quad (\text{S2.71})$$

3. Satisfying the matching condition

In this final step, we construct the invertible analytic matrix-valued function $E(z)$ to ensure that the matching function (P_c) is satisfied. In the $n \rightarrow \infty$ limit, by comparing Eqs. (S2.59), (S2.62) and (S2.68), we see that we must define E as

$$E(z) := N(z)z^{(1/2)\rho\sigma_3}e^{(\pi i/4)\sigma_3}\frac{1}{\sqrt{2}}\begin{pmatrix} 1 & -1 \\ 1 & 1 \end{pmatrix}f_n(z)^{\sigma_3/4}, \quad \text{for } z \in U_{\delta_2}. \quad (\text{S2.72})$$

It is straightforward to check that $E(z)$ so defined is indeed analytic and invertible (see [123], Remark 3.21). This ends the construction of the parametrix P near $z = 1$.

4. Summary of the local analysis near $z = 1$

Fixing an angle $\sigma \in (\pi/3, \pi)$, we have defined the contour Σ in a disk U_{δ_2} near $z = 1$ as the inverse image of the contour γ_σ under the map f_n defined in Eq. (S2.68). We have then found a solution

$$P(z) = E(z)\Psi(f_n(z))e^{-n\phi_n(z)\sigma_3}z^{-(1/2)\rho\sigma_3}, \quad \text{for } z \in \Sigma \cap U_{\delta_2} \quad (\text{S2.73})$$

to the RHP for P , where the matrix-valued function E is defined in Eq. (S2.72), and the matrix-valued function Ψ is defined in Eq. (S2.61). Furthermore, we have the asymptotic expansion

$$P(z)N(z)^{-1} \sim \mathbb{1} + \sum_{k=1}^{\infty} \Delta_k(z)\frac{1}{n^k}, \quad \text{as } n \rightarrow \infty, \quad (\text{S2.74})$$

uniformly for z in compact subsets of $\{0 < |z-1| < \delta_2\}$ and σ in compact subsets of $(\pi/3, \pi)$, where Δ_k is a meromorphic 2×2 matrix-valued function determined by Eqs. (S2.57), (S2.59), (S2.62), (S2.68) and (S2.72), and given explicitly by

$$\Delta_k(z) = \frac{1}{2(-\phi_n(z))^k}N(z)z^{(1/2)\rho\sigma_3}\begin{pmatrix} (-1)^k(s_k + t_k) & i(s_k - t_k) \\ -i(-1)^k(s_k - t_k) & s_k + t_k \end{pmatrix}z^{-(1/2)\rho\sigma_3}N(z)^{-1}, \quad (\text{S2.75})$$

where ϕ_n is defined in Eq. (S2.40), $N(z)$ is given in Eq. (S2.53), and the scalars s_k and t_k are defined in Eq. (S2.60). One can verify that $\Delta_k(z)$ is meromorphic in a neighbourhood of $z = 1$ by using the jump conditions of $\phi_n(z)$ and $N(z)$.

The first term in this asymptotic expansion is (suppressing z arguments to reduce notational clutter)

$$\Delta_1 = \frac{-1}{144\phi_n}\left[\begin{pmatrix} a^2 + a^{-2} & 2^{-\rho}i(a^2 - a^{-2}) \\ 2^\rho i(a^2 - a^{-2}) & -(a^2 + a^{-2}) \end{pmatrix} + 3\begin{pmatrix} (\varphi^\rho + \varphi^{-\rho})(a^2 - a^{-2}) & 2^{-\rho}i[\varphi^\rho(a + a^{-1})^2 + \varphi^{-\rho}(a - a^{-1})^2] \\ 2^\rho i[\varphi^{-\rho}(a + a^{-1})^2 + \varphi^\rho(a - a^{-1})^2] & -(\varphi^\rho + \varphi^{-\rho})(a^2 - a^{-2}) \end{pmatrix}\right].$$

Note that $\Delta_k(z)$ has a pole of order $(3k+1)/2$ at $z = 1$.

5. Parametrix near $z = -1$

We can use symmetry to carry over most of the analysis of the parametrix near $z = 1$ to obtain a parametrix near $z = -1$. In particular, consider the transformation

$$\tilde{\Psi}(z) := \sigma_3 \Psi(-z) \sigma_3. \quad (\text{S2.76})$$

Under the transformation $z \rightarrow -z$, the approach to a contour from the (+)-side gets mapped to the approach to the equivalent contour at $-z$ but from the (-)-side. This implies that the corresponding jump matrix is the *inverse* of the jump matrix at $-z$. For the set of jump matrices considered here, the extra conjugation by σ_3 is sufficient to correct for this inverse, i.e. $\sigma_3 v_j^{-1} \sigma_3 = v_j$, so that $\tilde{\Psi}(z)$ has the correct jump behaviour near $z = -1$.

We construct the rest of the parametrix in a similar way to before, with the result

$$P(z) = \tilde{E}(z) \tilde{\Psi}(-f_n(-z)) e^{-n\phi_n(-z)\sigma_3} (-z)^{-(\rho/2)\sigma_3}, \quad (\text{S2.77})$$

where $\tilde{E}(z)$ is an analytic matrix-valued function given by

$$\tilde{E}(z) = N(z) (-z)^{(\rho/2)\sigma_3} e^{(\pi i/4)\sigma_3} \frac{1}{\sqrt{2}} \begin{pmatrix} 1 & 1 \\ -1 & 1 \end{pmatrix} f_n(-z)^{\sigma_3/4}. \quad (\text{S2.78})$$

Notice the slight difference in the constant matrices in the definitions of $\tilde{E}(z)$ and $E(z)$, which comes about from conjugating with σ_3 . Note that for $\rho = 0$ we simply have $P(z) = \sigma_3 P(-z) \sigma_3$, but this is no longer quite true for $\rho \neq 0$, the reason being that the identity $\sigma_3 N(z) \sigma_3 = N(-z)$ holds only for $\rho = 0$.

As before, we have an asymptotic expansion

$$P(z) N^{-1}(z) \sim \mathbb{1} + \sum_{k=1}^{\infty} \tilde{\Delta}_k(z) \frac{1}{n^k}, \quad \text{as } n \rightarrow \infty, \quad (\text{S2.79})$$

uniformly for z in compact subsets of $U_{\delta_2} := \{0 < |z + 1| < \delta_2\}$ and σ in compact subsets of $(\pi/3, \pi)$, where $\tilde{\Delta}_k$ is a meromorphic 2×2 matrix-valued function given by

$$\tilde{\Delta}_k(z) = \frac{1}{2(-\phi_n(-z))^k} N(z) (-z)^{(1/2)\rho\sigma_3} \begin{pmatrix} (-1)^k (s_k + t_k) & -i(s_k - t_k) \\ i(-1)^k (s_k - t_k) & s_k + t_k \end{pmatrix} (-z)^{-(1/2)\rho\sigma_3} N(z)^{-1}. \quad (\text{S2.80})$$

The first term in this expansion is

$$\tilde{\Delta}_1(z) = \frac{-1}{144\phi_n(-z)} \left[\begin{pmatrix} a^2 + a^{-2} & i2^{-\rho}(a^2 - a^{-2}) \\ i2^{\rho}(a^2 - a^{-2}) & -(a^2 + a^{-2}) \end{pmatrix} - 3\Omega_1(z) \right], \quad (\text{S2.81})$$

where $\Omega_1(z)$ is defined for $U_{\delta_2} \cap \mathbb{C}_+$ as

$$\Omega_1(z) := \begin{pmatrix} (e^{-i\pi\rho}\varphi^\rho + e^{i\pi\rho}\varphi^{-\rho})(a^2 - a^{-2}) & 2^{-\rho}i [e^{i\pi\rho}\varphi^{-\rho}(a - a^{-1})^2 + e^{-i\pi\rho}\varphi^\rho(a + a^{-1})^2] \\ 2^{\rho}i [e^{i\pi\rho}\varphi^{-\rho}(a + a^{-1})^2 + e^{-i\pi\rho}\varphi^\rho(a - a^{-1})^2] & -(e^{-i\pi\rho}\varphi^\rho + e^{i\pi\rho}\varphi^{-\rho})(a^2 - a^{-2}) \end{pmatrix}, \quad (\text{S2.82})$$

and for $U_{\delta_2} \cap \mathbb{C}_-$ as

$$\Omega_1(z) := \begin{pmatrix} (e^{i\pi\rho}\varphi^\rho + e^{-i\pi\rho}\varphi^{-\rho})(a^2 - a^{-2}) & 2^{-\rho}i [e^{-i\pi\rho}\varphi^{-\rho}(a - a^{-1})^2 + e^{i\pi\rho}\varphi^\rho(a + a^{-1})^2] \\ 2^{\rho}i [e^{-i\pi\rho}\varphi^{-\rho}(a + a^{-1})^2 + e^{i\pi\rho}\varphi^\rho(a - a^{-1})^2] & -(e^{i\pi\rho}\varphi^\rho + e^{-i\pi\rho}\varphi^{-\rho})(a^2 - a^{-2}) \end{pmatrix}. \quad (\text{S2.83})$$

In these expressions we have suppressed for brevity the arguments of the functions a and φ , which are meant to be evaluated at z ; the only function evaluated at $-z$ is ϕ_n .

J. Local parametrix P near the origin

In this section we construct a local parametrix P which approximately solves the Riemann-Hilbert problem for S in a disk $U_{\delta_n} = \{z \in \mathbb{C} : |z| < \delta_n\}$ of radius $\delta_n = \gamma/\beta_n$ centered at the origin. Our analysis will be inspired by that of [27, 122, 123], but the main novelty will be that we construct the parametrix in a disk of radius shrinking like $\mathcal{O}(1/\beta_n)$. We do this to avoid having to deal with any singularities in the equilibrium measure; it was for this purpose that we assumed analyticity of the weight function in a region C_θ which is invariant under rescaling, as well as in a disk of constant radius centered at the origin. The price we will pay for shrinking the disk is error bounds in the matching condition $P(z)N(z)^{-1} \sim \mathbb{1} + o(1)$ which decay more slowly with n .

Riemann-Hilbert problem for P

(P_a) P is analytic in $U_{\delta_n} \setminus \Sigma$.

(P_b) $P_+(z) = P_-(z)v_S(z)$ for $z \in \Sigma \cap U_{\delta_n}$, with v_S the jump matrix for S .

(P_c) $P(z)N(z)^{-1} \sim \mathbb{1} + o(1)$ as $n \rightarrow \infty$, uniformly for z on the boundary ∂U_δ of the disk U_δ for δ in compact subsets of $(0, \delta_n)$.

As in Section S2I, we will first transform to a problem $P^{(1)}$ with constant jump matrices, and then construct an explicit solution to this problem using special functions.

1. Transformation to constant jump matrices

Following Ref. [27], in order to transform to constant jump matrices, we seek the parametrix P near 0 in the following form

$$P(z) = E_n(z)P^{(1)}(z)W(z)^{-\sigma_3}e^{-n\phi_n(z)\sigma_3}, \quad (\text{S2.84})$$

where $E_n(z)$ is an analytic matrix-valued function to be determined to ensure the matching condition (P_c), and $W(z)$ is defined by

$$W(z) := \begin{cases} z^{\rho/2}, & \text{if } \pi/2 < |\arg f_n(z)| < \pi, \\ (-z)^{\rho/2}, & \text{if } 0 < |\arg f_n(z)| < \pi/2, \end{cases} \quad (\text{S2.85})$$

where $f_n : U_{\delta_n} \rightarrow f_n(U_{\delta_n})$ is a biholomorphic map to be constructed in the next section. Note that $W(z)$ has a branch cut along the whole real axis. One can then verify that $P^{(1)}$ has a jump matrix which is piecewise constant [27]:

$$P_+^{(1)}(x) = P_-^{(1)}(x) \begin{pmatrix} 0 & 1 \\ -1 & 0 \end{pmatrix}, \quad \text{for } x \in \Sigma_1^o \cup \Sigma_5^o, \quad (\text{S2.86})$$

$$P_+^{(1)}(z) = P_-^{(1)}(z) \begin{pmatrix} 1 & 0 \\ e^{-i\pi\rho} & 1 \end{pmatrix}, \quad \text{for } z \in \Sigma_2^o \cup \Sigma_6^o, \quad (\text{S2.87})$$

$$P_+^{(1)}(z) = P_-^{(1)}(z)e^{\frac{i\pi\rho}{2}\sigma_3}, \quad \text{for } z \in \Sigma_3^o \cup \Sigma_7^o, \quad (\text{S2.88})$$

$$P_z^{(1)}(x) = P_-^{(1)}(z) \begin{pmatrix} 1 & 0 \\ e^{i\pi\rho} & 1 \end{pmatrix}, \quad \text{for } z \in \Sigma_4^o \cup \Sigma_8^o, \quad (\text{S2.89})$$

where the contours Σ_j^o , $j = 1, \dots, 8$ are sketched in Fig. S4(a), with the understanding that the notation Σ_i^o denotes Σ_i without the origin. We construct an explicit solution for this RHP using a model solution $\Psi_{\rho/2}(\zeta)$ for an auxiliary RHP in the ζ -plane, as given in [27, 122] and illustrated in Fig. S4(b).

Riemann-Hilbert problem for $\Psi_{\rho/2}$

($\Psi_{\rho/2,a}$) $\Psi_{\rho/2}$ is analytic in $\mathbb{C} \setminus \Gamma_\Psi$.

($\Psi_{\rho/2,b}$) $\Psi_{\rho/2}$ satisfies the following jump relations on Γ_Ψ :

$$\Psi_{\rho/2,+}(\zeta) = \Psi_{\rho/2,-}(\zeta) \begin{pmatrix} 0 & 1 \\ -1 & 0 \end{pmatrix}, \quad \text{for } \zeta \in \Gamma_1 \cup \Gamma_5, \quad (\text{S2.90})$$

$$\Psi_{\rho/2,+}(\zeta) = \Psi_{\rho/2,-}(\zeta) \begin{pmatrix} 1 & 0 \\ e^{-i\pi\rho} & 1 \end{pmatrix}, \quad \text{for } \zeta \in \Gamma_2 \cup \Gamma_6, \quad (\text{S2.91})$$

$$\Psi_{\rho/2,+}(\zeta) = \Psi_{\rho/2,-}(\zeta)e^{\frac{i\pi\rho}{2}\sigma_3}, \quad \text{for } \zeta \in \Gamma_3 \cup \Gamma_7, \quad (\text{S2.92})$$

$$\Psi_{\rho/2,+}(\zeta) = \Psi_{\rho/2,-}(\zeta) \begin{pmatrix} 1 & 0 \\ e^{i\pi\rho} & 1 \end{pmatrix}, \quad \text{for } \zeta \in \Gamma_4 \cup \Gamma_8. \quad (\text{S2.93})$$

($\Psi_{\rho/2,c}$) For $\rho < 0$, $\Psi_{\rho/2}$ has the following behavior as $\zeta \rightarrow 0$:

$$\Psi_{\rho/2}(\zeta) = \mathcal{O} \left(\begin{pmatrix} |\zeta|^{\rho/2} & |\zeta|^{\rho/2} \\ |\zeta|^{\rho/2} & |\zeta|^{\rho/2} \end{pmatrix} \right), \quad \text{as } \zeta \rightarrow 0. \quad (\text{S2.94})$$

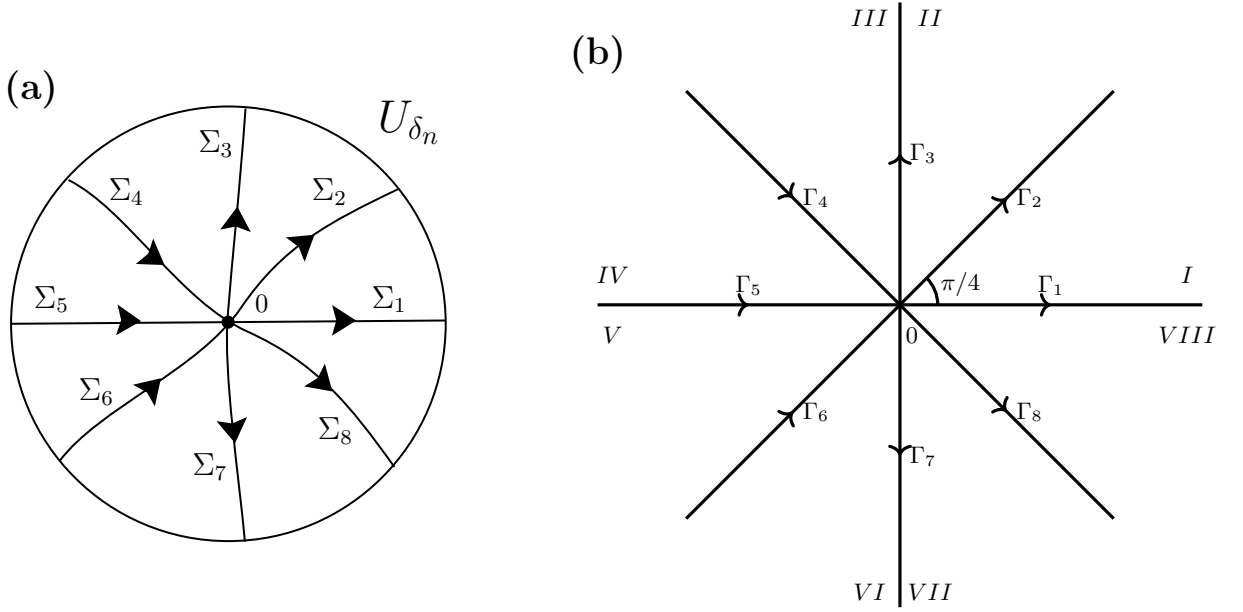


FIG. S4. **(a)** The contour $\Sigma = \bigcup_{i=1}^8 \Sigma_i$ in the z -plane on which $P^{(1)}(z)$ has jumps. We construct the parametrix in a disk U_{δ_n} of radius δ_n centered at the origin. **(b)** The contour Γ_Ψ for the auxiliary RHP in the ζ -plane used to obtain the parametrix near the origin.

For $\rho \geq 0$, $\Psi_{\rho/2}$ has the following behavior as $\zeta \rightarrow 0$:

$$\Psi_{\rho/2}(\zeta) = \begin{cases} \mathcal{O} \begin{pmatrix} |\zeta|^{\rho/2} & |\zeta|^{-\rho/2} \\ |\zeta|^{\rho/2} & |\zeta|^{-\rho/2} \end{pmatrix}, & \text{as } \zeta \rightarrow 0 \text{ with } \zeta \in \text{II, III, VI, VII}; \\ \mathcal{O} \begin{pmatrix} |\zeta|^{-\rho/2} & |\zeta|^{-\rho/2} \\ |\zeta|^{-\rho/2} & |\zeta|^{-\rho/2} \end{pmatrix}, & \text{as } \zeta \rightarrow 0 \text{ with } \zeta \in \text{I, IV, V, VIII}. \end{cases} \quad (\text{S2.95})$$

This RHP was solved in [122, Eqs. (4.26)-(4.33)]. It is built out of the modified Bessel functions $I_{\frac{1}{2}(\rho \pm 1)}$, $K_{\frac{1}{2}(\rho \pm 1)}$ and the modified Hankel functions $H_{\frac{1}{2}(\rho \pm 1)}^{(1)}$, $H_{\frac{1}{2}(\rho \pm 1)}^{(2)}$. The explicit formula for $\Psi_{\rho/2}$ in sector I is

$$\Psi_{\rho/2}(\zeta) = \frac{\sqrt{\pi}}{2} \zeta^{1/2} \begin{pmatrix} H_{\frac{1}{2}(\rho+1)}^{(2)}(\zeta) & -iH_{\frac{1}{2}(\rho+1)}^{(1)}(\zeta) \\ H_{\frac{1}{2}(\rho-1)}^{(2)}(\zeta) & -iH_{\frac{1}{2}(\rho-1)}^{(1)}(\zeta) \end{pmatrix} e^{-(\frac{\rho}{2} + \frac{1}{4})i\pi\sigma_3}, \quad \text{for } 0 < \arg \zeta < \frac{\pi}{4}, \quad (\text{S2.96})$$

and the expressions in the other sectors can be obtained from this one by following the jumps given in $(\Psi_{\rho/2,b})$. As $\zeta \rightarrow \infty$ in the first quadrant, we can use the asymptotic formulae [124, 9.2.7-9.2.10] for the Hankel functions to get the asymptotic expansion

$$\Psi_{\rho/2}(\zeta) \sim \frac{1}{\sqrt{2}} \sum_{k=0}^{\infty} \frac{i^k}{(2\zeta)^k} \begin{pmatrix} (-1)^k \left(\frac{1}{2}(\rho+1), k\right) & -i \left(\frac{1}{2}(\rho+1), k\right) \\ -i(-1)^k \left(\frac{1}{2}(\rho-1), k\right) & \left(\frac{1}{2}(\rho-1), k\right) \end{pmatrix} e^{\frac{i\pi}{4}\sigma_3} e^{-\frac{i\pi\rho}{4}\sigma_3} e^{-i\zeta\sigma_3}, \quad (\text{S2.97})$$

uniformly in ζ , where for $k=0$ we define $(v, 0) = 1$ and for $k \geq 1$

$$(v, k) := \frac{(4v^2 - 1)(4v^2 - 9) \cdots (4v^2 - (2k - 1)^2)}{2^{2k} k!}. \quad (\text{S2.98})$$

See Ref. [122] for expressions in the other quadrants.

We then define

$$P^{(1)}(z) := \Psi_{\rho/2}(nf_n(z)), \quad \text{for } z \in U_{\delta_n} \setminus f_n^{-1}(\Gamma), \quad (\text{S2.99})$$

where $f_n(z)$ is a biholomorphic map to be constructed in the next section.

2. Construction of biholomorphic map

Following Ref. [27], we define the map $f_n : U_{\delta_n} \rightarrow f_n(U_{\delta_n})$ by

$$f_n(z) := \begin{cases} i\phi_n(z) - i\phi_{n,+}(0), & \text{if } \text{Im } z > 0, \\ -i\phi_n(z) - i\phi_{n,+}(0), & \text{if } \text{Im } z < 0, \end{cases} \quad (\text{S2.100})$$

where $\phi_{n,+}(0) = i\pi/2$ for an even weight function. From Eqs. (S2.38) and (S2.40) we know that $\phi_n(z)$ is analytic in \mathbb{C}_{\pm} (within its domain) and flips sign across $(-1, 1)$, which implies that $f_n(z)$ is analytic in a neighborhood of $z = 0$. On the real line we have

$$f_n(x) = \pi \int_0^x \psi_n(s) ds, \quad \text{for } x \in (-\delta_n, \delta_n), \quad (\text{S2.101})$$

which implies that $f'_n(0) = \pi\psi_n(0) > 0$. The behavior of $f_n(z)$ near the origin is then given by

$$f_n(z) = \pi\psi_n(0)z + \mathcal{O}(z^3), \quad \text{as } z \rightarrow 0, \quad (\text{S2.102})$$

where $f''_n(0) = 0$ follows from the fact that $\psi_n(x)$ is even. The big- \mathcal{O} hides potential n -dependence, which we will need to be more careful about in order to guarantee that $f_n(z)$ is actually biholomorphic in a neighborhood of the origin.

Proposition S3. *There exists a $\gamma > 0$ such that for $\delta_n = \gamma/\beta_n$ and sufficiently large n , $f_n : U_{\delta_n} \rightarrow f_n(U_{\delta_n})$ satisfies the following properties.*

- (a) $f_n : U_{\delta_n} \rightarrow f_n(U_{\delta_n})$ is biholomorphic.
- (b) $f_n(U_{\delta_n} \cap \mathbb{R}) = f_n(U_{\delta_n}) \cap \mathbb{R}$, $f_n(U_{\delta_n} \cap \mathbb{C}_{\pm}) = f_n(U_{\delta_n}) \cap \mathbb{C}_{\pm}$.

Proof. Property (b) will follow as in Proposition S2. Regarding property (a), we have already established that f_n is analytic in a neighborhood of $z = 0$, so it remains to show that it is invertible. To that end, for $|z| \leq r_0$ we use Cauchy's theorem for derivatives on a circle of radius $r_1 > r_0$ to give

$$|f''_n(z)| = \left| \frac{2}{2\pi i} \oint_{|u|=r_1} \frac{f_n(u)}{(u-z)^3} du \right|, \quad (\text{S2.103})$$

$$\leq \frac{2r_1}{(r_1 - r_0)^3} \sup_{|u|=r_1} |f_n(u)|. \quad (\text{S2.104})$$

We are implicitly taking r_0 and r_1 to scale like $\mathcal{O}(1/\beta_n)$, but we will not explicitly denote their n dependence. Now, from Eqs. (S2.37), (S2.40) and (S2.100), we see that

$$\sup_{|u|=r_1} |f_n(u)| \leq \frac{r_1}{2} \sup_{|u|=r_1} |r(u)h_n(u)|. \quad (\text{S2.105})$$

We show in Lemma S9 that, for sufficiently large n , we have $h_n(z) = h_n(0)[1 + o(1)]$ uniformly for z in a sufficiently small disk of radius $\mathcal{O}(1/\beta_n)$ centered at the origin, where the $o(1)$ refers to scaling with n . Combined with the fact that $r(u) = (u+1)^{1/2}(u-1)^{1/2}$ is bounded near zero, for sufficiently large n we have

$$\sup_{|u|=r_1} |f_n(u)| \leq Cr_1 h_n(0). \quad (\text{S2.106})$$

for some constant $C > 1/2$ (independent of n). Inserting this into Eq. (S2.104) gives

$$|f''_n(z)| \leq 2C \frac{r_1^2}{(r_1 - r_0)^3} h_n(0), \quad \text{for } |z| \leq r_0 < r_1. \quad (\text{S2.107})$$

Again for $|z| \leq r_0$, we then have

$$|f'_n(z) - f'_n(0)| = \left| \int_0^z f''_n(s) ds \right| \leq 2C \frac{r_0 r_1^2}{(r_1 - r_0)^3} h_n(0). \quad (\text{S2.108})$$

We then set $r_0 = r_1/N$ for some large $N > 1$, and use $f'_n(0) = \pi\psi_n(0) = h_n(0)/2$, so that

$$|f'_n(z) - f'_n(0)| \leq 4C \frac{N^2}{(N-1)^3} f'_n(0). \quad (\text{S2.109})$$

By taking N sufficiently large (but independent of n), we can make the RHS less than, say, $f'_n(0)/2$, so we have a uniform (in z) nonzero lower bound on $|f'_n(z)|$ in the disk of radius r_0 . We can also make this uniform in n by using Lemma S8 to establish that $f'_n(0) = h_n(0)/2$ is $\Omega(1)$ as $n \rightarrow \infty$. This is enough to conclude that $f_n(z)$ is invertible and hence biholomorphic in a sufficiently small $\mathcal{O}(1/\beta_n)$ neighborhood of the origin. \square

3. Satisfying the matching condition

In this final step, we construct the invertible analytic matrix-valued function $E(z)$ to ensure that the matching function (P_c) is satisfied. Following Ref. [27], we define $E_n(z)$ by

$$E_n(z) := E(z) e^{n\phi_{n,+}(0)\sigma_3} e^{-\frac{\pi i}{4}\sigma_3} \frac{1}{\sqrt{2}} \begin{pmatrix} 1 & i \\ i & 1 \end{pmatrix}, \quad (\text{S2.110})$$

where the matrix valued function E is defined in different regions of the complex plane by

$$E(z) := \begin{cases} N(z)W(z)\sigma_3 e^{\frac{1}{4}\rho\pi i\sigma_3}, & \text{for } z \in f_n^{-1}(\text{I} \cup \text{II}), \\ N(z)W(z)\sigma_3 e^{-\frac{1}{4}\rho\pi i\sigma_3}, & \text{for } z \in f_n^{-1}(\text{III} \cup \text{IV}), \\ N(z)W(z)\sigma_3 \begin{pmatrix} 0 & 1 \\ -1 & 0 \end{pmatrix} e^{-\frac{1}{4}\rho\pi i\sigma_3}, & \text{for } z \in f_n^{-1}(\text{V} \cup \text{VI}), \\ N(z)W(z)\sigma_3 \begin{pmatrix} 0 & 1 \\ -1 & 0 \end{pmatrix} e^{\frac{1}{4}\rho\pi i\sigma_3}, & \text{for } z \in f_n^{-1}(\text{VII} \cup \text{VIII}). \end{cases} \quad (\text{S2.111})$$

This ends the construction of the parametrix P near $z = 0$.

4. Summary of the local analysis near $z = 0$

We have defined the contour Σ in a shrinking disk U_{δ_n} near $z = 0$ as the inverse image of the contour Γ_Ψ under the map f_n defined in Eq. (S2.100). We have then found a solution

$$P(z) = E_n(z) \Psi_{\rho/2}(nf_n(z)) W(z)^{-\sigma_3} e^{-n\phi_n(z)\sigma_3}, \quad \text{for } z \in \Sigma \cap U_{\delta_n} \quad (\text{S2.112})$$

to the RHP for P , where the matrix-valued function E_n is defined in Eq. (S2.110), the matrix-valued function $\Psi_{\rho/2}$ is defined in Eq. (S2.96), and $W(z)$ is defined in Eq. (S2.85). Furthermore, following Ref. [122], on the boundary ∂U_{δ_n} , we have the asymptotic expansion

$$P(z)N(z)^{-1} \sim \mathbf{1} + \sum_{k=1}^{\infty} \frac{\Delta(k, n)(z)}{[nf_n(z)]^k}, \quad \text{as } n \rightarrow \infty, \quad \text{for } z \in \partial U_{\delta_n}, \quad (\text{S2.113})$$

where the coefficient matrix $\Delta(k, n)(z)$ is determined by Eqs. (S2.97), (S2.99), (S2.100), (S2.110) and (S2.112), and given explicitly by

$$\Delta(k, n)(z) = \frac{i^k}{2^{k+1}} E(z) e^{n\phi_{n,+}(0)\sigma_3} \begin{pmatrix} (-1)^k s_{\rho/2, k} & -t_{\rho/2, k} \\ -(-1)^k t_{\rho/2, k} & s_{\rho/2, k} \end{pmatrix} e^{-n\phi_{n,+}(0)\sigma_3} E(z)^{-1}, \quad (\text{S2.114})$$

and the constants $s_{\rho/2, k}$ and $t_{\rho/2, k}$ are defined as

$$s_{\rho/2, k} := \left(\frac{1}{2}(\rho + 1), k \right) + \left(\frac{1}{2}(\rho - 1), k \right), \quad \text{and} \quad t_{\rho/2, k} := \left(\frac{1}{2}(\rho + 1), k \right) - \left(\frac{1}{2}(\rho - 1), k \right), \quad (\text{S2.115})$$

where the expression (v, k) was defined in Eq. (S2.98). For later, we note that

$$s_{\rho/2, 1} = \frac{\rho^2}{2} \quad \text{and} \quad t_{\rho/2, 1} = \rho. \quad (\text{S2.116})$$

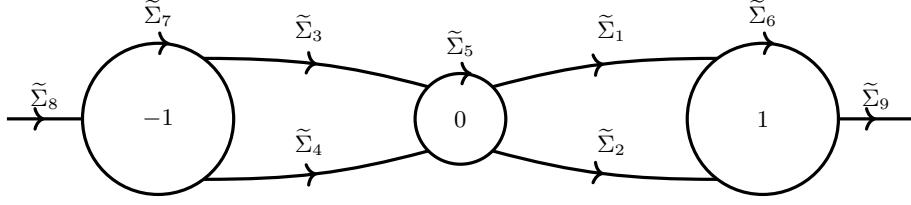


FIG. S5. The contour $\tilde{\Sigma}_R = \bigcup_{j=1}^9 \tilde{\Sigma}_j$ on which $R(z)$ has jumps. The circles $\tilde{\Sigma}_{j=5,6,7}$ are determined in the construction of the local parametrices in Sections S2I and S2J; note that $\tilde{\Sigma}_5$ has radius $\mathcal{O}(1/\beta_n)$, so as $n \rightarrow \infty$ it is much smaller than $\tilde{\Sigma}_{6,7}$ which have $\mathcal{O}(1)$ radius. The precise shape of the lens boundaries $\tilde{\Sigma}_{j=1..4}$ is given in Fig. S8.

We will soon discuss this in more detail, but let us note two things about $\Delta(k, n)(z)$: first, that it is analytic in a neighbourhood of $z = 0$, and second, that its only n dependence comes from the factors of $\exp[\pm n\phi_{n,+}(0)] = \exp[\pm n\pi i/2]$, where the value of $\phi_{n,+}(0)$ is fixed by the even symmetry of the weight function. Since this factor is $\mathcal{O}(1)$, the asymptotic n -decay of $P(z)N(z)^{-1} - \mathbb{1}$ will be determined solely by the factors of $[nf_n(z)]^k$ in Eq. (S2.113).

Finally, in the case $\rho = 0$, this whole construction reduces to $P(z) = N(z)$ exactly. This will mean that $R(z)$ has no jump near the origin if $\rho = 0$.

K. Riemann-Hilbert problem for R

Having constructed local parametrices $P(z)$ in disks centered at $z = 0$ and $z = \pm 1$, we define

$$S_{\text{par}}(z) := \begin{cases} P(z), & \text{if } |z - 1| < \delta_2 \text{ or } |z + 1| < \delta_2 \text{ or } |z| < \delta_n, \\ N(z), & \text{otherwise.} \end{cases} \quad (\text{S2.117})$$

Now we define

$$R(z) := S(z)S_{\text{par}}^{-1}(z). \quad (\text{S2.118})$$

One can verify that $R(z)$ is the unique solution of the following RHP, with jumps on the contour $\tilde{\Sigma}$ sketched in Fig. S5.

Riemann-Hilbert problem for R

(R_a) $R : \mathbb{C} \setminus \tilde{\Sigma}_R \rightarrow \mathbb{C}^{2 \times 2}$ is analytic.

(R_b) R has the following jump matrices.

$$R_+(s) = R_-(s) \begin{cases} N(s)v_i(s)N^{-1}(s), & \text{for } s \in \tilde{\Sigma}_i, i = 1, 2, 3, 4, 8, 9; \\ P(s)N^{-1}(s), & \text{for } s \in \tilde{\Sigma}_5 \cup \tilde{\Sigma}_6 \cup \tilde{\Sigma}_7; \\ \mathbb{1}, & \text{otherwise.} \end{cases} \quad (\text{S2.119})$$

Here $v_i(s)$ is the jump matrix for S on the relevant contour (see Eqs. (S2.46) to (S2.48)).

(R_c) $R(z) = \mathbb{1} + \mathcal{O}(1/|z|)$ as $|z| \rightarrow \infty$.

In particular, the jump matrix $v_R(z)$ of R is uniformly close to the identity, in the sense that, with $\Delta_R(z) := v_R(z) - 1$, as $n \rightarrow \infty$ we have $\|\Delta_R(z)\|_{L_\infty(\tilde{\Sigma})} \rightarrow 0$. In more detail, we have

$$\begin{aligned} \|\Delta_R\|_{L_\infty(\tilde{\Sigma}_{j=1..4})} &= o\left(\frac{1}{\text{poly}(\log n)}\right), & \|\Delta_R\|_{L_2(\tilde{\Sigma}_{j=1..4})} &= o\left(\frac{1}{n^{1/2}\text{poly}(\log n)}\right), & \|\Delta_R\|_{L_1(\tilde{\Sigma}_{j=1..4})} &= o\left(\frac{1}{n\text{poly}(\log n)}\right), \\ \|\Delta_R\|_{L_\infty(\tilde{\Sigma}_5)} &= \mathcal{O}\left(\frac{\beta_n}{nh_n(0)}\right), & \|\Delta_R\|_{L_2(\tilde{\Sigma}_5)} &= \mathcal{O}\left(\frac{\beta_n^{1/2}}{nh_n(0)}\right), \\ \|\Delta_R\|_{L_\infty(\tilde{\Sigma}_6)} &= \mathcal{O}\left(\frac{1}{n}\right), & \|\Delta_R\|_{L_2(\tilde{\Sigma}_6)} &= \mathcal{O}\left(\frac{1}{n}\right), \\ \|\Delta_R\|_{L_\infty(\tilde{\Sigma}_7)} &= \mathcal{O}\left(\frac{1}{n}\right), & \|\Delta_R\|_{L_2(\tilde{\Sigma}_7)} &= \mathcal{O}\left(\frac{1}{n}\right), \\ \|\Delta_R\|_{L_\infty(\tilde{\Sigma}_{8,9})} &= \mathcal{O}(e^{-cn}), & \|\Delta_R\|_{L_2(\tilde{\Sigma}_{8,9})} &= \mathcal{O}(e^{-cn}), \end{aligned} \tag{S2.120}$$

where $c > 0$ is a positive $\mathcal{O}(1)$ constant. When β_n is sublinear in n , the bounds on $\tilde{\Sigma}_5$ are polynomially small in n . In the marginal case $p = 1$ where $\beta_n \sim \mathcal{O}(n/\log^q n)$, the $L_\infty(\tilde{\Sigma}_5)$ bound decays polylogarithmically in n provided $q > -1$, given the logarithmic divergence $h_n(0) = (\log n)^{1+o(1)}$ of the equilibrium measure proved in Lemma S8. The precise rate of convergence for $\tilde{\Sigma}_{j=1..4}$ depends on p and q ; for $p > 1$ the convergence is actually superpolynomial, while for $p = 1$ the convergence may be superpolynomial or subpolynomial (but still super-polylogarithmic) depending on whether $q > 0$ or $q \leq 0$ (see the proof of Lemma S12 for details).

The bounds on $\tilde{\Sigma}_{6,7,8,9}$ are standard; see [22]. The L_∞ bound on $\tilde{\Sigma}_5$ follows from the fact that $\tilde{\Sigma}_5$ has a radius of $\mathcal{O}(1/\beta_n)$, combined with the asymptotic expansion Eq. (S2.113), the definition Eq. (S2.100) of $f_n(z)$, and the uniform lower bound for $h_n(z)$ given in Lemma S9. The $L_2(\tilde{\Sigma}_5)$ bound follows from the $L_\infty(\tilde{\Sigma}_5)$ bound by Hölder's inequality. The L_∞ bound on $\tilde{\Sigma}_{j=1..4}$ follows from the fact that the matrix elements of $\Delta_R(z)$ are proportional to $e^{-2n\phi_n(z)}D(z)^2\omega(z)^{-1}$ on the lens boundaries, and $D(z)^2\omega(z)^{-1} = \mathcal{O}(|z|^0)$ as $z \rightarrow 0$, while $|e^{-2n\phi_n(z)}| \xrightarrow{n \rightarrow \infty} 0$ super-polylogarithmically in n by Lemma S12. The $L_{1,2}(\tilde{\Sigma}_{j=1..4})$ bounds follows from the second part of Lemma S12.

1. Solution for R

We have constructed $R(z)$ such that its jumps are ‘small’, in the sense that its jump matrix $v_R(z)$ is uniformly close to the identity as $n \rightarrow \infty$. This will allow us to write down its solution using standard techniques (see [22, Appendix A]). For $f \in L_2(\tilde{\Sigma}_R)$, we can define the Cauchy-Stieltjes transform

$$(Cf)(z) := \frac{1}{2\pi i} \int_{\tilde{\Sigma}_R} \frac{f(s)}{s-z} ds, \quad z \in \mathbb{C} \setminus \tilde{\Sigma}_R. \tag{S2.121}$$

We denote by $(C_\pm f)(z)$ the limiting functions as z approaches $\tilde{\Sigma}_R$ from the \pm sides. Now with $\Delta_R(z) := v_R(z) - 1$, we define for matrix-valued functions $f : \tilde{\Sigma}_R \rightarrow \mathbb{C}^{2 \times 2}$ the weighted Cauchy-Stieltjes transform

$$C_{\Delta_R} f := C_-(f\Delta_R). \tag{S2.122}$$

Now, by the discussion in the previous section, for $n \rightarrow \infty$ we have $\|\Delta_R\|_{L_\infty} \rightarrow 0$, which by the boundedness of the Cauchy-Stieltjes transform implies that the L_2 -operator norm $\|C_{\Delta_R}\|_{L_2} \rightarrow 0$ as $n \rightarrow \infty$. Then for sufficiently large n , the operator $\text{Id} - C_{\Delta_R}$ can be inverted by a Neumann series, and so we can employ the standard solution [22]

$$R(z) = \mathbf{1} + C(\Delta_R + \mu_R \Delta_R)(z), \quad \text{where } \mu_R := (\text{Id} - C_{\Delta_R})^{-1} C_- \Delta_R, \tag{S2.123}$$

Expanding $R(z) = \mathbf{1} + R_1/z + \dots$, this formula gives

$$R_1 = -\frac{1}{2\pi i} \int_{\tilde{\Sigma}_R} [\Delta_R(y) + \mu_R(y)\Delta_R(y)] dy. \tag{S2.124}$$

From the definition of μ_R , we have $\|\mu_R\|_{L_2} \leq c\|\Delta_R\|_{L_2}$ for some $c > 0$ by the boundedness of the Cauchy-Stieltjes transform, and hence by Cauchy-Schwarz we have

$$R_1 = -\frac{1}{2\pi i} \int_{\tilde{\Sigma}_R} \Delta_R(y) dy + \mathcal{O}\left(\|\Delta_R\|_{L_2(\tilde{\Sigma}_R)}^2\right). \tag{S2.125}$$

2. Error bounds for R

By construction, we have $R(z) \rightarrow \mathbb{1}$ as $n \rightarrow \infty$. In this section we give the rate of this convergence, which follows from combining Eq. (S2.123) with Eq. (S2.120). In order to deal with points near the contour $\tilde{\Sigma}$, one can employ a contour deformation argument as in the proof of [22, Corollary 7.9]. The situation is most delicate for z near the origin. For $|z| \leq \mathcal{O}(1/\beta_n)$, we have the bound

$$\|R(z) - \mathbb{1}\| \leq \mathcal{O}\left(\frac{\beta_n}{nh_n(0)}\right), \quad \text{uniformly for } |z| \leq \mathcal{O}(1/\beta_n), \quad (\text{S2.126})$$

with the dominant contribution coming from integrating over the contour $\tilde{\Sigma}_5$. Again, this may decay only polylogarithmically in the worst case $p = 1, q > -1$. For larger $|z|$, similar arguments using Eq. (S2.120) lead to

$$\|R(z) - \mathbb{1}\| \leq \mathcal{O}\left(\frac{1}{\beta_n|z|} \frac{\beta_n}{nh_n(0)}\right) + \mathcal{O}\left(\frac{1}{n}\right), \quad \text{for } |z| \geq \Omega(1/\beta_n), \quad (\text{S2.127})$$

where the factor of $\mathcal{O}(1/\beta_n|z|)$ gets cut off at $\mathcal{O}(1)$ for $|z| \sim \mathcal{O}(1/\beta_n)$, and the factor of $\mathcal{O}(1/n)$ comes from the contours $\tilde{\Sigma}_{6,7}$. The proof of Lemma S12 shows that the contribution from the lens boundaries $\tilde{\Sigma}_{1..4}$ is $o(1/n \text{ poly}(\log n))$ and so is subleading.

One can similarly establish bounds on the derivatives: near the origin we have

$$\|R^{(k)}(z)\| \leq \mathcal{O}\left(\beta_n^k \frac{\beta_n}{nh_n(0)}\right), \quad \text{uniformly for } |z| \leq \mathcal{O}(1/\beta_n), \quad (\text{S2.128})$$

and for larger z this gets replaced with

$$\|R^{(k)}(z)\| \leq \mathcal{O}\left(\frac{1}{|z|^k} \frac{1}{\beta_n|z|} \frac{\beta_n}{nh_n(0)}\right) + \mathcal{O}\left(\frac{1}{n}\right), \quad \text{for } |z| \geq \Omega(1/\beta_n). \quad (\text{S2.129})$$

Remark 1. Note that these bounds imply that the derivatives of $R(z)$ could in principle grow with n , in contrast to the more standard situation where all derivatives of $R(z)$ are bounded [22, 27]. This is a consequence of shrinking the contour $\tilde{\Sigma}_5$ like $\mathcal{O}(1/\beta_n)$, which was necessitated by our fairly weak analyticity assumptions on Q . One might worry that these growing derivatives could dominate asymptotics for the Christoffel-Darboux (CD) kernel, which involves taking derivatives of $Y(z)$ (see Section S4). However, the contributions from R derivatives turn out to still be subleading relative to the derivatives of leading terms, since those derivatives themselves bring factors which grow with n . To illustrate this, a comparison one has to make for CD asymptotics in the bulk is between $\|R'(x)\|$ and $n\phi'_{n,+}(x)$, the latter coming from differentiating $e^{-n\phi_{n,+}(x)\sigma_3}$. From Eq. (S2.41) we have

$$n\phi'_{n,+}(x) = -i\pi n\psi_n(x) = \frac{-i\sqrt{1-x^2}}{2}nh_n(x). \quad (\text{S2.130})$$

In the bulk $\sqrt{1-x^2}$ is bounded away from 0, so one can then use the uniform lower bounds on $h_n(x)$ available from Lemmas S6 and S9 and Remark 3 to see that $n\phi'_{n,+}(x)$ dominates over $\|R'(x)\|$ as estimated from Eq. (S2.129). Similar conclusions can be made for asymptotics in the Bessel and Airy regions near $z = 0$ and $z = \pm 1$ respectively.

S3. EXTRACTING THE RECURRENCE COEFFICIENTS: PROOF OF THEOREM 1

A. Reversing the transformations

We have made a series of transformations from the original Riemann-Hilbert problem:

$$Y \mapsto U \mapsto T \mapsto S \mapsto R.$$

We will now reverse these transformations, with the goal of extracting the z -dependence of $Y(z)$ as $z \rightarrow \infty$.

Recall that $U(z) = \beta_n^{-(n+\rho/2)\sigma_3} Y(\beta_n z) \beta_n^{(\rho/2)\sigma_3}$. Making the expansions $U(z) = (\mathbb{1} + U_1/z + \dots)z^{n\sigma_3}$ and $Y(z) = (\mathbb{1} + Y_1/z + \dots)z^{n\sigma_3}$, linear independence gives

$$Y_1 = \beta_n \beta_n^{(n+\rho/2)\sigma_3} U_1 \beta_n^{-(n+\rho/2)\sigma_3}. \quad (\text{S3.1})$$

Next we recall that $U(z) = e^{\frac{1}{2}nl_n\sigma_3} T(z) e^{-\frac{1}{2}nl_n\sigma_3} e^{ng(z)\sigma_3}$. Expanding $T_1 = \mathbb{1} + T_1/z + \dots$ and $e^{ng(z)\sigma_3} = (\mathbb{1} + G_1/z + \dots)z^{n\sigma_3}$, we get

$$U_1 = e^{\frac{1}{2}nl_n\sigma_3} T_1 e^{-\frac{1}{2}nl_n\sigma_3} + G_1, \quad (\text{S3.2})$$

and hence

$$\begin{aligned} Y_1 &= \beta_n \beta_n^{(n+\rho/2)\sigma_3} e^{\frac{1}{2}nl_n\sigma_3} T_1 e^{-\frac{1}{2}nl_n\sigma_3} \beta_n^{-(n+\rho/2)\sigma_3} \\ &\quad + \beta_n \beta_n^{(n+\rho/2)\sigma_3} G_1 \beta_n^{-(n+\rho/2)\sigma_3}. \end{aligned} \quad (\text{S3.3})$$

Note that, since G_1 came from the expansion of $e^{ng(z)\sigma_3}$, which is a diagonal matrix, G_1 itself is also diagonal, and hence will not contribute to the off-diagonal elements of Y_1 , which are the ones that matter for the recurrence coefficients.

For the $T \rightarrow S$ transformation, we simply have $T_1 = S_1$, since S differs from T only for small values of z . Finally, for the $S \rightarrow R$ transformation, we have $S(z) = R(z)N(z)$ for $z \rightarrow \infty$, and hence

$$S_1 = R_1 + N_1. \quad (\text{S3.4})$$

Substituting into the formula for Y_1 and using $b_n^2 = (Y_1)_{12}(Y_1)_{21}$, we have

$$b_n^2 = \beta_n^2 (R_1 + N_1)_{12} (R_1 + N_1)_{21}. \quad (\text{S3.5})$$

Using the $z \rightarrow \infty$ asymptotics for $N(z)$, we get

$$b_n = \frac{\beta_n}{2} (1 + 2i [2^{-\rho}(R_1)_{21} - 2^\rho(R_1)_{12}] + 4(R_1)_{12}(R_1)_{21})^{1/2}. \quad (\text{S3.6})$$

Note that the leading order behaviour is given by $b_n \simeq \beta_n/2$, since R_1 is $o(1)$ as $n \rightarrow \infty$. From the solution for $R(z)$, we have

$$2^{-\rho}(R_1)_{21} - 2^\rho(R_1)_{12} = \frac{1}{2\pi i} \int_{\tilde{\Sigma}_R} [2^\rho(\Delta_R)_{12}(y) - 2^{-\rho}(\Delta_R)_{21}(y) + \dots] dy. \quad (\text{S3.7})$$

The $(R_1)_{12}(R_1)_{21}$ term in the formula for b_n will be subleading relative to this term because it is quadratic in R_1 .

B. Recurrence coefficients from residue calculus

Next we use the asymptotic expansions of Δ_R constructed in the various local parametrices to evaluate the RHS of Eq. (S3.7) using the residue theorem.

1. Integral over the circular contour $\tilde{\Sigma}_5$ near $z = 0$

Since $\Delta_R(z) = P(z)N(z)^{-1} - \mathbb{1}$ on this contour, taking the first term of the asymptotic expansion Eq. (S2.113) and using $[a(z) + a(z)^{-1}]^2 - [a(z) - a(z)^{-1}]^2 = 4$, we get

$$2^\rho(\Delta_R)_{12}(y) - 2^{-\rho}(\Delta_R)_{21}(y) = (-1)^{n+1} \frac{i\rho}{4n} \frac{1}{f_n(z)} \begin{cases} \left(e^{\frac{i\pi\rho}{2}} \varphi(z)^{-\rho} + e^{-\frac{i\pi\rho}{2}} \varphi(z)^\rho \right), & z \in \mathbb{C}_+, \\ \left(e^{-\frac{i\pi\rho}{2}} \varphi(z)^{-\rho} + e^{\frac{i\pi\rho}{2}} \varphi(z)^\rho \right), & z \in \mathbb{C}_-. \end{cases} \quad (\text{S3.8})$$

Near $z = 0$, we have

$$f_n(z) = \pi\psi_n(0)z + \mathcal{O}(z^3). \quad (\text{S3.9})$$

However, $\varphi(z)$ has a branch cut along the real axis, with

$$\varphi(z) = \begin{cases} i + \mathcal{O}(z), & z \in \mathbb{C}_+, \\ -i + \mathcal{O}(z), & z \in \mathbb{C}_-. \end{cases} \quad (\text{S3.10})$$

This cancels out the differing phase factors in \mathbb{C}_\pm , so we get the Laurent expansion

$$2^\rho(\Delta_R)_{12}(y) - 2^{-\rho}(\Delta_R)_{21}(y) = (-1)^{n+1} \frac{i\rho}{2n} \frac{1}{\pi\psi_n(0)} \frac{1}{z} + \mathcal{O}(z^0), \quad (\text{S3.11})$$

valid in both \mathbb{C}_+ and \mathbb{C}_- . Then the contour integral gives

$$\frac{1}{2\pi i} \int_{\tilde{\Sigma}_5} [2^\rho(\Delta_R)_{12}(y) - 2^{-\rho}(\Delta_R)_{21}(y) + \dots] dy = (-1)^n i\rho \frac{1}{nh_n(0)} + \dots, \quad (\text{S3.12})$$

where we note that $\tilde{\Sigma}_5$ is defined with clockwise orientation, and we have used $\psi_n(0) = h_n(0)/2\pi$.

2. Integral over the circular contour $\tilde{\Sigma}_6$ near $z = 1$

Since $\Delta_R(z) = P(z)N(z)^{-1} - \mathbb{1}$ on this contour, taking the first term of the asymptotic expansion Eq. (S2.74), we have

$$2^\rho(\Delta_R)_{12}(y) - 2^{-\rho}(\Delta_R)_{21}(y) = -\frac{i}{12n\phi_n(z)} [\varphi(z)^\rho - \varphi(z)^{-\rho}]. \quad (\text{S3.13})$$

Near $z = 1$, we have

$$\varphi(z)^\rho - \varphi(z)^{-\rho} = 2\sqrt{2}\rho(z-1)^{1/2} + \mathcal{O}[(z-1)^{3/2}]. \quad (\text{S3.14})$$

Since $\phi_n(z) \sim \mathcal{O}[(z-1)^{3/2}]$ near $z = 1$, the overall expression therefore has a simple pole at $z = 1$. Recalling that $\phi_n(z) = -(2/3)(z-1)^{3/2}\hat{\varphi}_n(z)$, with $\hat{\varphi}_n(z)$ analytic near $z = 1$, we get

$$2^\rho(\Delta_R)_{12}(y) - 2^{-\rho}(\Delta_R)_{21}(y) = \frac{i\rho}{2} \frac{1}{nh_n(1)} \frac{1}{z-1} + \mathcal{O}(z^0), \quad (\text{S3.15})$$

where we have used $\hat{\varphi}_n(1) = h_n(1)/\sqrt{2}$. Therefore the contour integral gives

$$\frac{1}{2\pi i} \int_{\tilde{\Sigma}_6} [2^\rho(\Delta_R)_{12}(y) - 2^{-\rho}(\Delta_R)_{21}(y) + \dots] dy = -\frac{i\rho}{2} \frac{1}{nh_n(1)} + \dots, \quad (\text{S3.16})$$

where again we take into account the clockwise orientation of $\tilde{\Sigma}_6$. Note that Lemma 1 tells us that $h_n(1) \sim \mathcal{O}(1)$ as $n \rightarrow \infty$, so this contribution scales as $\mathcal{O}(1/n)$.

3. Integral over the circular contour $\tilde{\Sigma}_7$ near $z = -1$

Similarly, taking into account the different expressions for $\tilde{\Delta}_1(z)$ in \mathbb{C}_\pm from Eq. (S2.79), we get

$$2^\rho(\Delta_R)_{12}(y) - 2^{-\rho}(\Delta_R)_{21}(y) = \frac{i}{12n\phi_n(-z)} [e^{\mp i\pi\rho} \varphi(z)^\rho - e^{\pm i\pi\rho} \varphi(z)^{-\rho}]. \quad (\text{S3.17})$$

To find the residue, we exploit analyticity and evaluate this expression as $z \rightarrow x + i0^+$ with $x < -1$. This gives

$$\varphi(x)^\rho = e^{i\pi\rho} \left(1 + \sqrt{2}\rho(-x-1)^{1/2} + \dots \right). \quad (\text{S3.18})$$

Then we have

$$e^{-i\pi\rho}\varphi(x)^\rho - e^{i\pi\rho}\varphi(x)^{-\rho} = 2\sqrt{2}\rho(-x-1)^{1/2} + \dots \quad (\text{S3.19})$$

Then again using $\phi_n(-z) = -(2/3)(-z-1)^{3/2}\hat{\varphi}_n(-z)$, we get

$$2^\rho(\Delta_R)_{12}(x) - 2^{-\rho}(\Delta_R)_{21}(x) = \frac{i\rho}{2} \frac{1}{nh_n(1)} \frac{1}{x+1} + \mathcal{O}(x^0), \quad (\text{S3.20})$$

so the residue is $i\rho/2nh_n(1)$. Hence the contour integral gives

$$\frac{1}{2\pi i} \int_{\tilde{\Sigma}_7} [2^\rho(\Delta_R)_{12}(y) - 2^{-\rho}(\Delta_R)_{21}(y) + \dots] dy = -\frac{i\rho}{2} \frac{1}{nh_n(1)} + \dots, \quad (\text{S3.21})$$

so to leading order we get the same contribution as from the circle around $z = 1$.

4. Contribution from the lens boundaries $\tilde{\Sigma}_{j=1..4}$

Let us focus on the lens boundary in the first quadrant, $\tilde{\Sigma}_1$, with the analysis for the other lens boundaries following similarly. From Eqs. (S2.46) and (S2.118) we have

$$\Delta_R(z) = e^{-2n\phi_n(z)}\omega(z)^{-1}N(z) \begin{pmatrix} 0 & 0 \\ 1 & 0 \end{pmatrix} N(z)^{-1}. \quad (\text{S3.22})$$

By using the solution Eq. (S2.53) for $N(z)$, one can check that the factor following $e^{-2n\phi_n(z)}$ is $\mathcal{O}(|z|^0)$ as $z \rightarrow \infty$. Then we have

$$\left| \int_{\tilde{\Sigma}_1} \Delta_R(z) dz \right| \leq \mathcal{O} \left(\left| \int_{\tilde{\Sigma}_1} |e^{-2n\phi_n(z)}| dz \right| \right) \quad (\text{S3.23})$$

In Lemma S12 we show that as $n \rightarrow \infty$ the RHS is $o(1/n \text{ poly}(\log n))$, so that the contribution from the lens boundary is subleading compared with the contributions from the local parametrices at $z = 0$ and $z = \pm 1$ (c.f. Eqs. (S3.12), (S3.16) and (S3.21)).

5. Combining the contributions

With the dominant contributions from the circular contours from the local parametrices, we get

$$b_n = \frac{\beta_n}{2} \left(1 + 2\rho \frac{1}{nh_n(1)} - (-1)^n 2\rho \frac{1}{nh_n(0)} + \dots \right)^{1/2}. \quad (\text{S3.24})$$

Expanding the square root gives

$$b_n = \frac{\beta_n}{2} \left(1 + \rho \left[\frac{1}{h_n(1)} - (-1)^n \frac{1}{h_n(0)} \right] \frac{1}{n} + \dots \right), \quad (\text{S3.25})$$

which concludes the proof of Theorem 1. The leading error term encoded in the dots depends on the growth exponents p and q of the potential $Q(x)$. For $p > 1$, the leading error is $\tilde{\mathcal{O}}(1/n^{2-1/p})$, with equal order contributions from the $k = 2$ term in the asymptotic expansion of the $z = 0$ local parametrix, and from the $\mathcal{O}(\|\Delta_R\|_{L_2(\Sigma_5)}^2)$ error in Eq. (S2.125). For $p = 1$, this error reduces to $\mathcal{O}(1/n(\log n)^{2+q+o(1)})$, which is subleading relative to the $1/nh_n(0) \sim 1/n(\log n)^{1+o(1)}$ term because we are assuming $q > -1$ if $p = 1$.

As a check of the theorem, we can consider the generalized Hermite polynomials, which have weight function $\Phi(x)/2\pi = |x|^\rho \exp[-x^2]$. With $Q(x) = x^2$, we have $\beta_n = \sqrt{2n}$, and $h_n(0) = h_n(1) = 4$ (c.f. Lemmas 1 and 2 with $p = 2$). Substituting into Theorem 1, we get agreement to $\mathcal{O}(1/n)$ with the exact recurrence coefficients, which are known to be $b_n = (1/\sqrt{2})\sqrt{n + \frac{1}{2}[1 - (-1)^n]\rho}$ [81].

C. Scaling of the leading coefficient y_n

The leading coefficients $y_n > 0$ of the polynomial $p_n(x) = y_n x^n + \dots$ can be extracted from the solution $Y(z)$ to the fundamental Riemann-Hilbert problem using Eq. (S2.6), which requires the matrix element $(Y_1)_{12}$. Reversing the transformations for Y as before gives

$$(Y_1)_{12} = \beta_n^{2n+1+\rho} e^{nl_n} \left(i2^{-(1+\rho)} + (R_1)_{12} \right). \quad (\text{S3.26})$$

The matrix element $(R_1)_{12}$ can be derived from a residue calculation like that for b_n , and takes the value

$$(R_1)_{12} = \frac{1}{n} \frac{i}{2^{1+\rho}} \left[\frac{\rho}{h_n(0)} \left(\frac{\rho}{2} - (-1)^n \right) + \frac{1}{12h_n(1)} \left(2(2 + 6\rho + 3\rho^2) - 3 \frac{h'_n(1)}{h_n(1)} \right) \right] + \dots. \quad (\text{S3.27})$$

The contribution to $(Y_1)_{12}$ from $(R_1)_{12}$ is therefore subleading by a factor of $1/n$ compared with the factor $i2^{-(1+\rho)}$ coming from $(N_1)_{12}$. Thus we have

$$(Y_1)_{12} = \frac{i}{2^{1+\rho}} \beta_n^{2n} \beta_n^{1+\rho} e^{nl_n} [1 + \mathcal{O}(1/n)]. \quad (\text{S3.28})$$

Then the leading coefficient y_n scales like

$$y_n = \frac{2^{\rho/2}}{\sqrt{\pi}} \beta_n^{-n} \beta_n^{-(1+\rho)/2} e^{-\frac{1}{2}nl_n} [1 + \mathcal{O}(1/n)]. \quad (\text{S3.29})$$

By Lemma S5, we know that the Lagrange multiplier l_n will be $\mathcal{O}(1)$ and negative as $n \rightarrow \infty$. On the other hand, $\beta_n \sim n^{1/p}$, so the leading order scaling of y_n will be dictated by the factor β_n^{-n} , such that

$$y_n \sim e^{-\frac{1}{p}n \log n + \mathcal{O}(n)}. \quad (\text{S3.30})$$

As a simple check of this scaling, we note that y_n is related to the recurrence coefficients by

$$y_n = (b_1 b_2 \dots b_n)^{-1}. \quad (\text{S3.31})$$

Since the recurrence coefficients scale to leading order like $b_n \sim \beta_n$, this validates the factorial-like scaling $y_n \sim \beta_n^{-n}$. In Ref. [10], by counting Dyck paths they give a lower bound for the moments

$$\mu_{2n} \geq y_n^{-2}, \quad (\text{S3.32})$$

so our result gives

$$\mu_{2n} \geq e^{\frac{2}{p}n \log n + \mathcal{O}(n)}, \quad (\text{S3.33})$$

so the moments grow at least as fast as a power of a factorial to leading order. Of course, this moment bound is immediate from just taking $b_n \sim n^{1/p}$, but our more precise estimate of y_n will be relevant in the next section.

S4. ASYMPTOTICS OF THE ORTHOGONAL POLYNOMIALS

In this section we will use our constructed asymptotic solution of the Riemann-Hilbert problem for $Y(z)$ to obtain the $n \rightarrow \infty$ asymptotics of the orthogonal polynomials $p_n(z)$, as well as the associated Christoffel-Darboux (CD) kernel $K_n(x, y) = \sum_{m=0}^{n-1} p_m(x)p_m(y)$. From Eq. (S2.4), the polynomials $p_n(z)$ and $p_{n-1}(z)$ will be determined by the first column of $Y(z)$ via

$$p_n(z) = y_n Y_{11}(z), \quad (\text{S4.1})$$

$$p_{n-1}(z) = \frac{-1}{2\pi i} \frac{1}{y_n b_n} Y_{21}(z), \quad (\text{S4.2})$$

where the recurrence coefficient b_n and the leading coefficient $y_n > 0$ of $p_n(x) = y_n x^n + \dots$ are determined from Y_1 as in Eqs. (S2.5) and (S2.6).

For the CD kernel, the Christoffel-Darboux formula gives

$$K_n(x, t) = b_n \frac{p_n(x)p_{n-1}(t) - p_{n-1}(x)p_n(t)}{x - t}, \quad (\text{S4.3})$$

Again, we can evaluate this in terms of the matrix elements of the solution Y to the Riemann-Hilbert problem:

$$K_n(x, t) = \frac{-1}{2\pi i} \frac{Y_{11}(x)Y_{21}(t) - Y_{21}(x)Y_{11}(t)}{x - t}. \quad (\text{S4.4})$$

We will mainly be interested in the diagonal case $t = x$, where we get

$$K_n(x, x) = \frac{-1}{2\pi i} (Y'_{11}(x)Y_{21}(x) - Y'_{21}(x)Y_{11}(x)), \quad (\text{S4.5})$$

$$= \frac{1}{2\pi i} \det \begin{pmatrix} Y_{11}(x) & Y'_{11}(x) \\ Y_{21}(x) & Y'_{21}(x) \end{pmatrix}. \quad (\text{S4.6})$$

A. Behavior near the origin

Here we discuss the asymptotics near the origin $z = 0$, where the scaling will be determined in terms of Bessel functions, by virtue of the local parametrix $\Psi_{\rho/2}$ constructed in Section S2 J 1. Following Ref. [27], we reverse the transformations $Y \mapsto U \mapsto T \mapsto S \mapsto R$ for $z \rightarrow 0$ in the upper lens, in the region enclosed by the local parametrix near the origin. Combining Eqs. (S2.7), (S2.34), (S2.45), (S2.112), (S2.117) and (S2.118), this gives

$$Y(\beta_n z) = \beta_n^{(n+\rho/2)\sigma_3} e^{(nl_n/2)\sigma_3} R(z) E_n(z) \Psi_{\rho/2}(nf_n(z)) z^{-(\rho/2)\sigma_3} e^{(i\pi\rho/2)\sigma_3} e^{-n\phi_n(z)\sigma_3} \times \begin{pmatrix} 1 & 0 \\ z^{-\rho} e^{-2n\phi_n(z)} & 1 \end{pmatrix} e^{-(nl_n/2)\sigma_3} e^{ng_n(z)\sigma_3} \beta_n^{-(\rho/2)\sigma_3}, \quad (\text{S4.7})$$

where we are taking z to be $\mathcal{O}(1/\beta_n)$. The first column of Y is then given by

$$\begin{pmatrix} Y_{11}(\beta_n z) \\ Y_{21}(\beta_n z) \end{pmatrix} = (\beta_n z)^{-\rho/2} e^{n[g_n(z) - \phi_n(z) - (ln/2)]} \beta_n^{(n+\rho/2)\sigma_3} e^{(nl_n/2)\sigma_3} R(z) E_n(z) \Psi_{\rho/2}(nf_n(z)) e^{(i\pi\rho/2)\sigma_3} \begin{pmatrix} 1 \\ 1 \end{pmatrix}. \quad (\text{S4.8})$$

For z in the sector $f_n^{-1}(I)$, we can combine Eq. (S2.96) with the Bessel function identities 9.1.3 and 9.1.4 of Ref. [124] to get

$$\Psi_{\rho/2}(nf_n(z)) e^{(i\pi\rho/2)\sigma_3} \begin{pmatrix} 1 \\ 1 \end{pmatrix} = e^{-i\pi/4} \sqrt{\pi} (nf_n(z))^{1/2} \begin{pmatrix} J_{\frac{1}{2}(\rho+1)}(nf_n(z)) \\ J_{\frac{1}{2}(\rho-1)}(nf_n(z)) \end{pmatrix}, \quad (\text{S4.9})$$

where J_α is a Bessel function of the first kind. Sending $z \downarrow x \in (0, \delta_n)$, Lemma S7 and Eq. (S2.42) tell us that

$$e^{n[g_{n,+}(x) - \phi_{n,+}(x) - (ln/2)]} = e^{\frac{n}{2}[g_{n,+}(x) + g_{n,-}(x) - ln]} = e^{\frac{n}{2}V_n(x)} = e^{\frac{1}{2}Q(\beta_n x)}, \quad (\text{S4.10})$$

where we used $2\phi_{n,+}(x) = g_{n,+}(x) - g_{n,-}(x)$. We therefore get

$$\begin{pmatrix} Y_{11}(\beta_n x) \\ Y_{21}(\beta_n x) \end{pmatrix} = e^{-i\pi/4} \sqrt{\pi} \beta_n^{-\rho/2} e^{\frac{1}{2}Q(\beta_n x)} \beta_n^{(n+\rho/2)\sigma_3} e^{(nl_n/2)\sigma_3} R(x) E_n(x) (nf_n(x))^{1/2} x^{-\rho/2} \begin{pmatrix} J_{\frac{1}{2}(\rho+1)}(nf_n(x)) \\ J_{\frac{1}{2}(\rho-1)}(nf_n(x)) \end{pmatrix}. \quad (\text{S4.11})$$

Since by construction $R(x) = \mathbf{1} + o(1)$, where the $o(1)$ refers to scaling with n , for large n we can approximate $R(x) \approx \mathbf{1}$. Then using the definition Eq. (S2.110) of $E_n(x)$, we can unpack this formula to get the explicit expressions (temporarily suppressing some function arguments to reduce notation)

$$Y_{11}(\beta_n x) \approx \frac{\pi e^{-i\pi/4}}{2^{3/2}} \sqrt{\frac{nf_n(x)}{w(\beta_n x)}} \beta_n^{n+\rho/2} e^{\frac{nI_n}{2}} 2^{-\rho/2} \left[e^{\frac{i\pi}{4}(2n-\rho)} \varphi_+^{\rho/2} (a_+ + a_+^{-1}) \left(e^{-\frac{i\pi}{4}} J_{\frac{1}{2}(\rho+1)} + e^{\frac{i\pi}{4}} J_{\frac{1}{2}(\rho-1)} \right) \right. \\ \left. + e^{-\frac{i\pi}{4}(2n-\rho)} \varphi_+^{-\rho/2} (a_+ - a_+^{-1}) \left(e^{\frac{i\pi}{4}} J_{\frac{1}{2}(\rho+1)} + e^{-\frac{i\pi}{4}} J_{\frac{1}{2}(\rho-1)} \right) \right], \quad (\text{S4.12})$$

$$Y_{21}(\beta_n x) \approx \frac{\pi e^{-i\pi/4}}{2^{3/2}} \sqrt{\frac{nf_n(x)}{w(\beta_n x)}} i \beta_n^{-(n+\rho/2)} e^{-\frac{nI_n}{2}} 2^{\rho/2} \left[e^{-\frac{i\pi}{4}(2n-\rho)} \varphi_+^{-\rho/2} (a_+ + a_+^{-1}) \left(e^{\frac{i\pi}{4}} J_{\frac{1}{2}(\rho+1)} + e^{-\frac{i\pi}{4}} J_{\frac{1}{2}(\rho-1)} \right) \right. \\ \left. + e^{\frac{i\pi}{4}(2n-\rho)} \varphi_+^{\rho/2} (a_+ - a_+^{-1}) \left(e^{-\frac{i\pi}{4}} J_{\frac{1}{2}(\rho+1)} + e^{\frac{i\pi}{4}} J_{\frac{1}{2}(\rho-1)} \right) \right], \quad (\text{S4.13})$$

with $w(x) = x^\rho e^{-Q(x)}$, and where the functions $a \equiv a(x)$ and $\varphi \equiv \varphi(x)$ are defined in Eqs. (S2.52) and (S2.54). In this region their + side expressions are $a_+(x) = e^{i\pi/4}(1-x)^{1/4}/(1+x)^{1/4}$ and $\varphi_+(x) = x + i\sqrt{1-x^2} = e^{i \arccos(x)}$. The Bessel functions $J_{\frac{1}{2}(\rho \pm 1)}$ should be evaluated with the argument $nf_n(x)$.

1. Proofs of Theorem 2 and Lemma 3

With these expressions for the first column of Y near the origin, we can now get expressions for the orthogonal polynomials $p_n(x)$ and $p_{n-1}(x)$ using Eqs. (S4.1) and (S4.2), as well as the expression Eq. (S3.29) for the leading coefficient y_n . For example, for p_n we get

$$p_n(\beta_n x) \approx \frac{e^{-i\pi/4}}{2^{3/2}} \sqrt{\frac{nf_n(x)}{\beta_n w(\beta_n x)}} \left[e^{\frac{i\pi}{4}(2n-\rho)} \varphi_+^{\rho/2} (a_+ + a_+^{-1}) \left(e^{-\frac{i\pi}{4}} J_{\frac{1}{2}(\rho+1)} + e^{\frac{i\pi}{4}} J_{\frac{1}{2}(\rho-1)} \right) \right. \\ \left. + e^{-\frac{i\pi}{4}(2n-\rho)} \varphi_+^{-\rho/2} (a_+ - a_+^{-1}) \left(e^{\frac{i\pi}{4}} J_{\frac{1}{2}(\rho+1)} + e^{-\frac{i\pi}{4}} J_{\frac{1}{2}(\rho-1)} \right) \right], \quad (\text{S4.14})$$

where the arguments of $\varphi_+ \equiv \varphi_+(x)$, $a_+ \equiv a_+(x)$ and $J_{\frac{1}{2}(\rho \pm 1)} \equiv J_{\frac{1}{2}(\rho \pm 1)}(nf_n(x))$ are suppressed as before. For $\rho = 0$, this reduces to Eq. (94) of the main text after using $nf_n(x) = \pi I_n(\beta_n x)$, with I_n defined in Eq. (92). By the discussion surrounding Eq. (S2.126), this expression has a multiplicative error of $\mathcal{O}(\beta_n/nh_n(0))$.

Using $f_n(x) = \pi \int_0^x \psi_n(s) ds \approx \pi \psi_n(0)x$, we can take the limit $x \rightarrow 0^+$, giving

$$p_n(0) \approx \cos\left(\frac{n\pi}{2}\right) \frac{2^{\frac{1}{2}-\frac{\rho}{2}}}{\Gamma\left[\frac{1+\rho}{2}\right]} e^{Q(0)/2} \frac{[\pi\sigma_n(0)]^{\rho/2}}{\beta_n^{1/2}}, \quad (\text{S4.15})$$

$$p'_n(0) \approx \sin\left(\frac{n\pi}{2}\right) \frac{2^{-\frac{1}{2}-\frac{\rho}{2}}}{\Gamma\left[\frac{3+\rho}{2}\right]} e^{Q(0)/2} \frac{[\pi\sigma_n(0)]^{1+\rho/2}}{\beta_n^{1/2}} \left(1 + \frac{(\rho+1)^2}{2\pi\beta_n\sigma_n(0)}\right), \quad (\text{S4.16})$$

where $\sigma_n(0) = n\psi_n(0)/\beta_n$ is the equilibrium density of the Coulomb gas at $\omega = 0$. This proves Theorem 2 in the main text. As a sanity check, we can see that $p_n(0)$ vanishes for odd n and $p'_n(0)$ vanishes for even n . One can also check using Eq. (S2.128) that the contribution from the derivative $R'(z)$ is subleading relative to the leading term by a factor of $\mathcal{O}(\beta_n/nh_n(0))$ (c.f. Remark 1), so the derivative $p'_n(0)$ has the same multiplicative error as $p_n(0)$.

Similarly, using Eqs. (S3.29), (S4.2) and (S4.13), for p_{n-1} we get

$$p_{n-1}(\beta_n x) \approx -\frac{e^{-i\pi/4}}{2^{3/2}} \frac{\beta_n}{2b_n} \sqrt{\frac{nf_n(x)}{\beta_n w(\beta_n x)}} \left[e^{-\frac{i\pi}{4}(2n-\rho)} \varphi_+^{-\rho/2} (a_+ + a_+^{-1}) \left(e^{\frac{i\pi}{4}} J_{\frac{1}{2}(\rho+1)} + e^{-\frac{i\pi}{4}} J_{\frac{1}{2}(\rho-1)} \right) \right. \\ \left. + e^{\frac{i\pi}{4}(2n-\rho)} \varphi_+^{\rho/2} (a_+ - a_+^{-1}) \left(e^{-\frac{i\pi}{4}} J_{\frac{1}{2}(\rho+1)} + e^{\frac{i\pi}{4}} J_{\frac{1}{2}(\rho-1)} \right) \right], \quad (\text{S4.17})$$

with the same argument suppression as before. Note that Theorem 1 tells us that the factor $\beta_n/2b_n = 1 + \mathcal{O}(1/n)$; for $\rho = 0$, this equation reduces to Eq. (93) of the main text after approximating $\beta_n/2b_n \approx 1$.

Keeping ρ general, again taking the limit $x \rightarrow 0^+$ gives

$$p_{n-1}(0) \approx \sin\left(\frac{n\pi}{2}\right) \frac{\beta_n}{2b_n} \frac{2^{\frac{1}{2}-\frac{\rho}{2}}}{\Gamma\left[\frac{1+\rho}{2}\right]} e^{Q(0)/2} \frac{[\pi\sigma_n(0)]^{\rho/2}}{\beta_n^{1/2}}, \quad (\text{S4.18})$$

$$p'_{n-1}(0) \approx -\cos\left(\frac{n\pi}{2}\right) \frac{\beta_n}{2b_n} \frac{2^{-\frac{1}{2}-\frac{\rho}{2}}}{\Gamma\left[\frac{3+\rho}{2}\right]} e^{Q(0)/2} \frac{[\pi\sigma_n(0)]^{1+\rho/2}}{\beta_n^{1/2}} \left(1 + \frac{\rho^2 - 1}{2\pi\beta_n\sigma_n(0)}\right), \quad (\text{S4.19})$$

For the CD kernel, the Christoffel-Darboux formula $K_n(0, 0) = b_n (p'_n(0)p_{n-1}(0) - p'_{n-1}(0)p_n(0))$ gives

$$K_n(0, 0) \approx \frac{1}{2^{1+\rho}\Gamma\left[\frac{1}{2}(1+\rho)\right]\Gamma\left[\frac{1}{2}(3+\rho)\right]} e^{Q(0)} [\pi\sigma_n(0)]^{1+\rho}. \quad (\text{S4.20})$$

This proves Lemma 3 of the main text, with a multiplicative error term of $\mathcal{O}(\beta_n/nh_n(0))$ coming from neglecting the $R(0) - 1$ and $R'(0)$ contributions.

B. Expressions for the spectral bootstrap

1. Bessel bootstrap: behavior near the origin

First let us derive Eq. (101) of the main text. Squaring Eqs. (S4.14) and (S4.17) and using the expressions $a_+(x) = e^{i\pi/4}(1-x)^{1/4}/(1+x)^{1/4}$ and $\varphi_+(x) = e^{i\arccos(x)}$, we get (after some algebraic simplifications)

$$p_{n-1}(\beta_n x)^2 + p_n(\beta_n x)^2 \approx \frac{nf_n(x)}{\beta_n w(\beta_n x)} \frac{1}{\sqrt{1-x^2}} \times \left[\left(J_{\frac{1}{2}(\rho-1)}^2 + J_{\frac{1}{2}(\rho+1)}^2 \right) (nf_n(x)) \right. \\ \left. - (-1)^n x \left(\left(J_{\frac{1}{2}(\rho-1)}^2 - J_{\frac{1}{2}(\rho+1)}^2 \right) (nf_n(x)) \sin[\rho \arcsin x] + 2 \left(J_{\frac{1}{2}(\rho-1)} J_{\frac{1}{2}(\rho+1)} \right) (nf_n(x)) \cos[\rho \arcsin x] \right) \right]. \quad (\text{S4.21})$$

Then we use the fact that $nf_n(x) = \pi I_n(\beta_n x)$ with I_n defined in Eq. (92). Rescaling $\beta_n x \mapsto \omega$, and using $w(x) = x^\rho \exp[-Q(x)]$, we get

$$e^{-Q(\omega)} \approx \frac{1}{p_{n-1}(\omega)^2 + p_n(\omega)^2} \frac{1}{\sqrt{\beta_n^2 - \omega^2}} \frac{\pi I_n(\omega)}{\omega^\rho} \left[\left(J_{\frac{1}{2}(\rho-1)}^2 + J_{\frac{1}{2}(\rho+1)}^2 \right) (\pi I_n(\omega)) \right. \\ \left. - (-1)^n \frac{\omega}{\beta_n} \left(\left(J_{\frac{1}{2}(\rho-1)}^2 - J_{\frac{1}{2}(\rho+1)}^2 \right) (\pi I_n(\omega)) \sin \left\{ \rho \arcsin \left(\frac{\omega}{\beta_n} \right) \right\} + 2 \left(J_{\frac{1}{2}(\rho-1)} J_{\frac{1}{2}(\rho+1)} \right) (\pi I_n(\omega)) \cos \left\{ \rho \arcsin \left(\frac{\omega}{\beta_n} \right) \right\} \right) \right]. \quad (\text{S4.22})$$

This simplifies to Eq. (101) upon dropping the term proportional to $\sin\{\rho \arcsin(\omega/\beta_n)\}$, which for $\omega/\beta_n \ll 1$ is subleading by a factor of $\mathcal{O}(\beta_n\sigma_n(\omega))$ relative to the term proportional to $\cos\{\rho \arcsin(\omega/\beta_n)\}$.

Now let us derive the expression Eq. (102) involving the diagonal Christoffel-Darboux kernel. The general strategy will be to use the Christoffel-Darboux formula $K_n(\omega, \omega) = b_n (p'_n(\omega)p_{n-1}(\omega) - p'_{n-1}(\omega)p_n(\omega))$, together with the expressions Eqs. (S4.14) and (S4.17) we derived for p_n and p_{n-1} . After a lengthy but straightforward algebraic computation, we get the expression

$$K_n(\omega, \omega) \approx \frac{1}{4} \frac{\pi I_n(\omega)}{w(\omega)} \left(\pi\sigma_n(\omega) \left[J_{\frac{1}{2}(\rho-1)}^2 + J_{\frac{1}{2}(\rho+1)}^2 - J_{\frac{1}{2}(\rho-3)} J_{\frac{1}{2}(\rho+1)} - J_{\frac{1}{2}(\rho-1)} J_{\frac{1}{2}(\rho+3)} \right] (\pi I_n(\omega)) + \frac{\rho \left(J_{\frac{1}{2}(\rho-1)}^2 + J_{\frac{1}{2}(\rho+1)}^2 \right) (\pi I_n(\omega))}{\sqrt{\beta_n^2 - \omega^2}} \right. \\ \left. + (-1)^n \frac{\beta_n}{\beta_n^2 - \omega^2} \left[\left(J_{\frac{1}{2}(\rho+1)}^2 - J_{\frac{1}{2}(\rho-1)}^2 \right) (\pi I_n(\omega)) \cos \left\{ \rho \arcsin \left(\frac{\omega}{\beta_n} \right) \right\} + 2 \left(J_{\frac{1}{2}(\rho-1)} J_{\frac{1}{2}(\rho+1)} \right) (\pi I_n(\omega)) \sin \left\{ \rho \arcsin \left(\frac{\omega}{\beta_n} \right) \right\} \right] \right), \quad (\text{S4.23})$$

where we used $\partial_\omega I_n(\omega) = \sigma_n(\omega)$. This expression reduces to Eq. (102) after dropping all but the first term proportional to $\pi\sigma_n(\omega)$ in the large curly bracketed expression, since for $\omega/\beta_n \ll 1$ the other terms are subleading by a factor of either $\mathcal{O}(\beta_n\sigma_n(\omega))$ or $\mathcal{O}(\beta_n^2/\omega^2)$.

2. Bulk bootstrap

Having already derived the spectral bootstrap equations near an algebraic divergence $\Phi(\omega) \sim |\omega|^\rho$, a quick way to arrive at the spectral bootstrap equations in the bulk is to simply send $\rho \rightarrow 0$ and then replace $\exp[-Q(\omega)] \mapsto \Phi(\omega)/2\pi$. One can check that properly doing the calculation by unpacking the expression for $Y(z)$ in the bulk gives the same expressions.

To derive Eq. (95) of the main text, we send $\rho \rightarrow 0$ in Eq. (S4.22); using $J_{-\frac{1}{2}}(x) = \sqrt{2/\pi x} \cos x$ and $J_{\frac{1}{2}}(x) = \sqrt{2/\pi x} \sin x$, we get

$$e^{-Q(\omega)} \approx \frac{1}{p_{n-1}(\omega)^2 + p_n(\omega)^2} \frac{1}{\sqrt{\beta_n^2 - \omega^2}} \frac{2}{\pi} \left[1 - (-1)^n \frac{\omega}{\beta_n} \sin[2\pi I_n(\omega)] \right], \quad (\text{S4.24})$$

which is equivalent to Eq. (95) once we set $\Phi(\omega) \equiv 2\pi \exp[-Q(\omega)]$.

To get Eq. (97) of the main text, we take $\rho \rightarrow 0$ of Eq. (S4.23) to get

$$K_n(\omega, \omega) \approx \frac{2\pi\sigma_n(\omega)}{\Phi(\omega)} \left(1 - (-1)^n \frac{\beta_n}{\beta_n^2 - \omega^2} \frac{\cos[2\pi I_n(\omega)]}{2\pi\sigma_n(\omega)} \right). \quad (\text{S4.25})$$

This reduces to Eq. (97) upon dropping the second term in the brackets, which is subleading by a factor of $\mathcal{O}(\beta_n\sigma_n(\omega))$. From Eqs. (S2.127) and (S2.129), this asymptotic has a multiplicative error of $\mathcal{O}(|\omega|^{-1}\beta_n/nh_n(0)) + \mathcal{O}(1/n)$, where the factor of $|\omega|^{-1}$ gets cut off by $\mathcal{O}(1)$ for $|\omega| \leq \mathcal{O}(1)$.

3. Airy bootstrap: behavior near the edge

In this section we will consider frequencies near the edge of the spectrum, $\omega \approx \beta_n$. Similarly to Section S4 A, we reverse the transformations $Y \mapsto U \mapsto T \mapsto S \mapsto R$, but now within the local parametrix centered at $z = 1$. With the aim of approaching the real axis, we will take z in the sector mapped to sector II of Fig. S3. Combining Eqs. (S2.7), (S2.34), (S2.45), (S2.57), (S2.117) and (S2.118), this gives

$$Y(\beta_n z) = \beta_n^{(n+\rho/2)\sigma_3} e^{(nl_n/2)\sigma_3} R(z) E(z) \Psi(f_n(z)) e^{-n\phi_n(z)\sigma_3} z^{-(\rho/2)\sigma_3} \\ \times \begin{pmatrix} 1 & 0 \\ z^{-\rho} e^{-2n\phi_n(z)} & 1 \end{pmatrix} e^{-(nl_n/2)\sigma_3} e^{ng_n(z)\sigma_3} \beta_n^{-(\rho/2)\sigma_3}. \quad (\text{S4.26})$$

The first column of Y is then given by

$$\begin{pmatrix} Y_{11}(\beta_n z) \\ Y_{21}(\beta_n z) \end{pmatrix} = (\beta_n z)^{-\rho/2} e^{n[g_n(z) - \phi_n(z) - (ln/2)]} \beta_n^{(n+\rho/2)\sigma_3} e^{(nl_n/2)\sigma_3} R(z) E(z) \Psi(f_n(z)) \begin{pmatrix} 1 \\ 1 \end{pmatrix}. \quad (\text{S4.27})$$

Taking $z \downarrow x < 1$, using Eq. (S4.10), and replacing Ψ with the sector II expression from Eq. (S2.61), we get

$$\begin{pmatrix} Y_{11}(\beta_n x) \\ Y_{21}(\beta_n x) \end{pmatrix} = \sqrt{2\pi} e^{-i\pi/4} (\beta_n x)^{-\rho/2} e^{\frac{1}{2}Q(\beta_n x)} \beta_n^{(n+\rho/2)\sigma_3} e^{(nl_n/2)\sigma_3} R(x) E(x) \begin{pmatrix} \text{Ai}(f_n(x)) \\ \text{Ai}'(f_n(x)) \end{pmatrix}, \quad (\text{S4.28})$$

where we recall that both $E(z)$ and $R(z)$ are analytic near $z = 1$, and the biholomorphic map $f_n(z)$ is defined in Proposition S2. Using the definition Eq. (S2.72) of $E(x)$, after some algebra this becomes

$$\begin{pmatrix} Y_{11}(\beta_n z) \\ Y_{21}(\beta_n z) \end{pmatrix} = \sqrt{\pi} e^{-i\pi/4} (\beta_n x)^{-\rho/2} e^{\frac{1}{2}Q(\beta_n x)} \beta_n^{(n+\rho/2)\sigma_3} e^{(nl_n/2)\sigma_3} R(x) 2^{-(\rho/2)\sigma_3} e^{(i\pi/4)\sigma_3} \\ \times \begin{pmatrix} [ia_+ \sin(\frac{\rho}{2} \arccos x) + a_+^{-1} \cos(\frac{\rho}{2} \arccos x)] f_n^{1/4} \text{Ai}(f_n) + [-a_+ \cos(\frac{\rho}{2} \arccos x) - ia_+^{-1} \sin(\frac{\rho}{2} \arccos x)] f_n^{-1/4} \text{Ai}'(f_n) \\ [-ia_+ \sin(\frac{\rho}{2} \arccos x) + a_+^{-1} \cos(\frac{\rho}{2} \arccos x)] f_n^{1/4} \text{Ai}(f_n) + [a_+ \cos(\frac{\rho}{2} \arccos x) - ia_+^{-1} \sin(\frac{\rho}{2} \arccos x)] f_n^{-1/4} \text{Ai}'(f_n) \end{pmatrix}, \quad (\text{S4.29})$$

where for notational simplicity we have suppressed the arguments of $f_n \equiv f_n(x)$ and $a_+ \equiv a_+(x) = e^{i\pi/4}(1-x)^{1/4}/(1+x)^{1/4}$, and used $\varphi_+(x) = e^{i \arccos x}$ for $0 < x < 1$. Approximating $R(x) \approx 1$, then using Eqs. (S4.1) and (S4.2) to

convert to $p_n(z)$ and $p_{n-1}(z)$, and the asymptotic Eq. (S3.29) for the leading coefficient y_n , we get

$$p_n(\beta_n x) \approx \frac{1}{\sqrt{\beta_n w(\beta_n x)}} \left([ia_+ \sin(\frac{\rho}{2} \arccos x) + a_+^{-1} \cos(\frac{\rho}{2} \arccos x)] f_n^{1/4} \text{Ai}(f_n) + [-a_+ \cos(\frac{\rho}{2} \arccos x) - ia_+^{-1} \sin(\frac{\rho}{2} \arccos x)] f_n^{-1/4} \text{Ai}'(f_n) \right), \quad (\text{S4.30})$$

$$p_{n-1}(\beta_n x) \approx \frac{\beta_n}{2b_n} \frac{1}{\sqrt{\beta_n w(\beta_n x)}} \left([-ia_+ \sin(\frac{\rho}{2} \arccos x) + a_+^{-1} \cos(\frac{\rho}{2} \arccos x)] f_n^{1/4} \text{Ai}(f_n) + [a_+ \cos(\frac{\rho}{2} \arccos x) - ia_+^{-1} \sin(\frac{\rho}{2} \arccos x)] f_n^{-1/4} \text{Ai}'(f_n) \right). \quad (\text{S4.31})$$

Note that, by Theorem 1, the prefactor $\beta_n/2b_n = 1 + \mathcal{O}(1/n)$, so we will henceforth approximate it as 1. Now, from the definition of $f_n(z)$ in Proposition S2, we can deduce that the behavior of $f_n(x)$ near $x = 1$ is approximately

$$f_n(x) \approx (x-1)f_n'(1), \quad x \rightarrow 1, \quad (\text{S4.32})$$

where the derivative $f_n'(1)$ is related to the equilibrium measure by

$$f_n'(1) = (n\hat{\varphi}_n(1))^{2/3} = \left(\frac{nh_n(1)}{\sqrt{2}} \right)^{2/3}. \quad (\text{S4.33})$$

This allows us to take the limit $x \rightarrow 1^-$ of Eqs. (S4.30) and (S4.31), with the result

$$p_n(\beta_n) \approx \frac{1}{\sqrt{\beta_n w(\beta_n)}} \left[(2nh_n(1))^{1/6} \text{Ai}(0) - (\rho+1)(2nh_n(1))^{-1/6} \text{Ai}'(0) \right], \quad (\text{S4.34})$$

$$p_{n-1}(\beta_n) \approx \frac{1}{\sqrt{\beta_n w(\beta_n)}} \left[(2nh_n(1))^{1/6} \text{Ai}(0) - (\rho-1)(2nh_n(1))^{-1/6} \text{Ai}'(0) \right], \quad (\text{S4.35})$$

where $\text{Ai}(0) = (3^{2/3}\Gamma[\frac{2}{3}])^{-1}$ and $\text{Ai}'(0) = -(3^{1/3}\Gamma[\frac{1}{3}])^{-1}$. By taking the ratio of these expressions we eliminate the unknown weight $w(\beta_n)$ and get a quadratic equation in $(2nh_n(1))^{1/6}$, either solution of which gives

$$h_n(1) \approx \frac{1}{2n} \left(\frac{\text{Ai}(0)}{\text{Ai}'(0)} \right)^3 \left[\rho - \left(\frac{p_n(\beta_n) + p_{n-1}(\beta_n)}{p_n(\beta_n) - p_{n-1}(\beta_n)} \right) \right]^3. \quad (\text{S4.36})$$

This gives a means of determining $h_n(1)$ solely in terms of the orthogonal polynomials, which can be computed in terms of the Lanczos coefficients using the three-term recurrence. One can then determine the weight $w(\beta_n)$ at the endpoint $\omega = \beta_n$ by inverting Eq. (S4.34):

$$w(\beta_n) \approx \frac{1}{\beta_n p_n(\beta_n)^2} \left[(2nh_n(1))^{1/6} \text{Ai}(0) - (\rho+1)(2nh_n(1))^{-1/6} \text{Ai}'(0) \right]. \quad (\text{S4.37})$$

To get the first of the bootstrap equations, we sum the squares of Eqs. (S4.30) and (S4.31) and rearrange for $w(\beta_n x)$ to give

$$w(\beta_n x) \approx \frac{2}{\beta_n} \frac{1}{p_n(\beta_n x)^2 + p_{n-1}(\beta_n x)^2} \frac{1}{\sqrt{1-x^2}} \left[-2x \text{Ai}(f_n(x)) \text{Ai}'(f_n(x)) \sin[\rho \arccos x] \right. \\ \left. + (-f_n(x))^{1/2} \text{Ai}(f_n(x))^2 (x \cos[\rho \arccos x] + 1) - (-f_n(x))^{-1/2} \text{Ai}'(f_n(x))^2 (x \cos[\rho \arccos x] - 1) \right]. \quad (\text{S4.38})$$

To get the second bootstrap equation concerning the derivative $f_n'(x)$, we need to compute the Christoffel-Darboux kernel $K_n(\beta_n x, \beta_n x)$, which involves differentiating the expressions Eqs. (S4.30) and (S4.31) for $p_n(\beta_n x)$ and $p_{n-1}(\beta_n x)$. Note that, because of the determinantal structure of K_n (c.f. Eq. (S4.6)), it is not necessary to differentiate the weight $w(\beta_n x)$, since all terms involving its derivative cancel exactly. It is then a matter of algebra to arrive at the expression

$$f_n'(x) \approx \frac{1}{2 \text{Ai}^2 f_n^2 - 2(\text{Ai}')^2 f_n - \text{Ai} \text{Ai}'} \left[-2\beta_n w(\beta_n x) K_n(\beta_n x, \beta_n x) f_n + \frac{2}{1-x^2} \text{Ai} \text{Ai}' \cos[\rho \arccos x] f_n \right. \\ \left. - \frac{\sin[\rho \arccos x]}{1-x^2} \left(\text{Ai}^2 (-f_n)^{3/2} - (\text{Ai}')^2 (-f_n)^{1/2} \right) - \frac{\rho}{\sqrt{1-x^2}} \left(\text{Ai}^2 (-f_n)^{3/2} + (\text{Ai}')^2 (-f_n)^{1/2} \right) \right], \quad (\text{S4.39})$$

where we have suppressed the arguments of $f_n \equiv f_n(x)$, $\text{Ai} \equiv \text{Ai}(f_n(x))$, and $\text{Ai}' \equiv \text{Ai}'(f_n(x))$. From Eqs. (S2.127) and (S2.129), this expression has a multiplicative error of $\mathcal{O}(1/n)$ from neglecting the contributions from $R(z) - \mathbb{1}$ and $R'(z)$.

C. Level- n Green's function

In this section we derive the expressions in Eqs. (81) and (84) for the level- n Green's function $G_n(z)$. From the definition in Eq. (78), we can deduce that

$$G_n(z) = \int_{\mathbb{R}} \frac{d\mu^{(n)}(x)}{z-x}, \quad z \in \mathbb{C} \setminus \mathbb{R}, \quad (\text{S4.40})$$

where $\mu^{(n)}$ is the spectral measure which generates the ‘associated orthogonal polynomials’ $\{p_m^{(n)}\}_{m=0}^{\infty}$, which are defined by the ‘ n -shifted’ recursion relation

$$b_{m+1+n}p_{m+1}^{(n)}(x) = xp_m^{(n)}(x) - b_{m+n}p_{m-1}^{(n)}(x), \quad m \geq 0, \quad (\text{S4.41})$$

with initial conditions $p_{-1}^{(n)}(x) = 0$, $p_0^{(n)}(x) = 1$. For $n = 0$ we have $d\mu^{(0)}(x) = w(x)dx$, where w is the original weight function.

The starting point for our analysis will be the relation

$$G_n(z) = \frac{1}{b_n} \frac{C_n(z)}{C_{n-1}(z)}, \quad (\text{S4.42})$$

where

$$C_n(z) = \int_{\mathbb{R}} \frac{p_n(x)}{z-x} w(x)dx, \quad z \in \mathbb{C} \setminus \mathbb{R}, \quad (\text{S4.43})$$

is the weighted Cauchy-Stieltjes transform of $p_n(x)$ with respect to the original weight function w . This relation appears as Eq. (3.7) in Ref. [29]. This reformulation is helpful because these weighted Cauchy-Stieltjes transforms appear (up to a normalization factor) in the second column of the solution $Y(z)$ to the fundamental Riemann-Hilbert problem discussed in Section S2 A. Indeed, a short computation gives

$$G_n(z) = \frac{1}{(Y_1)_{12}} \frac{Y_{12}(z)}{Y_{22}(z)}, \quad (\text{S4.44})$$

where we used the fundamental solution Eq. (S2.4), together with the relations $b_n = y_{n-1}/y_n$ and Eqs. (S2.5) and (S2.6). We have already determined the asymptotics of $(Y_1)_{12}$ in Eq. (S3.28), so it remains to determine the scaling of $Y_{12}(z)$ and $Y_{22}(z)$.

1. Behavior away from $z = 0$ and $z = \pm\beta_n$

Now let us derive the expression Eq. (81) for the level- n Green's function away from the special points $z = 0$ and $z = \pm\beta_n$. Unpacking the transformations Eqs. (S2.7), (S2.34), (S2.45) and (S2.118) for $Y(z)$, we have

$$\begin{pmatrix} Y_{12}(\beta_n z) \\ Y_{22}(\beta_n z) \end{pmatrix} = \beta_n^{\rho/2} e^{\frac{n!n}{2}} e^{-ng_n(z)} \beta_n^{(n+\rho/2)\sigma_3} e^{\frac{n!n}{2}\sigma_3} R(z)N(z) \begin{pmatrix} 0 \\ 1 \end{pmatrix}. \quad (\text{S4.45})$$

Note that, since we have focused only on the second column of $Y(z)$, this expression is accurate regardless of whether z is inside or outside the lens, provided it is not near the centers $z = 0$ and $z = \pm\beta_n$ of the local parametrices constructed in Sections S2 I and S2 J. Approximating $R(z) \approx \mathbb{1}$, and using the form Eq. (S2.53) for the outside solution $N(z)$, we get

$$\frac{Y_{12}(\beta_n z)}{Y_{22}(\beta_n z)} \approx -i2^{-\rho} \beta_n^{2n+\rho} e^{nl_n} \left(\frac{a(z) - a(z)^{-1}}{a(z) + a(z)^{-1}} \right). \quad (\text{S4.46})$$

Using the definition $a(z) = (z-1)^{1/4}/(z+1)^{1/4}$ and the asymptotic form Eq. (S3.28) for $(Y_1)_{12}$, we get Eq. (81) of the main text:

$$\beta_n G_n(\beta_n z) \approx 2 \left(z - \sqrt{z+1}\sqrt{z-1} \right). \quad (\text{S4.47})$$

There will be a multiplicative error from the $R(z) \approx \mathbb{1}$ approximation; by the discussion surrounding Eq. (S2.127), this error will be $\mathcal{O}(1/n)$ for $z = \mathcal{O}(1)$. For $\rho = 0$ it will remain of this order even as z shrinks to 0, but for $\rho \neq 0$ the error will grow like $\mathcal{O}(1/(nh_n(0)|z|))$, eventually reaching $\mathcal{O}(\beta_n/nh_n(0))$ at $z \sim 1/\beta_n$.

2. Behavior near the origin

We will focus on the limiting behavior as z approaches the positive real axis from \mathbb{C}_+ ; the other limits can be computed analogously. Starting from Eq. (S4.7), for z in the first quadrant and satisfying $|\beta_n z| \ll 1$, we have

$$\begin{pmatrix} Y_{12}(\beta_n z) \\ Y_{22}(\beta_n z) \end{pmatrix} = (\beta_n z)^{\rho/2} e^{-\frac{i\pi\rho}{2}} e^{-n[g_n(z) - \phi_n(z) - l_n/2]} \beta_n^{(n+\rho/2)\sigma_3} e^{\frac{nl_n}{2}\sigma_3} R(z) E_n(z) \Psi_{\rho/2}(nf_n(z)) \begin{pmatrix} 0 \\ 1 \end{pmatrix}. \quad (\text{S4.48})$$

Using the expression Eq. (S2.96) for $\Psi_{\rho/2}(nf_n(z))$ with z in the first quadrant, and taking the limit $z \downarrow x \in (0, \delta_n)$, this becomes

$$\begin{pmatrix} Y_{12,+}(\beta_n x) \\ Y_{22,+}(\beta_n x) \end{pmatrix} = \frac{\sqrt{\pi}}{2} e^{-\frac{i\pi}{4}} \sqrt{w(\beta_n x)} \beta_n^{(n+\rho/2)\sigma_3} e^{\frac{nl_n}{2}\sigma_3} \sqrt{nf_n(x)} R(x) E_n(x) \begin{pmatrix} H_{\frac{1}{2}(\rho+1)}^{(1)}(nf_n(x)) \\ H_{\frac{1}{2}(\rho-1)}^{(1)}(nf_n(x)) \end{pmatrix}. \quad (\text{S4.49})$$

Using Eq. (S2.110) for $E_n(x)$, approximating $R(x) \approx \mathbf{1}$, and using the asymptotic Eq. (S3.28) for $(Y_1)_{12}$, we get

$$G_{n,+}(\beta_n x) \approx -\frac{2}{\beta_n} \frac{\begin{pmatrix} H_{\frac{1}{2}(\rho+1)}^{(1)}(nf_n(x)) \left[e^{\frac{i\pi}{4}(2n-\rho-1)} \varphi_+^{\rho/2}(a_+ + a_+^{-1}) + e^{-\frac{i\pi}{4}(2n-\rho-1)} \varphi_+^{-\rho/2}(a_+ - a_+^{-1}) \right] \\ + H_{\frac{1}{2}(\rho-1)}^{(1)}(nf_n(x)) \left[e^{\frac{i\pi}{4}(2n-\rho+1)} \varphi_+^{\rho/2}(a_+ + a_+^{-1}) + e^{-\frac{i\pi}{4}(2n-\rho+1)} \varphi_+^{-\rho/2}(a_+ - a_+^{-1}) \right] \end{pmatrix}}{\begin{pmatrix} H_{\frac{1}{2}(\rho+1)}^{(1)}(nf_n(x)) \left[e^{-\frac{i\pi}{4}(2n-\rho-1)} \varphi_+^{-\rho/2}(a_+ + a_+^{-1}) + e^{\frac{i\pi}{4}(2n-\rho-1)} \varphi_+^{\rho/2}(a_+ - a_+^{-1}) \right] \\ + H_{\frac{1}{2}(\rho-1)}^{(1)}(nf_n(x)) \left[e^{-\frac{i\pi}{4}(2n-\rho+1)} \varphi_+^{-\rho/2}(a_+ + a_+^{-1}) + e^{\frac{i\pi}{4}(2n-\rho+1)} \varphi_+^{\rho/2}(a_+ - a_+^{-1}) \right] \end{pmatrix}}, \quad (\text{S4.50})$$

where we have suppressed the arguments of $\varphi_+ \equiv \varphi_+(x)$ and $a_+ \equiv a_+(x)$. Let us now rescale $\beta_n x \mapsto \omega$. As $\omega \rightarrow 0$, both $\varphi_+(\omega/\beta_n)$ and $a_+(\omega/\beta_n)$ tend to $\mathcal{O}(1)$ constants, while in general the Hankel functions will have an algebraic divergence. Thus, to leading order in $\omega/\beta_n \ll 1$, we can approximate $\varphi_+(\omega/\beta_n) \approx \varphi_+(0) = i$ and $a_+(\omega/\beta_n) \approx a_+(0) = e^{i\pi/4}$. With these approximations, we get the simpler expression

$$G_n(\omega + i0^+) \approx -\frac{2}{\beta_n} \frac{\cos\left(\frac{n\pi}{2}\right) H_{\frac{1}{2}(\rho-1)}^{(1)}(\pi I_n(\omega)) + \sin\left(\frac{n\pi}{2}\right) H_{\frac{1}{2}(\rho+1)}^{(1)}(\pi I_n(\omega))}{\cos\left(\frac{n\pi}{2}\right) H_{\frac{1}{2}(\rho+1)}^{(1)}(\pi I_n(\omega)) - \sin\left(\frac{n\pi}{2}\right) H_{\frac{1}{2}(\rho-1)}^{(1)}(\pi I_n(\omega))}, \quad (\text{S4.51})$$

where we have replaced $nf_n(\omega/\beta_n) = \pi I_n(\omega)$. Note that the difference between even and odd n is now manifest: for $-1 < \rho < 1$ we have $G_{2n}(\omega + i0^+) \sim \omega^\rho$ as $\omega \rightarrow 0$ while $G_{2n+1}(\omega + i0^+) \sim 1/\omega^\rho$, consistent with the recursion relation Eq. (79). Taking n even and approximating $I_n(\omega) = \int_0^\omega \sigma_n(\omega') d\omega' \approx \sigma_n(0)\omega$, we recover Eq. (84) of the main text. By the discussion surrounding Eq. (S2.126), this expression has a multiplicative error of $\mathcal{O}(\beta_n/nh_n(0))$.

3. Behavior near $z = \pm\beta_n$

Finally let us derive an expression for the level- n Green's function near the endpoints $z = \pm\beta_n$. We will focus on the behavior near $z = \beta_n$, with similar results holding near $z = -\beta_n$. Starting from Eq. (S4.26), the second column of Y in a neighborhood of β_n is given by

$$\begin{pmatrix} Y_{12}(\beta_n z) \\ Y_{22}(\beta_n z) \end{pmatrix} = (\beta_n z)^{\rho/2} e^{-n[g_n(z) - \phi_n(z) - l_n/2]} \beta_n^{(n+\rho/2)\sigma_3} e^{\frac{nl_n}{2}\sigma_3} R(z) E(z) \Psi(f_n(z)) \begin{pmatrix} 0 \\ 1 \end{pmatrix}, \quad (\text{S4.52})$$

where the Airy parametrix $\Psi(\zeta)$ was defined in Eq. (S2.61), and the map $f_n(z)$ was defined in Eq. (S2.68). Focusing on z in quadrant I of Fig. S3, this becomes

$$\begin{pmatrix} Y_{12}(\beta_n z) \\ Y_{22}(\beta_n z) \end{pmatrix} = \sqrt{2\pi} e^{\frac{i\pi}{12}} (\beta_n z)^{\rho/2} e^{-n[g_n(z) - \phi_n(z) - l_n/2]} \beta_n^{(n+\rho/2)\sigma_3} e^{\frac{nl_n}{2}\sigma_3} R(z) E(z) \begin{pmatrix} \text{Ai}(\xi_n(z)) \\ e^{\frac{4\pi i}{3}} \text{Ai}'(\xi_n(z)) \end{pmatrix}, \quad (\text{S4.53})$$

where $\xi_n(z) \equiv e^{4\pi i/3} f_n(z)$. Using the expression Eq. (S2.72) for $E(z)$, approximating $R(z) \approx \mathbf{1}$, and using the asymptotic formula Eq. (S3.28), substituting into Eq. (S4.44) gives

$$G_n(\beta_n z) \approx -\frac{2}{\beta_n} \frac{\begin{pmatrix} [a(z)(\varphi^{\rho/2} - \varphi^{-\rho/2})(z) + a(z)^{-1}(\varphi^{\rho/2} + \varphi^{-\rho/2})(z)] \xi_n(z)^{1/4} \text{Ai}(\xi_n(z)) \\ - [a(z)(\varphi^{\rho/2} + \varphi^{-\rho/2})(z) + a(z)^{-1}(\varphi^{\rho/2} - \varphi^{-\rho/2})(z)] \xi_n(z)^{-1/4} \text{Ai}'(\xi_n(z)) \end{pmatrix}}{\begin{pmatrix} [a(z)(\varphi^{\rho/2} - \varphi^{-\rho/2})(z) - a(z)^{-1}(\varphi^{\rho/2} + \varphi^{-\rho/2})(z)] \xi_n(z)^{1/4} \text{Ai}(\xi_n(z)) \\ - [a(z)(\varphi^{\rho/2} + \varphi^{-\rho/2})(z) - a(z)^{-1}(\varphi^{\rho/2} - \varphi^{-\rho/2})(z)] \xi_n(z)^{-1/4} \text{Ai}'(\xi_n(z)) \end{pmatrix}}, \quad (\text{S4.54})$$

where $a(z) = (z-1)^{1/4}/(z+1)^{1/4}$ and $\varphi(z) = z + (z-1)^{1/2}(z+1)^{1/2}$. Near $z = 1$, we have $f_n(z) \approx f'_n(1)(z-1)$, where $f'_n(1) = (nh_n(1)/\sqrt{2})^{2/3} \sim \mathcal{O}(n^{2/3})$. Then for $z = 1 + \mathcal{O}(n^{-2/3})$, we have $G_n(\beta_n z) \approx G_n(\beta_n) + \mathcal{O}(z-1)$, with

$$G_n(\beta_n) \approx \frac{2}{\beta_n} \left(\frac{2f'_n(1)^{1/2}\Gamma\left[\frac{1}{3}\right] - \sqrt{2}(-3)^{1/3}(\rho+1)\Gamma\left[\frac{2}{3}\right]}{2f'_n(1)^{1/2}\Gamma\left[\frac{1}{3}\right] - \sqrt{2}(-3)^{1/3}(\rho-1)\Gamma\left[\frac{2}{3}\right]} \right). \quad (\text{S4.55})$$

Since $f'_n(1) \sim \mathcal{O}(n^{2/3}) \rightarrow \infty$ as $n \rightarrow \infty$, we conclude that $G_n(\beta_n) \approx 2/\beta_n$ to leading order as $n \rightarrow \infty$. By the discussion surrounding Eq. (S2.127), this expression has a multiplicative error of $\mathcal{O}(1/n)$.

S5. AIRY BOOTSTRAP

Since it will be useful for Section VIII, we include here a version of the spectral bootstrap suited for recovering the spectral function near the ‘edge’ $\omega \approx \beta_n$. A modification is necessary because the polynomial asymptotics in this region are qualitatively different from those in the bulk of the spectrum: they are governed by the ‘Airy’ universality class rather than the ‘sine’ universality class. These Airy asymptotics hold in the ‘regular’ case where the density $\sigma_n(\omega)$ vanishes like a square root as $\omega \rightarrow \beta_n$ from below. For our class of spectral functions, we prove this is the case for large enough n (see Section S2D).

The Airy asymptotics are most easily stated in terms of a function $f_n(x)$ which is related to I_n by

$$f_n(x) = - \left(\frac{3\pi}{2} \left[\frac{n}{2} - I_n(\beta_n x) \right] \right)^{2/3}. \quad (\text{S5.1})$$

Since $I_n(\beta_n) = \int_0^{\beta_n} \sigma_n(\omega) d\omega = n/2$, we have $f_n(1) = 0$. Moreover, given the square root vanishing of the derivative $\partial_\omega I_n(\omega) = \sigma_n(\omega)$, using Eqs. (46) and (50) we have

$$f'_n(1) = \left(\frac{nh_n(1)}{\sqrt{2}} \right)^{2/3}. \quad (\text{S5.2})$$

The asymptotics of $h_n(1)$ are given in Lemma 1, where it is shown that $h_n(1)$ is $\mathcal{O}(1)$ as $n \rightarrow \infty$, so $f'_n(1) \sim \mathcal{O}(n^{2/3})$.

For the Airy bootstrap, we start at the endpoint $\omega = \beta_n$, and then work backwards to lower frequencies. The derivation of the following equations is given in Section S4B3.

First we approximate $h_n(1)$ using

$$h_n(1) \approx \frac{1}{2n} \left(\frac{\text{Ai}(0)}{\text{Ai}'(0)} \right)^3 \left[\rho - \left(\frac{p_n(\beta_n) + p_{n-1}(\beta_n)}{p_n(\beta_n) - p_{n-1}(\beta_n)} \right) \right]^3, \quad (\text{S5.3})$$

where Ai is the Airy function. Then we can estimate the spectral function at $\omega = \beta_n$ using Eq. (S5.2) and

$$\frac{\Phi(\beta_n)}{2\pi} \approx \frac{1}{\beta_n p_n(\beta_n)^2} \left[(2f'_n(1))^{1/4} \text{Ai}(0) - (1 + \rho)(2f'_n(1))^{-1/4} \text{Ai}'(0) \right]. \quad (\text{S5.4})$$

We can now proceed with the main bootstrap equations: with $x \equiv \omega/\beta_n$, the update of the spectral function is given by

$$\begin{aligned} \frac{\Phi(\omega)}{2\pi} \approx & \frac{2}{\beta_n} \frac{1}{p_n(\omega)^2 + p_{n-1}(\omega)^2} \frac{1}{\sqrt{1-x^2}} \left[-2x \text{Ai}(f_n(x)) \text{Ai}'(f_n(x)) \sin[\rho \arccos x] \right. \\ & \left. + (-f_n(x))^{1/2} \text{Ai}(f_n(x))^2 (x \cos[\rho \arccos x] + 1) - (-f_n(x))^{-1/2} \text{Ai}'(f_n(x))^2 (x \cos[\rho \arccos x] - 1) \right], \end{aligned} \quad (\text{S5.5})$$

while the update of the phase function $f_n(x)$ is given by

$$\begin{aligned} f'_n(x) \approx & \frac{1}{2 \text{Ai}^2 f_n^2 - 2(\text{Ai}')^2 f_n - \text{Ai} \text{Ai}'} \left[-2\beta_n \frac{\Phi(\omega)}{2\pi} K_n(\omega, \omega) f_n + \frac{2}{1-x^2} \text{Ai} \text{Ai}' \cos[\rho \arccos x] f_n \right. \\ & \left. - \frac{\sin[\rho \arccos x]}{1-x^2} \left(\text{Ai}^2 (-f_n)^{3/2} - (\text{Ai}')^2 (-f_n)^{1/2} \right) - \frac{\rho}{\sqrt{1-x^2}} \left(\text{Ai}^2 (-f_n)^{3/2} + (\text{Ai}')^2 (-f_n)^{1/2} \right) \right], \end{aligned} \quad (\text{S5.6})$$

where we have suppressed the arguments of $f_n \equiv f_n(x)$, $\text{Ai} \equiv \text{Ai}(f_n(x))$, and $\text{Ai}' \equiv \text{Ai}'(f_n(x))$.

Given a choice of frequency spacing $0 < \delta\omega \ll 1$ and a minimum frequency ω_{\min} , the main routine then works as follows.

0. Set $\omega = \beta_n$ and $f_n(1) = 0$. Compute $f'_n(1)$ using Eqs. (S5.2) and (S5.3), and $\Phi(\beta_n)$ using Eq. (S5.4).
1. Increment $\omega \mapsto \omega - \delta\omega$.
2. Set $f_n\left(\frac{\omega}{\beta_n}\right) = f_n\left(\frac{\omega + \delta\omega}{\beta_n}\right) - f'_n\left(\frac{\omega + \delta\omega}{\beta_n}\right) \times \frac{\delta\omega}{\beta_n}$.
3. Compute $\Phi(\omega)$ using Eq. (S5.5).
4. Compute $f'_n(\omega/\beta_n)$ using Eq. (S5.6).

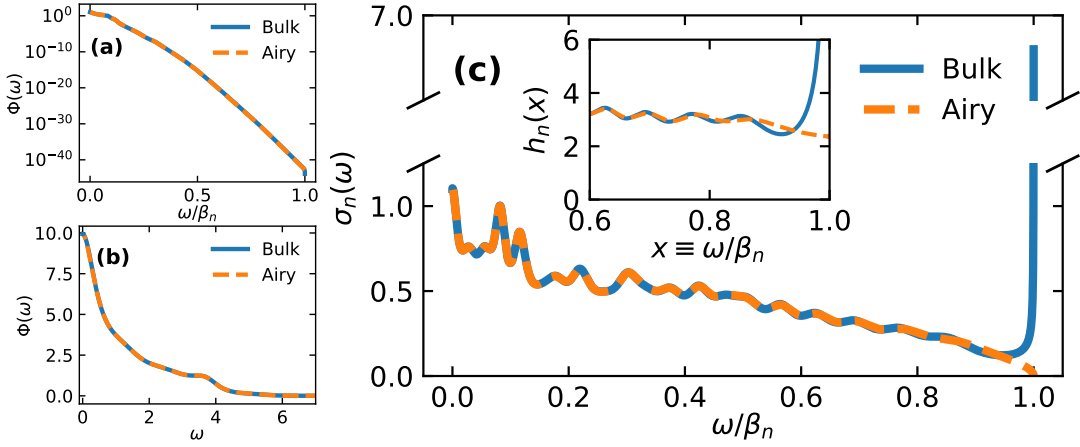


FIG. S6. **(a,b)** Log- and linear-scale spectral function $\Phi(\omega)$ of the energy current operator of the mixed field Ising model, as computed using the ‘bulk’ spectral bootstrap of Section VII A and the ‘Airy’ spectral bootstrap of Section S5. While they are intended to work in different frequency regimes, the estimates of $\Phi(\omega)$ agree remarkably well throughout the bulk. **(c)** Comparison between the extracted equilibrium measure $\sigma_n(\omega)$ for the same model. They agree throughout the bulk, but the bulk bootstrap breaks down near $\omega = \beta_n$, whereas the Airy bootstrap produces the expected square root vanishing of $\sigma_n(\omega)$ as $\omega \rightarrow \beta_n$. Indeed, the inset shows $h_n(x \equiv \omega/\beta_n) = 2\pi \frac{\beta_n}{n} \frac{\sigma_n(\omega)}{\sqrt{1 - (\omega/\beta_n)^2}}$; for the Airy bootstrap this is finite and as $x \rightarrow 1$ approaches the value $h_n(1) \approx 2$ expected from Lemma 1 with $p = 1$. Here we set $n = 40$, with $\beta_n \approx 2b_n \approx 46.1$.

5. Repeat steps 1–4 until $\omega = \omega_{\min}$, then terminate.

Note that in step 2 we divide the derivative by β_n because $f_n(x)$ is defined in terms of $x \equiv \omega/\beta_n$.

In Fig. S6 we show a benchmark of this ‘Airy bootstrap’ on the energy current operator of the mixed field Ising model (MFIM), as we did in Section VII A, and compare to the results from the ‘bulk bootstrap’ described in that section. These two methods are designed to work in different frequency regimes: the bulk bootstrap starts at $\omega = 0$ and iterates up to some $\omega_{\max} \ll \beta_n$, while the Airy bootstrap starts at $\omega = \beta_n$ and iterates down to some ω_{\min} . They should agree in frequency regimes where both methods are approximately valid, but *a priori* they could disagree elsewhere. In fact, in Fig. S6(a,b), we find that the extracted spectral functions $\Phi(\omega)$ agree remarkably well throughout almost the whole frequency range $\omega \in [0, \beta_n]$, with only some small deviation at $\omega \approx \beta_n$. This good agreement lends credence to our investigation of the high-frequency tail of $\Phi(\omega)$ in Section VII A, where we found $\Phi(\omega \rightarrow \infty) \sim \exp[-\mathcal{O}(\omega \log \omega)]$, consistent with locality bounds on operator growth in 1D [10]. It is also perhaps surprising that the Airy bootstrap can produce accurate estimates of the spectral function at moderate frequencies, since one might initially have worried about the numerical stability of a procedure which begins with the spectral function as small as $\Phi(\omega = \beta_n) \sim 10^{-43}$.

More significant deviation between the bulk and Airy bootstraps can be found by looking at their estimates for the equilibrium measure $\sigma_n(\omega)$, as shown in Fig. S6(c). This is computed directly as part of the bulk bootstrap, while for the Airy bootstrap we can recover it from $f_n(\omega/\beta_n)$ using Eq. (S5.1) and $\sigma_n(\omega) = \partial_\omega I_n(\omega)$. We find that the two methods give closely matching estimates of $\sigma_n(\omega)$ for $0 \leq \omega/\beta_n \lesssim 0.9$, but as ω approaches the spectral edge at $\omega = \beta_n$, the bulk bootstrap estimate blows up, while the Airy bootstrap produces the square root vanishing expected for ‘regular’ equilibrium measures (we remind the reader that we prove that this regularity property holds at large- n for our class of spectral function—see Section S2 D). To corroborate this, in the inset to Fig. S6(c) we plot the function (c.f. Eqs. (46) and (50))

$$h_n(x \equiv \omega/\beta_n) = 2\pi \frac{\beta_n}{n} \frac{\sigma_n(\omega)}{\sqrt{1 - (\omega/\beta_n)^2}}, \quad (\text{S5.7})$$

which should be finite at $x = 1$ if $\sigma_n(\omega)$ vanishes like a square root at $\omega = \beta_n$. For the Airy bootstrap estimate of $h_n(x)$, this is indeed the case, and we can also see that the limiting value of $h_n(x)$ as $x \rightarrow 1$ is close to 2, which is expected from Lemma 1 with $p = 1$, given the $\Phi(\omega \rightarrow \infty) \sim \exp[-\mathcal{O}(\omega \log \omega)]$ high frequency decay of the spectral function. On the other hand, the bulk bootstrap estimate does not successfully capture this behavior. Although the results of Fig. S6(a,b) show that this disagreement in estimating $\sigma_n(\omega)$ is not fatal for approximating the spectral function, it will be more relevant that we have an accurate estimate of $\sigma_n(\omega)$ in Section VIII, where we check for the emergence of universality.

S6. DETAILED ANALYSIS OF THE EQUILIBRIUM MEASURE

A. Behavior of the equilibrium measure near the origin

1. Behavior at the origin

Lemma S8. Consider $W = \exp(-Q(x))$ with $Q \in \text{VSLF}(p, q)$ for $p \geq 1$. If $p > 1$, then for all $q \in \mathbb{R}$ we have

$$\lim_{n \rightarrow \infty} h_n(0) = \frac{2p}{p-1}. \quad (\text{S6.1})$$

If $p = 1$ and $q > -1$, then as $n \rightarrow \infty$ we have

$$h_n(0) = (\log n)^{1+o(1)}. \quad (\text{S6.2})$$

Proof. (**Case: $p > 1$**) From Eq. (S2.13) we have

$$h_n(0) = \frac{2}{\pi} \int_0^1 \frac{V'_n(s)}{s} \frac{ds}{\sqrt{1-s^2}}. \quad (\text{S6.3})$$

From Lemma S1(v) we know that $\lim_{n \rightarrow \infty} V'_n(s) = (p/\lambda_p)s^{p-1}$, uniformly for s in any compact subinterval of $(0, \infty)$, where the constant λ_p is defined in Eq. (S1.14). This implies pointwise convergence of the integrand for $s \in (0, 1)$. In order to apply the dominated convergence theorem we appeal to Corollary S1 choosing ϵ so that $p-1-\epsilon > 0$. However, this upper bound is only available for $s \in [A/\beta_n, 1]$. Observe that the remaining part of the integral can be bounded by

$$\int_0^{A/\beta_n} \frac{|V'_n(s)|}{s} \frac{ds}{\sqrt{1-s^2}} \leq \frac{1}{\sqrt{1-(A/\beta_n)^2}} \frac{\beta_n}{n} \int_0^A \frac{|Q'(u)|}{u} du \leq \mathcal{O}\left(\frac{\beta_n}{n}\right), \quad (\text{S6.4})$$

because $Q'(0) = 0$ due to the assumed evenness of Q . As $\lim_{n \rightarrow \infty} \beta_n/n = 0$ for $p > 1$ by Eq. (S1.16) we have shown

$$\lim_{n \rightarrow \infty} h_n(0) = \frac{2}{\pi} \frac{p}{\lambda_p} \int_0^1 \frac{s^{p-2}}{\sqrt{1-s^2}} ds, \quad (\text{S6.5})$$

$$= \frac{2p}{p-1}, \quad (\text{S6.6})$$

where the last step follows from evaluating the integral and using the definition of λ_p .

(**Case: $p = 1$**)

The proof for $p > 1$ does not work for $p = 1$ because the limiting integrand is no longer integrable, having a logarithmic divergence at the origin. We will therefore need to be more careful about handling this divergence. From Eq. (S2.13), we have the integral expression for $h_n(0)$,

$$h_n(0) = \frac{2}{\pi} \frac{\beta_n}{n} \int_0^{\beta_n} \frac{Q'(u)}{u \sqrt{1-(u/\beta_n)^2}} du. \quad (\text{S6.7})$$

where we have changed variables for convenience. We split the integral into three parts, I_1 , I_2 , and I_3 ,

$$I_1 + I_2 + I_3 \equiv \left(\int_0^{A_n} + \int_{A_n}^{\beta_n/2} + \int_{\beta_n/2}^{\beta_n} \right) \frac{Q'(u)}{u \sqrt{1-(u/\beta_n)^2}} du, \quad (\text{S6.8})$$

where we define A_n as

$$A_n := (\log n)^\alpha, \quad \text{for some } \alpha > 0. \quad (\text{S6.9})$$

We show that the integrals I_3 and I_1 are dominated by I_2 . Estimating

$$1 \leq [1 - (u/\beta_n)^2]^{-1/2} \leq 2/\sqrt{3}, \quad \text{for all } A_n \leq u \leq \beta_n/2, \quad (\text{S6.10})$$

and using Lemma S1(iii) we obtain for I_2 lower and upper bounds

$$\Omega \left((\log \beta_n)^{q+1-\epsilon/2} \right) \leq I_2 \leq \mathcal{O} \left((\log \beta_n)^{q+1+\epsilon/2} \right), \quad (\text{S6.11})$$

where we have chosen ϵ so small that $q + 1 - \epsilon/2 > 0$. The dominance of I_2 now follows from

$$|I_3| \leq 2(\log \beta_n)^{q+\epsilon/2} \int_{\beta_n/2}^{\beta_n} \frac{1}{\beta_n \sqrt{1 - (u/\beta_n)^2}} du = \mathcal{O} \left((\log \beta_n)^{q+\epsilon/2} \right), \quad (\text{S6.12})$$

$$|I_1| = \mathcal{O} \left((\log A_n)^{q+1+\epsilon/2} \right), \quad (\text{S6.13})$$

where the latter estimate uses again Lemma S1(iii) and that $Q'(u)/u$ is bounded on any compact subset of \mathbb{R} due to $Q'(0) = 0$. Note further that $\beta_n/n = \Theta(1/Q'(\beta_n))$; see Lemma S1(iv). Then it follows from Eqs. (S6.7) and (S6.11) and Lemma S1(iii) that

$$\Omega \left((\log \beta_n)^{1-\epsilon} \right) \leq h_n(0) \leq \mathcal{O} \left((\log \beta_n)^{1+\epsilon} \right), \quad (\text{S6.14})$$

and the claim follows from Lemma S1(vi) as ϵ can be chosen arbitrarily small. \square

2. Uniform lower bounds near the origin

In this section we derive uniform lower bounds on the real part of $h_n(z)$ for z near the origin. The general strategy will be to reduce to the analysis we performed for $z = 0$.

Lemma S9. *Consider $Q \in \text{CVSLF}(p, q, \theta, \gamma)$. Let $0 < \gamma' < \gamma$, $0 < \theta' < \theta$, and $\alpha' \geq 0$ arbitrary for $p > 1$ but constrained to $\alpha' < 1 + q$ for $p = 1$. Define the set Λ_n by*

$$\Lambda_n := \{ \lambda \in \mathcal{C}_{\theta'} : |\lambda| < (\log n)^{\alpha'} \} \cup \{ \lambda : |\lambda| < \gamma' \}, \quad (\text{S6.15})$$

Then, as $n \rightarrow \infty$, we have uniformly for $z \in \Lambda_n/\beta_n$ that

$$h_n(z) = h_n(0) [1 + o(1)]. \quad (\text{S6.16})$$

Together with the scaling of $h_n(0)$ derived in Lemma S8, we conclude that, for sufficiently large n , one can obtain a uniform lower bound, say $h_n(0)/2$, for the real part of $h_n(z)$ if $z \in \Lambda_n/\beta_n$.

Proof. Choose $\alpha > \alpha'$ arbitrary for $p > 1$ but still constrained to $\alpha < 1 + q$ for $p = 1$. Set $A_n := (\log n)^\alpha$ and denote $r(z) = (z + 1)^{1/2}(z - 1)^{1/2}$. By the discussion in Section S2D, we may represent $h_n(z)$ as

$$h_n(z) = -2 \left[\frac{1}{2\pi i} \left(\int_{-1}^{-A_n/\beta_n} + \int_{A_n/\beta_n}^1 \right) \frac{V'_n(s)}{r_+(s)(s-z)} ds + \frac{1/2}{2\pi i} \oint_{\Gamma_n/\beta_n} \frac{V'_n(s)}{r(s)(s-z)} ds \right], \quad (\text{S6.17})$$

where $r_+(s) = i\sqrt{1-s^2}$, and Γ_n are simply closed clockwise oriented curves as sketched in Fig. S7. Important features of the contours are the following. i) Γ_n is contained in $\mathcal{C}_\theta \cup \{z : |z| < \gamma\}$ and has a positive n -independent lower bound on its distance from the set Λ_n (see (S6.15)) that is contained in the interior of Γ_n . ii) Moreover, the rightmost and leftmost points of Γ_n are A_n and $-A_n$ respectively. iii) The length of Γ_n is bounded by $\mathcal{O}(A_n)$.

First we employ the symmetries of Q and r and change variables in the integrals to $u = \beta_n s$. Denoting $\lambda \equiv \beta_n z$ we obtain

$$h_n(z) = \frac{2}{\pi} \frac{\beta_n}{n} \left[\int_{A_n}^{\beta_n} \frac{uQ'(u)}{(u^2 - \lambda^2)\sqrt{1 - (u/\beta_n)^2}} du + \frac{i}{4} \oint_{\Gamma_n} \frac{Q'(u)}{r(u/\beta_n)(u - \lambda)} du \right]. \quad (\text{S6.18})$$

In order to reduce to the $\lambda = 0$ case, we want to examine the effect of replacing $1/(u^2 - \lambda^2) \rightarrow 1/u^2$. To that end, we consider the difference

$$\frac{1}{u^2 - \lambda^2} - \frac{1}{u^2} = \frac{\lambda^2}{u^2(u^2 - \lambda^2)}, \quad (\text{S6.19})$$

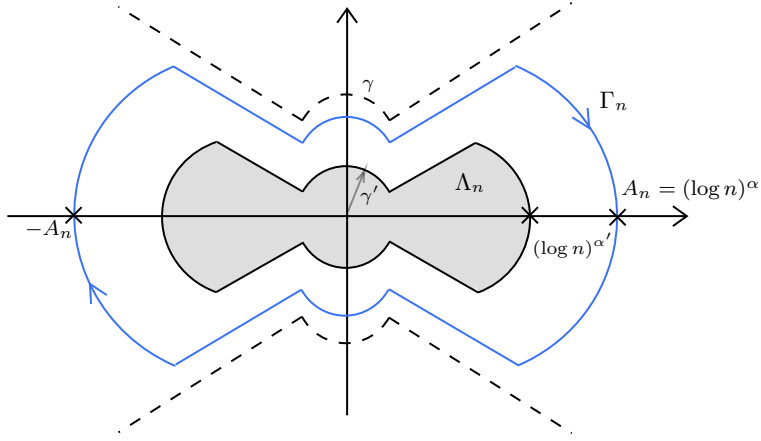


FIG. S7. Sketch of the contour Γ_n , and the sets Λ_n and $C_{\theta'} \cup \{z : |z| < \gamma\}$.

so that

$$\frac{\pi}{2} \frac{n}{\beta_n} h_n(z) = \int_{A_n}^{\beta_n} \frac{Q'(u)}{u \sqrt{1 - (u/\beta_n)^2}} \left(1 + \frac{\lambda^2}{u^2 - \lambda^2}\right) du + \frac{i}{4} \oint_{\Gamma_n} \frac{Q'(u)}{r(u/\beta_n)(u - \lambda)} du \equiv J_1 + J_2. \quad (\text{S6.20})$$

Recall from Eqs. (S6.7) and (S6.8) that

$$\frac{\pi}{2} \frac{n}{\beta_n} h_n(0) = I_1 + I_2 + I_3, \quad (\text{S6.21})$$

a representation that also holds in the case $p > 1$. We therefore need to establish $(J_1 + J_2)/(I_1 + I_2 + I_3) = 1 + o(1)$: We prove this by verifying that the following limits for $n \rightarrow \infty$ hold uniformly in z :

$$\frac{I_1}{I_1 + I_2 + I_3} \rightarrow 0, \quad \frac{J_1}{I_2 + I_3} \rightarrow 1, \quad \frac{J_2}{I_2 + I_3} \rightarrow 0. \quad (\text{S6.22})$$

The second claim follows from the observation that for $(\log n)^\alpha = A_n \leq u \leq \beta_n$ and $|\lambda| \leq (\log n)^{\alpha'}$ one has

$$\frac{\lambda^2}{u^2 - \lambda^2} \leq \mathcal{O}\left((\log n)^{-2(\alpha - \alpha')}\right). \quad (\text{S6.23})$$

The first claim has already been established in the case $p = 1$, see Eqs. (S6.11) to (S6.13). In the case $p > 1$, it follows from Lemma S1(iii) and from the boundedness of $Q'(u)/u$ on bounded sets that $I_1 = \mathcal{O}((\log n)^{\delta_1})$, whereas by Lemma S1(vi) and Lemma S8 we have $I_1 + I_2 + I_3 = \Omega(n/\beta_n) = \Omega(n^{\delta_2})$, for some positive numbers δ_1, δ_2 . Consequently $I_1/(I_1 + I_2 + I_3) \rightarrow 0$ as $n \rightarrow \infty$.

Finally, we turn to the third claim. Observe that by the choice of the path of integration Γ_n the denominator of the integrand of the term J_2 is uniformly bounded away from 0. Using Eq. (S1.24) we obtain the sup-norm bound $\mathcal{O}(A_n^{p-1}(\log A_n)^{q+\epsilon/2})$ on the integrand yielding $J_2 = \mathcal{O}(A_n^p(\log A_n)^{q+\epsilon/2})$. For $p > 1$ we have $I_2 + I_3 = \Omega(n/\beta_n)$ which establishes $J_2/(I_2 + I_3) \rightarrow 0$. In the case $p = 1$ we learn from Eqs. (S6.11) and (S6.12) that $I_2 + I_3 = \Omega((\log \beta_n)^{q+1-\epsilon/2})$ and the third claim follows from $\alpha - (q + 1) < 0$ by choosing ϵ small enough. This completes the proof. \square

Remark 2. By using a similar contour to that depicted in Fig. S7, one can combine the definition Eq. (S2.9) and Lemmas S1 and S2, in order to establish the following upper bounds on $|h_n(z)|$:

$$|h_n(z)| \leq \begin{cases} \mathcal{O}(\log n), & p > 1; \\ \mathcal{O}((\log n)^{1+\epsilon}), & p = 1, \end{cases} \quad (\text{S6.24})$$

where $\epsilon > 0$ can be made arbitrarily small. These bounds are uniformly valid for $z = x + iy$ with $|x| < 1 - \delta$ for arbitrary but fixed $\delta > 0$, and z in a suitable $\Theta(|x|)$ -sized neighborhood of x .

B. Uniform lower bounds for the equilibrium measure on the real line

Let us now prove Lemma S6 from Section S2D, which we restate here.

Lemma S6. *Suppose $Q \in \text{VSLF}(p, q)$ with $p \geq 1$, and q arbitrary for $p > 1$ but constrained to $q > -1$ for $p = 1$. Then there exists $n_0 \in \mathbb{N}$ such that, for every $M > 0$, there exists a constant $C > 0$ such that for all $n \geq n_0$ we have $h_n(x) > C$ for all $|x| < M$.*

Proof. Since $h_n(x)$ is even, it suffices to consider $x \geq 0$. The complexity of the proof depends on the magnitude of x , and whether it depends on n . Let $M > 0$ be given. It is our goal to construct a corresponding constant $C > 0$ uniformly for sufficiently large values of n as stated in the lemma.

Case 1 (near origin): $x \in [0, (\log n)^\alpha / \beta_n]$, with $\alpha > 0$ for $p > 1$ and $\alpha < 1 + q$ for $p = 1$

In this near-zero regime, we can apply Lemma S9 to conclude that $h_n(x) = h_n(0)[1 + o(1)]$ uniformly in x , where the $o(1)$ refers to scaling with n . Then the asymptotics of $h_n(0)$ from Lemma S8 suffice to give a uniform positive lower bound on $h_n(x)$ in this region. Thus, any choice, say $0 < C \leq 1$ would work for this region.

Case 2 (bulk): $x \in [(\log n)^\alpha / \beta_n, M]$, with α as in case 1

By Lemma S1(i), there exists $A > 0$ such that $uQ'(u)$ is increasing for $u > A$. This implies $sV'_n(s)$ is increasing for $s > A/\beta_n$, and therefore in this region of increase $xV'_n(x) - sV'_n(s)$ has the same sign as $x - s$. If we split the integral Eq. (S2.13) for $h_n(x)$ into two regions,

$$\begin{aligned} h_n(x) &= \frac{2}{\pi} \left(\int_0^{A/\beta_n} + \int_{A/\beta_n}^1 \right) \frac{xV'_n(x) - sV'_n(s)}{x^2 - s^2} \frac{ds}{\sqrt{1 - s^2}}, \\ &\equiv I_1 + I_2, \end{aligned} \quad (\text{S6.25})$$

the second integral I_2 is an integral of a manifestly positive integrand, so is positive. Let us first show that I_2 can be lower bounded by a positive constant. Since I_2 has a positive integrand, we can lower bound it by truncating the region of integration. In addition, we learn from Lemma S1(v) that for all $\epsilon > 0$ there exists $n_0 \in \mathbb{N}$ such that for all $n \geq n_0$ and $s \in [1/4, 1]$ we have

$$\left| sV'_n(s) - \frac{p}{\lambda_p} s^p \right| \leq \frac{\epsilon}{2}. \quad (\text{S6.26})$$

Using in addition the above mentioned monotonicity of $sV'_n(s)$ we obtain for $(\log n)^\alpha / \beta_n \leq x \leq 1/2$ that

$$\frac{\pi}{2} I_2 \geq \int_{3/4}^1 \frac{sV'_n(s) - xV'_n(x)}{s^2 - x^2} \frac{ds}{\sqrt{1 - s^2}} \geq \int_{3/4}^1 \left[\frac{3}{4} V'_n(3/4) - \frac{1}{2} V'_n(1/2) \right] ds \geq \frac{1}{4} \left[\frac{p}{\lambda_p} \left(\left(\frac{3}{4} \right)^p - \left(\frac{1}{2} \right)^p \right) - \epsilon \right], \quad (\text{S6.27})$$

and for $x \in [1/2, M]$ that

$$\frac{\pi}{2} I_2 \geq \int_{1/8}^{1/4} \frac{xV'_n(x) - sV'_n(s)}{x^2 - s^2} \frac{ds}{\sqrt{1 - s^2}} \geq \frac{1}{x^2} \int_{1/8}^{1/4} \left[\frac{1}{2} V'_n(1/2) - \frac{1}{4} V'_n(1/4) \right] ds \geq \frac{1}{8x^2} \left[\frac{p}{\lambda_p} \left(\left(\frac{1}{2} \right)^p - \left(\frac{1}{4} \right)^p \right) - \epsilon \right]. \quad (\text{S6.28})$$

From these estimates it follows that for any $p \geq 1$ one can choose $\epsilon > 0$ and an M -dependent constant $C > 0$ such that for all $n \geq n_0$ we have $I_2 \geq 2C$. In order to complete the proof we need to show that

$$|I_1| \leq \frac{I_2}{2}, \quad (\text{S6.29})$$

for all sufficiently large values of n . Let us start upper-bounding the modulus of I_1 by observing

$$\begin{aligned} I_1 &\equiv \frac{2}{\pi} \int_0^{A/\beta_n} \frac{xV'_n(x) - sV'_n(s)}{x^2 - s^2} \frac{ds}{\sqrt{1 - s^2}}, \\ &= \frac{2}{\pi} \frac{\beta_n}{n} \int_0^A \frac{vQ'(v) - uQ'(u)}{v^2 - u^2} \frac{du}{\sqrt{1 - (u/\beta_n)^2}}, \end{aligned} \quad (\text{S6.30})$$

where $v \equiv \beta_n x \in [(\log n)^\alpha, \beta_n M]$, and we rescaled the integration variable for convenience. With $f_Q(y) := \frac{d}{dy}[yQ'(y)] = Q'(y) + yQ''(y)$, we have

$$\frac{vQ'(v) - uQ'(u)}{v^2 - u^2} = \frac{1}{v+u} \int_0^1 f_Q[v - t(v-u)] dt. \quad (\text{S6.31})$$

The argument of f_Q is always between u and v , and since $u \in [0, A]$ while $v \rightarrow \infty$, this argument is always in $[0, v]$. For bounded arguments, we know $f_Q(u)$ is bounded due to our analyticity assumption on Q . For growing arguments, note that the condition Eq. (S1.2) on Q implies that

$$f_Q(y) = Q'(y) \left[1 + \frac{yQ''(y)}{Q'(y)} \right], \quad (\text{S6.32})$$

$$\leq Q'(y) \times 2p \quad \text{for large enough } y, \quad (\text{S6.33})$$

with $Q'(y) > 0$ also for large enough y , given condition Eq. (S1.1). Again for sufficiently large y , from Eq. (S1.12) we have the bound $Q'(y) \leq y^{p-1}(\log y)^{q+\epsilon}$ for $\epsilon > 0$. For $p > 1$ this bound increases with y , while for $p = 1$ it can increase or decrease depending on the sign of q . Taken together, these considerations of both bounded and growing arguments imply a bound, valid for $t \in [0, 1]$ and $u \in [0, A]$, of the form

$$\left| f_Q[v - t(v-u)] \right| \leq c v^{p-1} (\log v)^{\eta_q} \quad (\text{S6.34})$$

for some constant $c > 0$, where we have defined

$$\eta_q := \begin{cases} q + \epsilon, & q \geq 0; \\ 0, & q < 0, \end{cases} \quad (\text{S6.35})$$

where $\epsilon > 0$ can be made small by taking n large. Then we have the bound

$$|I_1| \leq \frac{2}{\pi} \frac{\beta_n}{n} c v^{p-1} (\log v)^{\eta_q} \times \int_0^A \frac{1}{v+u} \frac{du}{\sqrt{1 - (u/\beta_n)^2}}. \quad (\text{S6.36})$$

The integral can be upper bounded simply as

$$\int_0^A \frac{1}{v+u} \frac{du}{\sqrt{1 - (u/\beta_n)^2}} \leq \frac{1}{\sqrt{1 - (A/\beta_n)^2}} \int_0^A \frac{1}{v+u} du = \frac{1}{\sqrt{1 - (A/\beta_n)^2}} \log \left(1 + \frac{A}{v} \right) = \mathcal{O} \left(\frac{1}{v} \right), \quad (\text{S6.37})$$

since $A/v \rightarrow 0$ and $A/\beta_n \rightarrow 0$ as $n \rightarrow \infty$. Thus we conclude that

$$|I_1| \leq \mathcal{O} \left(\frac{\beta_n}{n} v^{p-2} (\log v)^{\eta_q} \right). \quad (\text{S6.38})$$

We now analyze this on a case by case basis.

Case \mathcal{A} : $p > 1$

Using $v = \mathcal{O}(\beta_n)$ and the asymptotics for β_n in Eq. (S1.16), for $p \geq 2$ we have $v^{p-2} = \mathcal{O}(\beta_n^{p-2})$, and so

$$|I_1| \leq \tilde{\mathcal{O}} \left(\frac{\beta_n^{p-1}}{n} \right) = \tilde{\mathcal{O}} \left(n^{-1/p} \right), \quad (\text{S6.39})$$

where the $\tilde{\mathcal{O}}$ notation hides polylogarithmic factors which are unimportant for $p > 1$. Equally, for $1 < p < 2$, v^{p-2} is $o(1)$, and hence in this case

$$|I_1| \leq \tilde{\mathcal{O}}(\beta_n/n) = \tilde{\mathcal{O}}(n^{-(p-1)/p}). \quad (\text{S6.40})$$

Overall we conclude for all $p > 1$ that $|I_1|$ vanishes as $n \rightarrow \infty$ and condition (S6.29) is satisfied for n large enough.

Case \mathcal{B} : $p = 1$

In this marginal case, we need to refine our lower bound on I_2 . First we rewrite the integrand of I_2 in terms of f_Q as in Eq. (S6.31), but this time we use the bound

$$f_Q(y) = Q'(y) \left[1 + \frac{yQ''(y)}{Q'(y)} \right], \quad (\text{S6.41})$$

$$\geq Q'(y) \times (p/2) \quad \text{for large enough } y, \quad (\text{S6.42})$$

which again follows from the condition Eq. (S1.2) on Q . Let $A' \geq A$ be so large that we can apply Eq. (S6.42) and the lower bound in Eq. (S1.12) on Q' throughout the slightly reduced domain of integration $[A', \beta_n]$. Then, as $p = 1$, we have the lower bound

$$I_2 \geq \frac{1}{\pi} \frac{\beta_n}{n} \int_{A'}^{\beta_n} \int_0^1 \frac{(\log[v - t(v - u)])^{q-\epsilon}}{v + u} dt du. \quad (\text{S6.43})$$

We can take A' large enough that the integrand is positive, such that we can lower bound I_2 by restricting the t integral domain. The argument $v - t(v - u)$ of the logarithm linearly interpolates between u and v , and if $q - \epsilon$ is positive (negative), we restrict to the half of the t -integral where $v - t(v - u)$ is lower (upper) bounded by its value $(v + u)/2$ at the midpoint. Evaluating the integrals then gives the lower bound

$$I_2 \geq \Omega \left(\frac{\beta_n}{n} \left[(\log(v + u))^{1+q-\epsilon} \right]_{u=A'}^{u=\beta_n} \right). \quad (\text{S6.44})$$

If $v \leq \mathcal{O}(\beta_n^\delta)$ for some $\delta < 1$, then this bound is of the order $\Omega((\beta_n/n)(\log \beta_n)^{1+q-\epsilon})$ since the upper and lower limits do not cancel to leading order. In that case, using Eq. (S6.38) to bound $|I_1|$, we have

$$\frac{|I_1|}{I_2} \leq \mathcal{O} \left(\frac{1}{v} \frac{1}{(\log \beta_n)^{1+q-\epsilon-\eta_q}} \right). \quad (\text{S6.45})$$

In the region $v \in [(\log n)^\alpha, \beta_n^{2/3}]$, we can bound $1/v$ by $1/(\log n)^\alpha$, so then

$$\frac{|I_1|}{I_2} \leq \mathcal{O} \left(\frac{1}{(\log \beta_n)^{1+q-\epsilon-\eta_q+\alpha}} \right). \quad (\text{S6.46})$$

For $q \geq 0$, the exponent is bounded by $1 + \alpha - 2\epsilon$, while for $q < 0$, it is bounded by $1 + q + \alpha - \epsilon$, which shows that in both cases the ratio goes to zero as $n \rightarrow \infty$. Equally, in the region $v \in [\beta_n^{2/3}, M\beta_n]$, the I_2 lower bound from Eq. (S6.44) becomes $\Omega((\beta_n/n)(\log \beta_n)^{q-\epsilon})$ because the leading term cancels, while the $1/v$ from the I_1 bound is at most $1/\beta_n^{2/3}$, so then

$$\frac{|I_1|}{I_2} \leq \mathcal{O} \left(\frac{1}{\beta_n^{2/3}} \frac{1}{(\log \beta_n)^{q-\epsilon-\eta_q}} \right), \quad (\text{S6.47})$$

which also goes to zero as $n \rightarrow \infty$. Thus Eq. (S6.29) holds in all cases considered. \square

Remark 3. Combining Lemma S9 and Eq. (S6.44), it follows that for $p = 1$ and $|x| < \beta_n^{-1/3}$, we have the uniform lower bound

$$h_n(x) \geq \Omega((\log n)^{1-\epsilon}), \quad (\text{S6.48})$$

where $\epsilon > 0$ can be made arbitrarily small by taking n large. (This bound remains true for $|x| < \beta_n^{-\delta}$ with $\delta > 0$.)

C. Behavior of the equilibrium measure near the endpoints

1. Behavior at the endpoint

Lemma S10. For $Q \in \text{VSLF}(p, q)$ with $p > 0$, we have

$$\lim_{n \rightarrow \infty} h_n(1) = 2p. \quad (\text{S6.49})$$

Proof. From the integral form Eq. (S2.13) we have

$$h_n(1) = \frac{2}{\pi} \int_0^1 \frac{V'_n(1) - sV'_n(s)}{1 - s^2} \frac{ds}{\sqrt{1 - s^2}}. \quad (\text{S6.50})$$

Similar to the proof of Lemma S8 for $p > 1$, we will use the result from Lemma S1(v) that $\lim_{n \rightarrow \infty} sV'_n(s) = (p/\lambda_p)s^p$, uniformly for s in compact subsets of $(0, \infty)$, which proves pointwise convergence of the integrand for $s \in (0, 1)$. In order to apply the dominated convergence theorem we argue differently for the integration domains $[0, 1/2]$ and $[1/2, 1]$. Choosing $A > 0$ according to Lemma S1(i) so that $sV'_n(s)$ is increasing on $[A/\beta_n, 1/2]$, the integrand is upper bounded by $(4/3)^{3/2}V'_n(1) \leq \mathcal{O}(1)$ on this interval. Since

$$\int_0^{A/\beta_n} sV'_n(s)ds = \frac{1}{n\beta_n} \int_0^A uQ'(u)du \rightarrow 0, \quad (\text{S6.51})$$

as $n \rightarrow \infty$, we may interchange the n -limit and integration on the domain $[0, 1/2]$. For the remaining part of the integral it suffices to show that

$$\frac{V'_n(1) - sV'_n(s)}{1-s} \leq \mathcal{O}(1), \quad (\text{S6.52})$$

uniformly for $s \in [1/2, 1]$. Here we use the function f_Q introduced in the proof of Lemma S6 and the relations presented in Eqs. (S6.31) and (S6.33). We obtain

$$\frac{V'_n(1) - sV'_n(s)}{1-s} = \frac{\beta_n \beta_n Q'(\beta_n) - \beta_n s Q'(\beta_n s)}{n(\beta_n - \beta_n s)} \leq 2p \frac{\beta_n}{n} \int_0^1 Q'(\beta_n[1-t(1-s)])ds. \quad (\text{S6.53})$$

Applying Corollary S1 with $\epsilon = 1$ and keeping in mind that $1-t(1-s) \in [s, 1] \subset [1/2, 1]$ for $0 \leq t \leq 1$ we conclude for sufficiently large n that

$$\frac{V'_n(1) - sV'_n(s)}{1-s} \leq 2p \frac{2p}{\lambda_p} \int_0^1 [1-t(1-s)]^{p-2} ds \leq \mathcal{O}(1). \quad (\text{S6.54})$$

In summary we may conclude that

$$\lim_{n \rightarrow \infty} h_n(1) = \frac{2}{\pi} \frac{p}{\lambda_p} \int_0^1 \frac{1-s^p}{1-s^2} \frac{ds}{\sqrt{1-s^2}} = 2p, \quad (\text{S6.55})$$

where the last step follows from evaluating the integral and using the definition of λ_p in Eq. (S1.14). \square

2. Uniform lower bounds near $z = \pm 1$

Let us now prove a uniform lower bound on $h_n(z)$ for z in a neighbourhood of $z = 1$, with the case $z = -1$ following by symmetry. This will follow by combining the following lemma about uniform continuity with Lemma S10, which shows that $h_n(1) = 2p + o(1)$ as $n \rightarrow \infty$.

Lemma S11. *Let $Q \in \text{CVSLF}(p, q, \theta, \gamma)$ and $p > 0$. Then there exist constants $C, \varrho > 0$ and $n_0 \in \mathbb{N}$ such that, for all sufficiently large $n \geq n_0$, we have*

$$|h_n(z) - h_n(1)| \leq C|z - 1|, \quad \text{for all } |z - 1| \leq \varrho. \quad (\text{S6.56})$$

Proof. Fix $\delta > 0$ such that the circle $\{z : |z - 1| = \delta\}$ is contained in the cone C_θ . Furthermore choose $0 < \varrho < \tilde{\varrho} < \delta$. Note that the claim follows if we can establish $|h'_n(z)| \leq C$ for all $|z - 1| \leq \varrho$. Since h_n is analytic in C_θ , we may obtain such a bound from the Cauchy integral formula for derivatives

$$h'_n(z) = \frac{1}{2\pi i} \oint_{|s-1|=\tilde{\varrho}} \frac{h_n(s)}{(s-z)^2} ds, \quad (\text{S6.57})$$

and from an upper bound C_1 for $|h_n(z)|$ on $\{z : |z - 1| = \tilde{\varrho}\}$ that then allows us to choose $C = \tilde{\varrho}C_1/(\tilde{\varrho} - \varrho)^2$. In order to obtain such a bound C_1 we use the representation of Eq. (S2.11) for $h_n(z)$ and $|z - 1| = \tilde{\varrho}$. We can deform the contour of integration to obtain

$$h_n(z) = \frac{1}{\pi} \int_{-1}^{1-\delta} \frac{V'_n(s) - V'_n(z)}{s-z} \frac{ds}{\sqrt{1-s^2}} + \frac{1}{2\pi i} \oint_{|s-1|=\delta} \frac{V'_n(s) - V'_n(z)}{s-z} \frac{ds}{r(s)}. \quad (\text{S6.58})$$

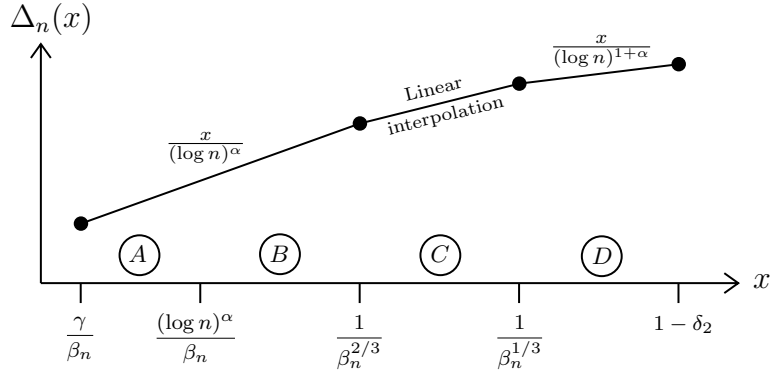


FIG. S8. Height function $\Delta_n(x)$ setting the imaginary part of the lens boundary $\tilde{\Sigma}_1$ (see Fig. S5), as a function of $x = \operatorname{Re} z$ in the different regions A, B, C, D . The contour is piecewise linear. The exponent α is chosen as in Lemma S12, and δ_2 and γ are as in Propositions S2 and S3. The specific exponents of $\beta_n^{2/3}$ and $\beta_n^{1/3}$ are not important; any decreasing pair of powers in $(0, 1)$ would suffice.

We have the following bounds on the integrals. First, for $|s - 1| = \delta$ and $|z - 1| = \tilde{\varrho}$ we obtain from Lemma S4 for n sufficiently large that

$$\left| \frac{V'_n(s) - V'_n(z)}{s - z} \frac{1}{r(s)} \right| \leq \frac{|V'_n(s)| + |V'_n(z)|}{(\delta - \tilde{\varrho}) \sqrt{\delta}} \leq \frac{4p(1 + \delta)^{p-1}}{\lambda_p(\delta - \tilde{\varrho}) \sqrt{\delta}}. \quad (\text{S6.59})$$

Second, we turn to the first summand on the right hand side of Eq. (S6.58). For $|z - 1| = \tilde{\varrho}$ we obtain

$$\left| \int_{-1}^{1-\delta} \frac{V'_n(s) - V'_n(z)}{s - z} \frac{ds}{\sqrt{1-s^2}} \right| \leq \frac{1}{(\delta - \tilde{\varrho}) \sqrt{\delta}} \left[2 \int_0^1 |V'_n(s)| ds + \frac{4p}{\lambda_p} (1 + \tilde{\varrho})^{p-1} \right], \quad (\text{S6.60})$$

for large n . We use Corollary S1 with $0 < \epsilon < p$ to bound the integral in the previous upper bound and obtain

$$\int_0^1 |V'_n(s)| ds \leq \frac{\beta_n}{n} \int_0^{A/\beta_n} |Q'(\beta_n s)| ds + \int_{A/\beta_n}^1 s^{p-1-\epsilon} ds \leq \frac{1}{n} \int_0^A |Q'(u)| du + \frac{1}{p - \epsilon}, \quad (\text{S6.61})$$

that finally yields the desired uniform bound C_1 on $|h_n(z)|$ for $|z - 1| = \tilde{\varrho}$ and large enough values of n . \square

D. Decay of contributions from the lens boundaries

Lemma S12. Consider $Q \in \text{CVSLF}(p, q, \theta, \gamma)$, and set $\alpha > 0$ arbitrarily for $p > 1$ but constrained to $\alpha < 1 + q$ for $p = 1$. Let the regions A, B, C, D and the height function $\Delta_n(x)$ be defined as indicated in Fig. S8. Then, for $\mathbb{X} \in \{A, B, C, D\}$, the following properties hold.

$$\sup_{x \in \mathbb{X}} \left| e^{-2n\phi_n(x+i\Delta_n(x))} \right| \xrightarrow{n \rightarrow \infty} 0. \quad (\text{S6.62})$$

$$n \operatorname{poly}(\log n) \int_{\mathbb{X}} \left| e^{-2n\phi_n(x+i\Delta_n(x))} \right| dx \xrightarrow{n \rightarrow \infty} 0. \quad (\text{S6.63})$$

Proof. The proof relies on the following basic equality which follows from Eqs. (S2.37) and (S2.41):

$$\left| e^{-2n\phi_n(x+i\Delta_n(x))} \right| = \exp \left[n \operatorname{Re} \left(\int_0^{\Delta_n(x)} ir(x+it)h_n(x+it) dt \right) \right], \quad (\text{S6.64})$$

where $r(z) = (z - 1)^{1/2}(z + 1)^{1/2}$. For $x \in \mathbb{X}$ and $t \in [0, \Delta_n(x)]$, one can check that $\arg r(x + it) \in [\pi/4, 3\pi/4]$.

We will define a function $\gamma_n(x)$ such that we can prove the bounds

$$|h_n(x + it)| \geq \gamma_n(x), \quad (\text{S6.65})$$

$$|\arg h_n(x + it)| \leq \pi/6, \quad (\text{S6.66})$$

for $x \in \mathbb{X}$ and $t \in [0, \Delta_n(x)]$. Then from Eq. (S6.64) we get

$$\left| e^{-2n\phi_n(x+it)} \right| \leq \exp \left[-\sin \left(\frac{\pi}{12} \right) n\gamma_n(x)\Delta_n(x) \right]. \quad (\text{S6.67})$$

We begin with the case $p = 1$, and will indicate how $p > 1$ can be treated at the end of the proof.

Region A

From Lemma S9, in this region we can choose $\gamma_n(x) = h_n(0)/2$ to satisfy Eq. (S6.65). With this choice, Eq. (S6.66) follows from $|h_n(x + it) - h_n(0)| \leq h_n(0)/2$. From Fig. S8 we recall that $\Delta_n(x) = x/(\log n)^\alpha$. Eq. (S6.62) then follows from Lemma S8 and

$$n\Delta_n(x)\gamma_n(x) \geq \Omega \left(\frac{n}{\beta_n} \frac{1}{(\log n)^\alpha} (\log n)^{1-\epsilon} \right) \geq \Omega \left((\log n)^{1+q-\alpha-2\epsilon} \right), \quad (\text{S6.68})$$

where the second inequality uses Eq. (S1.16); recall that $\alpha < 1 + q$ for $p = 1$, so the exponent can always be made positive by choosing ϵ small enough. Eq. (S6.63) then follows from a simple L_∞ bound.

Regions B–D

In all these regions, we choose $\gamma_n(x) = h_n(x)/2$, so that Eqs. (S6.65) and (S6.66) follow from $|h_n(x + it) - h_n(x)| \leq h_n(x)/2$. Let us now verify that this is a valid choice for $\gamma_n(x)$. From Remark 2 we have a uniform upper bound on $|h_n(z)|$ in a suitable $\Theta(|x|)$ -sized neighborhood of x . One can then use the Cauchy integral formula for derivatives to upper bound $|h'_n(x + it)| \leq \mathcal{O}((\log n)^{1+\epsilon}/|x|)$. Then we can bound the difference as $|h_n(x + it) - h_n(x)| \leq \mathcal{O}(\Delta_n(x)(\log n)^{1+\epsilon}/|x|)$. To show that this is less than $h_n(x)/2$, in regions B&C we use the lower bound $h_n(x) \geq \Omega((\log n)^{1-\epsilon})$ from Remark 3, while in region D we use $h_n(x) \geq \Omega(1)$ from Lemma S6.

With this choice of $\gamma_n(x)$, one can show that in regions C&D, Eqs. (S6.62) and (S6.63) are satisfied because $n\gamma_n(x)\Delta_n(x) \geq \Omega(n^{1/3-\epsilon})$. In region B, Eq. (S6.62) follows from

$$n\Delta_n(x)\gamma_n(x) \geq \Omega \left(\frac{n}{\beta_n} (\log n)^{1-\epsilon} \right) \geq \Omega \left((\log n)^{1+q-2\epsilon} \right), \quad (\text{S6.69})$$

where we used $x \geq (\log n)^\alpha/\beta_n$, the lower bound from Remark 3, and Eq. (S1.16). Since $1 + q > 0$, the exponent can be made positive by choosing ϵ sufficiently small. Eq. (S6.63) follows from the calculation

$$n \text{poly}(\log n) \int_B \exp \left[-\Omega \left(n (\log n)^{1-\epsilon} \frac{x}{(\log n)^\alpha} \right) \right] dx \leq \mathcal{O} \left(\frac{n \text{poly}(\log n)}{n (\log n)^{1-\epsilon-\alpha}} \exp \left[-\Omega \left(\frac{n}{\beta_n} (\log n)^{1-\epsilon} \right) \right] \right), \quad (\text{S6.70})$$

$$\leq \mathcal{O} \left(\text{poly}(\log n) \exp \left[-\Omega \left((\log n)^{1+q-2\epsilon} \right) \right] \right), \quad (\text{S6.71})$$

where we used Eq. (S1.16) for β_n . For $q > 0$ the upper bound converges to zero superpolynomially in n , while for $q \leq 0$ the convergence may be subpolynomial (but still super-polylogarithmic). This concludes the proof for $p = 1$.

For $p > 1$ the proof is much simpler. It suffices to take $\Delta_n(x) = x/(\log n)^2$ and $\gamma_n(x) = (1/2) \min_{x \in [0,1]} h_n(x) \geq \Omega(1)$. The bound $|h_n(x + it) - h_n(x)| \leq h_n(x)/2$ follows from Lemma S9 for $x \in A$, and for $x \in B, C, D$ by an upper bound on the derivative $h'_n(x + it)$ using Remark 2 as before. Overall one finds that

$$n\gamma_n(x)\Delta_n(x) \geq \Omega \left(\frac{n}{\beta_n} (\log n)^{-2} \right) \geq \Omega \left(n^{1-1/p-\epsilon} \right), \quad (\text{S6.72})$$

which suffices to prove Eqs. (S6.62) and (S6.63) for $p > 1$. \square

GLOSSARY OF SYMBOLS

We use standard asymptotic notation. Let $f, g : \mathbb{R}^+ \rightarrow \mathbb{C}$ be two functions. We write $f(x) = \mathcal{O}(g(x))$ iff there exist constants $C, x_0 > 0$ such that $|f(x)| < C|g(x)|$ for all $x > x_0$. We write $f(x) = o(g(x))$ iff, for every constant $C > 0$, there exists $x_0 > 0$ such that $|f(x)| < C|g(x)|$ for all $x > x_0$. We write $f(x) = \Omega(g(x))$ iff $g(x) = \mathcal{O}(f(x))$, and $f(x) = \omega(g(x))$ iff $g(x) = o(f(x))$. We write $f(x) = \Theta(g(x))$ iff $f(x) = \mathcal{O}(g(x))$ and $f(x) = \Omega(g(x))$. We write $f(x) = \tilde{\mathcal{O}}(g(x))$ iff $f(x) = \mathcal{O}(g(x)(\log |g(x)|)^k)$ for some finite k , and $f(x) = \tilde{\Omega}(g(x))$ iff $g(x) = \tilde{\mathcal{O}}(f(x))$. We write $f(x) = \text{poly}(g(x))$ iff $f(x) = \mathcal{O}((g(x))^k)$ for some finite k .

Symbol	Description	Definition
\mathcal{L}	Liouvillian superoperator	$\mathcal{L}(\cdot) = [H, \cdot]$
A	Initial Lanczos operator (not necessarily normalized)	System dependent
$C(t)$	Autocorrelation function	$C(t) = (A A(t)) = (A e^{i\mathcal{L}t}A)$
$\Phi(\omega)$	Spectral function	$\Phi(\omega) = \int_{\mathbb{R}} e^{-i\omega t} C(t) dt$
ρ	Low-frequency power-law exponent	$\Phi(\omega \rightarrow 0) \sim \omega ^\rho$
$G(z)$	Green's function (resolvent)	$G(z) = \left(A \left \frac{1}{z - \mathcal{L}} \right A \right)$
b_n	n th Lanczos coefficient	Eq. (23b)
O_n	n th Lanczos operator	Eq. (23c) (see also Eq. (31))
\mathcal{L}_n	Level- n Liouvillian	$\mathcal{L}_n = \mathcal{Q}_n \mathcal{L} \mathcal{Q}_n$ with $\mathcal{Q}_n = \mathbf{1} - \sum_{m=0}^{n-1} O_m\rangle\langle O_m $
$G_n(z)$	Level- n Green's function	$G_n(z) = \left(O_n \left \frac{1}{z - \mathcal{L}_n} \right O_n \right)$
$w(\omega)$	Weight function for orthogonal polynomials	$w(\omega) = \Phi(\omega)/2\pi$
$\Phi_n(\omega)$	n th spectral function (w.r.t. \mathcal{L}_n)	$\Phi_n(\omega) = \int_{\mathbb{R}} e^{-i\omega t} (O_n e^{i\mathcal{L}_n t} O_n) dt = 2 \text{Im}[G_n(\omega - i0^+)]$
$\tilde{\Phi}_n(\omega)$	n th spectral function (w.r.t. \mathcal{L})	$\tilde{\Phi}_n(\omega) = \int_{\mathbb{R}} e^{-i\omega t} (O_n e^{i\mathcal{L} t} O_n) dt$
$p_n(\omega)$	Degree n orthonormal polynomial w.r.t. $\Phi(\omega)/2\pi$	Eq. (10) (see also Eq. (30))
y_n	Positive leading coefficient of $p_n(\omega)$	$p_n(\omega) = y_n \omega^n + \mathcal{O}(\omega^{n-1}), \quad y_n > 0$
$P_n(\omega)$	Monic orthogonal polynomial	$P_n(\omega) = (1/y_n)p_n(\omega)$
$Q(\omega)$	Potential (for Coulomb gas)	Defined implicitly by $\Phi(\omega)/2\pi \equiv \omega ^\rho e^{-Q(\omega)}$
p, q	Polynomial growth exponents for potential	$Q(\omega \rightarrow \infty) \sim \omega^p (\log \omega)^{q+o(1)}$ (see Section S1 A)
$\sigma_n(\omega)$	Equilibrium density (with charge n)	Eq. (41)
β_n	n th Mhaskar-Rakhmanov-Saff (MRS) number	Eq. (43) (asymptotics in Eq. (44); satisfies $\beta_n = 2b_n[1 + \mathcal{O}(1/n)]$)
$V_n(x)$	Rescaled potential	$V_n(x) = Q(\beta_n x)/n$
$\psi_n(x)$	Rescaled equilibrium density	$\psi_n(x) = (\beta_n/n)\sigma_n(\beta_n x)$
$\psi^{(p)}(x)$	Ullman distribution	Eq. (49)
$h_n(x)$	Non-semicircle part of eq. measure	$h_n(x) = 2\pi\psi_n(x)/\sqrt{1-x^2}$ (see also Eq. (51))
$K_n(x, y)$	Christoffel-Darboux kernel	$K_n(x, y) = \sum_{m=0}^{n-1} p_m(x)p_m(y)$
$\tilde{K}_n(x, y)$	Weighted Christoffel-Darboux kernel	$\tilde{K}_n(x, y) = \sqrt{w(x)w(y)}K_n(x, y)$
$\mathbb{S}(u, v)$	Sine kernel	$\mathbb{S}(u, v) = \frac{\sin[\pi(u-v)]}{\pi(u-v)}$
$\mathbb{J}_{\rho/2}(u, v)$	Bessel kernel	$\mathbb{J}_{\rho/2}(u, v) = \pi\sqrt{u}\sqrt{v} \frac{J_{\frac{\rho+1}{2}}(\pi u)J_{\frac{\rho-1}{2}}(\pi v) - J_{\frac{\rho-1}{2}}(\pi u)J_{\frac{\rho+1}{2}}(\pi v)}{2(u-v)}$

Symbol	Description	Definition
$\mathbb{A}(u, v)$	Airy kernel	$\mathbb{A}(u, v) = \frac{\text{Ai}(u) \text{Ai}'(v) - \text{Ai}'(u) \text{Ai}(v)}{u-v}$
$\theta_n(\omega)$	(WKB) Phase factor	$\theta_n(\omega) = -\pi \int_{\omega}^{\beta_n} \sigma_n(\omega') d\omega' - \frac{\pi}{4}$
$I_n(\omega)$	Cumulative equilibrium measure	$I_n(\omega) = \int_0^{\omega} \sigma_n(\omega') d\omega'$
\mathcal{J}	Heat/spin/charge current operator	Hamiltonian-dependent (see Section VB)
$g_n(z)$	Logarithmic transform of equilibrium measure	$g_n(z) = \int_{-1}^1 \log(z-s) \psi_n(s) ds, \quad z \in \mathbb{C} \setminus \mathbb{R}$
l_n	Lagrange multiplier for Coulomb gas energy minimization	Eq. (S1.37)
$Y(z)$	Solution to fundamental Riemann-Hilbert problem	Eq. (S2.4)
σ_3	3rd Pauli matrix (not to be confused with $\sigma_n(\omega)$)	$\sigma_3 = \text{diag}(1, -1)$
Y_1	$\mathcal{O}(1/z)$ correction to leading $Y(z \rightarrow \infty)$ scaling	$z^{-n\sigma_3} Y(z) = \mathbf{1} + Y_1/z + \mathcal{O}(1/z^2)$ as $z \rightarrow \infty$
$U(z)$	$Y(z)$ rescaled by β_n	$U(z) = \beta_n^{-(n+\rho/2)\sigma_3} Y(\beta_n z) \beta_n^{(\rho/2)\sigma_3}$
$T(z)$	$U(z)$ rescaled by the log-transformed equilibrium measure	$T(z) = e^{-(nl_n/2)\sigma_3} U(z) e^{(nl_n/2)\sigma_3} e^{-ng_n(z)\sigma_3}$
$\hat{\psi}_n(z)$	Analytic continuation of equilibrium measure	Eq. (S2.37)
$\phi_n(z)$	Integral of equilibrium measure	$\phi_n(z) = -\pi i \int_1^z \hat{\psi}_n(s) ds, \quad z \in \mathbb{C} \setminus \mathbb{R}$
$S(z)$	Solution of intermediate RHP with contour deformation	Eq. (S2.45)
$N(z)$	Solution of RHP for outside region	Eq. (S2.53)
$D(z)$	Szegő function for $ x ^\rho$ on $[-1, 1]$	$D(z) = z^{\rho/2} / \varphi(z)^{\rho/2}$ with $\varphi(z) = z + (z+1)^{1/2}(z-1)^{1/2}$
$a(z)$	Generates solution of outside RHP for $\rho = 0$	$a(z) = (z-1)^{1/4} / (z+1)^{1/4}$
$r(z)$	Appears in solutions for RHPs on $[-1, 1]$	$r(z) = (z-1)^{1/2} (z+1)^{1/2}$
$P(z)$	Solution of RHP in local parametrices near $z = \pm 1$ and $z = 0$	Eqs. (S2.73) and (S2.77) for $z = \pm 1$, and Eq. (S2.112) for $z = 0$
$f_n(z)$	Biholomorphic map to auxiliary ζ -plane	Prop. S2 for z near $z = 1$, and Eq. (S2.100) for z near $z = 0$
$P^{(1)}(z)$	Solution of constant-jump RHP for local parametrices	Eq. (S2.62) for $z = 1$, and Eq. (S2.99) for $z = 0$
$\Psi(\zeta)$	Solution of auxiliary RHP for $z = \pm 1$ local parametrices	Eq. (S2.61)
$\Psi_{\rho/2}(\zeta)$	Solution of auxiliary RHP for $z = 0$ local parametrix	Eq. (S2.96)
$\omega(z)$	Analytic continuation of $ x ^\rho$, continuous across \mathbb{R}	Eq. (S2.44)
$W(z)$	Function related to $ x ^\rho$, discontinuous across \mathbb{R}	Eq. (S2.85)
$S_{\text{par}}(z)$	Approximate solution of RHP for $S(z)$ using local parametrices	Eq. (S2.117)
$R(z)$	Solution of residual RHP	$R(z) = S(z) S_{\text{par}}(z)^{-1}$, solved in Eq. (S2.123)
$\tilde{\Sigma}_j$	Contour on which $R(z)$ has a jump, $j = 1, \dots, 9$	See Fig. S5